

The Recycling of Resorcinol Formaldehyde Latex Coated Nylon 66

A thesis submitted to the University of Manchester
for the degree of
Doctor of Philosophy
in the Faculty of Engineering and Physical Sciences.

2013

Sarah Wroe

School of Materials

Table of Contents

Table of Contents	2
List of Tables.....	6
List of Figures	7
Abstract	13
Declaration	14
Copyright Statement	14
Acknowledgements	15
1.0 Introduction	16
1.1 Heathcoat Textiles.....	16
1.1.1 Background	16
1.1.2 Areas of Waste Production.....	16
1.1.3 Waste Management Systems.....	20
1.2 Raw Materials	21
1.2.1 Nylon.....	21
1.2.2 Fabric Construction.....	27
1.2.3 Resorcinol Formaldehyde Latex Coatings	29
1.2.4 Properties of Coated Fabrics	35
1.2.5 Summary	38
1.3 Research Objectives	38
1.4 References	39
2.0 Waste Disposal and Textile Recycling	41
2.1 Introduction	41
2.2 Legislation.....	41
2.3 Current Recycling Processes.....	44
2.3.1 The Primary Approach: Reclaimed Fibres.....	44
2.3.2 The Secondary Approach: Melt Processing.....	47
2.3.3 The Tertiary Approach: Chemical Recycling.....	52
2.3.4 The Quaternary Approach: Incineration	55
2.4 Innovation in Textile Recycling.....	56
2.5 Conclusions	60
2.6 References	61
3.0 The Effect of RFL Coating on Fabric Properties	64
3.1 Aim.....	64
3.2 Introduction	64
3.3 Materials.....	65
3.4 Experimental Methods	66
3.4.1 Tensile Properties.....	66
3.4.2 Bending Rigidity	67
3.4.3 Resistance to Tearing	67
3.5 Results and Discussion.....	68
3.5.1 Tensile Properties.....	68
3.5.2 Bending Rigidity	76
3.5.3 Resistance to Tearing	77

3.6 Summary and Hypothesised Effect of Coated Fabric Properties on Fabric Reduction Methods	80
3.7 References	80
4.0 Reduction Processes and their Effect on Fibre Length, Coating Integrity and Polymer Degradation	82
4.1 Aims.	82
4.2 Introduction to Reduction Processes.....	82
4.2.1 The Laroche Cadette Shredder.....	82
4.2.2 The Hollander Beater	83
4.2.3 The Intimus Disintegrator	84
4.3 Reduction of Coated and Uncoated Material	85
4.3.1 Materials.....	85
4.3.2 Reduction Procedures.....	85
4.3.3 Fibre Measurement.....	89
4.3.4 Results and Discussion.....	90
4.4 Microscopic analysis	107
4.4.1 Materials.....	107
4.4.2 Method	108
4.4.3 Results and Discussion.....	108
4.5 Thermal Analysis	127
4.5.1 Materials.....	128
4.5.2 Methods.....	129
4.5.3 Results and Discussion.....	130
4.6 Conclusions	153
4.7 References	155
5.0 Recycling Fibres Using Paper Technology.....	157
5.1 Aim.....	157
5.2 An Overview of the Papermaking Process.....	157
5.2.1 Pulping	158
5.2.2 Repulping, Beating and Refining.....	159
5.2.3 Screening and Cleaning	162
5.2.4 The Paper Machine	171
5.3 Paper and Textiles	172
5.3.1 Textiles Fibres in Paper.....	172
5.3.2 Paper in Textile Fabric	177
5.3.3 Synthetic Paper Yarns	179
5.4 Experimental – RFL Coated Nylon 66 Paper Handsheets	180
5.4.1 Materials.....	180
5.4.2 Handsheet Formation	181
5.4.3 Physical Testing of RFL Coated Nylon 66 Paper Handsheets.....	183
5.5 Results and Discussion – RFL Coated Nylon 66 Paper Handsheets	184
5.5.1 Forming of the Paper Sheet.....	184
5.5.2 Physical Testing of Handsheets	189
5.6 Conclusion – RFL Coated Nylon 66 Paper Handsheets	192
5.7 Experimental - Separation of Fibres	193
5.7.1 Materials.....	193
5.7.2 Length Fractionation using Centrifugal Cleaners	194
5.7.3 Calculating the Consistency.....	194

5.7.4 Colorimetric Analysis	195
5.7.5 Numerical Analysis	200
5.8 Results and Discussion – Separation of Fibres	201
5.8.1 Colorimetric Analysis	201
5.8.2 Numerical Analysis of Fibres.....	208
5.9 Conclusions – Separation of Fibres	211
5.10 References	213
6.0 Recycling of Fibres using Textile Technology	216
6.1 Aims	216
6.2 Introduction to Carding and Friction Spinning	216
6.2.1 Carding	216
6.2.2 Friction Spinning.....	217
6.3 Recycling Fibres using Spinning Processes.....	220
6.4 Experimental – Short Fibre Spinning.....	220
6.4.1 Materials.....	221
6.4.2 Spinning Studies	221
6.4.3 Yarn Testing.....	222
6.5 Results and Discussion – Short Fibre Spinning	223
6.6 Experimental – Web formation of RFL coated nylon 66 fibres	227
6.6.1 Materials.....	227
6.6.2 Carding.....	227
6.7 Results and Discussion – Web formation of RFL coated nylon 66 fibre..	228
6.8 Conclusions	230
6.9 References	230
7.0 Plastic Recycling.....	232
7.1 Aim.....	232
7.2 Introduction to Plastic Processing	232
7.2.1 Injection Moulding.....	232
7.2.2 Compression Moulding	234
7.3 Experimental	237
7.3.1 Injection Moulding.....	237
7.3.2 Compression Moulding	238
7.4 Results and Discussion.....	240
7.4.1 Injection Moulding.....	240
7.4.2 Compression Moulding	241
7.5 Conclusions	247
7.6 References	247
8.0 Using RFL Fibres as a Filler to Reinforce Rubber.	248
8.1 Aim.....	248
8.2 Rubber Technology.....	248
8.2.1 Introduction	248
8.2.2 Vulcanisation.....	250
8.2.3 Additives in Rubber	251
8.2.4 The Use of Textiles In rubber Technology	261
8.2.5 Rubber Processing.....	262
8.2.6 Applications of Rubber	263
8.3 Recycling of fibrous waste in rubber	264

8.3.1 Leather.....	264
8.3.2 Paper Fibres.....	266
8.4 Experimental	267
8.4.1 Materials.....	267
8.4.2 Preparation of Rubber Formulations.....	269
8.4.3 Cure Characterisation.....	272
8.4.4 Vulcanisation Procedure	273
8.4.5 Physical Test Methods - Tensile Properties.....	273
8.4.6 Physical test methods - Resistance to Tearing.....	274
8.5 Results and Discussion.....	274
8.5.1 Preparation of Specimen	274
8.5.2 Cure Profile	278
8.5.3 Curing of Rubber Sheets	284
8.5.4 Tensile Properties.....	286
8.5.5 Resistance to Tearing	291
8.6 Conclusions	294
8.7 References	295
9.0 Conclusions and Further Work	297
9.1 Conclusions	297
9.2 Further Work.....	301
Appendix 1: Fabric Properties	303
Appendix 2: Paper Physical Testing	305
Appendix 3: Yarn Physical Testing	308

Word Count: 73,412.

List of Tables

Table 1.1: Properties of Nylon	28
Table 3.1: Fabric Specifications.....	65
Table 3.2: Tensile Test Parameters	67
Table 3.3: Tensile Breaking Load of Nylon Fabrics.....	69
Table 3.4: Extension of T-00537 Nylon 66 Fabrics.....	72
Table 3.5: Toughness of T-00537 Nylon 66 Fabrics	75
Table 3.6: Bending Rigidity of T-00537 Nylon 66 Fabrics	77
Table 3.7: Maximum Tear Force of T-00537 Nylon 66 Fabrics.....	78
Table 4.1: Processing Conditions for Beating trial A (TU = Turns Up, D = Down Position ie biting point).....	86
Table 4.2: Processing Conditions for Beating trial B.....	88
Table 4.3: Effect of Coating on MFI.....	132
Table 4.4: Effect of Reduction Method on MFI.....	142
Table 5.1: Beating Procedure for Pulp Formation	181
Table 5.2: Composition of Handsheets	182
Table 5.3: Summary of Handsheet Formation	184
Table 5.4: Summary of RFL Coated Nylon 66/Cellulose Paper Weight per unit area and Thickness Results	189
Table 5.5: Summary of Tensile Properties.....	191
Table 5.6: Hydrocyclone Output Consistencies.....	195
Table 5.7: Paper Handsheets Manufactured from Separated Fibres	196
Table 5.8: Standard Paper Sheets Produced from Different Fibres	197
Table 5.9: Visual Colour Matching of Hydrocyclone Separated Fibres	201
Table 5.10: ΔE_{ab} Analyses of Batches against Standards with figures in bold showing closest standard for each hydrocyclone batch.	203
Table 5.11: ΔE_{94} Analyses of Batches against Standards	204
Table 5.12: Summary of Results from Colorimetric Analysis.....	205
Table 5.13: Numerical Analysis of Batch Samples.....	209
Table 5.14: Efficiency of Hydrocyclone Cleaners at Separating Fibres by Length	211
Table 6.1: Operating Conditions of the DREF 2 Spinning Machine	221
Table 6.2: Specification of Yarns Produced.....	222
Table 7.1: Injection Moulding Settings used in Study	237
Table 7.2: Compression Moulding Intimus Reduced Coated Waste (Particles)	241
Table 7.3: Compression Moulding of Uncoated Fabric using Open Flash Mould	242
Table 7.4: Compression Moulding of RFL Coated Fabric using Open Flash Mould.....	243
Table 7.5: Compression Moulding of Uncoated Fabric using a Positive Mould.....	244
Table 7.6: Compression Moulding of RFL Coated Fabric using a Positive Mould	245

Table 8.1: Controlling Vulcanizate Properties by Formulation Alteration (Brydson, 1988)	253
Table 8.2: The Effect of Filler Particle Size and Structure on Rubber Properties (Horn, 1982).....	258
Table 8.3: Beating Cycle to Produce Recycled Filler	268
Table 8.4: Rubber Mixes Produced.....	270
Table 8.5: 0% Filler Formulation.....	271
Table 8.6: 12.5% Filler Formulation.....	271
Table 8.7: 25% Filler Formulation.....	271
Table 8.8: 37.5% Filler Formulation.....	272
Table 8.9: Summary of Cure in Uncoated Nylon Filler.....	280
Table 8.10: Summary of Cure in RFL Coated Nylon Filler	280
Table 8.11: Reinforcement Factor.....	283
Table 8.12: Tensile Strength of Rubber Sheets.....	287
Table 8.13: Tear Strength of Filled Rubber Sheets.....	291

List of Figures

Figure 1.1: Spindle Texturising Process (Hatch, 1993).....	17
Figure 1.2: Cross-section of Passage of Warp Yarn Through a Loom (Modified-redrawn (Marks et al., 1976)).....	19
Figure 1.3: Synthesis of Nylon 6 (Durairaj, 2005).	21
Figure 1.4: Reaction Synthesis for Nylon 66 (Durairaj, 2005).....	22
Figure 1.5: Melt Spinning (Billmeyer, 1971).	23
Figure 1.6: Drawing Process (Billmeyer, 1971)	24
Figure 1.7: Stress-strain Curves of Nylon Compared to other Popular Fibres (Moncrieff, 1975).....	25
Figure 1.8: Reaction Schemes to Produce (a) RF Resole and (b)RF Novolak (Durairaj, 2005).....	31
Figure 1.9: Styrene-Butadiene Copolymer	32
Figure 1.10: Vinyl Pyridine Terpolymer.....	32
Figure 1.11: Dip Coating (Sen and Damewood, 2001).....	32
Figure 1.12: Reaction Scheme to Form Chemical Bond between RFL and Nylon (Durairaj, 2005).....	33
Figure 1.14: Possible Bonding Mechanisms between Nylon,	35
RFL and Rubber (Durairaj, 2005).....	35
Figure 1.15: Simplified Cross-section of a Coated Fabric.....	36
Figure 2.1: Tearing Technology Utilising Pin and Sawtooth Clothing (Laroche, 2012).	45
Figure 2.2: Mini Garnett Machine for Yarn Opening (Scoleri, 2008).....	45
Figure 2.3: Four-Shaft Shredder (Scheirs, 1998).....	48
Figure 2.4: Granulator Knife Action (Scheirs, 1998).	49
Figure 2.5: Agglomeration by Densifying Discs (Scheirs, 1998).....	50
Figure 2.6: Compression Agglomeration.....	50
Figure 2.7: Reaction Scheme of Acid Catalysed Depolymerisation of Nylon 6 to give Caprolactam (Scheirs, 1998).	53
Figure 2.8: Schematic Diagram of Acidolysis Plant (Scheirs, 1998).	53
Figure 2.9: Aminolytic Reaction Scheme of Nylon 6 and Nylon 66.....	54

Figure 2.10: Schematic Diagram of Aminolysis Process (Scheirs, 1998).....	55
Figure 3.1: Wing-rip specimen size and arrangement for clamping.....	68
Figure 3.2: The Effect of Coating on Fabric Breaking Strength.....	69
Figure 3.3: The Effect of Coating on Thread Breaking Strength.....	69
Figure 3.4: The Effect of Coating on Fabric Extension.....	72
Figure 3.5: Generalised Load-extension Curve of Woven Fabrics. (Grosberg, 1969)	73
Figure 3.6: Tensile Curves of Fabric in Warp Direction.	75
Figure 3.7: Tensile Curves of Fabric in Weft Direction	75
Figure 3.8: The Effect of Coating on Fabric Flexural Rigidity	77
Figure 3.9: The Effect of Coating on Fabric Tear Strength.....	78
Figure 4.1: The Laroche Cadette with 2 opening sections (Laroche, 2012).....	83
Figure 4.2: Diagram of the Hollander Beater (University of Minnesota, 1998)..	84
Figure 4.3: Intimus Power Disintegrator(Martin Yale International, 2010).....	84
Figure 4.4: Typical Breakdown Output from the Laroche Cadette Shredder.....	91
Figure 4.6: Typical Breakdown Output from the Hollander Beater	93
Figure 4.7: Average Fibre Length of Uncoated and RFL Coated Reduced Material Throughout Beating Trial A. (Error bars = Standard deviation of fibre length)	94
Figure 4.8: Fibre Length Distribution of Uncoated and RLF Coated Material after 10 minutes Beating..... = Fibre length suitable for spinning	95
Figure 4.9: Fibre Length Distribution of Uncoated and RFL Coated Material after 50 minutes Beating.....	96
Figure 4.10 The Effect of Consistency on the Amount of Fibre to Fibre Contact causing Friction and Fibre to Metal Contact causing Cutting Action. (Smook, 2002)	97
Figure 4.11: Average Fibre Length of Uncoated and RFL Coated Reduced Material Throughout Beating Trial B.	98
Figure 4.12: RFL Coated Fibre Length Distribution at 15 minutes 10TU 1.5% (Trial B).....	99
Figure 4.13: RFL Coated Fibre Length Distribution at 30 minutes 10TU, 2% (Trial B).....	100
Figure 4.14: RFL Coated Fibre Length Distribution at 45 minutes, 7TU, 2% (Trial B).....	100
Figure 4.15: RFL Coated Fibre Length Distribution at 55 minutes, 5TU, 2% (Trial B).....	101
Figure 4.16: RFL Coated Fibre Length Distribution at 65 minutes, 2TU, 2% (Trial B).....	101
Figure 4.17: RFL Coated Fibre Length Distribution at 75 minutes, D, 2% (Trial B)	102
Figure 4.18: Typical Breakdown Output from the Intimus disintegrator.	103
Figure 4.19: Particle Size Distribution of RFL Coated Material Reduced by the Intimus Disintegrator (Trial A).	104
Figure 4.20: Particle Size Distribution by Weight of RFL Coated Material Reduced by the Intimus Disintegrator Trial A, Analysed using Fractionation by Sieving.	105
Figure 4.21: Size Descriptors in Particles.....	106

Figure 4.22: Fibre Length Distribution of Uncoated and RFL Coated Material Initial Laroche Cadette Shredding Followed by Intimus Disintegration.	107
Figure 4.23: SEM Micrographs of Face side of Two Common Types of Coated Fabric Waste, at a Magnification of x25	109
Figure 4.24: SEM Micrographs of Face side of Two Common Types of Uncoated Fabric Waste, at a Magnification of x25	110
Figure 4.25: SEM Micrograph of Coated Fabric A at a Magnification x250....	111
Figure 4.26: SEM Micrograph of Coated Fabric B at a Magnification x250....	111
Figure 4.27: SEM Micrograph of Uncoated Fabric A at a Magnification x250	112
Figure 4.28: SEM Micrograph of Uncoated Fabric B at a Magnification x250	113
Figure 4.29: SEM Micrographs of Coated Material Reduced by Means of the Laroche Cadette, at a Magnification of x250.....	115
Figure 4.30: SEM Micrograph of Uncoated Material Reduced by Means of the Laroche Cadette, at a Magnification of x250.....	116
Figure 4.31: SEM Micrograph of Surface Abrasion of Nylon Caused by a Rotating Pin (Hearle, 1998)	117
Figure 4.32: SEM Micrograph of Twist Break (Hearle, 1998).....	117
Figure 4.33: SEM Micrograph of Fibre to Metal Abrasion Causing Axial Splitting of the Fibre (Hearle, 1998).....	118
Figure 4.34: SEM Micrograph of Coated Material Reduced by Means of the Hollander Beater, at a Magnification of x250.....	119
Figure 4.35: SEM Micrograph of Uncoated Material Reduced by Means of the Hollander Beater, at a Magnification of x250.....	120
Figure 4.36: SEM Micrograph of Fibre Breaks Occurring from Nylon Fibre held under Tension against a Rotating Pin (Hearle, 1998)	121
Figure 4.37: SEM Micrograph of Nylon Fibre Cut with a Knife (Hearle, 1998)	122
Figure 4.38: SEM Micrograph of Polyester Cut with Scissors (Hearle, 1998) .	122
Figure 4.39: SEM Micrograph of Nylon Fibres Broken due to Impact (Hearle, 1998).	122
Figure 4.40: SEM Micrograph of Coated Material Reduced by Means of the Intimus Disintegrator, at a Magnification of x250.....	124
Figure 4.41: SEM Micrograph of Uncoated Material Reduced by Means of the Intimus Disintegrator, at a Magnification of x250.....	125
Figure 4.42: SEM Micrograph of Coated Material Reduced by Means of the Intimus Disintegrator, Forming Flake-like Particles, at a Magnification of x5 (image a) and x40 (image b).	126
Figure 4.43: SEM Micrograph of Coated Material Reduced by Means of the Intimus Disintegrator, Forming Flake-like Particles, at a Magnification of x250	127
Figure 4.44: DSC Thermograms Showing the Initial (top) and Second (bottom) Heat Cycle of Finished (Uncoated) and Dipped (Coated) Fabric.....	131
Figure 4.45: Preferential Polymer Break Points in Thermal Degradation of Nylon.	133
Figure 4.46: Degradation Reactions of Nylon 66 (Steppan et al., 1991).....	134
Figure 4.47: TGA Analysis of Finished and Dipped Fabric	135
Figure 4.48: Structure of RFL Coated Nylon and Bonding Mechanism Involved (Durairaj, 2005).....	136
Figure 4.49: FTIR Spectral Analysis of Finished Fabric (top) and Dipped Fabric (bottom) in Relation to Temperature.....	137

Figure 4.50: Identification of Volatiles Produced using FTIR Analysis from Finished (top) and Dipped (bottom) Fabric.	138
Figure 4.51: DSC Analysis Showing the Initial (top) and Second (bottom) Heat Cycle of Fabric Samples from Mixed Coated Waste Prior to Reduction.	139
Figure 4.52: DSC Analysis Showing the Initial (top) and Second (bottom) Heat Cycle of Reduced Mixed Coated Waste.	141
Figure 4.53: TGA Analysis of Fabric Samples from Mixed Uncoated Waste Prior to Reduction.	143
Figure 4.54: FTIR Spectral Analysis of Uncoated A Fabric (top) and Uncoated B Fabric (bottom) in Relation to Temperature.	145
Figure 4.55: TGA Analysis of Reduced Mixed Uncoated Waste.	145
Figure 4.56: FTIR Spectral Analysis of Reduced Mixed Uncoated Waste in Relation to Temperature, Laroche Cadette (top), Hollander beater (centre) Intimus Disintegrator (bottom).	146
Figure 4.57: Identification of Volatiles Produced using IR Analysis from Laroche Cadette (top) and Hollander Beater (bottom) Reduced Uncoated Waste.	147
Figure 4.58: TGA Analysis of Fabric Samples from Mixed Coated Waste Prior to Reduction.	148
Figure 4.59: FTIR Analysis of Coated A Fabric (top) and Coated B Fabric (bottom) in Relation to Temperature.	148
Figure 4.60: Identification of Volatiles Produced using IR Analysis from Coated B Fabric in Mixed Coated Waste Prior to Reduction.	149
Figure 4.61: TGA Analysis of Reduced Mixed Coated Waste.	149
Figure 4.62: FTIR Spectral Analysis of Reduced Mixed Coated Waste in Relation to Temperature, Laroche Cadette (top), Hollander Beater (centre) Intimus disintegrator (bottom).	150
Figure 4.63: Identification of Volatiles Produced using IR Analysis from Laroche Cadette (top) and Hollander Beater (centre) and Intimus Disintegrator (bottom) Reduced Coated Waste.	151
Figure 4.64: FTIR Spectral Analysis of Intimus Disintegrator Reduced Coated Waste (Particles) in Relation to Temperature.	152
Figure 4.65: Identification of Volatiles Produced using IR Analysis from Intimus Disintegrator Reduced Coated Waste (Particles).	152
Figure 5.1: An Overview of Pulping and Papermaking Processes (Inform, 2009)	158
Figure 5.2: Illustration of a Hydropulper (Smook, 2002)	160
Figure 5.3: Diagram of Screening System (Smook, 2002)	162
Figure 5.4: Centrifugal Cleaner (Smook, 2002)	164
Figure 5.5: Flow Patterns within Hydrocyclones (Bliss, 1996)	164
Figure 5.6: Forward Flow Cleaner Operating Conditions (Bliss, 1996)	165
Figure 5.7: Core Bleed Cleaner (Bliss, 1996)	166
Figure 5.8: Reverse Cleaner (Bliss, 1996)	167
Figure 5.9: Through Flow Cleaner (Bliss, 1996)	167
Figure 5.10: The Fourdrinier Paper Machine (Smook, 2002)	171
Figure 5.11: Example of a sheet with no faults	185
Figure 5.12: Photographic examples of sheets with minor faults such as the hole in the left sheet and small areas of thinness in the right sheet.	185

Figure 5.13: Photographic Examples of Sheets with Major Faults, such as the Large hole in the Left sheet and Many Smaller Holes and Large Areas of Thinness in the Second Sheet.	185
Figure 5.14: Photographs of Nylon Papers Formed from Various RFL coated Nylon 66/Cellulose Pulp Compositions.....	188
Figure 5.15: Weight per Unit area of Paper Handsheets Formed.....	190
Figure 5.16: Thickness of Paper Handsheets Formed.....	190
Figure 5.17: Tensile Index of Synthetic Nylon Fibre Paper Handsheets.....	192
Figure 5.18 CIE L*a*b* colour model.....	199
Figure 5.19: Visual Comparison Between Standard and Hydrocyclone Outlet Batches.....	202
Figure 5.20: Reflectance Spectra of Feed, Forward Flow “Accepts” and Through Flow “Accepts” in Comparison to the 70% Long/30% Short and the 50% Long/50% Short Standards.....	206
Figure 5.21: Reflectance of Through Flow “Rejects” in Comparison to the 100% Long Fibre and 90% Long Fibre/10% Short Fibre Standards.....	207
Figure 5.22: Reflectance of Forward Flow “Rejects” in Comparison to the 20% Long Fibre/80% Short Fibre and 30% Long Fibre/70% Short Fibre.....	208
Figure 5.23: Pie Charts Showing the Proportion of Long and Short Fibres Counted within each Batch.....	210
Figure 5.24: Recommended Processing Set up for an Industrial Application... ..	212
Figure 6.1: Position of Constituent Rollers on a Roller Clearer Card.....	216
Figure 6.2: Carding and Stripping Actions (Dahiya et al., 2004).....	217
Figure 6.3: The Friction Spinning Process (Ishtiaque et al., 2003).....	218
Figure 6.4: DREF-2 Spinning System (Ishtiaque et al., 2003).....	219
Figure 6.5: The Effect of Fibre Length on Yarn Tenacity.....	223
Figure 6.6: The Effect of Fibre Percentage on Yarn Tenacity in a 30mm/10mm Blended Yarn.....	224
Figure 6.7: The Effect of Fibre Percentage on Yarn Tenacity in a 25mm/10mm Blended Yarn.....	225
Figure 6.8: The Effect of Fibre Percentage on Yarn Tenacity in a 30mm/15mm and 25mm/15mm Blended Yarn.....	226
Figure 6.9: The Effect of Short Fibre Percentage on Yarn Tenacity in a 30mm/4mm Blended Yarn.....	227
Figure 6.10: Photograph of RFL Fibre Web.....	228
Figure 7.1: Injection Moulding (Crowther et al., 1982).....	233
Figure 7.2: The Injection Moulding Cycle (Brydson, 1990).	233
Figure 7.3: Compression Moulding (Rosato, 1997).....	234
Figure 7.4: The Compression Moulding Cycle (Brydson, 1990).....	235
Figure 7.5: Open Flash Mould.....	236
Figure 7.6: Positive Mould.....	236
Figure 7.7: Picture Frame Mould.....	239
Figure 7.8: Compression Moulding Construction.....	239
Figure 7.9: Fabric Layers Prior to Moulding.....	240
Figure 7.10: Example of a Moulded Piece Produced from Uncoated and RFL Coated Fabric using an Open Flash Mould.....	243
Figure 7.11: Example of a Moulded Piece Produced from Uncoated and RFL Coated Fabric using a Positive Mould.....	245

Figure 7.12: Light Micrograph Cross-section of Moulded Piece Produced from RFL Coated Fabric using an Open Flash Mould, with a Magnification of 5x. .. 246

Figure 8.1: Polyisoprene Structure	249
Figure 8.2: Styrene Butadiene Rubber (SBR) Polymer Structure	250
Figure 8.3: Sulphur Bonding Structures in a Vulcanisate Network.....	251
Figure 8.4: Molecular Structures in Plasticisers (Brydson, 1988)	259
Figure 8.5: Uncoated (left) and Coated (right) Beaten Waste Fabric used in Rubber Processing.....	269
Figure 8.6: The Monsanto Rheometer 100 (Monsanto).....	273
Figure 8.7: Rubber Behaviour During Milling.....	276
Figure 8.8: Rubber Mixes Incorporating the Uncoated Waste Reduced using the Hollander Beater.	277
Figure 8.9: Rubber Mixes Incorporating the RFL Coated Waste Reduced using the Hollander Beater.	277
Figure 8.10: Typical Cure Trace (Monsanto)	279
Figure 8.11: The Effect of Filler Percentage and RFL Content on Rubber Cure Time	280
Figure 8.12: The Effect of Filler on Minimum (M_L) and Maximum (M_{HF}) Torque	281
Figure 8.13: The Effect of Filler on Scorch Time ($t_s(5)$) and Cure Time ($t_c(90)$)	282
Figure 8.14: The Effect of Filler on Cure Rate Index.....	282
Figure 8.15: The Effect of RFL on Filler on Reinforcing Factor (α_F)	283
Figure 8.16: Vulcanised Moulded Rubber Sheets.	285
Figure 8.17: Defects in 25% Non-Coated Rubber Sheet.	285
Figure 8.18: The Effect of Recycled Filler Content on Tensile Strength of Rubber Compounds.	288
Figure 8.19: The Effect of Recycled Filler Content on the Tensile Extension of rubber compounds.....	290
Figure 8.20: The Effect of Recycled Filler on Tear Strength of Rubber Compounds.	293
 Figure 9.1: Recommended recycling processing route for RFL coated nylon 66 fibres.....	 300

Abstract

The University of Manchester

Sarah Eirene Wroe

Doctor of Philosophy

The Recycling of Resorcinol Formaldehyde Latex Coated Nylon 66.

September 2012

The Waste (England and Wales) Regulations encourage business to recycle their waste, as an alternative to landfill. This study has evaluated a number of processing techniques with respect to a difficult to recycle, technical textile, in order to develop recycling opportunities. Resorcinol formaldehyde latex (RFL) coated nylon 66 is a high performance fabric used as an interface to reinforce rubber products such as timing belts.

The characteristics of the RFL coated woven fabric, assessed in comparison to equivalent uncoated fabrics, showed increased stiffness and decreased tear resistance. This was followed by the evaluation of three reduction processes:

- 1) The Laroche Cadette shredder;
- 2) The Hollander beater;
- 3) The Intimus disintegrator.

The fibre length, coating integrity and degradation properties were assessed for each of the reduction techniques. The longest fibres were produced by the Laroche Cadette shredder, this method proved most suitable for textile processing. The coating was unaffected and little degradation occurred. The Hollander beater produced mid-length fibres; however, fibres as short as 2mm could also be achieved. The material did not degrade, as water used within the process reduced heat build up, the coating remained adhered to the fibre. The Intimus Disintegrator produced the smallest fibre length and produced the greatest processing problem due to heat build up and degradation. Particles in addition to fibres were formed but were not crystalline in nature, and were difficult to process further.

Processing using paper, textile, plastic and rubber technology were trialled with varying success. The recommended recycling route was found to be through reduction using the Hollander beater followed by incorporation of the waste as filler in rubber composites. RFL coated fibres gave additional strength to the rubber at high filler contents of 37.5% in comparison to uncoated waste filler also trialled. This was due to the surface chemistry of the RFL coated nylon fibre. The RFL coated nylon 66 filler also enabled the composites to exceed tear specifications required for hardwearing footwear. Fibres were effectively separated by length using forward flow and reverse flow hydrocyclones, separating 10mm and 3mm length fibres, which would prove useful for obtaining optimum particle size for reinforcement during the reduction process.

Alternate processed trialled enabled the RFL fibres to be formed into a paper sheet using 50% cellulose pulp but textile processes proved unsuccessful. Moulded pieces formed though compression moulding were able to be produced from coated and uncoated fabric pieces, however many voids were present, limiting the usability.

Declaration

No portion of the work referred to in this thesis has been submitted in support of any of an application for another degree of qualification of this or any other university or institute of learning.

Copyright Statement

- i.** The author of this thesis (including any appendices and/or schedules to this thesis) owns certain copyright or related rights in it (the “Copyright”) and she has given The University of Manchester certain rights to use such Copyright, including for administrative purposes.
- ii.** Copies of this thesis, either in full or in extracts and whether in hard or electronic copy, may be made **only** in accordance with the Copyright, Designs and Patents Act 1988 (as amended) and regulations issued under it or, where appropriate, in accordance with licensing agreements which the University has from time to time. This page must form part of any such copies made.
- iii.** The ownership of certain Copyright, patents, designs, trade marks and other intellectual property (the “Intellectual Property”) and any reproductions of copyright works in the thesis, for example graphs and tables (“Reproductions”), which may be described in this thesis, may not be owned by the author and may be owned by third parties. Such Intellectual Property and Reproductions cannot and must not be made available for use without the prior written permission of the owner(s) of the relevant Intellectual Property and/or Reproductions.
- iv.** Further information on the conditions under which disclosure, publication and commercialisation of this thesis, the Copyright and any Intellectual Property and/or Reproductions described in it may take place is available in the University IP Policy (see <http://www.campus.manchester.ac.uk/medialibrary/policies/intellectual-property.pdf>), in any relevant Thesis restriction declarations deposited in the University Library, The University Library’s regulations (see <http://www.manchester.ac.uk/library/aboutus/regulations>) and in The University’s policy on presentation of Theses

Acknowledgements

The author would like to thank all people who have made this project possible, and for all the advice, help and encouragement that has been received.

Particularly to Cameron Harvie and Brian Roocroft at Heathcoat Fabrics and academic and technical staff at the University of Manchester, Prof Chris Carr, Dr Arthur Wilkinson, Polly Crook, Alison Harvey, Robert Wilde, Philip Tougher, Adrian Handley, Peter Moroz and Andy Zadoroshnyj.

To all who have aided in reviewing this thesis, particularly Richard Seacome and Philippa Duffus, many thanks

Thanks also to the EPSRC for funding this project.

Finally, the author would like to thank all family and friends that have supported and encouraged her in the completing of this work.

1.0 Introduction

1.1 Heathcoat Textiles

1.1.1 Background

Heathcoat Textiles is a global market leader in timing belt applications, manufacturing high performance fabrics for rubber interfaces using unique adhesion and priming systems (Heathcoat Fabrics, 2011). 2.5 million metres of fabric for timing belts is sold each year by the company. The solid waste produced from this process equates to 2 tonnes per week, inclusive of all texturising weaving and inspection processes where the waste occurs. The waste produced is nylon based, 70% of which is untreated, 30% is treated with a resorcinol formaldehyde latex (RFL) coating (Harvie, 2008).

With increased pressure on the environmental impact of waste products, it is important to reduce waste as much as possible. Due to manufacturing requirements, the company feels it cannot further decrease the waste in the production process without increased labour cost or decreased production. It is therefore necessary to reuse or recycle the waste products in order to cut down on waste sent to landfill. An alternative use of this waste (both uncoated nylon 6.6 and RFL coated nylon 6.6) is required.

1.1.2 Areas of Waste Production

Nylon waste is produced throughout the manufacturing process of fabrics at Heathcoat fabrics. The main areas of waste production have been identified and are outlined in the following sections.

1.1.2.1 Texturising

Texturising is a process used to impart bulk and elasticity to filament yarns (Hatch, 1993). Heathcoat Fabrics use the False Twist method of texturising yarn where the

tensioned, moving, filament yarn is twisted using a spindle or belt and heat set. The direction of twist above and below the spindle is imparted in opposite directions, as the twist occurs at a central point on the yarn length. For each 'Z' twist an 'S' twist has also been inserted, so there is no overall twist and the term false twist is applied. The terms 'S' and 'Z' are used in textiles to describe the direction of twist in a yarn, 'S' twist having twist occurring in the same direction as the letter 'S' shape when observed along the length of the yarn and 'Z' twist occurring in the opposite direction causing twist to be in the direction of the letter 'Z'. In false twist texturing, illustrated in Figure 1.1, as the yarn approaches the spindle it becomes twisted due to the false twist spindle, in Figure 1.1 an 'S' twist is imparted below the spindle. The twisted part of the yarn, below the spindle, passes over a heater which sets the yarn in its twisted shape. The yarn passes through the spindle, where twist is inserted in the opposite direction to which it was set as it is now above the spindle. It is untwisted from its set shape, producing the textured yarn (Hatch, 1993). This process is illustrated below (Figure 1.1). Heathcoat Fabrics produce six-fold yarns in this way that are then subsequently spun for further uniformity and strength (Harvie, 2008). The final yarn has increased elasticity and bulk due to the texturing process (Hatch, 1993).

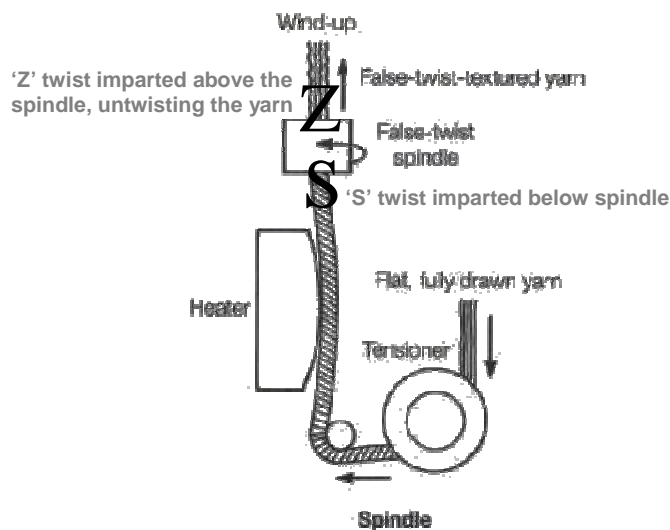


Figure 1.1: Spindle Texturing Process (Hatch, 1993).

The two areas of waste production in this process are due to feedstock waste and yarn faults. Feedstock waste relates to yarn that is unsuitable to be twisted due to faults within the fibre. This can be sent back to the yarn manufacturing mill at its full price,

therefore it can be excluded from this study. Waste from faults occurs where the yarn breaks during processing or contamination occurs within the yarn. The yarn is then unsuitable for further processing and is stripped off the packages and bagged for storage. This accounts for a large proportion of the entire waste produced by the factory (Harvie, 2008).

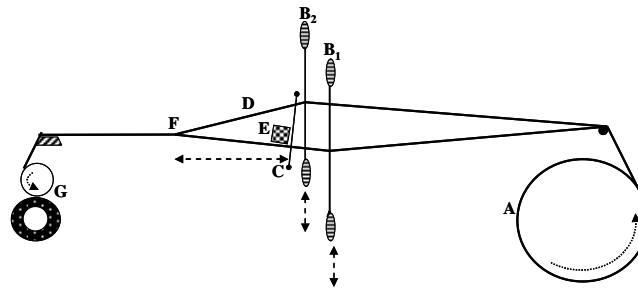
The production rate of the textured yarn is approximately 10 tonnes per week, and the waste percentage is approximately 3% of production. This gives a waste production of 300 kg per week of from the texturing process alone, 15% of the entire waste production, which then requires disposal or reprocessing. This waste is entirely uncoated nylon material, however may include contaminants introduced during processing (Harvie, 2008).

1.1.2.2 Weaving

Heathcoat Fabric's have approximately 110 looms which are run 24 hour a day, 7 days a week, to produce 15,000 metres of fabric per week. The main waste that is produced within the weaving process is warp ends and selvedge waste (Harvie, 2008).

Warp yarn waste is produced at roll ends, due to the working length of the weaving process. Figure 1.2 illustrates the passage of warp yarns through a loom, leading to this waste production. Warp yarns are prepared on a warp beam prior to weaving and this is mounted on the loom. The warp yarns are threaded through healds (B) which separate the warp yarns, producing a shed (D) allowing a woven pattern to be created. This occurs in the picking stage, where the weft yarns are inserted through the shed of the warp yarns (E). The warp yarns are also threaded through dents within a reed (C) which beats the weft yarn into the fell of the fabric (F). Warp yarns are let off from the warp beam (A) and the fabric is taken up by use of the take up roller onto the cloth beam (G) in order for the weaving process to continue and a length of fabric to be produced (Marks *et al.*, 1976). Warp yarns are held in tension during weaving due to the intricate system of letting off and taking up. The distance between the warp beam and cloth beam is known as the working length of the loom. Since the warp yarns on the beam are a finite length, there comes a point where no more letting off can occur. There is a length of warp yarns at the end of the weaving process, from the warp beam

to the fell, that do not become part of the finished fabric. It is these warp ends that form the wastage that occurs during the weaving process.



A. Warp beam

B. Healds

C. Reed

D. Shed

E. Weft Insertion

F. Fell

G. Take up roller and Cloth beam

Figure 1.2: *Cross-section of Passage of Warp Yarn Through a Loom (Modified-redrawn (Marks et al., 1976)).*

The second type of waste produced within the weaving process is from selvedge waste. Due to the nature of shuttleless looms, a false selvedge is often created in order to temporarily control each pick extending from the true selvedge and momentarily hold it in place. False selvedges are created where leno or helical selvedges are utilised as the true selvedge. False selvedges are particularly necessary at the non-supply side, but can occur at both sides. The false selvedge contains approximately 6 warp yarns which are placed a few centimetres away from the true selvedge. It is woven in a plain or sometimes leno pattern to ensure that inserted picks are held in place rather than slipping back through to the shed during the beat up process. The false selvedge is removed near to the fell of the fabric by cutting through the weft yarns at a point just outside the true selvedge. The false selvedge is then wound onto a reel separate to the cloth beam. Alternatively it can be twisted together at the fell and drawn forward at the same rate as the fabric, producing a string-like structure which is dropped into a waste bin at the front of the loom. The second method allows the weft yarns to be trapped more effectively within the selvedge due to the twisting action (Vincent, 1980). 3-4% of weft yarn and 1-2% of warp yarn used goes into the creation of the false selvedge and the resultant waste produced (Seyam, 2000).

Waste produced by Heathcoat Fabrics during the weaving processes is bagged up for storage. The majority of fabric waste produced in the weaving process is 100% nylon. Some fabrics have aramid yarns blended with nylon, for example, when using an aramid for weft yarns (Harvie, 2008).

1.1.2.3 Inspection

At the inspection stage the fabric is checked for any faults. Simultaneously, the fabric is slit using an ultrasonic beam to create a straight and neat edged roll. The ultrasonic beam seals the edge of the fabric to prevent any fraying. This occurs so that the fabric has a continuous width. The waste produced from this slitting process is known as tape waste. In addition to this waste there is waste produced from faulty areas of fabric that are cut from the roll.

Waste produced during inspection can be 100% nylon, blended fabric, for example with aramid yarns, or coated fabric having a resorcinol formaldehyde latex (RFL) coating. The RFL coating consists of a range of compounds which can vary, depending on the type of rubber that the fabric is to be bonded to. Waste from the inspection stage is the main focus of this study, as the RFL coating stage occurs after weaving, making all coated waste from the inspection stage. Coated tape waste makes up the majority of waste that is currently not recycled by the company (Harvie, 2008).

1.1.3 Waste Management Systems

Heathcoat fabrics separate waste produced into treated and untreated material. It is then packed into bales of 300kg – 400kg. Fabric waste and fibre waste are not separated and therefore bales are produced with these types of waste mixed within a single bale (Harvie, 2008).

1.2 Raw Materials

The waste from Heathcoat Fabrics that is within the remit of this study is either 100% uncoated nylon or resorcinol formaldehyde latex (RFL) coated nylon. It is therefore necessary to understand the background production processes and chemistry involved in manufacturing this material and the properties that it possesses, prior to assessing how it can be processed further.

1.2.1 Nylon

1.2.1.1 Nylon Production

Nylon fibre is made of linear macromolecules, which are linked by the chemical amide group -NH-CO- . The two main types of nylon used within industrial textiles are nylon 6 and nylon 6.6. Nylon 6 is formed from the ring opening polymerisation of the monomer caprolactam (Durairaj, 2005), as shown in the reaction scheme in Figure 1.3. The number of carbon atoms within the monomer is conveyed within the polyamide name, for example nylon 6 is composed of 6 carbon atoms. The polymerisation of caprolactam is carried out by the addition of water which opens up the lactam ring via hydrolysis. The water is then removed at an elevated temperature to form the linear polymer. This can be carried out in an autoclave or continuous reactor. Caprolactam and monomers that do not react to form the polymer are subsequently removed by washing with water in order for good yarn properties to be achieved (Billmeyer, 1971).

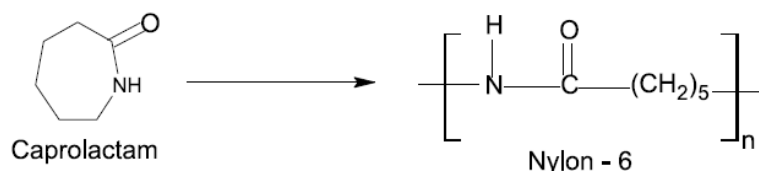


Figure 1.3: Synthesis of Nylon 6 (Durairaj, 2005).

Nylon 6.6 is made from a condensation reaction of a diamine with an activated diacid. The numbers within the polyamide name express the number of carbon atoms in the diamine and diacid, respectively (Richards, 2005). The reaction scheme is shown in

Figure 1.4. Hexamethylene diamine and adipic acid can form a salt which can be isolated due to its low solubility in methanol. The salt is then dissolved in water and added to an autoclave. At raised temperature (270-280 °C) and pressure (250 psi), the reaction takes place to form the polymer over 3 to 4 hours. Nitrogen pressure is then used to extrude the nylon as a ribbon through a valve in the autoclave from which the polymer chips are made (Billmeyer, 1971). Products produced by Heathcoat Fabrics are composed of nylon 6.6, the waste used within this study being composed only of this type of polyamide.

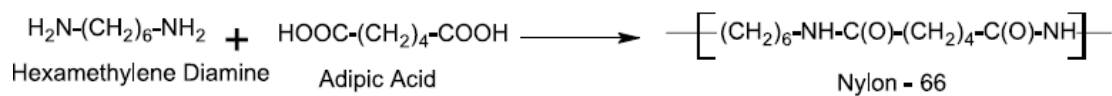


Figure 1.4: Reaction Synthesis for Nylon 66 (Durairaj, 2005).

1.2.1.2 Fibre Production

Nylon filaments are produced through the process of melt spinning. Molten polymer is pumped under a constant rate and high temperature through a spinneret. The spinneret contains many holes producing jets of polymer which are then cooled in the air and solidified. The filaments are brought together to form a yarn and wound onto a bobbin. This process is illustrated in Figure 1.5. At this point, the polymer chains are almost completely unorientated as the molecular orientation is able to relax before the fibre cools and crystallises (Billmeyer, 1971). Drawing is required to align the polymer chains thereby increasing the crystallinity of the polymer to approximately 50% (Richards, 2005).

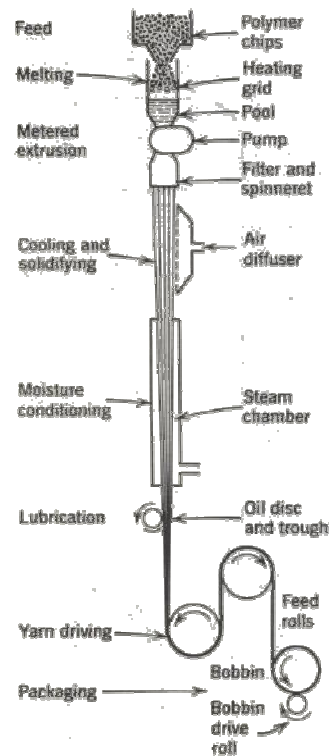


Figure 1.5: Melt Spinning (Billmeyer, 1971).

The drawing process traditionally occurred as a separate process to the melt spinning process as much slower speeds were utilised, however this can now usually be achieved in one process. The drawing process utilises two sets of rollers, the second of which rotate at 4 times the speed of the first. This process is illustrated in Figure 1.6. When the unorientated fibre is stretched at this speed it becomes thinner at one point, known as “necking down”. As drawing continues, the thin section increases in length, however, the diameters of the drawn and undrawn portions remain constant. This process does not drastically change the degree of crystallinity, although this can be increased if the undrawn polymer is amorphous or partially crystalline. Instead the crystalline regions are deformed with tilting and slipping of chains. Once these defects have been formed, blocks of folded chains break off and are incorporated into the new fibre structure alongside unfolded chains. This causes the number of chain folds to be decreased and orientated fibrils to be formed linking crystalline regions to amorphous regions, known as tie molecules. The increase of tie molecules, in addition to the entwined nature of the crystal lamellae formed, causes fibre properties, such as tensile strength mechanical stability and stiffness, to increase (Billmeyer, 1971).

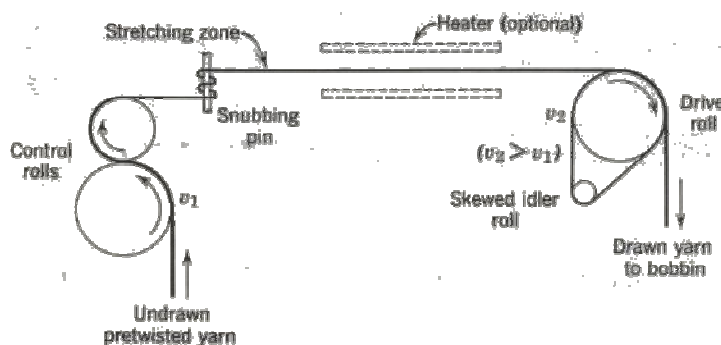


Figure 1.6: Drawing Process (Billmeyer, 1971)

1.2.1.3 Properties of Nylon 66

The density of nylon is 1.14 g/cm^2 , which is lower than most fibres. This property makes it a good fibre for producing lightweight fabrics with high cover factors often used in sporting applications (Moncrieff, 1975).

Nylon 6,6 has a similar tenacity to that of polyester of $0.4\text{-}0.6 \text{ N tex}^{-1}$, however, its breaking extension is slightly higher, between 20-30%, rather than the 10-20% in polyester (Richards, 2005). The high tenacity of nylon is due to the crystalline polymeric structure, strengthened by the presence of numerous hydrogen bonds. Nylon fibres can be produced with different tenacities depending on the intended application. Nylon made for industrial applications have higher tenacities than nylon for apparel applications. High tenacity nylon has lower extensibility than standard nylon. Nylon also retains its strength when wet, with a wet strength of 80-90% of the dry strength. The high extension at break is also accompanied with good elasticity properties. Nylon can stretch up to 8% (regular) or 4% (high tenacity) while maintaining 100% recovery (Hatch, 1993). The initial modulus of a fibre indicates its behaviour at small strains and stresses. Nylon 66 has a lower initial modulus than polyester at $2.0\text{-}3.5 \text{ N tex}^{-1}$ and $8\text{-}10 \text{ N tex}^{-1}$, respectively (Hatch, 1993). The initial modulus affects the fabric handle where the nylon will bend more easily than polyester, be softer and have increased drape. Due to its high elongation, the work of rupture for nylon 6,6 is higher than polyester, the former having a work of rupture of $60\text{-}70 \text{ mN tex}^{-1}$, compared to the latter's work of rupture at $50\text{-}60 \text{ mN tex}^{-1}$ (Hatch, 1993). The high work of rupture of nylon makes it suitable to be used in applications

such as climbing ropes. These tensile properties are summarised in the stress-strain curve of nylon shown in Figure 1.7 compared to other popular fibres.

Nylon also has very high abrasion resistance allowing it to withstand rubbing, flexing and scraping forces with little damage. This is due to the zigzag configuration of the polymers; polymers on the outside of a bend are able to lengthen while contraction of the polymers occurs on the inside (Hatch, 1993).

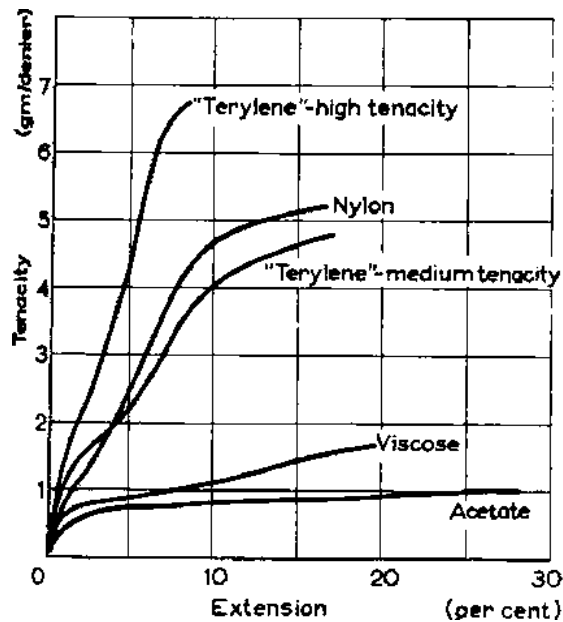


Figure 1.7: Stress-strain Curves of Nylon Compared to other Popular Fibres (Moncrieff, 1975).

The melting point of nylon, and other thermal properties, depends on the number of amide linkages and the extent of hydrogen bonding present in the molecule. Nylon 66 has a melting point of 264°C compared to nylon 6 which melts at 215°C (Brydson, 1999). Nylons have sharp melting points due to their high crystallinity, and unlike other thermoplastics, do not have any appreciable flow below their melting point (Imperial Chemical Industries). The glass transition point of nylon occurs at 40-50°C. At this point there is mobility within the chain segments of the amorphous regions of the fibre. A fibre needs to be above its glass transition point for processes such as dyeing, drawing and texturing to occur. The optimum steam setting temperature of nylon 6.6 is 130°C, and its maximum setting temperature is 225°C (Brydson, 1999). Between these temperatures the polymer starts to become plastic at 210 °C. If it is

heated further it will reach its softening point at 235°C, until it has no strength at 240°C (Brydson, 1999).

At increased temperature the tensile properties of the fibre will be affected. As the temperature increases the tenacity and initial modulus will reduce and the extension at break will increase. This change in tensile behaviour occurs due to the increasing mobility of the polymer chains, in both the crystalline and amorphous areas of the fibre. Nylon also shrinks approximately 5% when heated in a dry state from room temperature to 100°C (Richards, 2005). This shrinkage is greater in wet yarns due to water penetrating the structure and increasing the chain mobility (up to 10 %). Shrinkage occurs due to orientated amorphous polymer regions reverting to their pre-drawn less orientated state. Stresses are removed from the crystalline areas and these areas also become shorter. Additionally, shrinkage can occur with polymer chains forming crystalline areas by folding or moving relative to each other, or by crystallites melting, allowing the molecules to shrink into a random coil. If the fibre has previously undergone thermal treatments this will affect how the fibre will behave when heated again. When previously heated under no tension, the fibre does not shrink further when heated again. However, if the tension is present during the initial heating, shrinkage will occur in subsequent heating (Richards, 2005).

Chemically, nylon is very stable, having good resistance to organic solvents, being unaffected by the majority. However, it is attacked by phenol, formaldehyde, benzyl alcohol and nitrobenzene. Resistance of nylon to alkaline solutions and dilute caustic alkalis is good and they also have moderate resistance to acids. Other than hydrogen peroxide and chlorine bleaching, nylon is generally inert to inorganic reagents.

Nylon is degraded by light due to free radical mechanisms, but this is minimised by use of stabilisers within the fibre. No discolouration takes place from photochemical degradation (Cockett, 1966). However, exposure to strong sunlight will adversely affect the mechanical properties (Imperial Chemical Industries).

Moisture absorption of nylon is low at about 4.2% at equilibrium when the fibre is at standard conditions of 65% RH and 20°C (Moncrieff, 1975). The mechanical properties will be affected by the degree of moisture absorption, as the moisture

absorbed is increased the mechanical properties will be reduced (Imperial Chemical Industries).

This information on nylon 66 and additional information on the properties of nylon 6 is summarised in the Table 1.1.

1.2.2 Fabric Construction

Nylon 66 yarn is processed at Heathcoat Fabrics by means of texturising, weaving and coating as described in section 1.1.2. A number of fabric qualities are manufactured using a range of weave patterns, including plain weave, basket weave and twill weaves.

Plain weave is the simplest type of construction interlacing two sets of yarns in a one up, one down fashion. This gives the maximum possible number of warp and weft intersections, making plain weave the strongest and stiffest type of woven structure (Sen and Damewood, 2001).

Basket weave is a derivative of plain weave, having 2 or more yarns warp and weft yarns simultaneously interlaced with each other. This gives a 2x2, 3x3 or 4x4 pattern, resembling that of a basket. Basket weaves have fewer intersections than plain weave allowing more threads to be inserted per cm. This gives a higher cover factor, but also allows the fabric to have good drape. Basket weaves are often preferred to plain weave in applications where tear strength is important (Sen and Damewood, 2001).

Twill weaves are distinctive by their diagonal twill lines occurring at a 45° angle to the direction of the threads. The yarns are woven so that the first weft yarn interlaces with the first warp yarn, the second weft with the second warp, and the third weft with the third warp, continuing in this way with as many warps and wefts as are in the repeat. Twill weaves enable heavier cloth to be created, having better draping qualities than if a plain weave were used (Sen and Damewood, 2001).

Table 1.1: Properties of Nylon

Property	Nylon 66	Nylon 6
<i>Molecular</i> (Durairaj, 2005)		
Molecular diagram	$\left[\text{-(CH}_2\text{)}_6\text{-NH-C(O)-(CH}_2\text{)}_4\text{-C(O)-NH-} \right]$	$\left[\begin{array}{c} \text{H} \\ \\ \text{N} \\ \\ \text{C=O} \\ \\ \text{(CH}_2\text{)}_5 \end{array} \right]_n$
<i>Density</i> (Moncrieff, 1975)		
Density (gcm ⁻³)	1.14	1.13
<i>Tensile Properties</i> (Hatch,1993)		
Tenacity (N tex ⁻¹)	0.4-0.6	0.4-0.6
Breaking Extension (%)	20-30	20-40
Initial Modulus (N tex ⁻¹)	2.0-3.5	1.5-3.5
Work of Rupture (mN tex ⁻¹)	60-70	70-80
<i>Thermal Properties</i> (Hatch,1993)		
Melting Point (°C)	255-260	215-220
Zero Strength (°C)	240	220
Maximum setting temperature (°C)	225	190
Softening Point (°C)	235	170
Starts to become Plastic (°C)	210	160
Maximum ironing temperature (°C)	180	150
Optimum setting temperature with steam (°C)	130	128
Glass transition temperature (°C)	40-50	40-50
<i>Moisture</i> (Moncrieff, 1975)		
Moisture Regain 20°C, 65% R.H. (%)	4	4

1.2.3 Resorcinol Formaldehyde Latex Coatings

1.2.3.1 Purpose of RFL coatings

Products such as tyres, hoses and belts are composite materials made up of natural or synthetic rubbers that are reinforced with fibres, carbon black and other reinforcing fillers. In order to enhance these types of product there is a constant effort to improve both the reinforcing element and the elastomeric material used in the rubber composite. More effective reinforcement leads to lower volumes of rubber needed in many applications, and therefore, reduced heat build up and enhanced the fatigue resistance in applications where friction occurs, such as tyres and transmission belts.

High tenacity fibres, such as nylon, polyester and aramid have been developed for use in reinforcing rubbers. Although these synthetic fibres have good tensile properties, their smooth polymer surface and low reactivity makes it difficult for them to adhere directly to the rubber. It is therefore necessary to use an adhesive to bond the two together effectively (Durairaj, 2005).

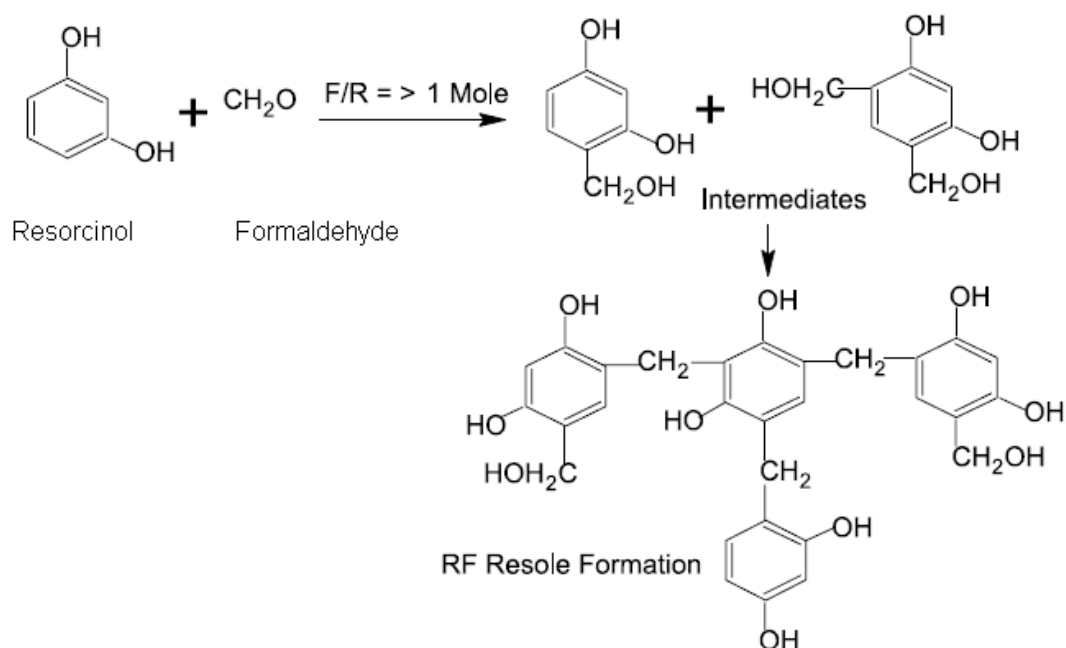
The first adhesive system was developed for rayon and consisted of a blend of casein and natural rubber latex. This gave acceptable results where rayon was used but was less successful when synthetic fibres were introduced as reinforcements. The need to develop improved adhesives and adhesion promoters, for enhanced strength in rubber composite products, was recognised (Durairaj, 2005). This led to the development of resorcinol formaldehyde latex adhesives.

The high tenacity fibres used within rubber composites have high strength but low elongation in comparison to the rubber matrix which has low strength but high elongation. The role of the adhesive is to combine these two material properties to give the best composite product characteristics. The adhesive is required to transfer the load stress from the rubber matrix to the reinforcing fibres. In order to achieve this, the adhesive is required to have a high degree of bonding strength with both the fibres and the rubber, with intermediate tensile properties to the two materials. Within the RFL adhesive, the resorcinol formaldehyde resin component preferably bonds to the fibre and the latex component bonds to the rubber through co-vulcanisation giving high bonding strength to both components (Durairaj, 2005).

1.2.3.2 Chemical Formulation of RFL

The RFL coating can be formed using either an *in-situ* RF (resole) resin or a pre-condensed RF (novolak) resin. Novolaks describe a phenol-formaldehyde resin with formaldehyde to phenol ratio of less than one, where the reaction is catalysed in acidic conditions, whereas, resoles are resins with formaldehyde to phenol ratio of more than one where the reaction is catalysed in basic conditions. In order to produce an RF resole resin rather than novolac resin, an increased formaldehyde concentration under alkaline conditions are required in addition to a lower temperature (25°C or less), this enables the methylol groups to form, this reaction is shown in Figure 1.8a. Sodium hydroxide is generally used as the base catalyst. Alternatively, the RF resin can be formed using a pre-condensed RF novolac resin (Figure 1.8b) then reacting this with formaldehyde. As the pre-condensed RF resin is normally prepared under acidic conditions, the resin must first be neutralised, using sodium hydroxide and ammonia, before adding the latex to avoid coagulation (Durairaj, 2005).

(a) RF resole formation



(b) RF novolak formation

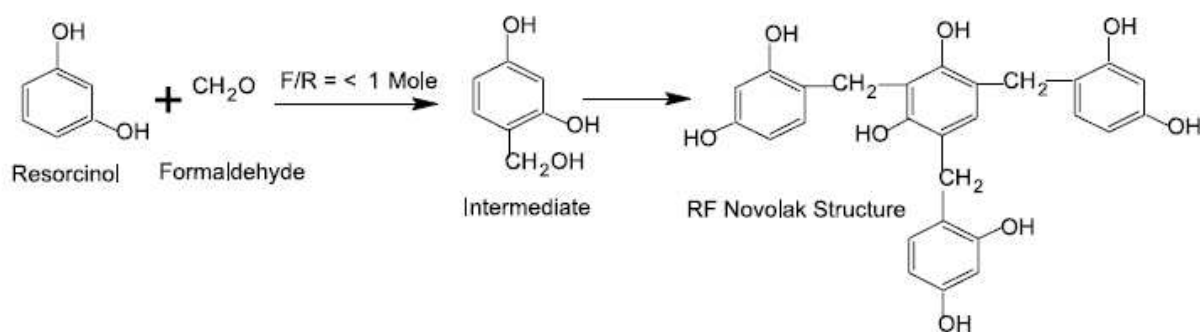


Figure 1.8: Reaction Schemes to Produce (a) RF Resole and (b) RF Novolak
(Durairaj, 2005)

Once the RF resin has been formulated, either using the resole system or novolak system, it is then dispersed within latex to form the final RFL dip solution. The latex component is generally natural rubber, styrene butadiene rubber (SBR) or vinyl pyridine terpolymer (VP) (Sen and Damewood, 2001). For nylon an SBR-VP latex mixture is often used at a ratio of 80:20, for higher tenacity yarns, higher proportions of VP, up to 80% can be used. SBR and VP polymers are shown in Figure 1.9 and 1.10. The bonding between the RF resole and latex occurs in the curing stage after application to the fabric (Sen and Damewood, 2001).

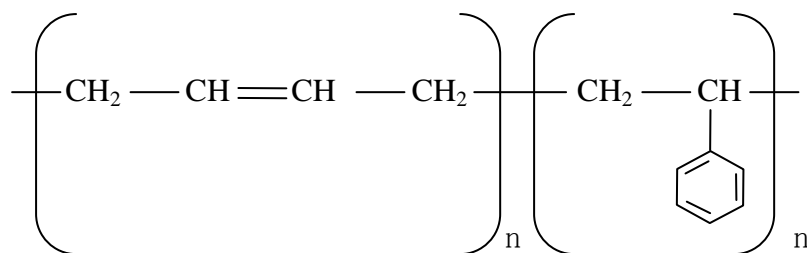


Figure 1.9: Styrene-Butadiene Copolymer

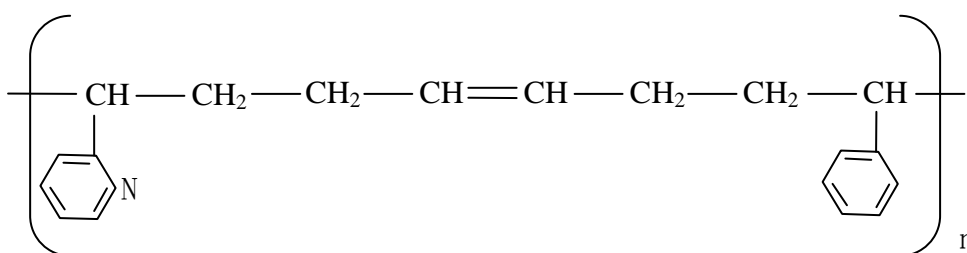


Figure 1.10: Vinyl Pyridine Terpolymer

1.2.3.3 Application of RFL coating to Fabric.

The aqueous RFL solution is applied to the nylon 66 fabric by means of submersion of the fabric into the aqueous RFL solution in a process known a dip coating. Excess solution is then squeezed out by passing the fabric through nip rollers (Sen and Damewood, 2001). This process is illustrated in Figure 1.11.

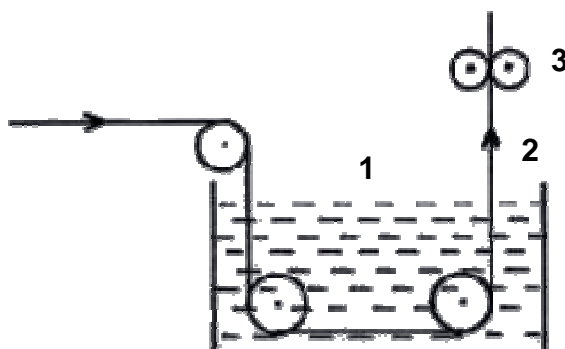


Figure 1.11: Dip Coating (Sen and Damewood, 2001)

The aqueous RFL solution has a low viscosity resulting in good wetting of the fabric and increasing the interaction between fibre and adhesive. The amount of adhesive that is picked up by the fabric will depend upon the fibre surface characteristics and the concentration of the RFL dip solution. The dip pick up relates to the amount of

adhesive that is deposited on the fibre surface. This, in addition to the ability of the adhesive to penetrate the fibre surface will determine the adhesion performance. Adhesion increases linearly with pick up, but reaches a maximum at about 6-8% of fibre weight. At this point, the effect of increased stiffness of the fabric caused by excessive dip pick up will reduce the adhesive strength to the rubber due to a reduction contact points between the fabric and the rubber as the two flex differently during the curing process (Durairaj, 2005).

The fabric is passed through ovens in order for drying and curing to take place. Drying ovens allow the solvent to be evaporated leaving only the RFL formulation. The curing process allows strong interaction between the fibre's amide group and adhesive's methylol group to take place. Optimal temperature, time and tension are used to balance the fabric strength against adhesion properties to give the best characteristics for the product application. Drying temperatures of 130°C-170°C and curing temperatures of 190°C-240°C are normally used. Both over-curing and under-curing will affect the final adhesion properties (Durairaj, 2005).

1.2.3.4 RFL Bonding Systems in Nylon and Rubber.

The RFL adhesive utilises the amide (-CO-NH-) groups within the nylon polymer chain in order to create strong bonds with methylol (-CH₂-OH-) groups formed in the creation of the RF resin. A primary covalent bond is formed between the nylon polymer and RFL adhesive as shown in the reaction sequence in Figure 1.12.

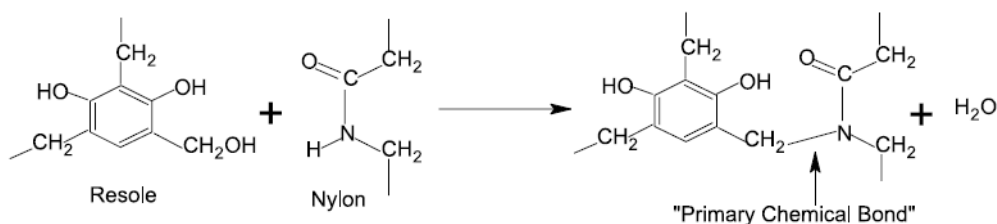


Figure 1.12: Reaction Scheme to Form Chemical Bond between RFL and Nylon (Durairaj, 2005).

For this reaction to occur, the resorcinol methylol has to have penetrated the nylon surface. The Hildebrand solubility parameter is the square root of cohesive energy density and provides a numerical estimate of the degree of interaction between two materials. Solubility parameters of nylon, 16.0, and resorcinol, 15.9, closely match

making the nylon and RFL compatible for both penetration and chemical interaction. The resorcinol is also able to swell the polyamide fibres, increasing the likelihood of penetration. Curing conditions are carried out above the glass transition temperature of the polyamide, increasing the molecular chain mobility and interaction between RF resins within the RFL and the amide groups in the nylon. This chemical bonding between methylol and amide groups is the primary method of adhesion between the RFL and the nylon.

Hydrogen bond formation also occurs between the resorcinol hydroxyl and nylon amide groups. This can occur in two different ways as shown in Figure 1.13. This strengthens the adhesion between the RFL and nylon further (Durairaj, 2005).

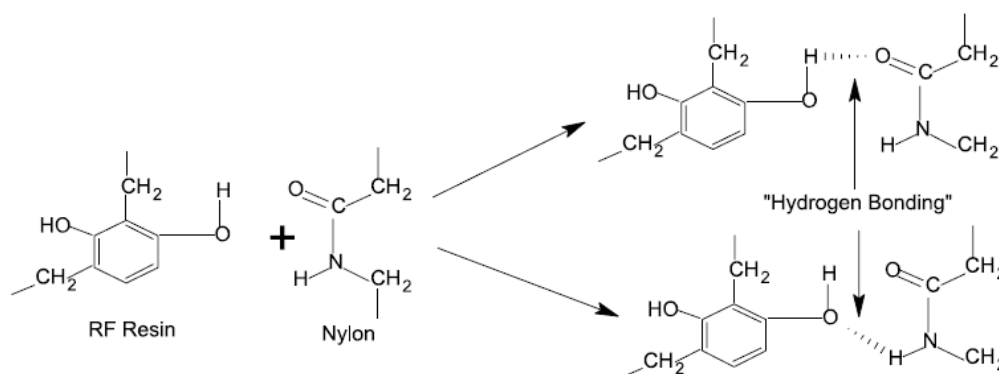


Figure 1.13: Reaction Scheme to Form Hydrogen Bonds between Resorcinol and Nylon

The RF can be bonded to the SB-VP latex mixture in two ways. Chemical bonds are formed through reaction of the methylol resorcinol with the carbon-carbon bond of the SB or VP latex, resulting in a chroman-type structure. The second bonding mechanism is through hydrogen bonding between resorcinolic hydroxyl groups and the nitrogen of the pyridine nucleus of the VP latex. Both bonding structures are illustrated in Figure 1.14.

The RFL adhesive, bonds to any olefin rubbers due to the latex composition and structure, which contains high numbers of unsaturated carbon-carbon bonds within the mixture. Even after reaction with the RF component (described above), high numbers of unsaturated bonds are still present. The remaining unsaturated compounds, are therefore, used in the bonding to the rubber compound. A chemical bond associated with sulphur cross-linking is formed between the latex and rubber

compounds, this occurs during the vulcanisation process (Durairaj, 2005). These bonding mechanisms between the nylon, RFL, and rubber are summarised in Figure 1.14.

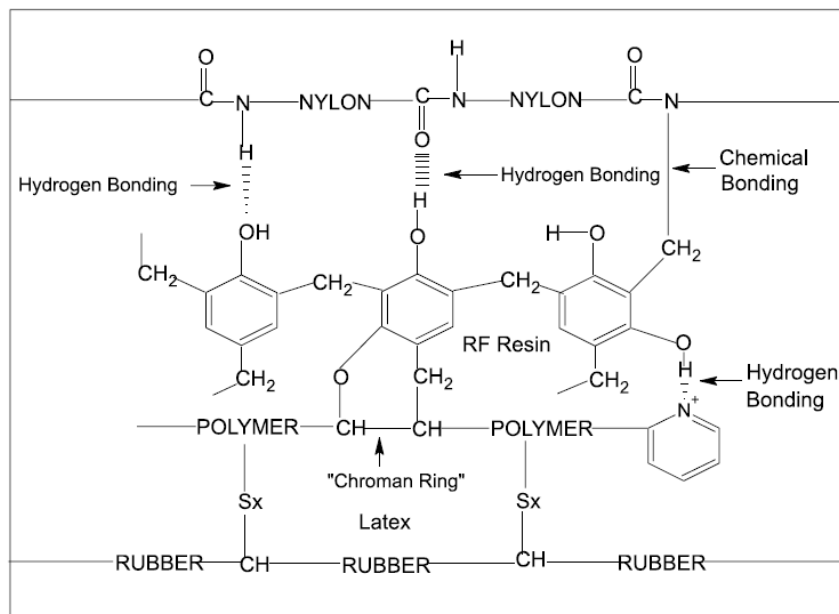


Figure 1.14: Possible Bonding Mechanisms between Nylon, RFL and Rubber (Durairaj, 2005).

The bonding mechanisms seen in RFL coated fabric are important to understand in order to comprehend how the coating may be removed or how the fabric is able to interact with other materials in the recycling processes.

1.2.4 Properties of Coated Fabrics

Since the RFL waste examined in this study is a type of coated fabric, the process for which is described in section 1.2.3.3, it is important to assess how coatings in general affect the physical properties of a fabric. Coating a fabric rather than fibres or yarns allow for continuous processing to be implemented which would not be possible with fibre bales or packages and hanks of yarn. By incorporating the coating into the latter stages of processing, problems associated with the coating are avoided from disrupting the spinning and weaving processes. The physical properties of a coated fabric will depend upon the textile substrate, the coating formulation, the application technique, and the processing conditions during coating. Due to coating being applied

while the fabric is in tension longitudinally, the positions of the yarns within the textile substrate are altered. The warps become more aligned in parallel and the wefts become more crimped (Sen and Damewood, 2001). The minimum coating thickness is applied to the top of the weft yarns as shown in Figure 1.15. The fabric properties will be changed from the uncoated fabric because of this change in structure and composition.

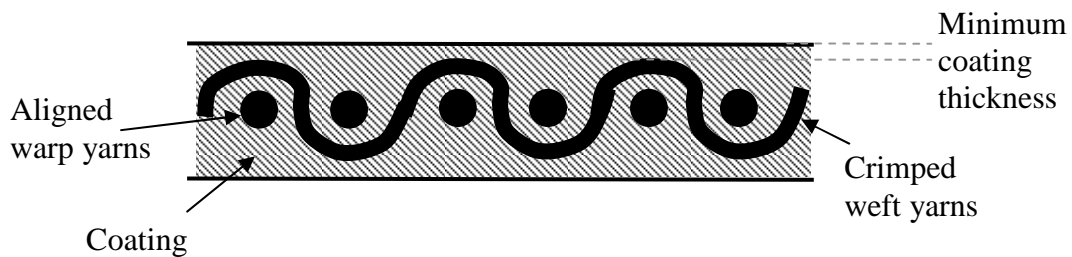


Figure 1.15: Simplified Cross-section of a Coated Fabric.

Due to the difference in break elongation between the textile substrate and coating, it is unlikely that the coating compound will contribute to the strength of the coated fabric. However, due to the tension and heat of the coating compound during the coating process, there is shrinkage in the fabric leading to an increase in yarn packing density in the warp direction. This leads to an increase in tensile strength as the load is distributed across a higher number of threads. However calculations by Eichert (1994), who considered the higher thread count seen in coated fabrics, found that the effective strength of coated fabrics was reduced. This is thought to be due to transversal strain and heating of the yarns during processing.

Similarly the effect of fabric shrinkage affects the elongation of the fabric. Coated fabrics were found to have much lower elongation in the warp direction compared to the weft direction, with the warp direction elongation being similar to the yarn elongation (Sen and Damewood, 2001). This is due to the crimp transfer that occurs from longitudinal tensioning during the coating process. Warp yarns are stretched so that they are taut and parallel which decreases the elongation in this direction, whilst the looping of the weft yarns is increased, enhancing the elongation (Sen and Damewood, 2001).

The coating will also have an effect on the tear properties of a fabric. In an uncoated fabric, tear strength is dependent on the weave pattern, yarn fineness and yarn density. As the coating surrounds the yarns, the coating material (formulation and bonding system) and the penetration of the coating material on the textile substrate will also affect the tear strength (Sen and Damewood, 2001). Coating leads to reduced deformability of the yarns within a fabric. Thus, each yarn is more likely to be broken individually and the tear strength reduced. Where fabric is able to deform, yarns move and become closer together, in the region of stress concentration, allowing the tear force to be distributed across yarns, therefore increasing the tear strength.

There is also a relationship between the coating adhesion and fabric tear strength. As the adhesion of the coating to the substrate increases, the tear strength is reduced (Sen and Damewood, 2001). Increased adhesion is likely to lead to decreased deformation, decreasing the tear strength due to the reasons above. Loss in tear strength is also more severe across the weft direction than the warp direction in a coated fabric (Sen and Damewood, 2001). This has been reasoned to be due to the direction of spread in knife coating applications, where the knife runs parallel to the weft yarns. The dragging action of the knife over the yarns opens up the filaments or fibres which results in more penetration of the coating into the weft yarns. As the fabric is tensioned, warp yarns are less crimped, and therefore the crimped weft yarns have more interaction with the knife. Because of this, and as the knife is running perpendicularly to the direction of the warp yarns, the fibres are opened up less and the coating does not penetrate into the yarn as far as occurred in the weft yarns. The weft yarns are therefore less deformable than the warp yarns and the tear strength across the weft is more affected after coating (Sen and Damewood, 2001). However, since material from Heathcoat Fabric's is coated by a dip coating process, rather than knife coating, this phenomenon should not occur, as fibres are not opened up in the same way when passing through rollers as occurs in dip coating, and therefore the penetration of the coating into the yarns will be approximately equal in warp and weft yarns..

1.2.5 Summary

The coated waste material produced by Heathcoat Fabrics consists of nylon 6.6 textured filaments, woven to produce the fabric substrate. This is coated with an RFL adhesive, dried and cured. The fabric has not yet undergone the vulcanisation process to bond to the rubber, as this occurs in the production processes of Heathcoat Fabrics' customer base. The material, therefore, has a chemical structure similar to the one shown in Figure 1.14 with the rubber polymer and sulphur cross linking omitted. Due to the variety of applications Heathcoat Fabrics produce fabric for, the fabric specifications of the waste fabric produced are numerous and varied.

The previous sections outline the production techniques and chemistry involved in manufacture of the RFL coated waste and the general properties related to nylon and coated fabrics. As a composite material the properties of the waste fabric will be affected by the substrate nylon fabric properties, coating properties and the processing carried out within production of the material.

1.3 Research Objectives

It is the aim of this research project to investigate ways in which the RFL coated nylon waste fabric can be recycled. Currently there are routes available for pure nylon waste to be recycled as discussed in chapter 2. However due to the composite nature of the RFL coated waste, it is much harder to recycle. This study considers recycling possibilities that do not require separation prior to processing and examines how the coated fabric behaves in comparison to the non coated fabrics in each of the areas investigated. The aims of this thesis are as follows:

- To understand current methods of recycling;
- To understand the effect RFL coating has on fabric properties and how this will affect fabric breakdown during recycling;
- To investigate fabric breakdown methods and their effect on coating integrity and polymer degradation;
- To investigate recycling possibilities through synthetic paper formation and opportunities for separation of fibres using paper technology;

- To investigate recycling possibilities regarding yarns containing recycled fibres;
- To investigate recycling opportunities in plastic moulding;
- To investigate recycling using RFL fibres as rubber fillers.

The following chapters address these aims, introducing previous work carried out in these areas and experimental work that has been completed within this research. The thesis covers a broad spectrum of technologies with the aim to introduce a range of recycling possibilities and highlight areas where research could be focussed in future. Conclusions and suggestions for the most successful recycling streams will be made.

1.4 References

- BILLMEYER, F. W. (1971) *Textbook of polymer science*, New York Chichester, Wiley-Interscience.
- BRYDSON, J. A. (1999) *Plastics materials*, Oxford, Butterworth-Heinemann.
- COCKETT, S. R. (1966) An introduction to man-made fibres. London, Pitman.
- DURAIRAJ, R. B. (2005) *Resorcinol [electronic resource]: Chemistry, Technology and Applications*, Berlin, Heidelberg, Springer-Verlag Berlin Heidelberg.
- EICHERT, U. (1994) Weaving and Coating Processing Influences (Fabric Rendement). *Journal of Coated Fabrics*, 24, 20-39.
- HARVIE, C. (2008) Heathcoat Fabrics Factory Visit. (Personal Communication 10th September 2008)
- HATCH, K. L. (1993) *Textile science*, Minneapolis/Saint Paul, West Publishing Company.
- HEATHCOAT FABRICS (2011) Automotive Market. Heathcoat Fabrics. [online] Available at: <http://www.heathcoat.co.uk/automotive> [Accessed 16th August 2011].
- IMPERIAL CHEMICAL INDUSTRIES, L. *Nylon its nature properties and uses*, I.C.I. Ltd.
- MARKS, R., TEXTILE, I. & ROBINSON, A. T. C. (1976) *Principles of weaving*, Manchester, Textile Institute.
- MONCRIEFF, R. W. (1975) *Man-made fibres*, London, Newnes-Butterworths.

RICHARDS, A. F. (2005) Nylon Fibres. In McIntyre, J. E. (Ed.) *Synthetic fibres: nylon, polyester, acrylic, polyolefin*. Cambridge, Woodhead Publishing Limited.

SEN, A. K. & DAMEWOOD, J. (2001) *Coated textiles: principles and applications*, Boca Raton, FL ; London, Taylor & Francis.

SEYAM, A. M. (2000) 3. Advances in Weaving and Weaving Preparation. *Textile Progress*, 30, 22-40.

VINCENT, J. J. (1980) *Shuttleless looms*, Manchester (Greater Manchester), Textile Institute.

2.0 Waste Disposal and Textile Recycling

2.1 Introduction

In England industrial waste makes up 13%, by weight, of the annual total in comparison to the household waste stream which contributes 9% of the total waste (DEFRA, 2009). A survey of 4500 industrial and commercial businesses in England, carried out by an environment agency in 2002/3 found that industrial waste amounted to 38 million tonnes per annum, of which the chemicals industries (which included fibre, rubber and plastics) contributed 7.2 million tonnes. Of the total waste produced by commercial and industrial businesses 6.1 million tonnes (9%) was being dealt with by reuse, 22.6 million tonnes (33%) by recycling, 2.5 millions tonnes (4%) by thermal treatment, 1.6 millions tonnes (2%) by other recovery systems and 27.7 million tonnes (41%) by landfill. A comprehensive national survey on this scale has not been repeated since, however, from these results it can be seen that there is considerable room to increase reuse, recycling and recovery rates in order to reduce waste going to landfill (DEFRA, 2009).

This chapter aims to outline the issues facing textile companies regarding waste they produce, and the pressure from government for waste of this type to be reduced. Furthermore, current recycling systems and technologies that are available for the recycling of both post consumer and post industrial textile waste will be discussed and current research themes related to textile recycling will be examined.

2.2 Legislation

Fabric manufacturers in addition to all other industrial and commercial businesses are under increasing pressure to divert waste away from landfill and instead to reuse and recycle. A key component of this pressure comes from the Council Directive 1999/31/EC of 26 April 1999 on the landfill of waste also known as the Landfill Directive (Commission of the European Communities, 2005). This directive aims to reduce the negative effects on the environment from the land filling of waste. In order

to achieve this objective stringent technical requirements for waste and landfills were introduced. In addition targets were set for the reduction of biodegradable municipal waste that was going to landfill (DEFRA, 2011b). These targets were based on a reduction to 75% by July 2006, to 50% by July 2009 and to 15% by July 2016 of the waste produced in 1995 (Commission of the European Communities, 2005).

Prior to this directive the government introduced a landfill tax in October 1996 in order to reduce waste that was sent to landfill. Rates for the year 2010/11 were £48/tonne (+VAT) for “active” waste and £2.50/tonne (+VAT) for “inactive” waste. Since the RFL coated nylon 66 waste is plastic material it is classed as “active” waste. In the 2010 budget the government announced that the rate for “active” waste would continue to rise by £8 per year until at least 2014/2015, at which point it will be £80/tonne (DEFRA, 2003). This tax has therefore increased the disposal charges incurred by industrial businesses and provided a strong incentive to tackle the problem.

In 2008 the European parliament introduced a further directive setting out ways in which waste could be reduced. The European Waste Framework Directive 2008/98/EC included information on the collection, transport, recovery and disposal of waste. The directive described a comprehensive definition of waste. The directive required all member states to take the necessary measures to ensure waste was recovered or disposed of without endangering human health or causing harm to the environment. In addition member states were primarily; to take measures to encourage the prevention or reduction of waste, and secondly; to encourage recovery of waste by recycling, re-use and reclamation (DEFRA, 2011a).

This framework has been transposed into national law in The Waste (England and Wales) Regulations 2011 which came into force on 29 March 2011 (DEFRA, 2011b). The regulations outline the establishment of waste prevention programmes, waste management plans and related duties and responsibilities. The waste hierarchy is outlined as:

- a. prevention;
- b. preparing for re-use;
- c. recycling;
- d. other recovery (for example energy recovery);
- e. disposal.

Through these regulations all businesses, organisations, producers and handlers of waste were required to prevent waste as far as possible and to apply this waste hierarchy whenever waste is transferred. In doing so businesses are encouraged to use less material in the design and manufacture of their products, enabling the prevention of waste occurring. Where possible businesses should check, clean, repair, refurbish whole items or spare parts, thus enabling reuse rather than disposal. This approach is currently more relevant to machinery parts within the textile manufacturing sector rather than textile waste products. Waste is encouraged to be recycled, turning it into a new substance or product, hence avoiding disposal. Finally any methods of energy recovery such as anaerobic digestion and incineration would also be encouraged over disposal by landfill or incineration without energy recovery (DEFRA, 2012b).

There was also mention in these regulations of producer responsibility but this is in relation to packaging waste rather than production waste. This was outlined in further detail within the Producer Responsibility Obligations (Packaging Waste) Regulations, 2005, (Producer Responsibility Obligations (Packaging Waste) Regulations 2005) which was further amended in 2008. However there is no current legislation outlining specific manufacturer responsibility with regards to waste minimisation. This may be due to the fact that improvements have been seen in the amount of industrial waste being recycled with 52% of commercial and industrial waste being recycled or reused in England in 2009 compared to 42% in 2002/3 (DEFRA, 2012a). Environmental regulators are also currently working towards making the rules clearer and removing old unworkable regulations. By doing this they aim to provide savings to businesses whilst enforcement is targeted on companies who are not following the rules set out. With this in mind the advice set out in the European Waste Framework Directive 2008/98/EC and the Waste (England and Wales) Regulations 2011 have substantial advice for manufacturing businesses to work with in order to help reduce waste produced.

2.3 Current Recycling Processes.

Recycling technologies can be classed into four approaches in relation to how synthetic textile waste can be processed (Wang, 1998). The primary approach is to recycle in its original form, which would involve the breakdown of fabrics to fibres and processing of the recycled fibres. The secondary approach is to melt process plastics into a new product with lower physical and chemical properties. Tertiary recycling involves converting plastic wastes to basic chemicals or fuels, for example this can be by pyrolysis or hydrolysis reactions. Finally quaternary recycling is where waste is converted to energy through incineration.

2.3.1 The Primary Approach: Reclaimed Fibres.

Most tearing machines require preliminary cutting of the fabric (Gulich, 2004). The most common technology used is based on rotary cutters, although drop knives are also used. Cutting technology operates at a faster rate than downstream reduction processes, having capacities of 6 to 10 tonnes/hour. Rotary cutting machines exhibited at ITMA 2003 included a special knife geometry to guarantee exact cuts across widths of up to 920mm (Gulich, 2004).

Tearing technology, utilising cylinders with pin clothing for coarsely opening fabrics and saw tooth clothing for fine opening, is a widely used form of size reduction. Technology is focussed on refinement of the equipment in order to produce high quality recycled fibres, having long lengths and little contamination, for a specific use. In order to optimise the opening process large cylinders of 1m diameter with coarsely opening pin clothing are used at the beginning of the line, whereas small diameter cylinders of 0.6m with fine opening saw tooth clothing are used at the end of the line, as illustrated in Figure 2.1. Energy efficiency is also optimised by using cylinders at the same peripheral speed. Fabric chunks or yarns that manage to get through the tearing machine are extracted and fed back into the system at a suitable stage. Tearing machines have a capacity of 1000-1250kg/h per metre of working width, with the typical maximum working width being 2 metres (Gulich, 2004).

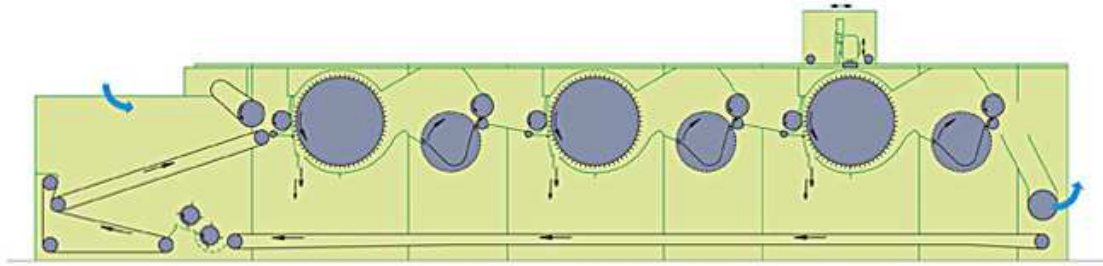


Figure 2.1: *Tearing Technology Utilising Pin and Sawtooth Clothing (Laroche, 2012).*

Specific opening machinery is available for selvedge strips for internal recycling in the nonwovens industry. These make use of twin-roller intakes alongside the previously discussed pin drums and saw tooth rollers. It is important that these machines are able to process material to keep up the supply rate into the nonwoven production line. Technology for internal recycling for thermally sensitive fibre material also exists with an internal spray system incorporated for cooling (Gulich, 2004).

Machinery specifically for yarn opening utilises technology similar to that of carding, using a number of roller worker units against a larger saw tooth clothing drum (Figure 2.2). This allows for more robust yarn structures to be opened to fibres with minimal fibre damage allowing for the recovery of higher quality recycled fibres (Gulich, 2004).

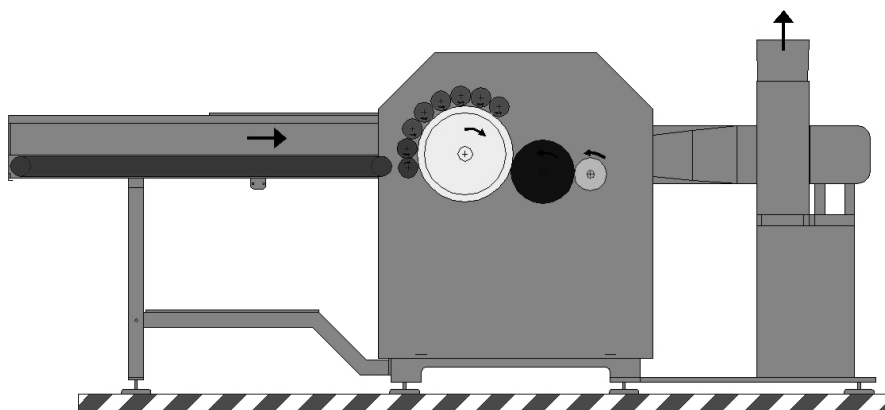


Figure 2.2: *Mini Garnett Machine for Yarn Opening (Scoleri, 2008).*

By recycling textiles using the primary approach the fibre quality characteristics are maintained, for example non-flammability and high fibre strength, and can be made use of several times. Reclaimed fibres are low cost in comparison to fibres recycled by chemical methods (Gulich, 2004). New fibres and downstream disposal are also becoming more expensive. Energy consumption is also lower than other forms of physical and chemical recycling such as granulation and fibre production (Gulich, 2004).

Reclaimed fibres by nature have a high proportion of short fibres as well as threads and fabric pieces not fully broken up. The fibre lengths need to be high enough in order to allow for spinning or web formation to take place. Short fibres, dust and fabric pieces will cause challenges in the production processes. Yarn pieces are able to contribute to a nonwoven matrix and will be further broken down to fibres in carding processes. Present day technology produces reclaimed fibres with 25% to 50% being above 10mm in length (Gulich, 2004).

Once fabric has been successfully reduced to fibre the most common way of reprocessing is through nonwoven technology. Web formation can take place using a vibration chute feeder and card technology; however the challenge arises in nonwoven technology in being able to produce increased range of web weights and thicknesses. This can be achieved using a self regulating fibre distribution system that utilises air streams alongside profile monitors (Pourdeyhimi, 2008). Machines utilising this technology can produce webs in the range of 600-2000g/m² (Gulich, 2004).

Aerodynamic web formers are another advanced way of achieving web formation and are particularly relevant to the recycling industry as they are able to offer considerable versatility regarding fibre type, managing both natural and synthetic, pure and mixed fibres, recycled fibre and granulated material (Hussey, 2011). The technology consists of tower feeders to supply fibres to rotating pin or saw tooth rollers which open the fibres which are then supported by air extractor screens. Using this process fibres are able to be deposited in three-dimensional layers with gravimetric, optoelectronic and radiometric sensors able to measure/control feed

intensity, feeder opening, change in air feed and web weight and thickness (Gulich, 2004).

Once formed into a web, traditional bonding technologies such as needling, and thermobonding can be used. Thermobonding is more commonly used in recycling of fibres, utilising heat-sensitive fibres or bonding powder, as bulk and thickness can be preserved in the web or structure using through-flow dryers and heat setting (Gulich, 2004).

Recycled fibres are also used in stuffing, carpet underlay, automotive components and building insulation (Gulich, 2004). Reclaimed fibres can also be respun into yarn to be subsequently woven or knitted into new products. By reusing fibres in this way, value is added to the material, which would otherwise end up being land filled or incinerated.

An increasing amount of reclaimed fibre is being utilised in technical textiles (Gulich, 2004). This is a market which is growing and therefore the demand for fibres both virgin and reclaimed is also growing. The quality of this fibre is the most important aspect considered in this industry, however if the quality can be maintained, using reclaimed fibres allows for the use of cheaper raw materials. As high functionality fibres are expensive, the recycling of these allows for better cost savings, particularly as the cost of recycling increases (Gulich, 2004).

2.3.2 The Secondary Approach: Melt Processing

In order to recycle material through a melt processing, input material is required to be smaller and more consistent in size and shape. Shredders for plastic recycling, therefore, operate using a different process, cutting rather than opening the material. These shredders can be single, double or four shaft machines. Single shaft shredders use a large rotor up to 2 metres in length with a ram that forces material into the rotor. The material then passes through a screen (Hawn, 2001). Alternatively where two or four shafts are used the shredding occurs between adjacent disks. The capabilities of cutting a crushing depend on the number of hooks on the circumference of the disk and the size of the cutting disk. Shredders work by tearing and cutting the material

and are suitable for film, sheet, and bulky objects such as bales (Hawn, 2001). Figure 2.3 illustrates the principle of operation of a four shaft shredder. The throughput will depend upon the density, shape and nature of the material to be processed, the cutter capabilities (disk width, number of cutting teeth, size of cutter opening) and the diameter of the sieve holes (Scheirs, 1998).

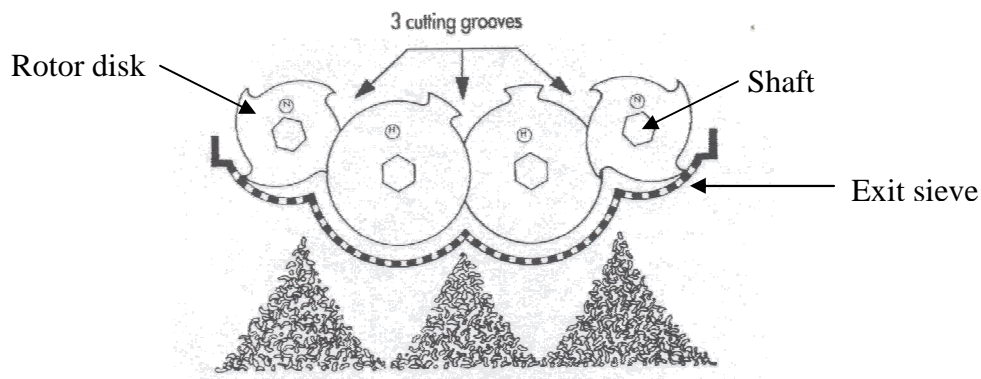


Figure 2.3: Four-Shaft Shredder (Scheirs, 1998).

In order to provide for products that are more difficult to reduce, such as fine yarn, fibre, drawn tow and thin film, technology now includes a higher number of cutters, special knives, modified screens, heavier drive systems (including independently driven shafts utilising gear transmissions) and programmed vertical rams which help to compress the material to cover the rotor and preventing wrapping and wedging within the machine (Hawn, 2001).

Granulators are one of the most common reduction techniques used in the plastics recycling industry. They consist of a system of rotating knives alongside three or four stationary knives, Figure 2.4 and are also referred to as rotary knife cutters. Both the rotary knives and stationary knives are set at an angle in order to provide constant cutting across the width of the knife, ensuring good efficiency from close knife to knife clearances (Scheirs, 1998). Knife gaps are typically in the range of 0.2-0.3mm with the number and configuration of the knife blades able to be changed depending on the material to be reduced. Many small knives with a small inclination would be used for high bulk density material, whereas an open steep angle rotor would be used for sheet, film, and fibre with thicknesses up to 5mm. Granulators can work at capacities of 10,000 kg/hour (Scheirs, 1998).

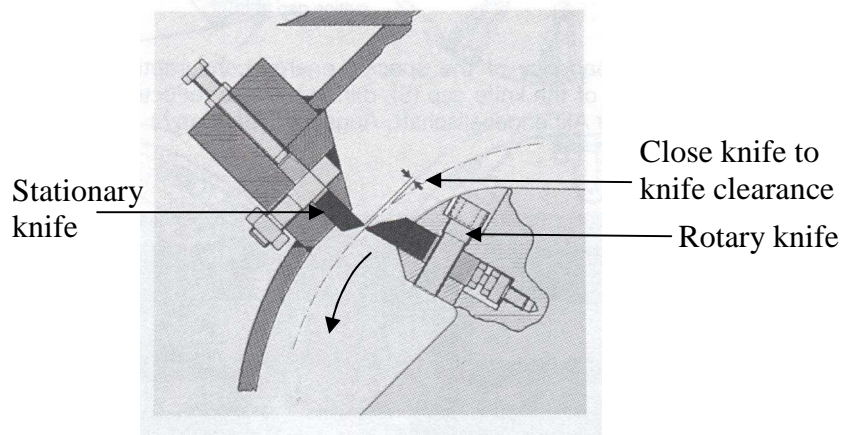


Figure 2.4: *Granulator Knife Action (Scheirs, 1998).*

Size reduction can be combined with a washing stage in wet granulation, this is useful for processing of dirty materials (Scheirs, 1998). This also allows for the knives to be directly cooled by water and prevents contaminants being incorporated into the plastic. The friction caused from the cutting intensifies the washing stage. The water also helps to prevent blocking of the screen. Due to the cooling action of the water, thermal stress of the polymer fibre is avoided (Scheirs, 1998).

After shredding, materials generally go through a densification process; forming the material into a more compact form for better handling. It is often used for packaging film, textile fibres or foam since these materials are particularly voluminous. These materials have a bulk density between 20-40 kg/m³ which is increased to around 400kg/m³ for further processing. The polymer is softened from the frictional heat of 135-140°C, ensuring that the melting temperature of the polymer is not reached. The advantages of incorporating an agglomeration/consolidation process are that storage space is reduced, transport is more economical, polymer flowing properties are improved and dust is removed. Densification can be done using densifying discs, compression or agitation (Scheirs, 1998).

Densifying discs (Figure 2.5) have grooves running from the centre to the circumference which are tapered outwards. One disc remains stationary whilst the other rotates. Plastic material is fed into the system by a feeding screw, the frictional

heat and the forces occurring between the discs lead to material being extruded from the outer areas of the discs (Scheirs, 1998).

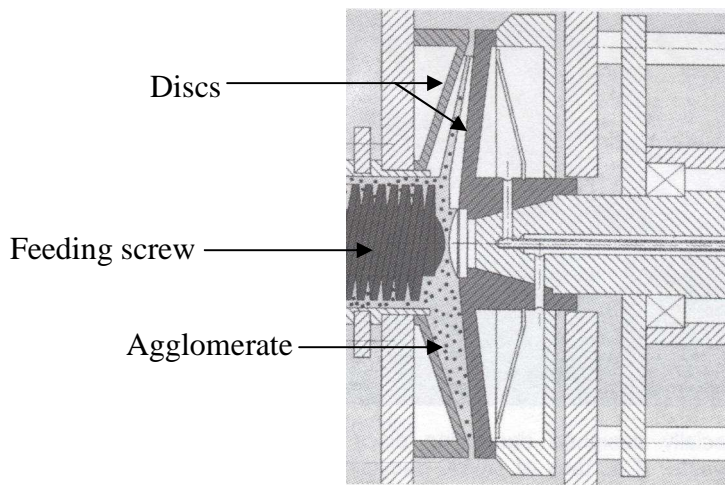


Figure 2.5: *Agglomeration by Densifying Discs (Scheirs, 1998).*

An alternative is to compact the material by compression until pellets are formed. Granulated material is then fed onto a die to form a layer, and rollers are then used to compact this layer, forcing it through the die channels, as illustrated in Figure 2.6. The material is extruded as a continuous strand that is then cut using a rotary cutter (Scheirs, 1998).

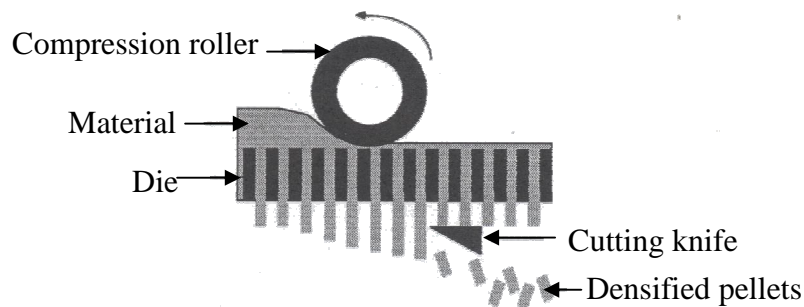


Figure 2.6: *Compression Agglomeration*

The final agglomeration method is to vigorously agitate the waste, using rotating blades, which causes the material to reach near melting point. Jets of water are used to control the temperature so that the melting point is not reached. The water is then evaporated off leaving the dry agglomerate.

Some material will go through a pulverisation stage, converting cleaned plastic waste into a fine powder. Pulverised PVC waste can be reused for extrusion, whilst pulverised PR waste can be moulded directly into a sheet. Pulverised waste material can be used as fillers, sintered powder coatings, and moulding powders. Pulverisation allows for excellent flow characteristics, high bulk density, narrow particle size distribution, and homogeneous composition. Technology such as disc mills and pin mills are used to achieve this in temperature sensitive polymers attaining particle size of less than 50 μ m. Waste is reduced to this size using a fan wheel and a screen, where the fineness of the powder is defined by the mesh size of the screen. Pulverisation can also be useful where impurities are involved as once ground down to this particle size the impurities tend to act as inert fillers. Problems can occur with high temperature zones with blade edges causing polymer sticking, reducing the cutting effectiveness (Scheirs, 1998). Disc pulverisers offer an alternative way of reducing material to dust form, consisting of two discs having tooth-like protrusions. These do not contain a screen and therefore have a short dwell time, allowing for better processing of temperature sensitive polymers. Discs have diameters of around 1.25m and capacities of 3500kg/hr. Pulverisation can also be performed using rotors or hammers. More advanced technology utilises liquid nitrogen causing the polymer to become more brittle and easing the grinding process for hard to grind polymers. Solid state shear extrusion is also used, subjecting the polymer to high shear and high pressure within a twin screw extruder whilst removing any heat. This causes the polymer to shatter into powdered form rather than melting and can be used as a single process to create particulate material (Scheirs, 1998).

Once the appropriate size reduction has taken place the plastic can be extruded or moulded. Polypropylene is commonly compounded with additional polymers and additives before injection moulding to create new products. Polyester on the other hand is extruded to produce staple fibre (Hawn, 2001). The above size reduction techniques are also required for chemical recycling, as discussed in section 2.3.3, and incineration, section 2.3.4, to enable the waste to be in a regular and consistent form that can be easily metered and fed into these processes (Scheirs, 1998).

Although traditional melt spinning extrusion is possible, many reclaimed fibres are put through compact short staple fibre spinning as an alternative. This process cools

the extruded filaments in a very short distance, less than one inch from the extrusion die in comparison to cooling zones up to 4 storeys high in tradition spinning. The spinning speed is also much lower having a maximum of 250m/min in comparison to thousands of metres per minute in traditional spinning. Finally the spinnerets are larger with more holes, generally producing filaments with higher linear densities than traditional spinning. Fibre production can be done in a single process with up to 1,000,000 filaments being extruded, cooled, lubricated, drawn and heat set (Hawn, 2001). This requires less floor space and less labour, due to the continuous nature of the process. Fibre quality is also easier to control due to the low spinning speeds used, this is an advantage where polymer quality may not be as high as virgin polymers used in traditional fibre extrusion. Newer technology utilises circular heads with annular spinnerets which offers higher fibre to fibre uniformity and deniers as low as 1 denier per filament being produced (Hawn, 2001).

2.3.3 The Tertiary Approach: Chemical Recycling

Chemical recycling involves depolymerisation of the polymer back to its constituent monomers. This is a popular way of recycling nylon 6 and can be done by acidolysis, hydrolysis or depolymerisation in vacuo. It is harder to recycle nylon 66 in this way but can be done thorough aminolysis, a technology patented by DuPont.

Acidolysis refers to the addition of an acid catalyst to reduce the polymer chain length. However initially nylon 6 is first cut and then melted in a continuous reactor and treated with steam. Hydrolysis of the polymer occurs producing the monomer caprolactam as shown in the reaction scheme in Figure 2.7. The caprolactam is then distilled, while the caprolactam-water vapour is concentrated and treated with potassium permanganate which oxidises impurities. The caprolactam is recovered in a filtration stage, which can then be polymerised to produce a good quality polymer product. Figure 2.8 shows a plant schematic of the acidolysis process (Scheirs, 1998).

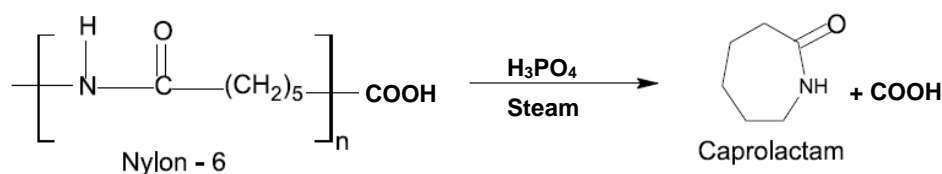


Figure 2.7: Reaction Scheme of Acid Catalysed Depolymerisation of Nylon 6 to give Caprolactam (Scheirs, 1998).

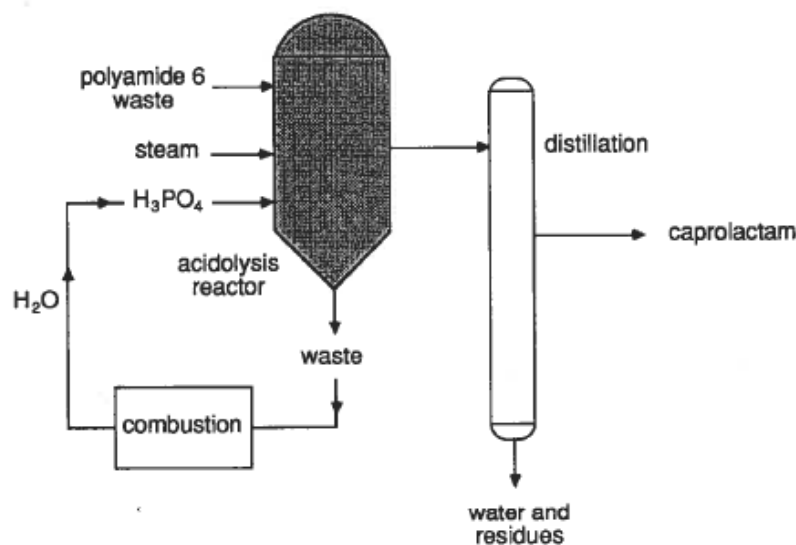


Figure 2.8: Schematic Diagram of Acidolysis Plant (Scheirs, 1998).

The disadvantages to this process are that filler or fibre reinforcement in the polymer can react with the acid which lowers the efficiency of the reaction. Also this is an expensive method due to the high cost and consumption of the acid catalyst and the treatment of the byproducts and waste water (Scheirs, 1998). It is also not possible to recycle nylon 66 in this way.

Another way to convert nylon 6 back to its monomer caprolactam is through hydrolysis, again this method is not possible for nylon 66. Rather than using the above method with high pressure steam an aqueous system under pressure is used. Yields of 60%-70% can be achieved without the use of a catalyst using a water to polymer ratio of 10:1 (Scheirs, 1998). A distillation stage is still required to remove the water and this alongside the high temperatures and pressure required makes this method relatively expensive. Higher yields are technically able to be achieved using higher temperatures; however this adds pressure to the system and requires a more robust reactor, increasing the investment costs needed.

In order to depolymerise nylon 6 without the need for the expensive distillation process a vacuum method can alternatively be used. This method is able to produce

caprolactam of high purity from nylon 6 in yields of more than 80%. A catalyst is required for this reaction in order to limit the number of byproducts (such as cyclic olefins and nitriles) that are produced. Potassium carbonate allows for high yields and short reaction times, however, other options for catalysts exist (Scheirs, 1998).

A final process, aminolysis, patented by DuPont in 1994 is able to process both nylon 6 and nylon 6.6 into their constituent monomers. The nylon 6 and nylon 6.6 is mixed with ammonia gas and a phosphate catalyst and reacted at a temperature of 330°C and a pressure of 7MPa. The reaction scheme for this process is shown in Figure 2.9. The reaction mixture is then distilled in order to recycle the ammonia involved and remove the by-products produced. The nylon monomers produced are then fractionally distilled in order to achieve separation of caprolactam, hexamethylenediamine (HMD), aminocapronitrile (ACN), and adiponitrile (ADN), Figure 2.10. ACN and ADN are subsequently able to be hydrogenated to give pure HMD, whilst the caprolactam produced is either converted further to ACN by another aminolysis process or refined to a pure caprolactam. The monomers produced are used to produce “new” nylon 6 and nylon 6.6 which can then be spun into bulked continuous filament.

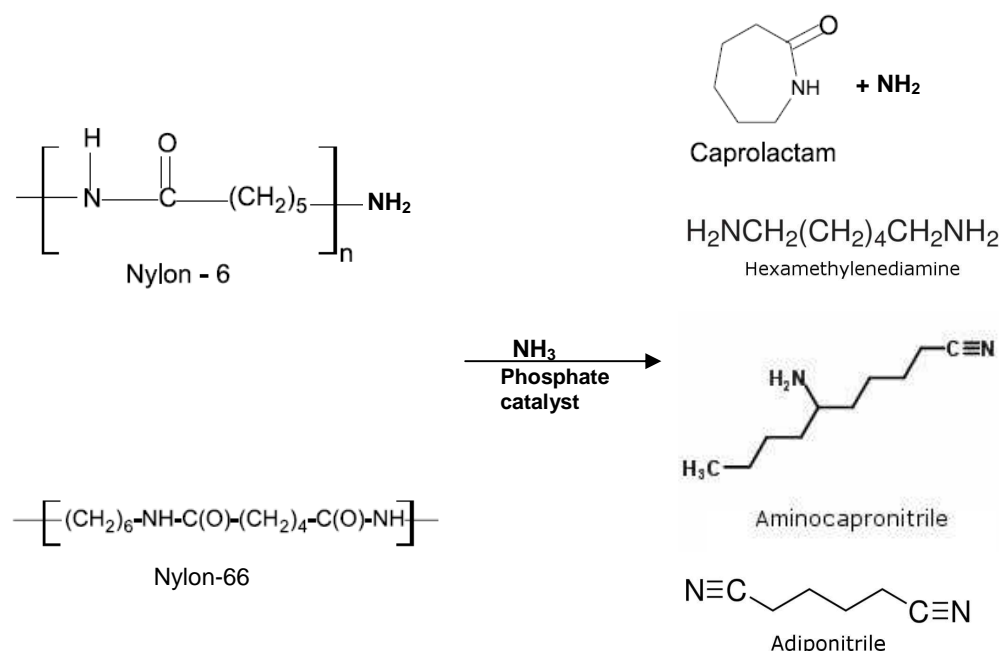


Figure 2.9: Aminolytic Reaction Scheme of Nylon 6 and Nylon 6.6.

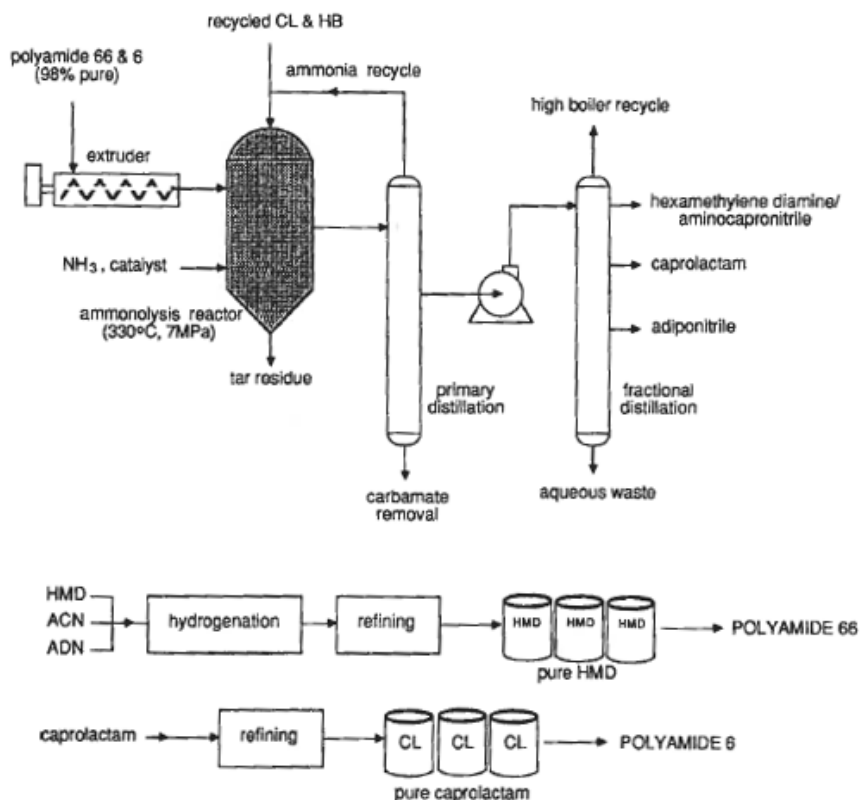


Figure 2.10: Schematic Diagram of Aminolysis Process (Scheirs, 1998).

2.3.4 The Quaternary Approach: Incineration

Waste sorted to go to land fill or incineration, are avoided if possible as there is a charge applied to these processes and accordingly less than 7% of post consumer textiles in the USA (Hawley, 2006) and 7% in the UK (Samuels, 2012) are sorted to this category. Nevertheless incineration of textiles for energy production is an waste stream that is increasing in popularity, particularly in European countries such as Germany (Parker, 2008). Incineration is also a common form of municipal waste disposal. As municipal waste is not sorted prior to incineration a problem still exists in that 40% ends up as ashes which are difficult to dispose of (Huang, 1995). If incineration is to become a viable option for the disposal of polymers in future it will be necessary to sort polymer wastes prior to incineration as the combustion of purer polyolefins generates too much heat for traditional furnaces and ceramic liners are also needed. There is also concern over how incineration contributes to carbon emissions and the greenhouse effect. This has brought about barriers to new incinerators being built in the United States (Huang, 1995).

2.4 Innovation in Textile Recycling

Current research in textile recycling is focussed on the following topics:

- Characterisation of reclaimed fibres (Rodríguez, 2006) (Turner, 2011);
- Optimal fabric reduction (Rodríguez, 2006) (Turner, 2011) (Ortlepp et al., 2004) (Ortlepp and Lutzkendorf, 2006) (Saffert, 1994);
- Reclaimed technical fibres (Palmer et al., 2010) (Ortlepp et al., 2004) (Ortlepp and Lutzkendorf, 2006);
- After treatment of reclaimed fibres (Rodríguez, 2006) (Palmer et al., 2010).

Together this research will enable higher quality reclaimed fibres to be produced suitable for a higher number of applications.

Of particular interest in the current study is the recycling of textiles that are contaminated with a finish or coating that is adhered to the fibre surface. There is little literature on the recycling of coated textiles, however there have been some studies on the recycling of PVC coated material (Takahahi and Kimura, 2003) (Saffert, 1994).

Saffert (1994) found that PVC coated tarpaulin material was able to be ground at low temperatures producing low bulk blended material. The PVC was not removed from the fabric prior to grinding. This material could then be used as filler in standard plasticised PVC compounds. However, the mechanical properties of these compounds quickly decreased as the quantity of filler was increased, for example 10% drop in tear resistance was seen with a regrind to virgin material ratio of 10:100, a better grind was therefore required. Saffert further developed the pulverisation method using low temperatures of -196°C causing the plastics to become brittle, and therefore more easily ground. An average particle diameter of 80-90 μm was achieved. The powder produced was able to be used as a filler in PVC plastisols, however the method was not commercially viable due to the high cost.

Saffert (1994) also looked at ways the PVC coating could be removed from the polyester fabric using solvents. Since PVC is soluble in tetrahydrofurane but PET is insoluble in this solvent, tetrahydrofurane was thought to be an ideal solvent for separation. However, this solvent is flammable and has an strong odour and for this

reason a closed system had to be used in laboratory scale recycling experiments. The solvent also forms explosive mixtures in air at concentrations between 1 and 14% by volume and is classed as an environmental hazard. It is also difficult to degrade in effluent or sewage treatment plants. In laboratory experiments by Saffert (1994), the PVC was precipitated as bulky fibres that clumped easily, and once the tetrahydrofurane had been eliminated the PVC was not of equivalent quality to virgin PVC as it contained impurities such as dirt and additives. The separation method was therefore not viable to continue development to a commercial scale.

Takahahi and Kimura (2003) studied how PVC coated glass fabric could be recycled by compression and injection moulding techniques. A safe and easy moulding method was developed which produced moulded products with satisfactory mechanical properties. However they found that hydrogen chloride gas produced during moulding affected the mould structures and therefore their mechanical properties. The moulding process was developed further with the addition of hydrotalcite and zinc stearate to inhibit the generation of the hydrogen chloride gas, producing superior structures.

Rodríguez et al (2006) have studied the milling times of flax fibre – vinyl ester composites in order to assess the most efficient milling time. It was found that when using a Janke and Kunkel milling machine and assessing powder size through sieving that the powder size did not decrease any further after 20 minutes. This information was subsequently used in order to plan further investigations relating to the incorporation of this powder in a vinyl ester matrix.

Turner et al. (2011) also characterised recyclate from prepregnation materials having a variety of fibre and types and resin types, comparing the breakdown of the different weave types used. The materials were cut into 1m x 300mm sections and heated in an oven to fully cure the resin. The cured material was then cut into 300 x 150mm sections to enable efficient feeding to the granulator. The granulator used had 3 sets of 10 knives arranged in a v-pattern on a rotor diameter of 180mm. The knives cut against fixed anvils which were situated at opposite ends of the cutting chamber. A cutting width of 300mm was used at a speed of 150 rpm, resulting in a striking velocity of 1.4m/s. Screens of 6mm, 8mm, 15mm 20mm and 25mm were assessed and the granulated material was assessed through sieving and also image analysis.

The authors found that granulation caused significant dust production. Heat build up was also a problem causing melting of the polymer material and build up on the blades surfaces if more than 30 minutes of continuous granulation was used. Errors in the work were introduced from clumping of the granulated material during sieving used to characterise the granulated size produced. These clumps were unable to pass through the mesh, giving higher proportions of material being analysed as larger particles due to this. This typically occurred in smaller sieve mesh sizes of less than 4mm. It was also found that dust production increased with smaller granulator mesh size. Dust was defined as material which passed through a sieve aperture of 600 μ m. Dust levels were found to be unacceptably high making up more than 25% on material output where granulator screen sizes of 6mm and 8mm were used. Useful material was defined as having a mean fibre length of 1-10mm. 6mm and 8mm screens were seen to be the most efficient overall, the 6mm granulating screen producing 79% of material below 10mm fibre length.

Research based on technical fibres aims to make recycled fibres more economically viable in a range of applications. Virgin carbon fibres are particularly costly at over £10,000 per tonne (Palmer et al., 2010), and are therefore only cost effective for very high end markets. In order to utilise carbon fibres in a greater range of applications the market for recovered and recycled carbon fibre is growing. The simplest approach to this is mechanical grinding but this produces short fibres of less than 2mm, limiting the carbon fibres to use as a reinforcement material. Other chemical techniques have been used in order to remove the resin component in composites including extraction by thermal decomposition, dissolution using supercritical fluids and use of molten salt solutions, nitric acid (Palmer et al., 2010). Fibres produced by these methods are unaligned and cannot be cut to the required lengths for sheet moulding compounds (SMC) processing. Sheet and dough moulding processes are able to utilise shorter fibres providing a potential application for ground fibres. Carbon fibres have been used in a ground form as a filler in SMC formulations, however this is not cost effective (Palmer et al., 2010).

In order to make use of the reinforcing properties of recycled carbon fibres in sheet moulding compounds (SMC) formulations research was done by Palmer et al., (2010) introducing carbon fibre recyclate in a fibre form, adding these fibres to the paste in a

similar manner to the incorporation of virgin fibres. Waste was granulated using an 8mm screen and was then refined and graded in order to add value. The fibres were separated out into 4 grades using air classification and sieving. This produced a grade consisting of fine fibres having a carbon fibre content of 72%, the remaining 28% being resin based. This grade provided up 24% of the original carbon recycle.

A new processing unit was devised by Palmer et al, (2010) to be able to use these fibres for SMC manufacture. Production lines for virgin fibres supply continuous strands which are chopped and continuously sprinkled onto the paste. Similarly it is necessary to ensure that precise quantities of evenly distributed recycle fibres are supplied to the web, and this can be achieved through a processing unit involving a hopper, a recycle feed unit, a rotating shaft with steel pins and vibrating sieve section. SMC structures were able to be formed by this process which had comparable mechanical properties to conventional formulations. In addition by control of mould charge a good surface finish could be produced.

Work has also been done to maintain fibre length in technical fibres such as p-aramids (Ortlepp et al., 2004) and carbon fibres (Ortlepp and Lutzkendorf, 2006) in order to enable their reinforcing characteristics to be better used. A novel milling technique was devised using a crushing type action to extract long fibres, by reverse engineered separation of the constituent parts of the material (Ortlepp et al., 2004). Reversed engineered reduction processes are processes in which fibres are extracted by first deconstructing the fabric structure to yarn constituents, and then separating the fibres from the yarn. By reducing fabrics in this way fibres should be less damaged than if fibres are extracted by pulverising the fabric. Ballistic cloth produced from p-aramid filament fibres was reduced in length by initially using drop knives in an L shaped formation to produce pieces of up to 70mm x 70mm. A moisture content of 10-15% was also recommended to accelerate subsequent disintegration processes and protect the material. After cutting, the material was conveyed to the modified crushing mill where the disintegration was done in a semi-continuous process. Fibres produced were suitable to supply conventional textile processing. Similarly heat protection fabrics based on staple fibres were reduced by first cutting with drop knives to 50mm x 50mm size, before wetting and using the novel crushing reduction process. This produced open tangled fibres which were able to be separated using a one or two

drum tearer utilising a specific periphery speed pin configuration dependent on the fibre properties. From analysis of the material produced and comparison to traditional tearing processes it was found that reduction using tearing machinery resulted in fibrillation of the fibres, which in turn led to a reduction in tensile strength. In comparison the new reduction process was gentler on the material. In addition to fibrillation, tearing machines also caused fibrils to split off, this resulted in dust-like particles which cause depositions in transport devices and machinery. A build up of these dust depositions leads to processing problems with the formation of neps in yarn or nonwoven fabric when the fibres are subsequently processed. These products are therefore of reduced quality due to the nep formation. This novel reduction process was able to produce fibres of relatively long lengths. Fabrics based on filament fibres were reduced to fibres of an average length of more than 50mm, whereas fabrics based on staple fibres were reduced to fibres having an average length of more than 25mm.

A web shredding method suitable for carbon fibres was also described by Ortlepp and Lutzkendorf (2006) utilising pre-crushing drop knives to obtain material pieces of 30-70mm before a milling process in place of traditional tearing. The same theory of disintegration of the fabric in the prescribed staggered steps applied. With carbon fibres this method has the added advantage that carbon fibre fly or dust is controlled and prevented from leaving the mill by using a low pressure process. The reclaimed carbon fibres are high value having a length of more than 30mm, and free from dust. The fibre reclaimed from woven fabrics and braids is suitable for production of non-woven webs which were able to be formed with no processing problems.

2.5 Conclusions

Although there is increasing pressure on companies to reuse and recycle their waste, the government is aware that introducing too many regulations will cause excessive bureaucracy and increase cost to industrial businesses. Instead it is putting the advice and structure in place to allow companies to voluntarily reduce, reuse and recycle waste, hence diverting it from landfill.

There are multiple technologies that allow for fabric and polymer recycling, that are available to fabric manufacturers. With the added need for better quality reclaimed fibres this technology is advancing further. Research is focused on the characterisation of reclaimed fibres in order to assess optimal fabric reduction processes. In addition much research is focussed on high value reclaimed technical fibres and the associated development of newer recovery technologies that will increase the commercial viability and flexibility of the textile recycling industry.

2.6 References

COMMISSION OF THE EUROPEAN COMMUNITIES (2005) Report from the commission to the council and the European parliament on the national strategies for the reduction of biodegradable waste going to landfills pursuant to the article 5(1) of directive 1999/31/EC on the landfill of waste.

DEFRA (2003) ARCHIVE: EU landfill directive. Crown copyright. [online] Available at:

<http://archive.defra.gov.uk/environment/waste/strategy/legislation/landfill/index.htm>
[Accessed 14th July 2012]

DEFRA (2009) Commercial and Industrial Waste in England - Statement of aims and actions in 2009. Crown Copyright. [online] Available at:
<http://archive.defra.gov.uk/environment/waste/topics/documents/commercial-industrial-waste-aims-actions-091013.pdf> [Accessed 14th July 2012]

DEFRA (2011a) EU Waste Framework Directive. Crown Copyright. [online] Available at: <http://www.defra.gov.uk/environment/waste/legislation/eu-framework-directive/> [Accessed 14th July 2012]

DEFRA (2011b) Waste Legislation. Crown copyright. [online] Available at: <http://www.defra.gov.uk/environment/waste/legislation/> [Accessed 14th July 2012]

DEFRA (2012a) Waste and recycling. Crown Copyright. [online] Available at: <http://www.defra.gov.uk/environment/waste/> [Accessed 14th July 2012]

DEFRA (2012b) Waste Hierarchy Guidance Review 2012. Crown copyright. [online] Available at: <http://www.defra.gov.uk/environment/waste/legislation/waste-hierarchy/> [Accessed 14th July 2012]

- GULICH, B. (2004) What is the machinery industry offering textile recycling? *Melliand International*, 10, 52-53.
- HAWLEY, J. M. (2006) Textile recycling: a system perspective. In Wang, Y. (Ed.) *Recycling in Textiles*. Cambridge, Woodhead Publishing Limited.
- HAWN, K. (2001) An Overview of Commercial Recycling Technologies and Textile Applications for the Products. *The Sixth Annual Conference on Recycling of Polymer, Textile, and Carpet Waste*. North West Georgia Trade & Convention Center, Dalton, Georgia.
- HUANG, S. J. (1995) Polymer Waste Management, Biodegradation, Incineration, and Recycling. *Journal of Macromolecular Science, Part A*, 32, 593-597.
- HUSSEY, C. (2011) Waste Textiles, Recycling. *Textiles Magazine*, 38, 36-37.
- LAROCHE (2012) Our Activities - Jumbo. OZ-média. [online] Available at: <http://www.laroche.fr/domaine-activite-recyclage.php?pge=14&lang=en> [Accessed 18th June 2012]
- ORTLEPP, G. & LUTZKENDORF, R. (2006) Long carbon fibers from textile wastes. *Technical Textiles / Technische Textilien*, 49, E117-E119.
- ORTLEPP, G., WEIß-QUASDORF, M. & GULICH, B. (2004) New recycling process for p-aramid fibers from fabric wastes. *Technical Textiles / Technische Textilien*, 47, 63-78.
- PALMER, J., SAVAGE, L., GHITA, O. R. & EVANS, K. E. (2010) Sheet moulding compound (SMC) from carbon fibre recycle. *Composites: Part A*, 41, 1232-1237.
- PARKER, S. (2008) An Explanation Of The Waste Incineration Directive. [online] Available at: <http://www.articlesbase.com/environment-articles/an-explanation-of-the-waste-incineration-directive-526306.html> [Accessed 4th August 2009]
- POURDEYHIMI, B. (2008) ITMA 2007 Review: Implications for the Nonwoven Industry. *Journal of Engineered Fibers and Fabrics*, 3, 38-46.
- PRODUCER RESPONSIBILITY OBLIGATIONS (PACKAGING WASTE) REGULATIONS 2005.
- RODRÍGUEZ, E., ALVAREZ, V. A., MORAN, J., MORENO, S., PETRUCCI, R., KENNY, J. M. & VÁZQUEZ, A. (2006) Mechanical Properties Evaluation of a Recycled Flax Fiber-reinforced Vinyl Ester. *Journal of Composite Materials*, 40 (30), 245-256.
- SAFFERT, R (1994) Recycling of PVC coated fabrics. *Journal of Industrial Textiles*, 23, 274-279.

SAMUELS, G (2012) Diverting clothes from landfill could save £140m [online] Available at <http://www.letsrecycle.com/news/latest-news/textiles/diverting-clothes-from-landfill-2018could-save-ps140m2019> [Accessed 26th January 2013]

SCHEIRS, J. (1998) *Polymer recycling: science, technology, and applications*, Chichester, Wiley.

SCOLERI (2008) Mod. Mini-Garnett. Rome, Officina Meccanica Tessile. [online] Available at <http://www.scoleri.it/mod.mini-garnett.htm> [Accessed 18th June 2012]

TAKAHASHI, T & KIMURA, T. (2003) Recycling of glass fabric coated by polyvinyl chloride. *Progress in rubber, plastics and recycling technology*. 19 (2), 93-116.

TURNER, T. A., PICKERING, S. J. & WARRIOR, N. A. (2011) Development of recycled carbon fibre moulding compounds. Preparation of waste composites. *Composites: Part B, Engineering*, 42, 517-525.

WANG, Y. (1998) An Overview of Activities on Recycling of Fibrous Textile and Carpet Waste at the Georgia Institute of Technology. In Horrocks, A. R. (Ed. *Ecotextile '98*. Bolton, England, Woodhead Publishing Limited.

3.0 The Effect of RFL Coating on Fabric Properties

3.1 Aim

To evaluate the fabric properties of comparable coated and uncoated fabric and hence assess how the RFL coating is likely to affect the ease of fabric reduction in recycling.

3.2 Introduction

Details on the general effect that coatings have on fabric properties have previously been discussed in section 1.2.3. However, in order to assess how the RFL coating will behave in reduction processes it is necessary to quantitatively assess the properties of the RFL fabric against non-coated fabric. Tensile strength, bending rigidity and tear strength have been chosen to be assessed, as these properties are likely to influence on how the fabric behaves whilst being broken up. The tensile strength and tear strength of a fabric will affect how easily the fabric is reduced when utilising tearing technology, pin rollers will apply force to the fabric in opposing directions, causing tensile or tear breaks. Grinding reduction techniques are more likely to be affected by the toughness of the fabric, an expression of the energy required to break the fabric, which can be assessed through tensile tests. The bending rigidity of a fabric will vary how the material feeds into rollers and how forces act upon the fabric, for example a fabric bends easily will drape around object providing the force, causing the action by opposing forces to work across the fabric, producing an abrasive action of the fabric. Whereas, a stiff fabric will remain at 90° to the opposing forces causing a cutting action on the fabric. These tests will also take into account the properties of the RFL coating studied within this thesis as opposed to PVC (Abbott et al., 1971) (Mewes, 1989) (Harris et al., 1994) and PU coatings (Mewes, 1989) (Wilkinson, 1996) that have been studied previously.

3.3 Materials

Three fabrics were supplied by Heathcoat Fabrics from different stages of the fabric manufacture. Heathcoat Fabrics' T-00537 quality was used as its composition of 100% nylon 66 and twill woven structure offered an ideal means to assess the effect of the coating on fabric performance. The fabric construct is a 2x2 twill weave, as defined in section 1.2.2, using a 13 tex multifilament textured nylon yarn for both warp and weft yarns containing 78 filaments. The fabric is designed to have a final weight of 130g/m². Loomstate fabric, intermediate heat set finished fabric, and RFL dipped fabric with a coating pickup of 5% was provided.

The effective warp and weft density of each fabric was measured using a method based on British Standard BS EN 1049-2:1994 Method 1 Dissection of Fabric (British Standards, 1994). A 5x5cm sample of each fabric was used and dissected completely to assess the number of warps and wefts. The weight per unit area of each fabric was also assessed using a British Standard 12127:1998 (British Standards, 1998). Table 3.1 summarises the results found.

Table 3.1: Fabric Specifications

Sample	Weight (g/m ²)	Thread Density	
		Warp	Weft
T-00537 Loomstate	112	80 ends/cm	38 picks/cm
T-00537 Finished	124	60 end/cm	38 picks/cm
T-00537 Dipped	113	60 ends/cm	30 picks/cm

These results show the opposite to the described effect of coating discussed in section 1.2.3, with warp packing density reducing with finishing and coating processes, and weft packing densities also reducing at the coating stage. Changes in warp and weft packing densities due to crimp transfer would result in increase in warp packing densities and decrease in waft packing densities due to the tensions and heat involved in the coating process causing the fabric to shrink in the weft direction. Weft packing density does decrease with the coating process, as expected. A decrease in the warp packing density from the loomstate to finished fabric is observed suggesting the fabric has been stretched and held in place in the weft direction to fix the width of the fabric

during the finishing procedure. Oddly this procedure has also increased the weight of the fabric, unexpected particularly since the amount of yarn per area is reduced, which would result in a reduced fabric weight. It is unknown why this anomaly has occurred. During the coating procedure the width was also held in place giving the same warp density as the finished fabric. However there does seem to be increased tension in the warp direction as the weft density is reduced by 21%. The fabric weight of the coated fabric would also be expected to be heavier due to the coating pickup, however its is similar to that of the loomstate fabric, this highlights the variation that can occur in fabrics from batch to batch.

3.4 Experimental Methods

3.4.1 Tensile Properties

Tensile properties of the fabrics were assessed using British Standard BS EN ISO 13934-1:1999 (British Standards, 1999). The fabric was put under a constant rate of extension and the load needed to stretch the fabric alongside the extension was measured until the fabric broke. Five samples of each specimen were taken in both warp and weft directions. Samples were cut to a length of 250mm and width of 50mm, and tested using a gauge length of 200mm and crosshead speed of 100mm/min. This length was chosen to align the test to the British standard procedure, however a gauge length of 0mm may have been more appropriate to assess how the fabrics would behave in a reduction process, since forces act across short roller or knife clearances. Table 3.2 summarises the parameters were used within the test. Specimens were conditioned at 20°C and 65% RH for 24 hours prior to testing. The toughness of the fabric was also assessed through this test, calculated by the area under the tensile curve. This gives a description of the energy required to break the material up the material and hence will describe the resistance the fabric has to reduction.

Table 3.2: Tensile Test Parameters

Instron Model	Instron Series IX Automated Materials Testing system.
Gauge Length	200mm
Rate of Extension	100mm/min
Load cell	5kN
Sample Rate	10pts/sec

3.4.2 Bending Rigidity

The British standard test BS 3356:1990 (British Standards, 1990) was used to assess the bending rigidity of the fabric in both the warp and weft directions. This method measures the length of fabric overhang required for the fabric to drop to a line inclined at 41.5° below the horizontal, and is a popular method for testing the stiffness of woven fabrics in textile technology. The bending length is defined to be the length of a rectangular strip of material that will bend under its own mass to an angle of 7.1° (British Standards, 1990). The Shirley Stiffness measurer used in this test is designed so that the overhang to 41.5° , is twice that of the bending length due to the trigonometric functions of angles. The Shirley stiffness measurer, however, is designed so that the bending length can be read of the scale directly. Three test specimens were cut for each sample in both warp and weft directions. Specimens were tested both face up and face down, giving six repetitions for each sample direction. Test specimens were conditions at 20°C and 65% RH for 24 hours before testing. The flexural rigidity, defined to be the ratio of small change in bending moment per unit width, was then calculated according to the standard using equation 3.1 where G is the bending rigidity in $\text{mg}\cdot\text{cm}$, C is the mean bending length in cm and M is the mass per unit are of the fabric in g/m^2 (British Standards, 1990).

$$G = 0.1MC^3 \quad (\text{equation 3.1})$$

3.4.3 Resistance to Tearing

Tearing was assessed using the wing rip technique detailed in British Standard BS 4303:1968 (British Standards, 1968). Initially the Elmendorf method was used but the load required to tear the fabric was higher than the available pendulum testing machine, therefore, it was decided to use the wing rip technique instead. The wing rip

technique measures the maximum force required to tear a specimen a set distance. A Series IX Instron Machine was utilised for this test with a 5kN load cell. The sample is cut and fixed within the Instron machine jaws as shown in Figure 3.1. Five repetitions were performed for each sample both across the warp and across the weft except for the loomstate fabric where four repetitions in each direction were taken due to limited fabric available. Specimens were conditions at 20°C and 65% RH for 24 hours before testing.

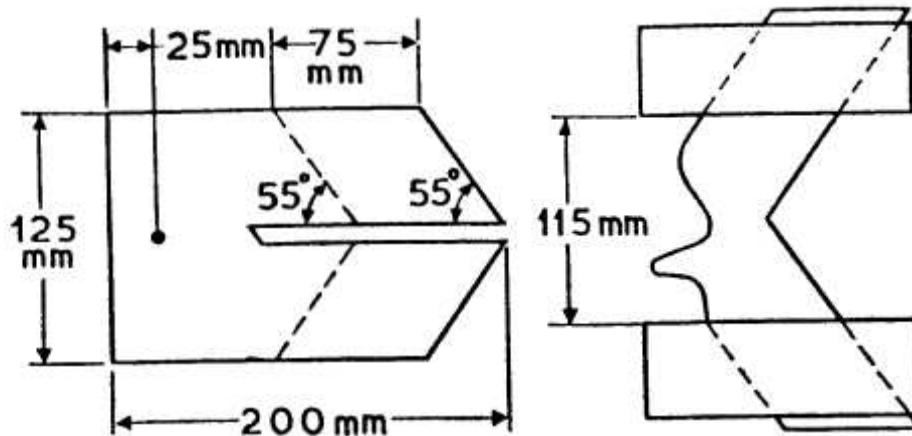


Figure 3.1: Wing-rip specimen size and arrangement for clamping.

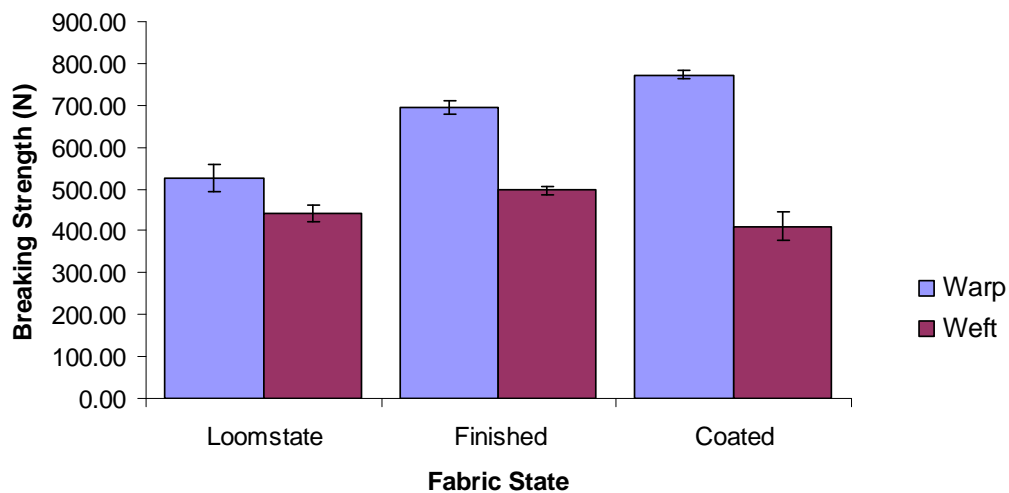
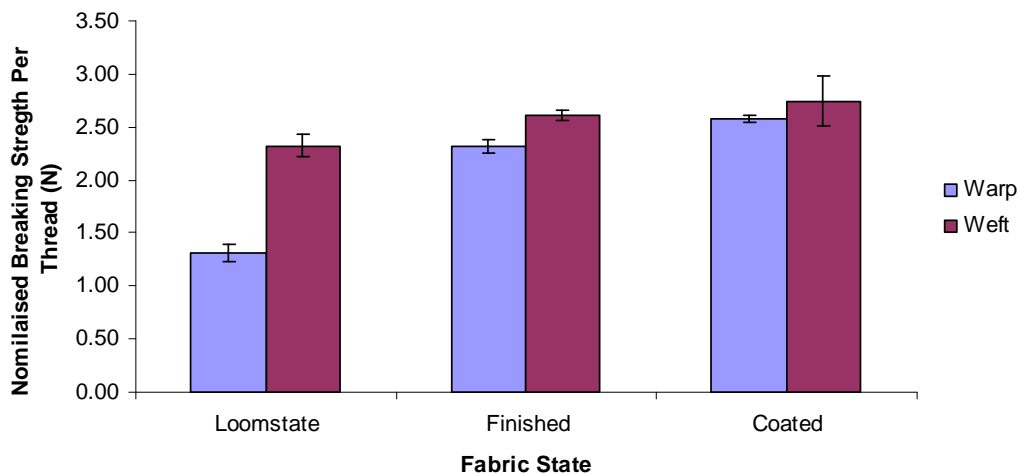
3.5 Results and Discussion

3.5.1 Tensile Properties.

Despite the warp thread density having decreased after finishing and dipping, the breaking strength increased in both the finished and coated fabric, as shown in Table 3.3 and Figure 3.2, see Appendix 1 for raw data. This suggests that the finishing process and RFL coating are altering the tensile properties of the fabric, rather than just the crimp interchange as described in most literature (Sen and Damewood, 2001) (Eichert, 1994) and explained within section 1.2.3. This is possibly due to increased yarn to yarn adhesion allowing better force distribution across the fabric.

Table 3.3: Tensile Breaking Load of Nylon Fabrics

	Warp			Weft		
	Loomstate	Finished	Coated	Loomstate	Finished	Coated
Mean Breaking Load (N)	526.6	695.0	772.7	440.9	496.3	410.9
St.Dev. (N)	32.5	18.0	11.0	19.5	8.4	35.2
Coef.Var. (%)	6.2	2.6	1.4	4.4	1.7	8.6
Minimum (N)	490.7	671.4	757.9	418.5	484.0	375.8
Maximum (N)	563.0	720.8	785.2	462.4	504.7	462.1
Thread Density (cm ⁻¹)	80.0	60.0	60.0	38.0	38.0	30.0
Breaking Load Per Thread (N)	1.3	2.3	2.6	2.3	2.6	2.7

*Figure 3.2: The Effect of Coating on Fabric Breaking Strength**Figure 3.3: The Effect of Coating on Thread Breaking Strength*

As the tensile strength is related to the number of yarns within a specified distance the force is distributed across a normalised breaking strength has been calculated using equation 3.2. These results are shown in Table 3.1 and Figure 3.3.

$$\text{Normalised fabric breaking load (N)} = \frac{\text{Mean breaking load (N)}}{\text{Fabric width (cm)} \times \text{Thread density (cm}^{-1}\text{)}} \quad (\text{Equation 3.2})$$

An increase in warp breaking strength of 95% was observed for the normalised breaking strength per yarn, from 1.32N in the loomstate, to 2.58N in the coated fabric. Normalised breaking strength is also increased in the weft direction to a lesser degree of 18%. The majority of this strength increase occurred during the finishing process rather than coating process. The coating, however, has also added further strength. The finishing process increased the nominal yarn strength by 76% in the warp direction, the coating then increased the strength by a further 10%. The weft strength is affected less by the processes, however, a significant increase in strength of 13% in the finishing process and a further 5% in the coating process was observed.

Earlier literature suggests that coating can increase the strength of a fabric (Mattinson, 1960), (Abbott et al., 1971). In Mattinson's (1960) study an increase of 32% in warp strength was seen in PVC coated fabric where a warp gain of 11% was due to the fabric weft shrinkage, suggesting that both the warp gain and coating contributed to the strength increase.

Abbott et al (1971) suggest that an increase in strength of coated fabric was due to increased fibre to fibre adhesion. It is likely that the RFL coating does hold the fibres within the yarns together so that the load is dispersed across the fibres better, however, the fibre to fibre adhesion is more likely to increase the strength of spun yarns rather than the multifilament yarns that the fabrics tested in this study contain, and it is therefore unlikely that this is the sole reason for the increase in strength.

It has also been considered that an increase in breaking strength could be due to increased yarn crystallinity occurring during heating procedures in the coating process (Wilkinson, 1996), but again it seems unlikely that this would cause a 10% increase in yarn breaking load. In a study on warp knit fabrics undertaken by Wilkinson (1996)

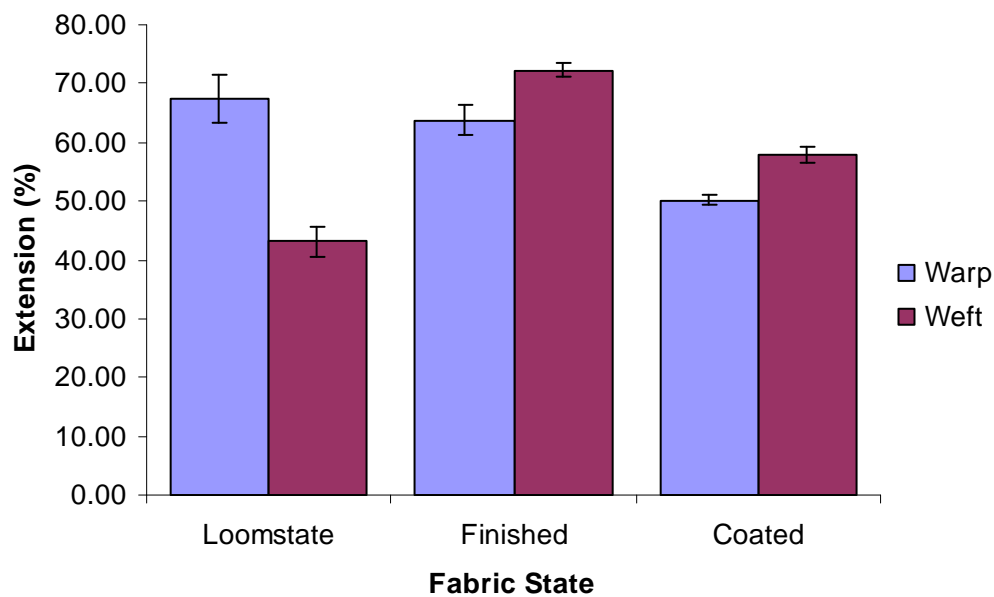
coating fabric increased tensile strength by 2-4% which in this case is not due to crimp transfer as this will not occur in knitted fabrics. These figures are much lower than the increase in strength seen in this study. It is suggested that the finishing procedure carried out on the TL-00537 loomstate fabric was used to set the fabric to eliminate internal tensions within the weave. However stress strain properties are significantly affected when synthetic fibres, yarns or fabrics are heat set. Work by Statton (1971) shows that the crystallinity of nylon 6.6 fibres increased with increased heat setting temperature however the orientation of the crystalline regions did not increase. This work was carried out whilst fibres were in an unconstrained condition. If however, the fibres were in a tensioned state as occurs in heat setting treatment it is likely that orientation would also increase and this would contribute to the increase in tensile strength of the fabric. Hearle (1971) summarised structural mechanisms involved in the setting treatment, both at a fabric and fibre level. Between fibres frictional forces are present, and bonding can also occur in the form of weak hydrogen bonds and strong adhesive bonding. Within the fibres chain stiffness, temporary crosslinks, crystallisation and chemical crosslinks can occur (Hearle, 1971) resulting in these mechanisms together achieving a higher tensile strength in the yarn.

The RFL coating then adds further to this strength through impregnation with the matrix. The adhesive sticks the structure together, distributing the load across fibres. The latex polymer may also add to the strength of the coated yarns.

The extension of the fabric exhibited more expected behaviour with the warp direction decreasing gradually during each process. Warp extension is expected to reduce during the coating process due to the tension within the process that straightens the warp yarn and sets it in this position within the heating processes. This in turn causes a reduction in the warp extension as the warp crimp has been reduced. The crimp is transferred to the weft yarn, causing an increase in weft extension. An increase in weft extension has occurred in the first finishing process presumed to be a heat setting finish, however, the addition of the RFL coating causes the weft extension to subsequently reduce. These results are shown in Table 3.4 and Figure 3.4, raw data is contained within Appendix 1.

Table 3.4: Extension of T-00537 Nylon 66 Fabrics

	Strain (%)						
	Loomstate	Warp			Weft		
		Finished	Coated	Loomstate	Finished	Coated	
Mean	67.4	63.8	50.2	43.2	72.3	57.8	
S.D	4.1	2.5	0.8	2.5	1.1	1.3	
C.V	6.1	3.9	1.5	5.8	1.6	2.3	
Minimum	61.5	59.7	49.4	40.3	71.1	56.3	
Maximum	71.3	66.4	51.2	46.4	73.8	59.0	

**Figure 3.4:** The Effect of Coating on Fabric Extension

Due to the adhesive nature of the RFL coating it is thought that the coating inhibits the weft yarn from stretching due to the bonds it forms, making connections both between fibres and within fibres. This limits slippage between fibres and ultimately makes the yarn more brittle.

A similar reduction in elongation was observed in work evaluating the effect of RFL coating on tyre cords. Raumann (1968) found that the latex caused an increase in breaking extension whilst the RF component served to lower both the breaking strength and elongation. Combining both the properties of the RF resin and the latex, the complete RFL dip did reduce breaking strength by 5% and elongation by 4%, however it was concluded that the dip material are of minor importance in the overall load elongation behaviour of the nylon cords.

Further properties of the fabrics can also be analysed by examining the full tensile curve, shown in Figures 3.5 and 3.6. Three areas of fabric tensile behaviour can be analysed from these curves: the inter-fibre friction effect, the decrimping region, the yarn extension region (Grosberg, 1969) as shown in the generalised load extension curve shown in Figure 3.5. The area under the curve also describes the toughness, or energy required to break the fabric. This gives an expression of how the fabric will resist reduction processes.

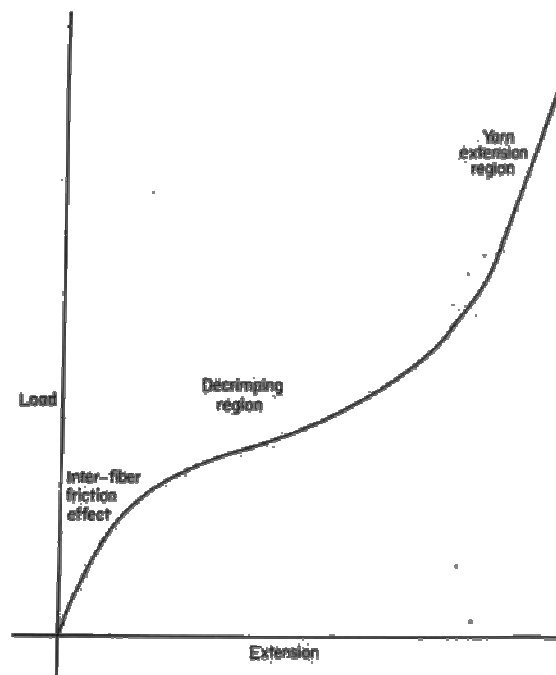


Figure 3.5: Generalised Load-extension Curve of Woven Fabrics. (Grosberg, 1969)

The area of inter-fibre friction effect cannot be seen on the tensile curves of the nylon fabrics (Figures 3.6 and 3.7). Due to the smooth fibre surface of the nylon fibre minimal friction will occur between fibres causing the decrimping action to occur straight away. In the warp direction (Figure 3.6) the loomstate and finished fabric require a similar force to straighten the threads, as seen by the similar height of the decrimping region. However, the loomstate fabric is elongated more in this initial stage. In contrast the initial modulus of the coated fabric is higher, showing that more force is required to straighten the yarns within the fabric. This will be due to the adhesive nature of the RFL coating bonding the fibres and yarns together. The coated fabric is also much less elongated during this stage suggesting that there is less crimp within the coated structure than the finished and loomstate fabrics due to the tension

applied in the coating process. In contrast in the weft direction (Figure 3.7) the coated fabric has a much lower load required for decrimping indicating the increased crimp in this direction that is being straightened out. The coated fabric maintains a higher gradient within the decrimping region than the finished fabric showing the increased force needed due to the bonding between fibres and yarns. The change in fabric structure of the loomstate to finished fabric is also evident from the decrimping region as the loomstate fabric has minimal elongation in this region in comparison to the finished fabric.

Within the yarn extension region the difference in gradient in the warp direction portrays the increase in stiffness from the loomstate, finished and coated fabric, the latter having the steepest gradient and hence the stiffest fabric. This difference in gradient cannot be seen in the weft direction with the finished and coated fabric having a similar gradient and hence stiffness. The loomstate fabric has the highest gradient in the weft direction rendering it to be the stiffest fabric. This suggests that the coating penetrates further into the warp yarns causing more fibres to be bonded together and thus increasing the tensile modulus.

The brittle nature of the coated fabric was also evident in the load-elongation curve. In both warp and weft directions the break of the coated fabric is immediate upon initial failure. The loomstate and finished fabrics, however, maintain some of the load after the initial failure as some yarns remain intact. This is due to the increased mobility of the yarns within the fabric allowing them to redistribute the load across remaining yarns. The bonds between yarns in the coated fabric allow the load to be distributed more effectively throughout the yarn extension region and hence the yarns will fail at the same time.

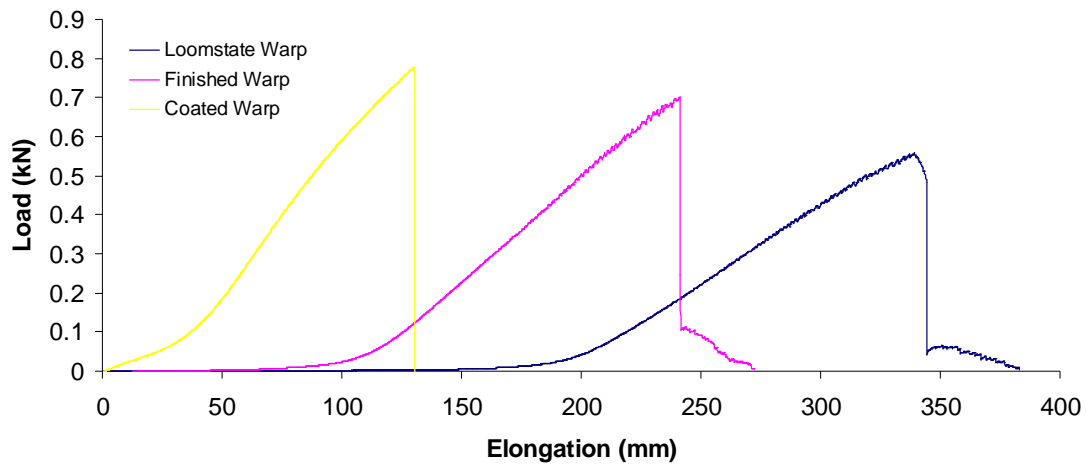


Figure 3.6: Tensile Curves of Fabric in Warp Direction.

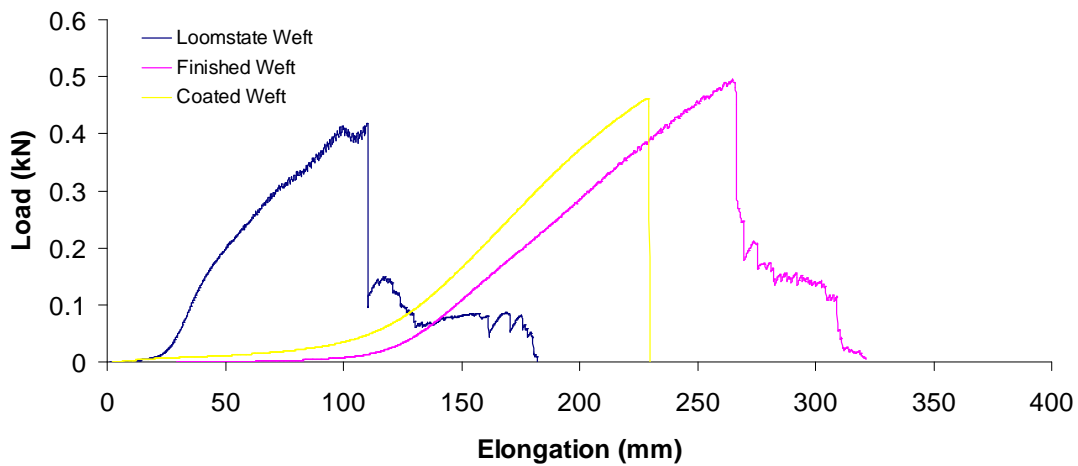


Figure 3.7: Tensile Curves of Fabric in Weft Direction

The energy required to break the sample, or toughness, is equivalent to the area under each curve, these values have been calculated from the raw data and are shown in Table 3.5.

Table 3.5: Toughness of T-00537 Nylon 66 Fabrics

	Energy (kJ)		
	Loomstate	Finished	Coated
Warp	83.03	59.74	24.56
Weft	15.56	61.92	34.42

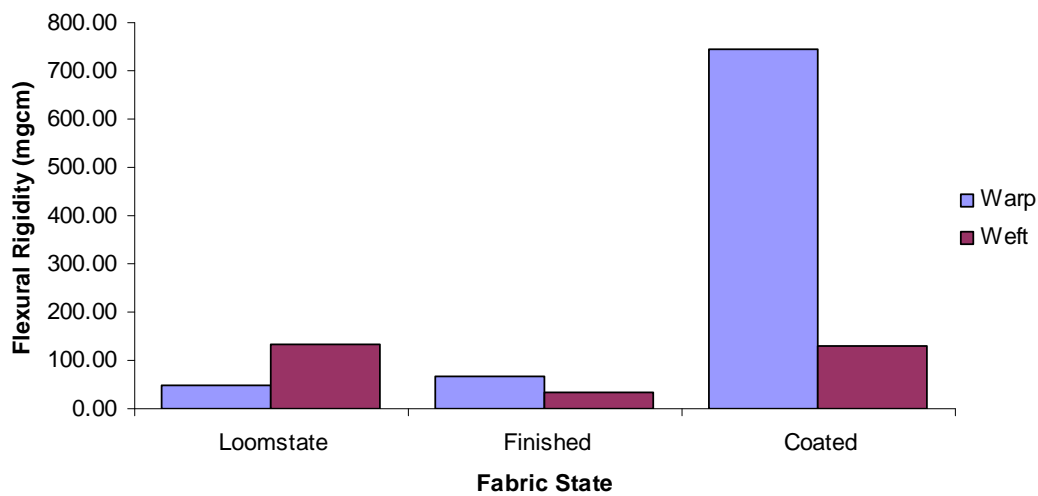
The finishing and dipping processes have made the toughness of the fabric more equivalent in each direction, whereas the initial loomstate fabric has high toughness in the warp and low toughness in the weft. The coated fabrics have a reduced toughness in comparison to the finished fabric, which will make them less resistant to the reduction techniques and therefore are likely to be pulverised to a smaller fibre length in a reduced timeframe.

3.5.2 Bending Rigidity

The bending rigidity data is summarised in Table 3.6 and Figure 3.8, raw data can be found in Appendix 1. As suggested from results in section 3.5.1 the coating causes an increase in rigidity in the warp direction but is not greatly affected in the weft direction. The warp flexural rigidity is increased more than tenfold. This increase in rigidity is similar to that found by Raumann (1968) who also related the rigidity to the number of filament layers the RFL coating had penetrated into the yarn. The reduction in rigidity of the yarns measured by Raumann (1968) related to the calculated rigidity of yarn having 1.5-2.5 filament layers bonded together. It can therefore, be presumed that a similar amount of filaments are bonded together within the yarns in the RFL fabric structure studied, causing the reduction in rigidity of the fabric. Porter (1992) also suggested that the penetration of the RFL adhesive should be 2-3 filaments for optimum adhesion with deeper penetration not contributing to the adhesion properties. The flexural rigidity in the weft direction was reduced by the finishing process before returning to a similar value observed with the loomstate fabric. The rigidity of the coated fabric was only approximately 4 times that of the finished fabric, much reduced from the increase that occurred in the warp direction. The penetration of the coating may therefore be lower in the weft yarns than occurred in the warp yarns. In addition to the penetration the surrounding layer of coating will have an effect on the bending rigidity. As the warp yarn is more parallel than the weft yarn and runs down the centre of the matrix, it has a more constant coating thickness around it, giving a higher rigidity, in comparison the weft yarns have areas of low coating thickness at the peak of their curve and higher coating thickness at the centre, as shown in Figure 1.13. The areas of low coating thickness will therefore increase the weft flexibility at these areas in comparison to the warp yarns.

Table 3.6: Bending Rigidity of T-00537 Nylon 66 Fabrics

	Warp			Weft		
	Loomstate	Finished	Coated	Loomstate	Finished	Coated
Mean Bending Length (cm)	1.63	1.75	4.04	2.28	1.38	2.25
St.Dev. (cm)	0.26	0.09	0.17	0.12	0.08	0.14
Coef.Var. (%)	16.16	5.11	4.10	5.12	5.90	6.29
Minimum (cm)	1.30	1.65	3.90	2.15	1.30	2.10
Maximum (cm)	1.90	1.85	4.35	2.45	1.50	2.45
Fabric Weight (g/m ²)	112	124	113	112	124	113
Flexural Rigidity (mg.cm)	49.5	66.5	745.1	133.7	32.6	128.7

**Figure 3.8:** The Effect of Coating on Fabric Flexural Rigidity

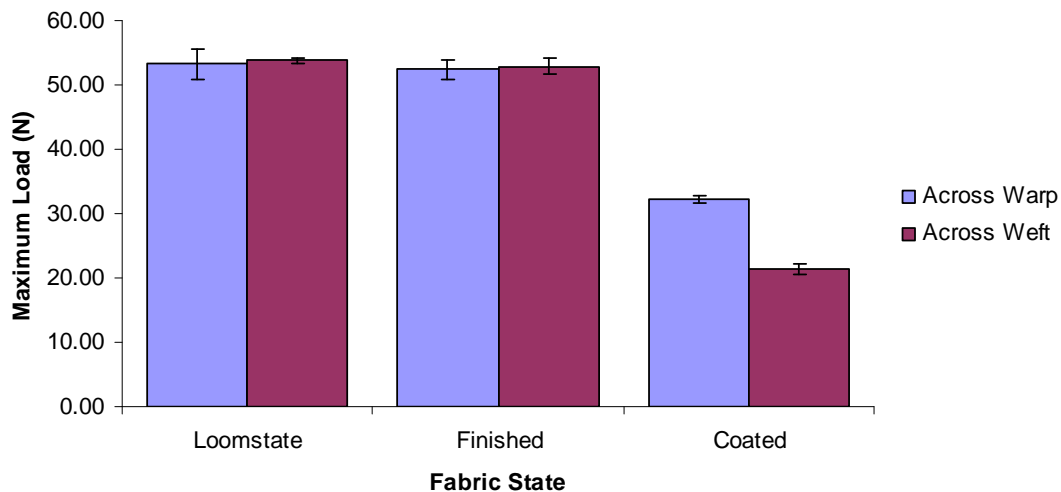
3.5.3 Resistance to Tearing

The tear strength of the fabric was drastically reduced by the coating procedure, Table 3.7 and Figure 3.9. Raw data is available in Appendix 1. As explained in section 1.2.3 this is due to the reduced deformation of the fabric caused by the coating. The coating enables crosslinks to be formed between yarns, holding the yarns in place within the structure. This does not allow for “bunching” of the yarns when a tearing force is applied, and each yarn is therefore broken separately. This reduces the tear strength as the maximum force attained is dependent on an individual yarn rather than a group of yarns working together.

Table 3.7: Maximum Tear Force of T-00537 Nylon 66 Fabrics

Maximum Tear Force (N)						
	Warp			Weft		
	Loomstate	Finished	Coated	Loomstate	Finished	Coated
Mean	53.22	52.37	32.29	53.82	52.91	21.47
S.D.	2.43	1.61	0.54	0.36	1.26	0.79
C.V.	4.56	3.06	1.68	0.68	2.38	3.66
Minimum	56.10	54.09	32.88	54.09	54.49	22.41
Maximum	50.46	50.06	31.67	53.28	51.40	20.67

This reduction in tear strength has occurred in both warp and weft directions; however, it is more severe across the weft yarns. This suggests that although the warp yarns are more rigid they are more able to move across weft yarns and bunch together more easily than the weft yarns. Due to the warp density being much higher than the weft density in the fabric, the warp yarns are able to bunch together more easily than the weft yarns as they are a smaller distance away from each other. Although there is a similar difference in thread density in the loomstate and finished fabrics, the yarns within the finished fabric are able to bunch to a suitable level that its effect on tear strength is not noticeable. When the yarns are unable to move in the coated structure the distance between the yarns means that the force at the point of tearing is distributed between fewer yarns, making the tear strength lower.

**Figure 3.9:** The Effect of Coating on Fabric Tear Strength

This relationship between the thread densities of coated fabrics and the tear strength using the trapezoidal tear test was also seen by Eichert (1994) and Mewes (1989) who noted an increase in tear strength with increased end and pick density. These results

were, however not replicated when leg tear tests were used (Eichert, 1994). This was said to be due to the difference in restraint of the thread system being tested. In trapezoidal testing the thread system being torn is restrained within clamps, whereas in leg tear tests the opposite thread system to the one being torn is held.

Alongside fabric construction, the coating material, coating formulation, adhesion, bonding system and penetration may also have an effect on the tear strength (Mewes, 1989). Wilkinson (1996) suggests the most critical coating factors affecting tear strength to be the location of the coating on the thread system and the penetration of the coating into the fabric interstices, which the fabric structure would affect. As the coating has been applied via a dip process on the fabric tested the location of the coating will not affect how the fabric behaves in the warp and weft direction both the face and back of the fabric have been coated. The way the coating penetrates the fabric interstices may however have more of an effect on the tear strength measured. With the interstices being larger between weft yarns more coating is likely to penetrate between the weft yarns than between the warp yarns, therefore the preferential coating adhesion to the weft yarns would further reduce the tear strength in this direction. However, previous results in section 3.5.2 would suggest that the preferential adherence of the coating is to the warp yarns as the flexural rigidity in this direction was affected more severely. This is likely to be due to the increased number of warp yarns within the fabric structure in comparison to the number of weft yarns. The penetration of coating to the fabric interstices is therefore not seen to have made a great effect on the tear strength between warp and weft in this fabric.

It has also previously been suggested in section 3.5.2 that the penetration of coating into the weft yarns may be lower than occurs in the warp yarns. This will also affect the tear strength as lower penetration will result in less bonds being able to be created and a reduction in adhesion. In turn this reduction in adhesion will allow the yarns to move more easily. The effect of penetration of the coating into the yarn would therefore cause a more severe drop in tear strength in the warp yarns. As this is not seen in Figure 3.9 it can be suggested that the degree of coating penetration into the yarn is not the main cause of the difference in tear strength in the warp and weft direction of the fabric tested. This agrees with literature on the subject where Mewes (1989) found that there was no relationship between tear propagation and adhesion

when coated fabrics with the same substrate from different coaters were compared. Similarly Wilkinson (1996) notes that there is no direct relationship between the degree of coating penetration and tearing strength.

3.6 Summary and Hypothesised Effect of Coated Fabric Properties on Fabric Reduction Methods

The effect that the coating has on the fabric as a whole was to increase its stiffness in the warp direction and reduce the tear resistance in both directions. It was also evident that the coated fabric has increased breaking strength in the warp direction, but reduced energy is required to reach break point. It is likely that during traditional textile reduction methods incorporating pin penetration and shredding the main form of fabric breakdown will occur from tear propagation. The coated fabric will therefore, break up more easily than non-coated fabric initially. Where cutting implements are used in granulator type reduction techniques the stiffness will allow shear forces to have a greater impact upon the yarns and fibres making cutting occur more readily, as the fabric remains at 90° to the forces rather than draping and allowing the knives to abrade across the surface. Once the fabric is reduced to yarns it will be harder to reduce further without a cutting action due to the increased tensile strength of the yarns. As the coating also bonds the fibres together within the yarn it will be more difficult to achieve individual fibres from the coated fabric.

3.7 References

ABBOTT, N. J., LANNEFIED, T. E., BARISH, L. & BRYSSON, R. J. (1971) A Study of Tearing in Coated Cotton Fabrics. *Journal of Coated Fibrous Material*, 1, 4-17.

BRITISH STANDARDS (1968) BS 4303:1968 Determination of the resistance to tearing of woven fabrics by the wing-rip technique. 22 March 1968 ed., British Standards Online.

BRITISH STANDARDS (1990) BS 3356:1990 Determination of bending length and flexural rigidity of fabrics. 31 August 1990.

BRITISH STANDARDS (1994) BS EN 1049-2:1994 Textiles. Woven fabrics. Construction. Methods of analysis. Determination of number of threads per unit length. 15 March 1994 ed.

BRITISH STANDARDS (1998) BS EN 12127:1998 Textile. Fabrics. Determination of mass per unit area using small samples. British Standards Online.

BRITISH STANDARDS (1999) BS EN ISO 13934-1:1999 Textiles. Tensile Properties of Fabrics. Determination of maximum force and elongation at maximum force using the strip method. 15 May 1999 ed., British Standards Online.

EICHERT, U. (1994) Weaving and coating processing influences (Fabric Rendement). *Journal of Coated Fabrics*, 24, 20-39.

GROSBURG, P. (1969) The Tensile Properties of Woven Fabrics. In Hearle, J. W. S., GROSBURG, P. & BACKER, S. (Eds.) *Structural mechanics of fibers, yarns and fabrics*. New York, Chichester, Wiley-Interscience.

HARRIS, A. P., METCALFE, R. A. & PATRICK, S. G. (1994) PVC [Polyvinyl Chloride] Plastisol Bonding Agents: The Influence of Formulation Variables on Performance. *Journal of Coated Fabrics*, 23, 260.

HEARLE, J. W. S. (1971) The Nature of Setting. In Hearle, J. W. S. & Miles, L. W. C. (Eds.) *The setting of fibres and fabrics*. Watford (276 Hempstead Rd, Watford, Herts.), Merrow Publishing Co. Ltd.

MATTINSON, E. H. (1960) The coating of fabrics with P.V.C. *Journal of the Textile Institute Proceedings*, 51, P690-P698.

MEWES, H. (1989) Adhesion and tear resistance of coated fabrics from polyester and nylon. *Journal of Industrial Textiles*, 19, 112-128.

PORTER, N. K. (1992) RFL dip technology *Journal of Coated Fabrics*, 21, 230.

RAUMANN, G. (1968) Some mechanical properties of resorcinol-formaldehyde latex (RFL) tyre cord adhesive. *Textile Research Journal*, 38, 627 - 633.

SEN, A. K. & DAMEWOOD, J. (2001) *Coated textiles: principles and applications*, Boca Raton, FL; London, Taylor & Francis.

STATTON, W. O. (1971) Synthetic Fibres: Structure and Setting. In Hearle, J. W. S. & Miles, L. W. C. (Eds.) *The setting of fibres and fabrics*. Watford (276, Hempstead Rd, Watford, Herts.), Merrow Publishing Co. Ltd.

WILKINSON, C. L. (1996) A review of industrial coated fabric substrates. *Journal of Industrial Textiles*, 26, 45-64.

4.0 Reduction Processes and their Effect on Fibre Length, Coating Integrity and Polymer Degradation

4.1 Aims.

In order to further process the RFL coated nylon fabric, it is likely that the substrate will need be broken down into a workable form, suitable to be used as a base material for other production routes. This chapter evaluates three approaches to “reducing” the fabric: 1) The Laroche Cadette shredder - a traditional textile shredding method; 2) The Hollander beater – a traditional method of reduction in the paper industry; and 3) The Intimus disintegrator - an innovative alternative reduction processes, to establish the forms of fibrous material that are able to be created for use in recycling routes. In addition, the coating integrity on the reduced forms has been assessed with regard to the possibility of coating removal. The effect that these processes have on polymer degradation has also been explored through thermal analysis so the nylon polymer quality can be determined.

4.2 Introduction to Reduction Processes.

4.2.1 The Laroche Cadette Shredder.

The Laroche Cadette shredder (Figure 4.1) is a traditional textile recycling reduction machine designed for in-house recycling of fibrous material. It is suitable for all types of production waste from spinning, weaving, knitting and dry laid nonwovens. It consists of between one and six opening sections, each of which contain two cylinders, the first of these is made up of flat teeth, while the second is made up of steel wire card clothing. This shears the fabric against a bedplate. The working width can be between 500 mm and 1000 mm and it is capable of production speeds of up to 250kg/hour (Laroche, 2012). The Laroche Cadetter Shredder used for this work was based at the University of Leeds, School of design.

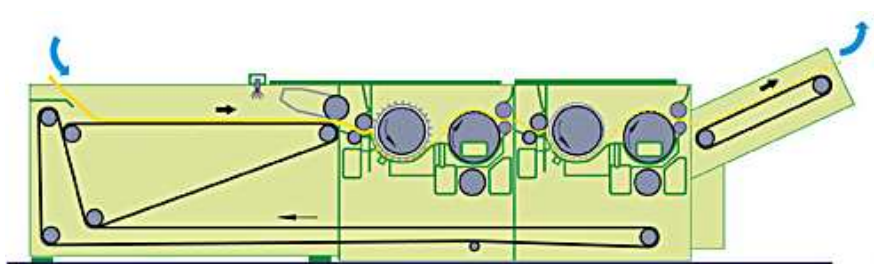


Figure 4.1: The Laroche Cadette with 2 opening sections (Laroche, 2012)

4.2.2 The Hollander Beater

The Hollander beater was invented in the 18th century and consists of an oval tank around which the pulp slurry circulates. Figure 4.2 illustrates the main parts of the Hollander beater where the tank is divided on one of its lengths by a large cylinder roll and bedplate. The cylinder has a number of bars attached, parallel to its axis. Similarly, the bedplate also consists of bars across its surface. The roll revolves causing the pulp to circulate around the tub. At the divide, the pulp is forced between the cylinder and the bedplate, causing the rubbing and brushing action on the fibres.

In order to control this action, the cylinder roll can be raised or lowered. This enables fibres to pass the roll with little shear action. Alternatively, increased pressure between the cylinder roll and bedplate enables a cutting action, rather than an abrasive action to work on the fibres. The beater roll position is measured from the down position (D) which is the biting point between the roll and bedplate where they are just touching. Positions higher and lower than this are measured using turns up (TU) and turns down (TD), respectively. The backfall is used to ensure the circulation of the pulp (Swanson, 1964). This machine is designed for use within the paper industry for beating and refining paper stock, however, it was initially created for reducing cotton rags to a paper pulp. Traditionally, the Hollander beater uses pulp consistencies of about 6% by weight of cellulose to water.

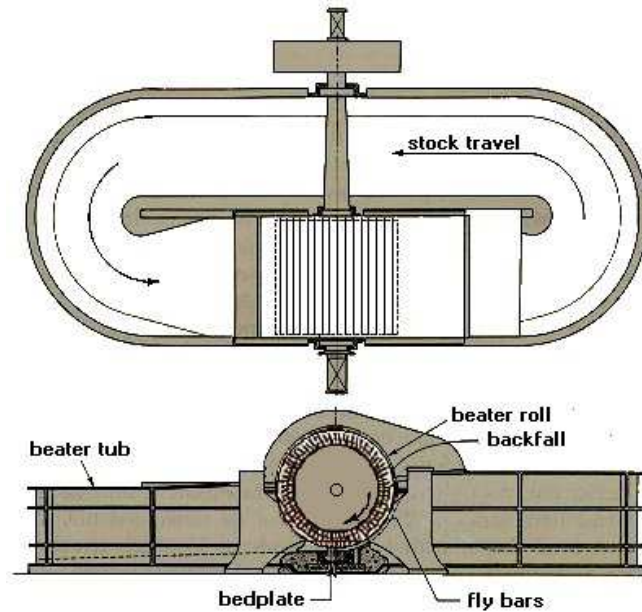


Figure 4.2: Diagram of the Hollander Beater (University of Minnesota, 1998).

4.2.3 The Intimus Disintegrator

This machine is traditionally used for the destruction of bank notes, paper and electronic media (Martin Yale International, 2010). It utilises rotary knives that feed and cut the material against stationary knives. The reduced material leaves the cutting chamber via a screen, ensuring that all reduced material is smaller than the mesh of the screen. The screen can be changed to permit a range of shred sizes in order to optimise the user's needs.

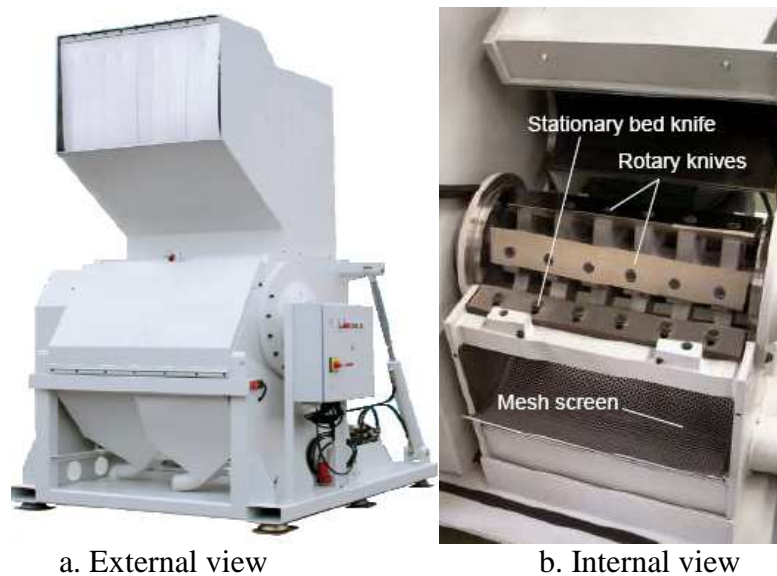


Figure 4.3: Intimus Power Disintegrator (Martin Yale International, 2010).

4.3 Reduction of Coated and Uncoated Material

The aim of this work was to determine the potential for breaking the coated fabric down to fibre form. Secondly, to analyse what fibre lengths could be achieved from the use of each of the three reduction methods. It was also important to see the type of damage caused to the fibres from the processes and how the coating integrity was affected.

4.3.1 Materials

Waste fabric from Heathcoat Textiles consisting of a mixture of fabric specifications was used for this work. The waste was primarily false selvages from the weaving process and faulty fabric offcuts identified during inspection. The fabric was separated into RFL coated nylon 6.6 waste and uncoated nylon 6.6 waste, in order to assess how the coating affected how the material was reduced.

All waste used in this study was from one batch of waste sent from Heathcoat Fabrics and as such the raw material used within the study has remained as constant as possible given that it is a waste product that is being dealt with.

4.3.2 Reduction Procedures

4.3.2.1 Laroche Cadette.

500g of waste fabric was cut into strips of approximately 30cm long in order to be a suitable input to the Laroche Cadette. The material was inputted through the feed of the Laroche Cadette shredder with 1 opening section. This was repeated 3 times in order for the majority of the material to be broken down to fibre form.

4.3.2.2 The Hollander Beater

A guillotine was used to cut the fabric to strips of approximately 30 cm in length so that they were a suitable size for use in the Hollander beater. The roll was positioned to “4 turns up” (TU) from the contact point with the bed plate and the fabric strips

were added to the Hollander beater to reach a consistency of 1% by weight of solids to water. A reduced consistency was used to that traditionally used when processing pulp slurries since the nylon behaves differently to cellulose fibres, the increased water content helps with the flow of the fibres and separation. Increased solid content is used in pulp slurries to cause better fibrillation of the fibre which was not required for the nylon. To achieve this 3.5 kg of fibres were used with 350 L of water. The beating procedure was as described in Table 4.1. Samples were taken at 0 minutes (before the strips had been added to the beater) then at 10, 20, 30, 40 and 50 minutes after the first waste had been added. Small samples, of approximately 2 g were taken at various points in the rotation of the slurry to form the full sample of approximately 20 g representing the fibre population of the pulp.

Table 4.1: Processing Conditions for Beating trial A
(TU = Turns Up, D = Down Position ie biting point)

Time (min)	Beater Roll Setting	Amps	Remarks	Sample Taken
0	4TU	11-25	To fill for 10 mins.	Raw Material
5	4TU	11-25	All waste added to beater	No
10	4TU	11-25	Dewatering drum engaged.	Sample 1
15	1TU	11-22	To further beat fibres.	No
20	1TU	11-25		Sample 2
30	D	13-18		Sample 3
40	D	13-18		Sample 4
50	1TD	13.0	Amps become constant	Sample 5
51	20 TU		Beating stopped	

A second beating trial was undertaken to subject the fibres a lower shearing action and potentially produce longer fibres. This was achieved by using a higher consistency of fibres and lowering the beater roll at a slower rate.

Coated fabric was cut into strips of approximately 30cm x 5cm and added to the beater at a consistency of 1.5% solids with the beater roll set at 10 turns giving a gap between the beater roll and bedplate of 2.5 mm. The first sample was taken before adding more fabric to a consistency of 2%. Beating was continued at this consistency and beater roll position, taking samples at 5 and 10 minutes. The beater roll was then lowered to 7 turns up, then 5 turns up and 2 turns up before finally lowering to datum. Fibre samples were taken at 5, 10, 15, 20, 30, 40 and 50 and minutes after the roll being lowered. The beater roll was left in some settings for a longer period of time if it was observed that work was still being done on the fibres at that setting. Work being done on the fibres can be seen by observing the current changes of the beater motor, as well as looking at the changes in the fibres. Samples were continued to be taken at 5 minute intervals and the beating procedure is summarised in Table 4.2.

Table 4.2: Processing Conditions for Beating trial B

Time From First Addition to Beater (mins)	Conc.	Beater Roll Setting	Amps	Remarks	Samples Taken
0	0	10TU	11-18	Start adding fabric to beater.	No
15	1.5%	10TU	13-18		Sample 1
20	2%	10TU	13-35	Stop adding fabric to beater	No
25	2%	10TU			Sample 2
30	2%	10TU			Sample 3
31	2%	7TU	14-18	Roll turned down	No
35	2%	7TU			Sample 4
40	2%	7TU			Sample 5
45	2%	7TU			Sample 6
46	2%	5TU	14-18	Roll turned down	No
50	2%	5TU			Sample 7
55	2%	5TU			Sample 8
56	2%	2TU	16-30	Roll turned down	No
60	2%	2TU			Sample 9
65	2%	2TU			Sample 10
66	2%	D	22-32	Roll Turned down	No
70	2%	D			Sample 11
75	2%	D			Sample 12

4.3.2.3 The Intimus Disintegrator

Initial investigations, described as “trial A” were based on 500g, inputted into the Intimus disintegrator. The Intimus Disintegrator is a batch process requiring all the material to be inputted at one time point. A mesh size of 2 mm was used to filter the shredded material at the output of the Intimus disintegrator. A second investigation, “trial B” was also undertaken which used a decreased materials input quantity of 100g.

Output material from the Laroche Cadette was used for this trial as oppose to the fabric waste. The same mesh filter size as the initial investigation was used.

4.3.3 Fibre Measurement

Fibres samples from each of the reduction processes were measured in one of three ways, depending on the fibre lengths and density of the output material achieved from the reduction procedures: 1) projection of fibres onto a screen; 2) image analysis from light microscopy; and 3) sieve fractionation.

4.3.3.1 Projection

Fibres were arranged on slides then using an overhead projector, images were projected onto a screen. The fibre images were measured by an opisometer (BS ISO 6989:1981). Ten slides were made up for each sample. To make each slide, one milligram (approx.) of fibres were taken from the sample using tweezers, and laid on the slide. The fibres were then separated using the tweezers and a needle. Each slide was then laid on a projector parallel to a gradicule and the image projected onto a screen. Ten fibres from each slide were measured by tracing the projected image with the opisometer and compared to the gradicule scale. A total of 100 fibre lengths were taken for each sample. This method may have some bias with longer fibres more likely to be selected when picking out fibres from the sample using tweezers. Although a random selection of fibre lengths were selected to be measured, the process was done manually, picking fibres that “focused well”. Therefore, a true random selection of measured fibres may not have been obtained. Due to the fibre length being up to 160mm, light microscopy could not be used for all samples and this alternative method provided an appropriate level of accuracy for fibres of this length.

4.3.3.2 Microscopy and Image Analysis

Shorter fibres could be analysed, avoiding the bias mentioned above, through light microscopy using a Projectina microscope and PIA-4000 imaging software. Slides were made using the previous method, micrographs of the fibres were taken and the fibre lengths traced on screen. The PIA-4000 program calculated their length from known calibrated measurements, which were set from known lengths on each of the

images. All fibres within the image could be analysed as images were able to be focussed more effectively due to the shorter fibre lengths lying flat against the slide. An objective magnification of 1.0x and an eyepiece magnification of 10x was used for this work. Replicates of either 100 or 500 fibres were used in this method.

4.3.3.3 Fractionation by Sieving

Hard particulate material formed during use of the Intimus disintegrator was separated by size using a sieve method. Sieves of mesh size 10, 12, 16, 30, 44, 60 and 85 were used to separate the material into 8 fractions. 25 g of particle material was separated by shaking the sieve system by hand for a period of 5 minutes. The resultant material within each fraction was then weighed and the percentage by weight for each fraction was calculated. Triplicates of this method were performed each using 25g as a starting sample size.

4.3.4 Results and Discussion

4.3.4.1 The Laroche Cadette Shredder

The Laroche Cadette shredder was successful at opening up the coated fabric. However, it was difficult to reduce the material down to single fibres, instead the coated material stayed within a yarn form as shown in Figure 4.4. In contrast the uncoated fabric was broken down more effectively; however small pieces of fabric still remained. Multiple operations or many opening systems would be required in the reduction process to provide fibres suitable for further processing. Reduction of coated fabric to fibre form is likely to be more challenging because the coating used to bond the polyamide fibres to the rubber acts to bond the fibres within the yarn together. The methylol groups in the RF resole and the amide groups of the nylon form a covalent bond, and hydrogen bonding also occurs as discussed in section 1.2.2.4. The shear stresses the fabric is subjected to during the shredding process are neither likely to be strong enough nor directed accordingly to break these bonds to separate the coating from the polymer chains.

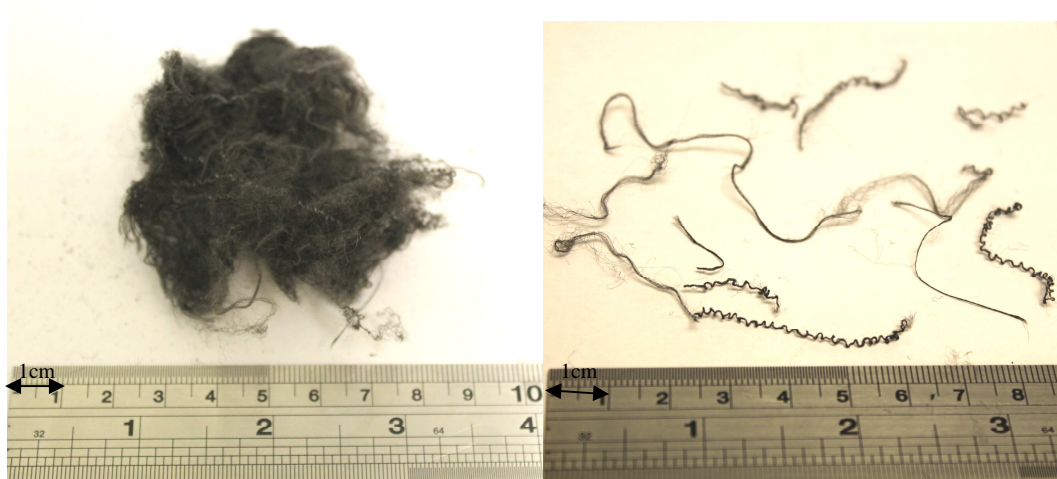


Figure 4.4: Typical Breakdown Output from the Laroche Cadette Shredder.

Fibres were measured using the projection and opisometer method. One hundred fibres from each sample were measured and the results can be seen in the histogram depicted in Figure 4.5. It was found that the RFL coated material was more likely to be reduced to a shorter length and a lower range of fibre lengths were also seen. This is likely to be due to the added stiffness that the coating brings to the fibre, shown in section 3.5.2. Increased stiffness will cause the fabric and yarn pieces to remain straight allowing the flat teeth and steel wire clothing act upon the entire piece. When the pin clothing is unable to pull apart the yarns within the fabric, increased force on the yarns will cause increased breakages. In comparison more flexible uncoated fabric and yarn pieces will move with the force provided by the flat tooth and pin clothing allowing yarns and fibres to be untangled and picked out of the fabric, keeping the force imparted on the fibres to a minimum and allowing fewer breakages to occur.

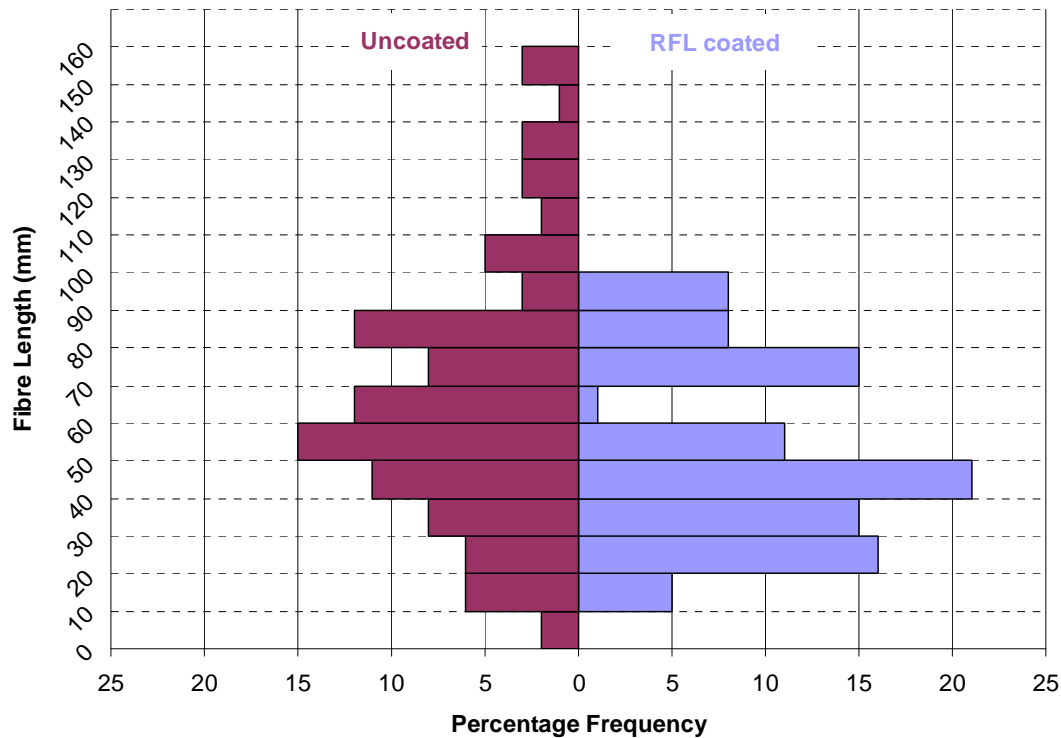


Figure 4.5: Fibre Length of Material Reduced by Laroche Cadette Shredder.

4.3.4.2 The Hollander Beater

It was observed during the beating process there was excessive foam formation which was kept under control using the dewatering wheel and hose. This would be unsuitable in a mass production environment, due to the manual labour required and it is suggested that defoamer would be used. The resultant foam affected the circulation of the pulp in the Hollander beater, which in turn affected the rate of breakdown of the fibres. Therefore, it is essential that the production of foam is kept to a minimum. It is probable the foam occurred due to chemicals added to the fabric in previous finishing processes, such as surfactants or lubricants.

Another point to note is that the nylon fibres floated on the surface of the water. This did not affect the breakdown of the fibres although it could possibly present a problem in mass production processes where the pulp has to flow through pipes. Nevertheless after 50 minutes of beating, the fibres were more evenly dispersed throughout the water, although when the agitation was stopped the fibres rose to the surface.

It was evident that the fibres were broken down easily using the Hollander beater, offering a range of fibre output as shown in Figure 4.6. This method is a viable method for breaking down the fibres and offers a suitable material for further study.

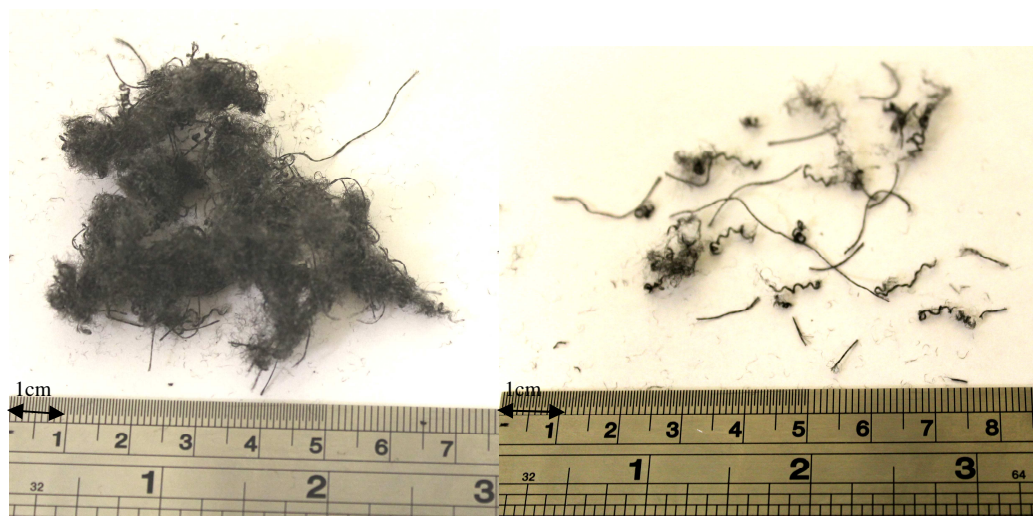


Figure 4.6: Typical Breakdown Output from the Hollander Beater

Initial studies to assess how the fabric reduced with beating time showed that fibre length decreased very quickly within the first 20 minutes. Investigations were performed with both uncoated and RFL coated fabric to compare the difference in their breakdown. Beating was undertaken and samples obtained as described in Trial A, Table 4.1. 100 fibres from each sample were measured using the microscopy method. It was found that for the RFL coated fabric the fibre is reduced to a short length over the first 20 minutes, but with further beating the rate of reduction was considerably reduced. This effect is illustrated in Figure 4.7 where the fibre length plateaus at 30 minutes which coincides with the time the beater roll was lowered to D. This is to be expected, as large clumps within the beater will be trapped within the metal bars on the roll and bed plate causing a shearing action to break up the material further. Once the small fibres have been formed, they are passed through the roll and bed plate without being affected. In comparison, the uncoated fabric is reduced to this short length almost immediately with the first sample taken having a mean length of just 4.4mm. This observation demonstrates the comparative ease of reduction of the uncoated fabric due to the absence of a binding substance. The standard deviation of the values from the mean fibre length, shown as error bars in Figure 4.7, reduces with time to a constant value, indicating that with both the coated and uncoated fabrics the

lowering of the beater roll and increased time helps to create a more uniform length, by breaking down the longer fibres further.

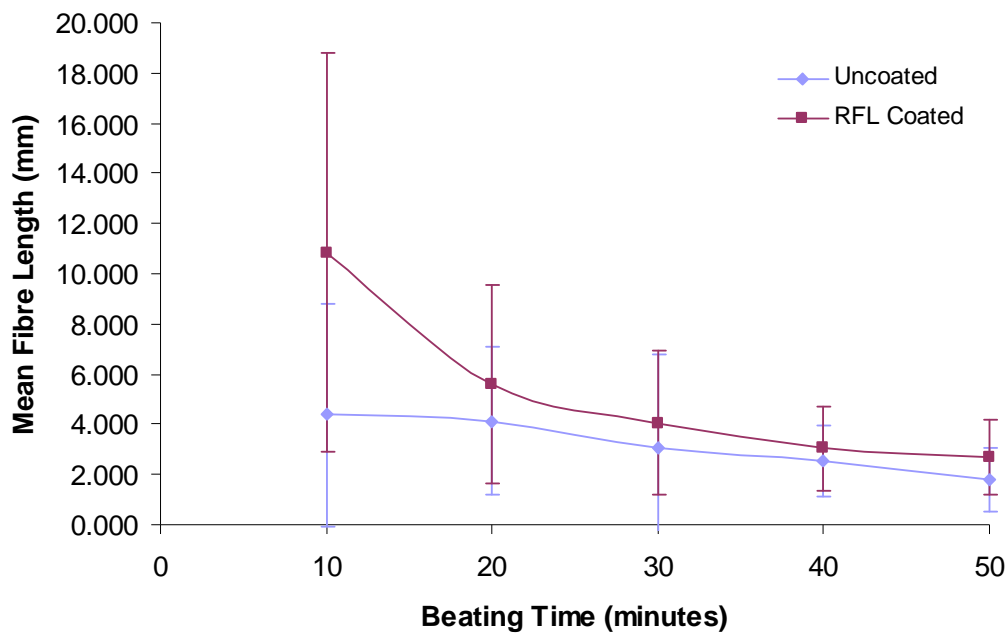


Figure 4.7: Average Fibre Length of Uncoated and RFL Coated Reduced Material Throughout Beating Trial A. (Error bars = Standard deviation of fibre length)

After 10 minutes of RFL fabric reduction in the beater, there were many cut yarns that had not been fully broken down to their individual filament form. These consisted of both fairly straight cut yarns which originate from the warp yarns within the fabric and highly crimped yarns that originate from the weft yarns within the fabric. The cut yarns were surrounded by very small fibres the majority of which are 2 mm or less. There were also some longer fibres that have been broken to individual filaments from the cut yarn. The uncoated fibre sample after 10 minutes reduction time consisted of very few cut yarns, rather most fibres were in a single cut filament form and there were also many small “dust-like” fibres. Figure 4.8 shows a comparison between the two fibre length distributions after 10 minutes beating time.

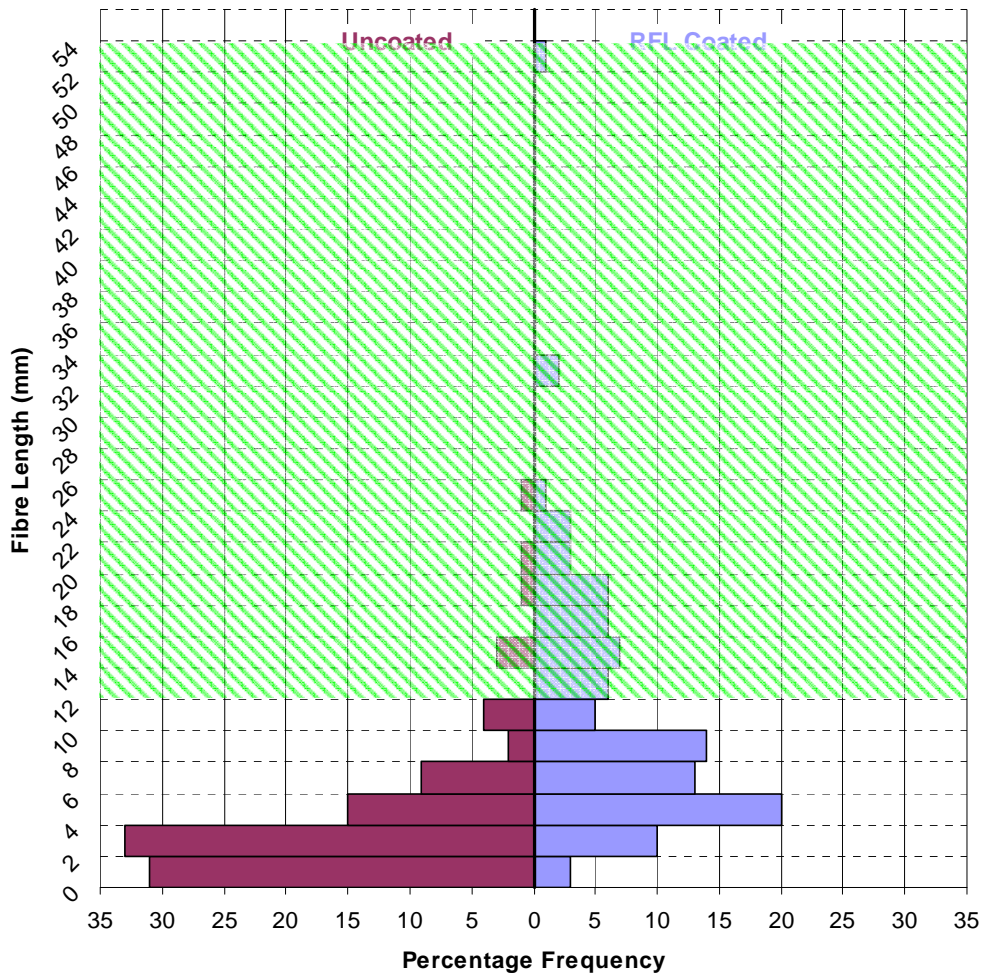



Figure 4.8: Fibre Length Distribution of Uncoated and RFL Coated Material after 10 minutes Beating.  = Fibre length suitable for spinning

After 50 minutes of beating time, as suggested by the reduced standard deviation, shown as error bars in Figure 4.7, the fibre length distribution significantly reduced with all fibres being in the range of 0mm to 7mm. There was also less variation between the fibre lengths of RFL material and uncoated material, Figure 4.9, suggesting that although the RFL fibre were initially more difficult to break up, with sufficient time the Hollander beater will reduce material to this fibre range.

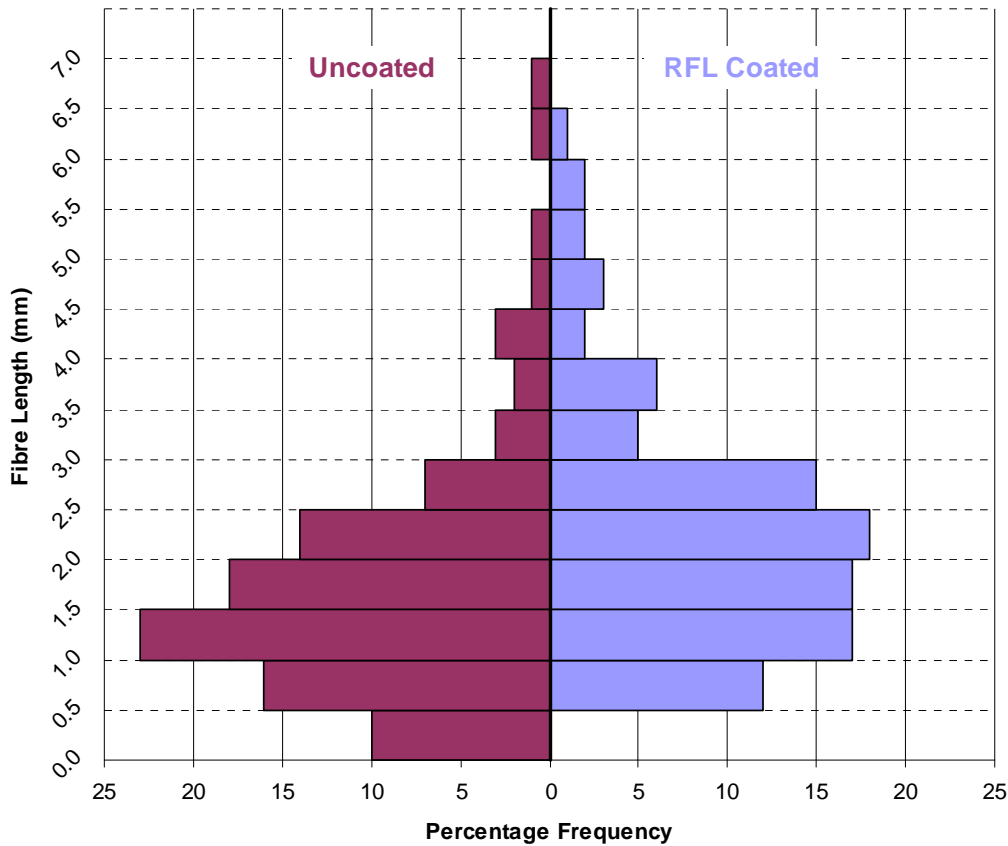


Figure 4.9: Fibre Length Distribution of Uncoated and RFL Coated Material after 50 minutes Beating.

In order to achieve lengths suitable for textile spinning, fibres should be over 15 mm long (Klein, 1986). Fibres less than 4 - 5 mm will be lost as fly waste during the spinning process, whilst fibres of 5 - 12 mm offer bulk to the yarn, but will not contribute to its strength properties. Fibres above 12 - 15 mm offer the positive characteristics necessary for spinning yarns suitable for use in further processes such as weaving and knitting. The reduction results at 10 minutes (Figure 4.8) indicate that this method of breakdown could produce fibres suitable for textile processing. However, as the majority of fibres are too short for spinning, the reduction method would need to be adjusted, or separation of the short fibres via an alternative route would need to be developed.

In order to gain a higher percentage of fibres above 12 - 15mm in length, the RFL coated fibres in a cut yarn form need to be broken down further without causing the yarns to be cut. Similarly, reduced cutting is required on the uncoated fibres where

breakdown to filaments has occurred. This could be achieved by continuing to beat the fibres with a wide gap between the beater roll and bedplate. Consequently, this would cause less cutting action to the fibres, as there is more space maintained for the fibres to circulate past the beater roll. The consistency of the fibre suspension could also be increased causing more fibre to fibre contact, rather than fibre to metal contact. A second effect would be an increase in the friction occurring between fibres as they are forced between the roll and bedplate, enabling breakdown of the fabric with minimal cutting action (as is caused by the fibre to metal abrasion). Figure 4.10 demonstrates this concept of higher consistency causing less cutting action to the fibres.

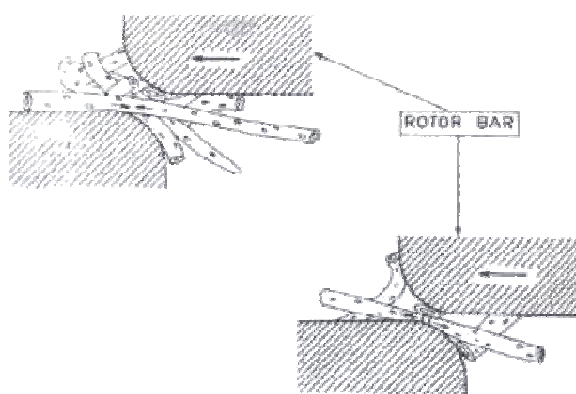


Figure 4.10 *The Effect of Consistency on the Amount of Fibre to Fibre Contact causing Friction and Fibre to Metal Contact causing Cutting Action. (Smook, 2002)*

In order to test this proposal, Trial B in the Hollander beater was completed using a 1.5% consistency of RFL coated fabric to water by weight. A sample of 500 fibres were measured from each batch collected using the opisometer method for samples 1-10 and microscopy for sample 11 and 12 as these fibres were too small to get clear projected images. The trial was completed on the RFL material only, as during trial A at a beating drum position of 4TU the initial 10 minute sample consisted of 94% 12mm or less in the uncoated fabric, in comparison to 65% in the RFL coated material. The remaining 35% of RFL material was mostly in a cut yarn form and therefore would make up a larger percentage by weight. The RFL material therefore offered a better opportunity to produce long fibres by this method.

The results of the trial (illustrated in Figure 4.11) concurred with the result of trial A and demonstrated that the fibre lengths prior to the beater being in full contact with

the bedplate at Datum (D) were very varied with samples having a high standard deviation. At the Datum point, the fibres were quickly reduced down to a uniform length of 2.4 mm having a very small standard deviation of 1.3mm within sample 11. Prior to reaching this point, a step wise pattern is seen in the fibre length each time the beater roll is turned down, this is most evident at 45 minutes and 55 minutes. The first 10 samples were generally made up of cut yarn samples and as such they could be identified as being from warp or weft yarns. Warp yarns were straight, whereas weft yarns have been crimped in the manufacturing process prior to fabric production and coating, therefore having a curly appearance. This distinction can be seen in Figure 4.6. The projection and the microscope measurement methods allowed measurements to be taken with the weft fibres in their curled state. The lengths of the warp and weft yarns were also compared to each other with each sample containing 250 warp yarns and 250 weft yarn pieces. It was found that the weft yarns were generally of a longer length in comparison to the warp yarns, this was the case in all samples. A possible explanation is their crimped nature, as in their relaxed state they are shorter and statistically less likely to come into contact with the beater roll at this length.

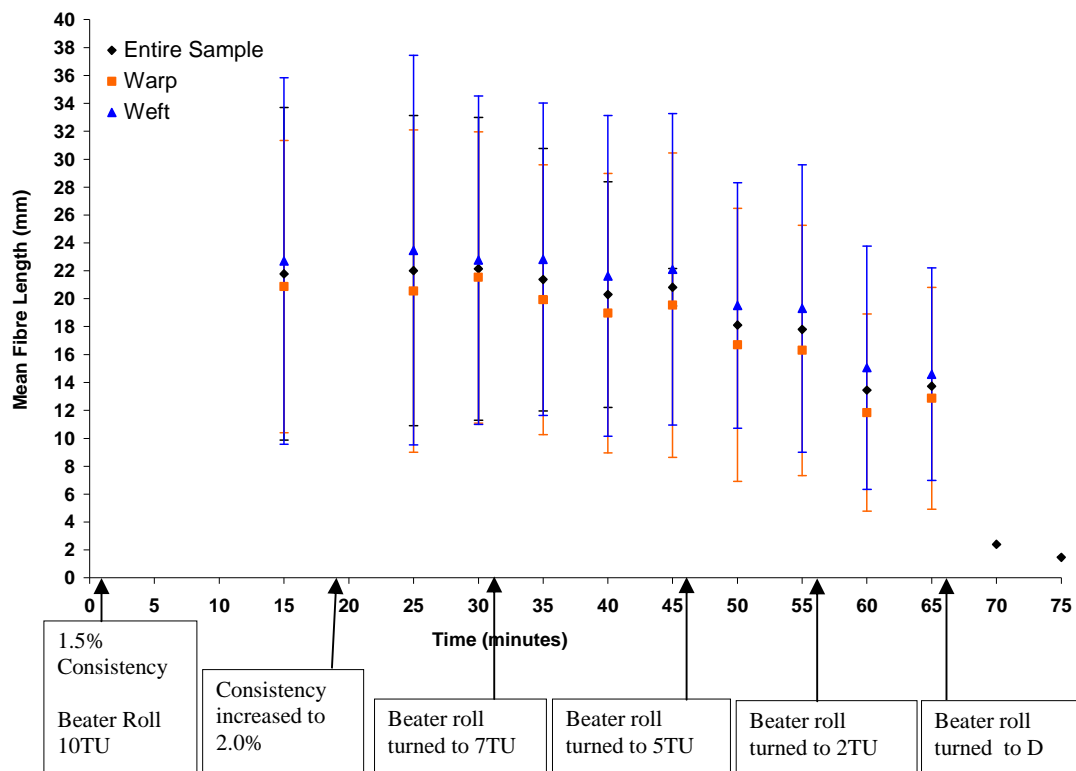


Figure 4.11: Average Fibre Length of Uncoated and RFL Coated Reduced Material Throughout Beating Trial B.

Although individual filaments were unable to be extracted in most cases, by controlling the beater roll setting, cut yarn lengths could be maintained. This has enabled the majority of yarns to be above 15 mm in length in a 66% of samples, whilst eliminating fabric pieces. Although lengths were produced within the suitable range for spinning it is unlikely that this method could be used to reclaim fibres for spinning processes as the fibres remain bonded to one another resulting in stiffness being maintained. In this form, the fibres are unlikely to be pliable enough to maintain the twist imparted to the yarn in the spinning process.

Figures 4.12 to 4.17 show the fibre length distributions at each beater roll step taken within trial B. As suggested in the overview of the fibre lengths in Figure 4.12, there is little difference between the fibre length achieved at 10TU, 7TU and 5TU. Any of these positions could therefore be used over a prolonged length of time to produce this fibre distribution. It is only when the beater roll was lowered to 2TU that above 50% of the fibres become less than 15 mm. Significant reduction then takes place when the beater roll was lowered to D.

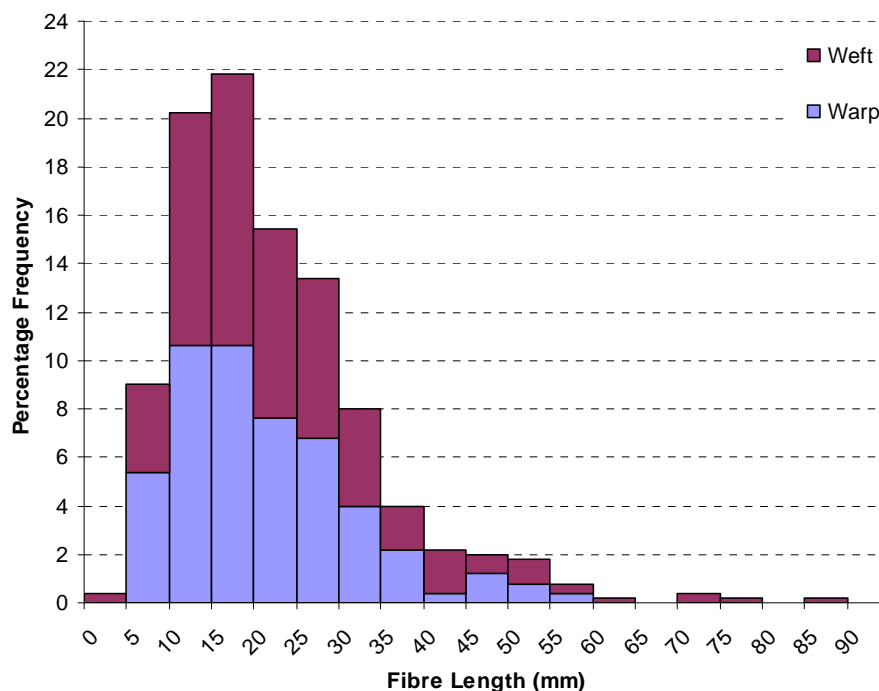


Figure 4.12: RFL Coated Fibre Length Distribution at 15 minutes 10TU 1.5%
(Trial B).

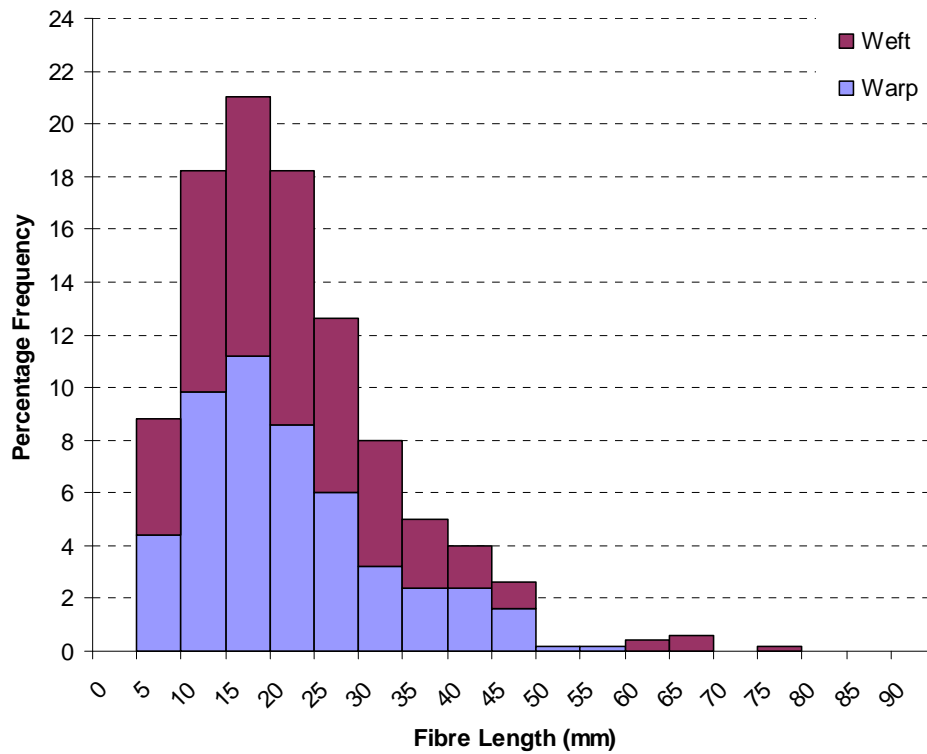


Figure 4.13: RFL Coated Fibre Length Distribution at 30 minutes 10TU, 2% (Trial B)

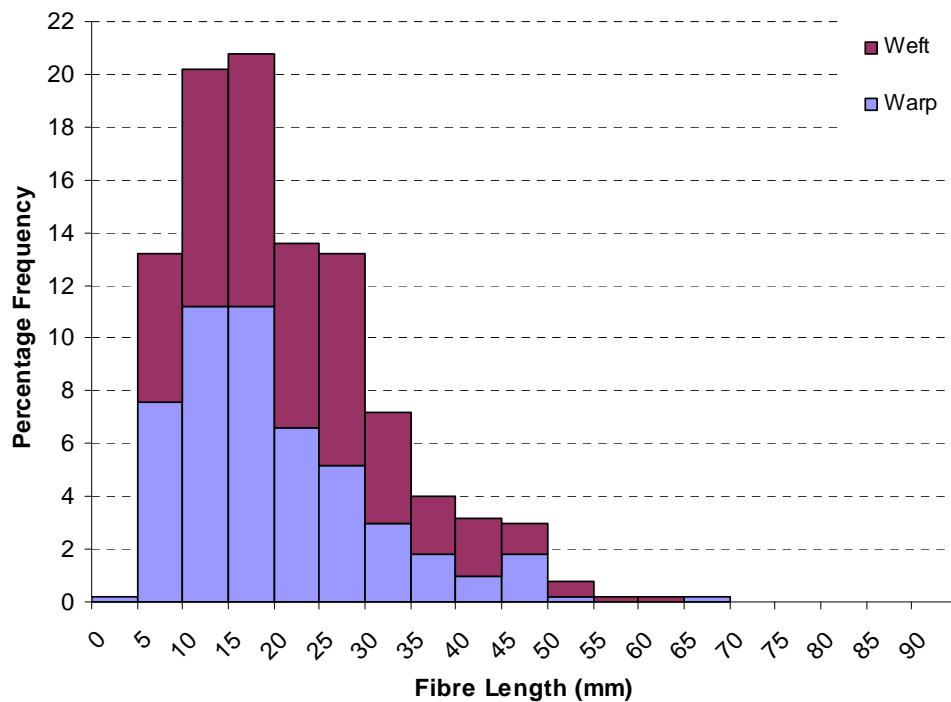


Figure 4.14: RFL Coated Fibre Length Distribution at 45 minutes, 7TU, 2% (Trial B)

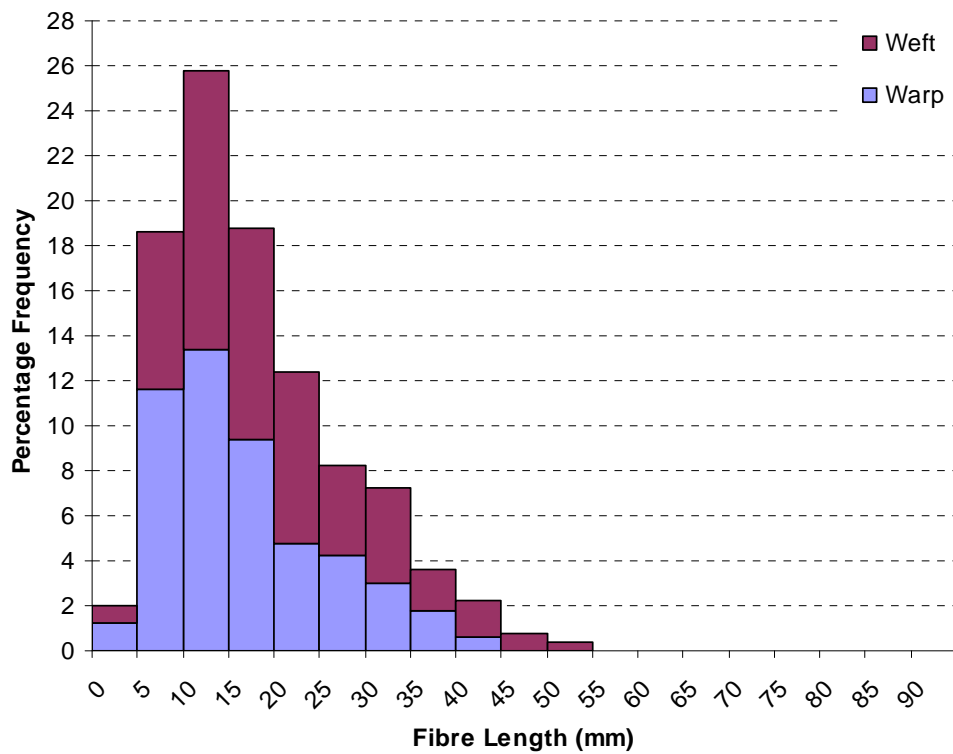


Figure 4.15: RFL Coated Fibre Length Distribution at 55 minutes, 5TU, 2% (Trial B)

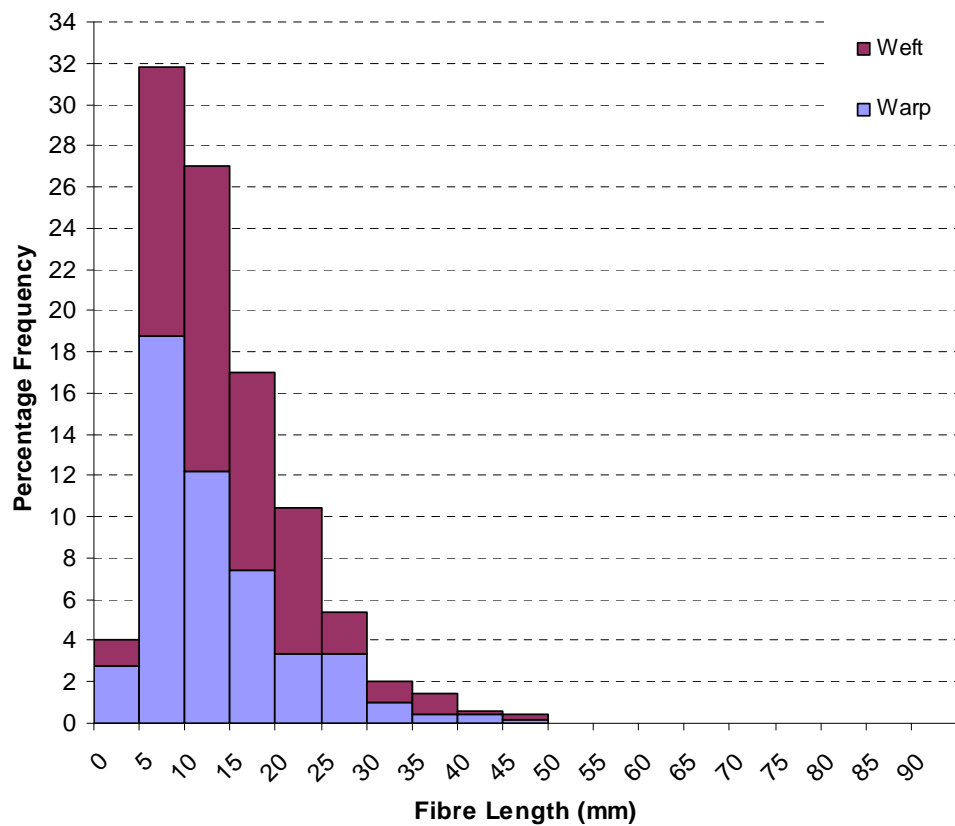


Figure 4.16: RFL Coated Fibre Length Distribution at 65 minutes, 2TU, 2% (Trial B)

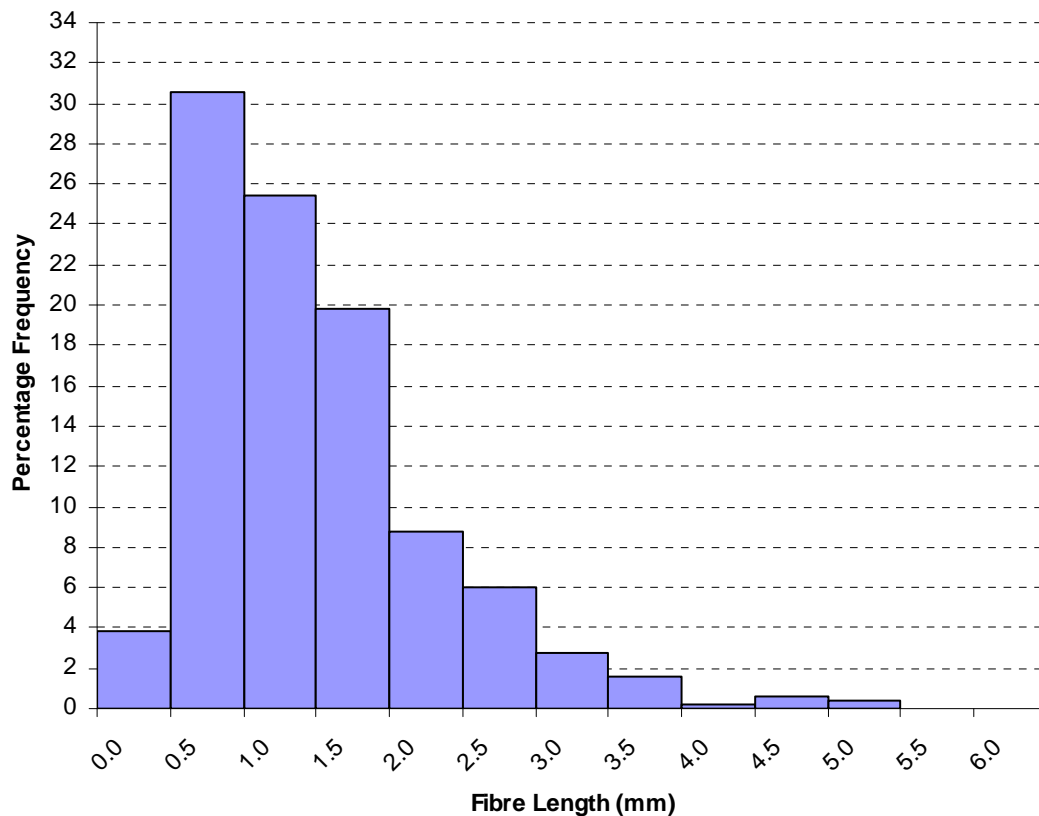


Figure 4.17: RFL Coated Fibre Length Distribution at 75 minutes, D, 2% (Trial B)

4.3.4.3 The Intimus Disintegrator

The output from the Intimus beater in trial A was low, as frictional heat build-up limited the amount of fibre throughput that could be achieved. Initial work produced flaky particulate material as due to the action of the disintegrator, as shown in Figure 4.18(a). This was expected to be due to the polymer reaching near melting point and smearing against the chamber sides. The flakes were irregular in shape and often had a folded structure. In order to minimise heat build up within the cutting chamber it was necessary to use low batch sizes, and pre-cut the waste prior to shredding. This type of output could be useful for further plastic recycling processes. Trial B produced fibres from this process (depicted in Figure 3.18(b)), allowed through utilisation of pre-reduced material from the Laroche Cadette shredder. The throughput of material was reduced, using a batch size of 100g as appose to the 500g used in trial A, to stop heat build-up so that fibres could be produced. In addition to the low output, material was easily contaminated with fibres from previous processing operations. The

disintegrator would therefore require thorough cleaning between each material change to maintain the recyclate quality.

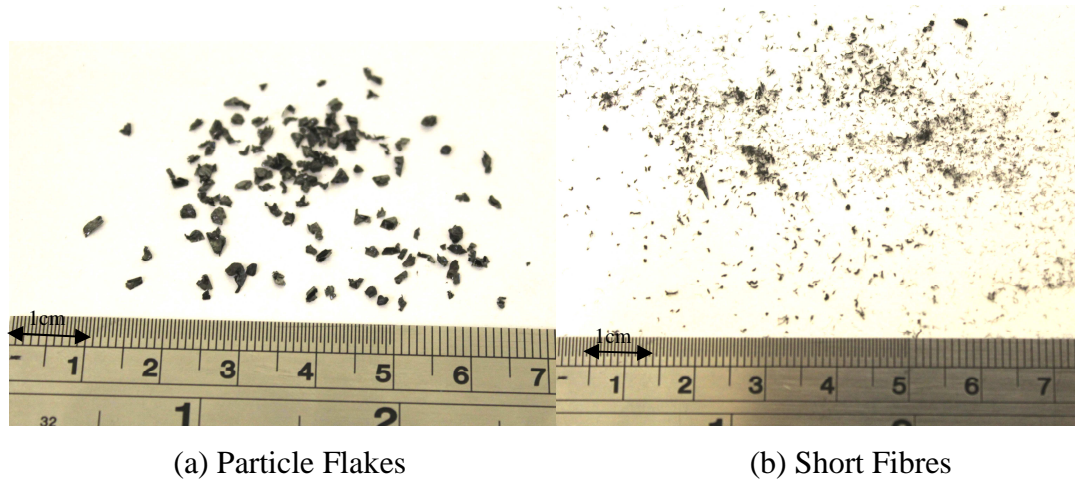


Figure 4.18: Typical Breakdown Output from the Intimus disintegrator.

The particulate material formed in trial A was measured using the microscopy technique (section 4.3.3.2). Outlines of the particle perimeters were measured and from this, the equivalent diameter was calculated using the PIA-4000 software. Figure 4.19 shows the particle size distribution and it is evident that the particles were of a smaller size than the lengths produced using the Hollander beater at the Datum point. In addition it is clear that they were also a more uniform size than previously observed with the fibres having a standard deviation of 0.53 mm. This is likely to be due to the screen used on the materials exit from the cutting chamber as particles larger than the mesh size cannot escape from the cutting chamber.

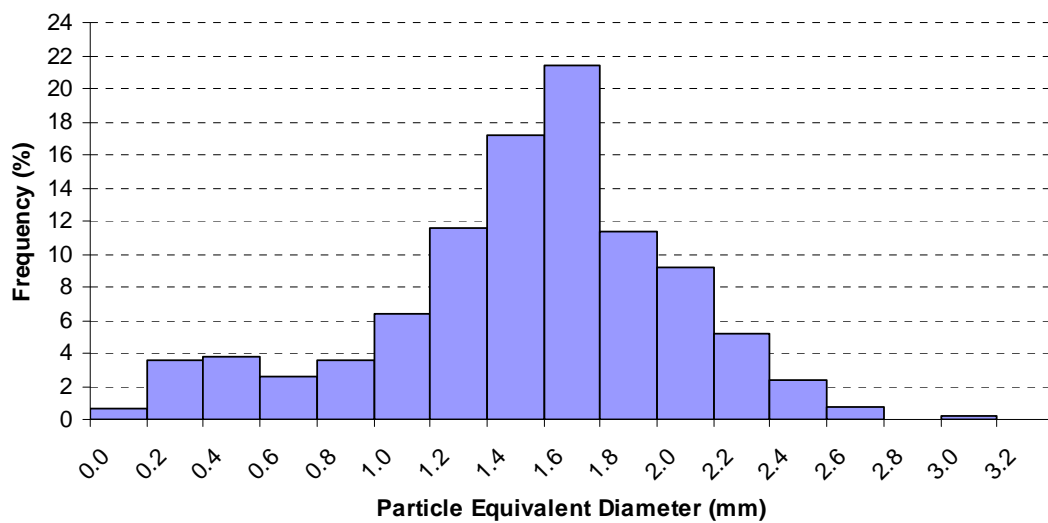


Figure 4.19: Particle Size Distribution of RFL Coated Material Reduced by the Intimus Disintegrator (Trial A).

The material was also assessed by the sieving fractionation technique (section 4.3.3.3), results of which can be seen in Figure 4.20. However differences are evident between the two data sets; with both sets of data showing a normal distribution as would be expected, however, the peak of this distribution shows particles having a lower size in the sieve fractionation data. The mean peak occurs at 1.6 - 1.8 mm equivalent diameter in the image analysed data, whereas the majority of material was within the sieve mesh sizes of 1 - 1.4mm. Further analysis of the larger particles shows that 50.6% of material over 1.8 mm equivalent diameter in the image analysed data compared to only 1.44% left in the sieve with a mesh size of 1.7 mm. It is likely that the sieve fractionation data set is more accurate for smaller particles than the microscopy method. The microscopy method relies on the resolution of the human eye, there will also be human error when sampling particles from the image as particles that focused well were selected and the outline could be identified easily.

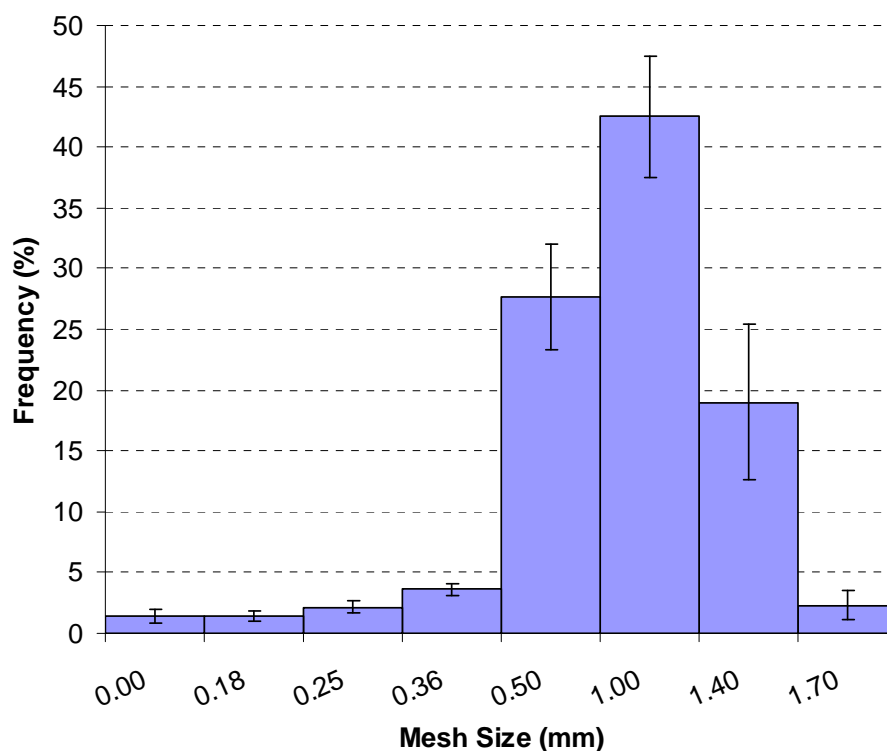


Figure 4.20: Particle Size Distribution by Weight of RFL Coated Material Reduced by the Intimus Disintegrator Trial A, Analysed using Fractionation by Sieving.

The anomaly within the larger particles was probably due to the flake-like structure of the particles. When assessed via image analysis, particles were shown in a 2D perspective. Since the particles were flake-like, the thickness of the particles was smaller than the length and width measured in the image analysis. The larger particles found in the image analysis may have been sieved through a smaller mesh size as due to agitation they are able pass through in any direction. The fraction into which they are grouped would therefore be determined from the minimum feret diameter. The equivalent diameters in the image analysis data were calculated from the perimeter lengths, assuming circular particles. In reality the particles were a range of shapes and aspect ratios, the equivalent diameter is therefore likely to be longer than the minimum feret diameter. Figure 4.21 describes these measurements with an example particle shape.

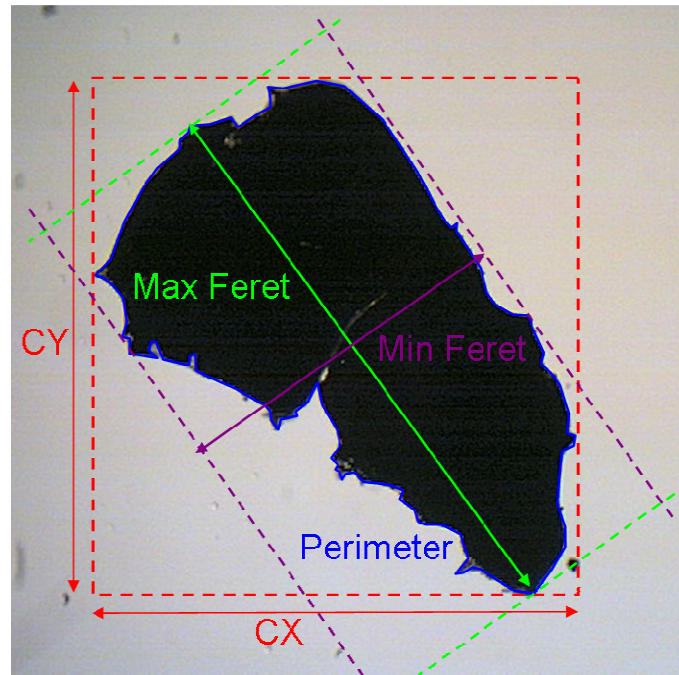


Figure 4.21: Size Descriptors in Particles.

Material from the trial B where RFL coated and uncoated pre-shredded material from the Laroche Cadette was disintegrated into fibres was also compared. Samples of 500 fibres from both batches were measured using the microscopy technique. A comparison of the fibre distributions is illustrated in Figure 4.23. The maintenance of fibre length of the uncoated material compared to the coated material mirrored previous observations in section 4.3.4.1. This may be due to the difference in the input material, the uncoated material from the Laroche Cadette having a longer fibre length than the coated material. In comparison to the input material, the output material was less varied. Fibres used for reinforcement generally have a length of around 6.4 mm (Boonstra, 1982). Fibres created during the Intimus disintegration process were all lower than this, but this length could be increased by using a more open mesh size in the screen.

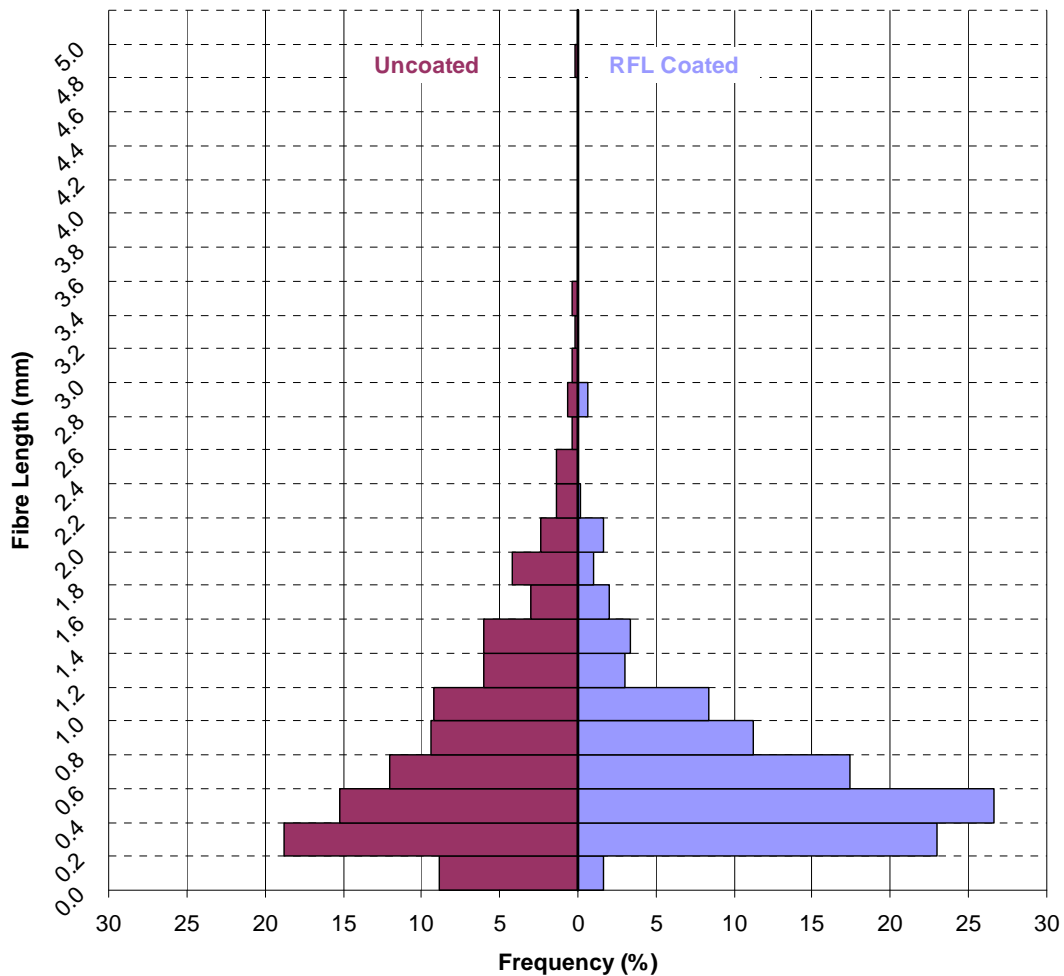


Figure 4.22: Fibre Length Distribution of Uncoated and RFL Coated Material Initial Laroche Cadette Shredding Followed by Intimus Disintegration.

4.4 Microscopic analysis

4.4.1 Materials

Waste fabric from Heathcoat Textiles (as described in section 4.3) and the material produced from the reduction processes outlined in 4.3.2 was used for this work. The waste material consisted of a mixture of fabric specifications; two types of coated material and two types of uncoated material made up the majority of the waste. The material analysed prior to breakdown includes both these fabric types for comparison, referred to as Coated A, Coated B and Uncoated A, Uncoated B. The output material was reduced from a mixture of all coated or all uncoated waste.

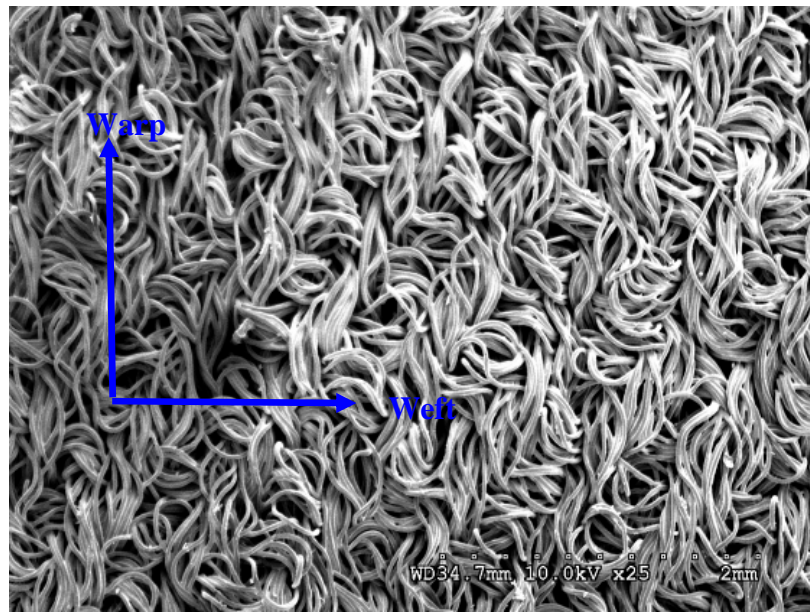
4.4.2 Method

A Hitachi S-3000N scanning electron microscope (SEM) was used to picture both the broken ends of the samples and the coating integrity after reduction processes. Stubs were prepared using black carbon tape to stick fibres or fabric to the metal stub. The fibres were not gold coated; however, acceptable quality micrographs were obtained using an acceleration voltage of 10kV to limit charging.

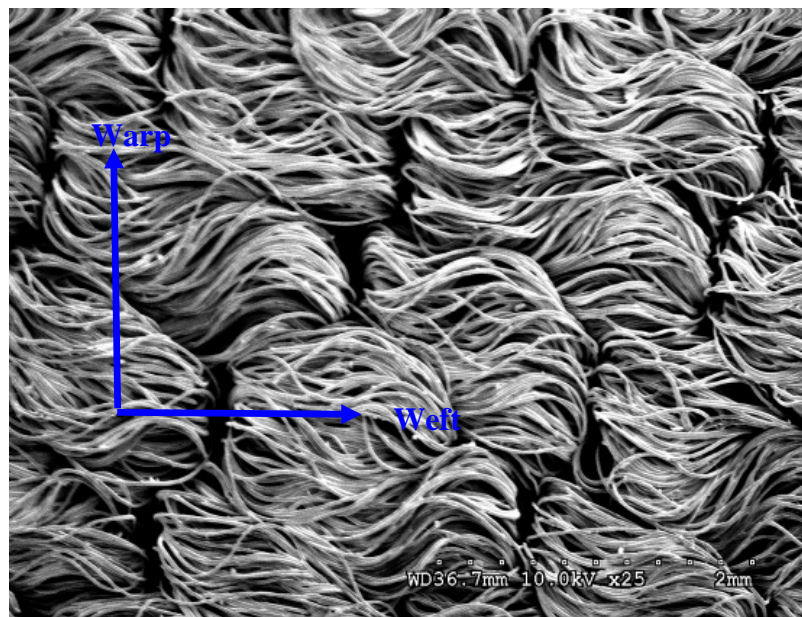
4.4.3 Results and Discussion

4.4.3.1 Original Waste Fabric

Figure 4.23 illustrates the surface topography of the coated fabrics A and B at a low magnification. It is unclear at this magnification how the coating behaves on the fibre surface and its integrity before the reduction process. In comparison to Figure 4.24 (which illustrates two uncoated fabrics at the same magnification), there is no appreciable difference between the fibre surfaces. Nevertheless the filament fibre structures are clear in both coated fabric and uncoated fabric micrographs with the coating not masking the fibres completely.

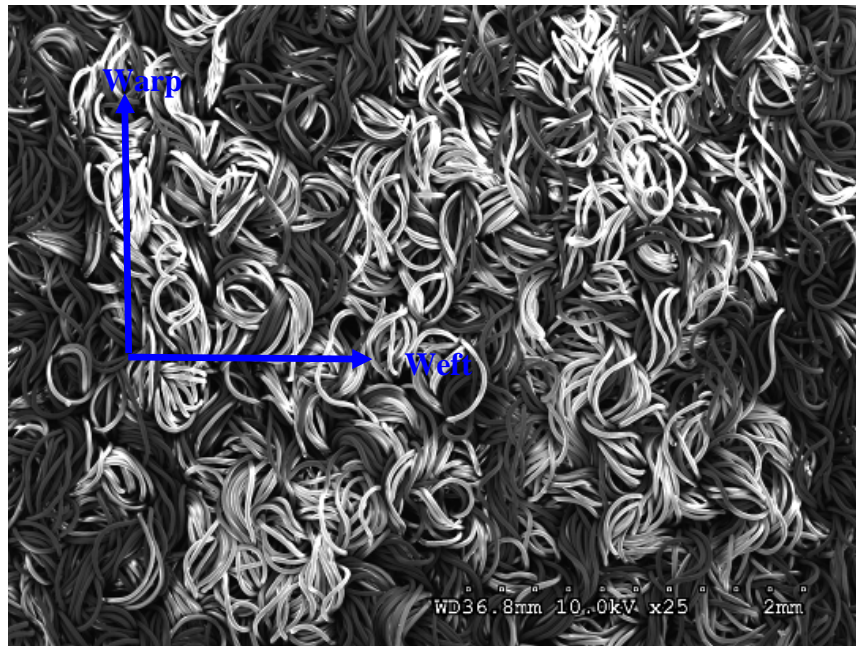


Coated A

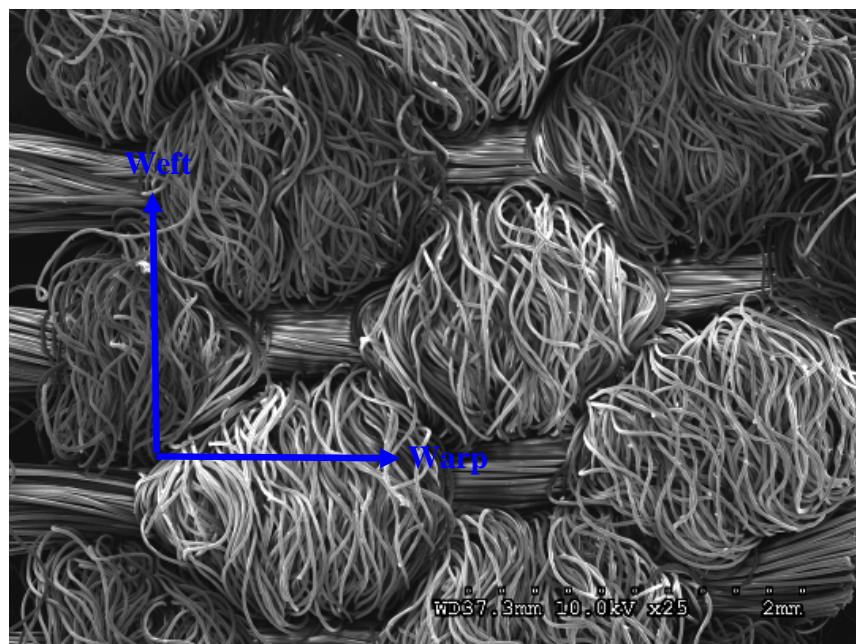


Coated B

Figure 4.23: SEM Micrographs of Face side of Two Common Types of Coated Fabric Waste, at a Magnification of x25



Uncoated A



Uncoated B

Figure 4.24: SEM Micrographs of Face side of Two Common Types of Uncoated Fabric Waste, at a Magnification of x25

At the higher magnification of x250, Figure 4.25, for fabric “Coated A” and Figure 4.26 for fabric “Coated B”, it is clear that the coating is bonding fibres together where they are adjacent to each other in the structure. This can be observed clearly in Figure 4.25(b) and Figure 4.26(b) where 6 or more fibres are bonded together in both cases. The adhesive coating can also be observed at yarn crossover points in Figure 4.25(a)

and 4.24(b). However, even before the reduction processes have been carried out, there are areas on the yarn where the coating is cracking between the fibres (as Figure 4.25(b)), or does not cover the surface of the yarn evenly (as centre of Figure 4.25(a)). The uncoated fabrics illustrated at the same magnification in Figure 4.27 and 4.28 are more smooth and reflective. Although the coating is not always obvious on the yarn structure from the adherence between fibres, the dulling aspect is seen more clearly when the coated and uncoated fabrics are compared.

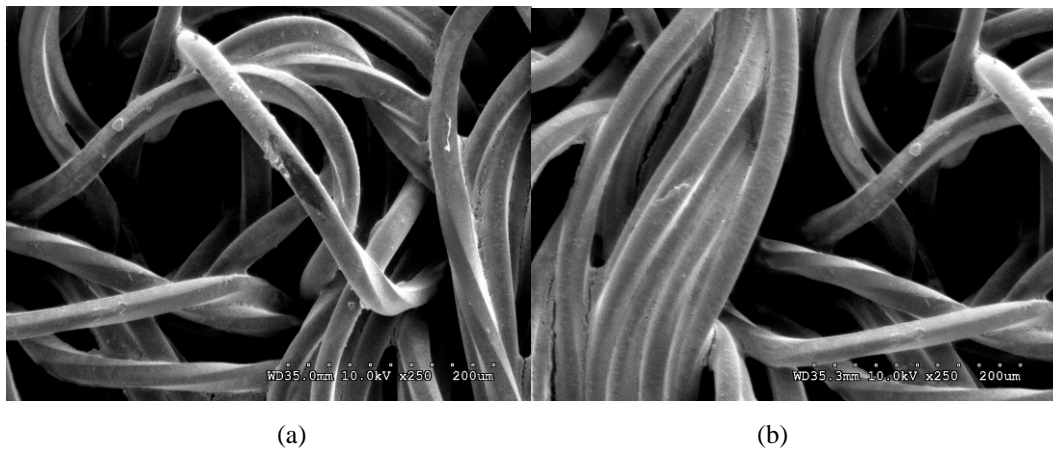


Figure 4.25: SEM Micrograph of Coated Fabric A at a Magnification x250

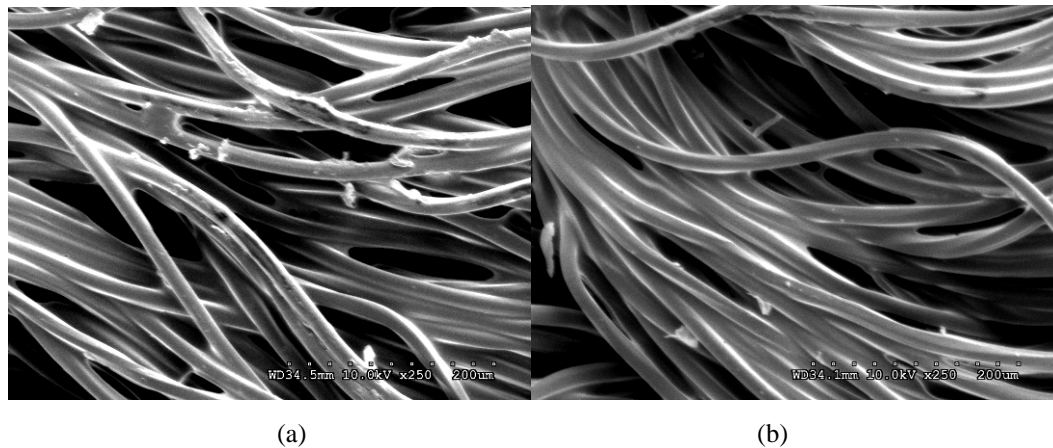


Figure 4.26: SEM Micrograph of Coated Fabric B at a Magnification x250

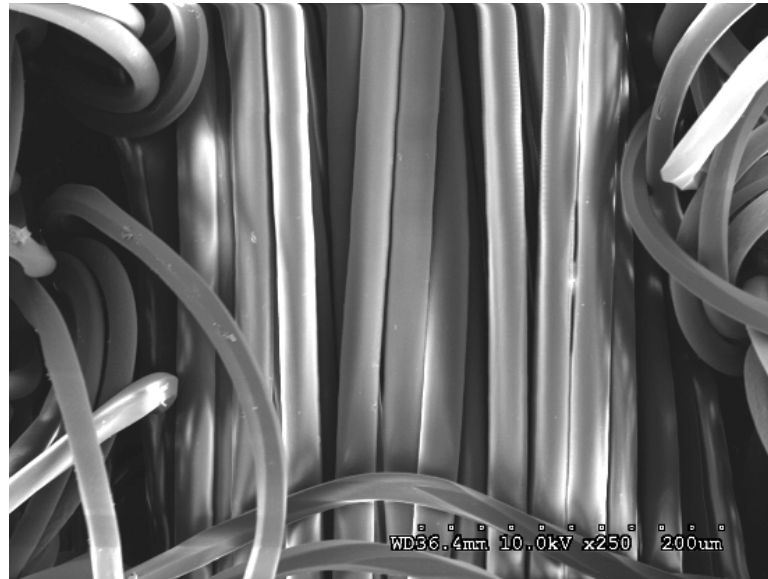


(a)

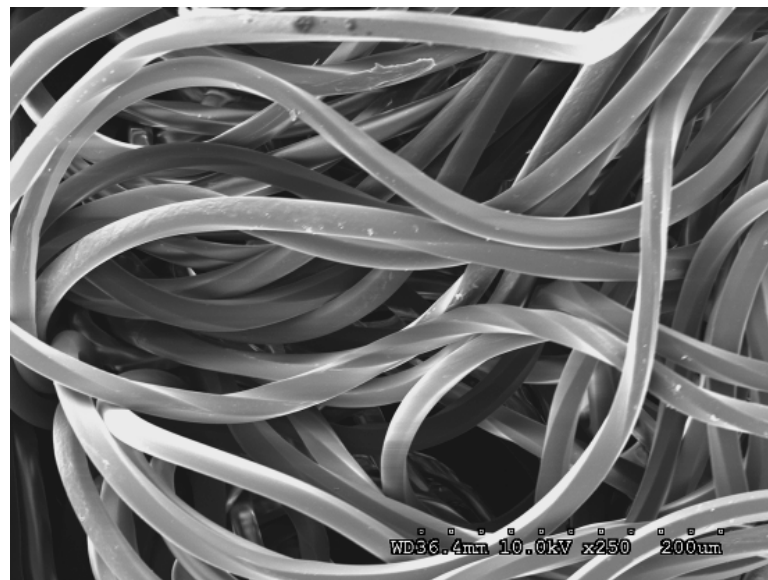


(b)

Figure 4.27: SEM Micrograph of Uncoated Fabric A at a Magnification x250



(a)



(b)

Figure 4.28: SEM Micrograph of Uncoated Fabric B at a Magnification x250

4.4.3.2 Laroche Cadette Reduced Material

The effect that the Laroche Cadette reduction process had on the coating integrity and the breakage points can be seen in Figure 4.29(a) and (b). From the SEM micrograph image (a), it can be seen that the coating has been relatively unaffected with two fibres still adhering together along their length. However, there seems to be less bonding contact between fibres at cross over points in comparison to Figure 4.26(b). It is possible that where the coating links fibres together with a small area of surface contact, the Laroche Cadette can pull these fibres apart. Where the surface contact

areas are greater, the pin clothing of the Laroche Cadette is unable to disrupt the coating in order to separate the fibres. It is likely that a similar rule will apply to that of fibre pull out which is used to assess failure of composite structures and the energy required to debond the fibres in the matrix. Equation 4.1 describes the factors associated with this function.

$$Wd = \frac{\pi d^2 \sigma_f^2 l_d}{24 E_f} \quad (\text{equation 4.1})$$

Where d = fibre diameter

σ_f^2 = fibre strength

l_d = the length of the debonded region

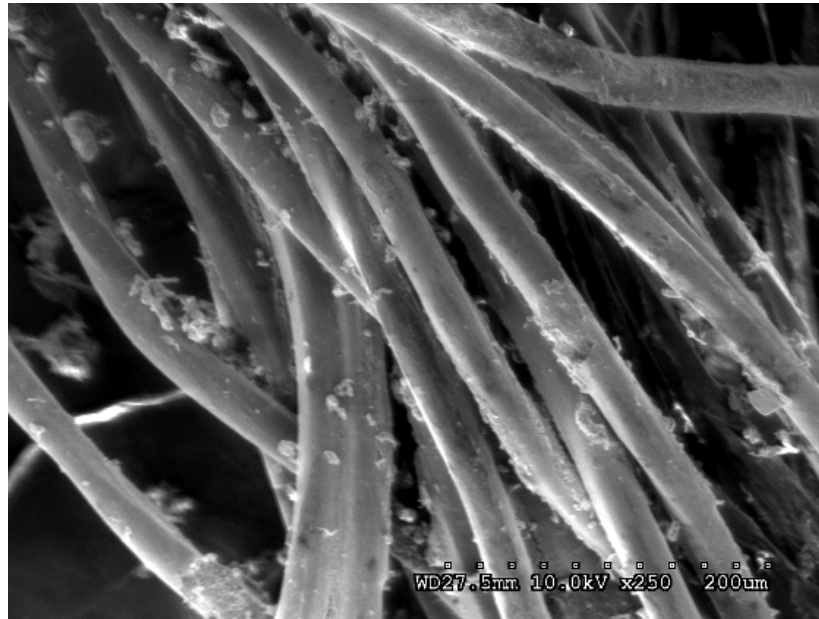
E_f = fibre modulus

Within composites a crack would first penetrate through the matrix, also causing interfacial debonding of the fibre. Fibre pull out then occurs as the individual fibres fracture. In the coated fabric similarly the yarns will be debonded from surrounding yarns initially enabling forces to be concentrated on individual yarns which are then fractured. The yarn itself will act as a composite as the coating penetrates into the yarn. Therefore in order to achieve individual fibres the debonded region would be required to be high to achieve separation from the coating, however, it would be beneficial for fibre diameter, fibre strength to be low to also lower the work required to pull out the fibre, also the fibre modulus should be high for the same reason.

Additional material is seen on the fibre surface in Figure 4.29(a) that was not present on images of the coated material prior to reduction. This is likely to be dust deposits from abrasion of the material during the reduction process, or signs of surface wear of the yarns. Figure 4.31 illustrates an example of surface wear on nylon caused by a rotating pin, the fibre surface seen in Figure 4.29 is also indicative of this mechanical action. The uncoated material depicted in Figure 4.30 also has areas where surface wear can be seen.

These observations indicate that the uncoated fibres have been more damaged than the coated fibres from this process as many imperfections on the uncoated fibres can be seen, in comparison to the pre reduced material depicted in Figure 4.27 and 4.27

where the fibres are very smooth. The reduced coated fibres also appear to be smooth in general beneath the deposits.

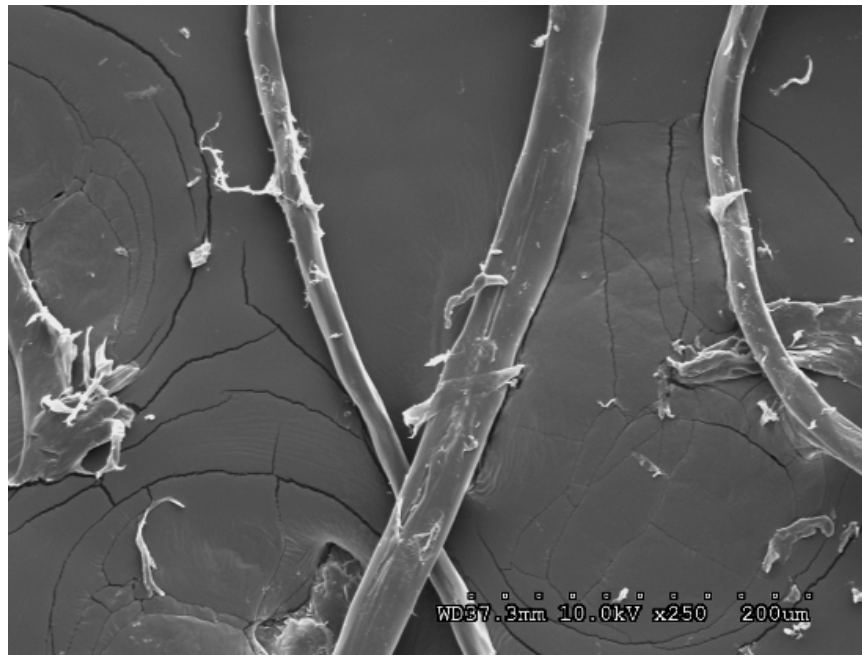


(a)



(b)

Figure 4.29: SEM Micrographs of Coated Material Reduced by Means of the Laroche Cadette, at a Magnification of x250



(a)



(b)

Figure 4.30: SEM Micrograph of Uncoated Material Reduced by Means of the Laroche Cadette, at a Magnification of x250.

The filament breaks observed in Figure 4.29(b) and Figure 4.30(b) are indicative of some type of twist break, an example of which is shown in Figure 4.32. It is unclear from Figure 4.29(b) of the appearance of the break surface but the break length is short and the edge has multiple segments. Twist breaks are a type of ductile break,

characterised by a v-notch at the fibre surface followed by a catastrophic break region (Hearle, 1998). Cyclic twisting leads to torsional breaks, causing multiple splitting in nylon (Hearle, 1998). This multiple splitting may be the cause of the uneven fibre end shown in Figure 4.29(b). The break seen in the uncoated fibres has a much longer length. This is more characteristic of an axial break which can occur through fibre to metal abrasion. It is likely that the metal pin clothing on the Laroche Cadette would impart significant fibre damage due to abrasion. It is also possible that the RFL coating may protect the nylon fibre during the reduction process so that the filament breaks are more likely to be “short and clean” since abrasion does not occur on the nylon only the RFL coating.

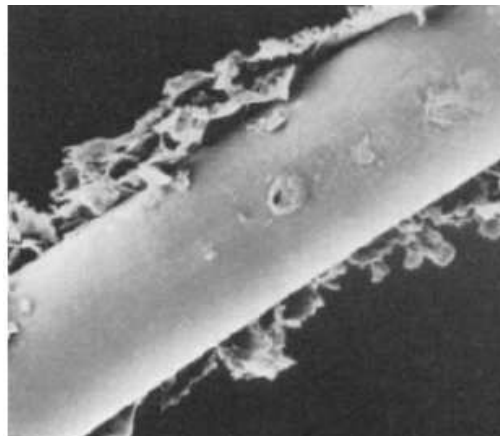


Figure 4.31: SEM Micrograph of Surface Abrasion of Nylon Caused by a Rotating Pin (Hearle, 1998)

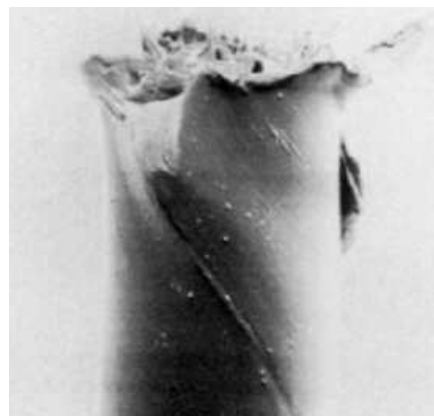


Figure 4.32: SEM Micrograph of Twist Break (Hearle, 1998)

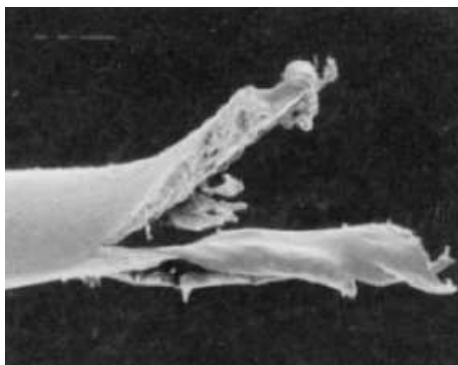
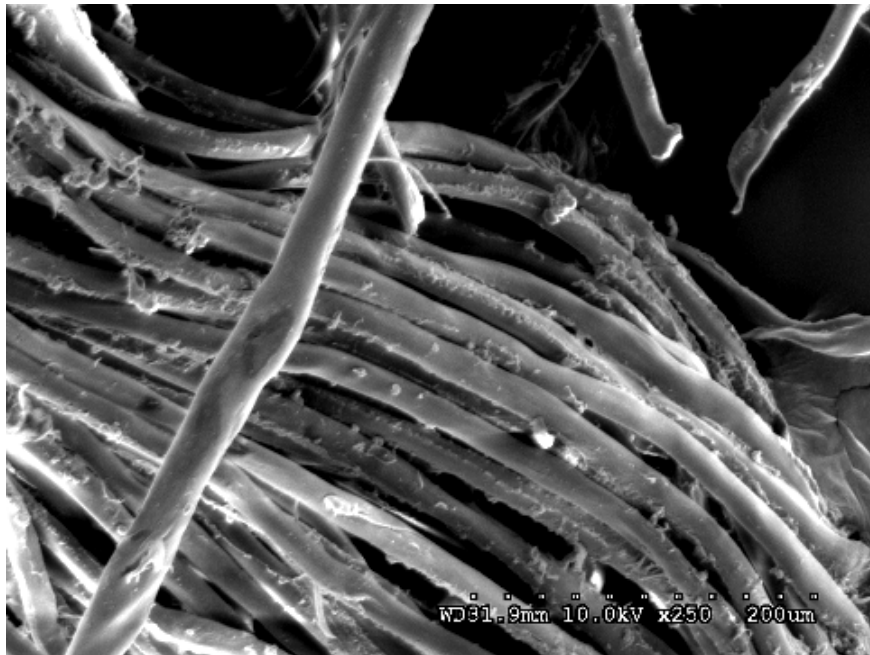


Figure 4.33: SEM Micrograph of Fibre to Metal Abrasion Causing Axial Splitting of the Fibre (Hearle, 1998)

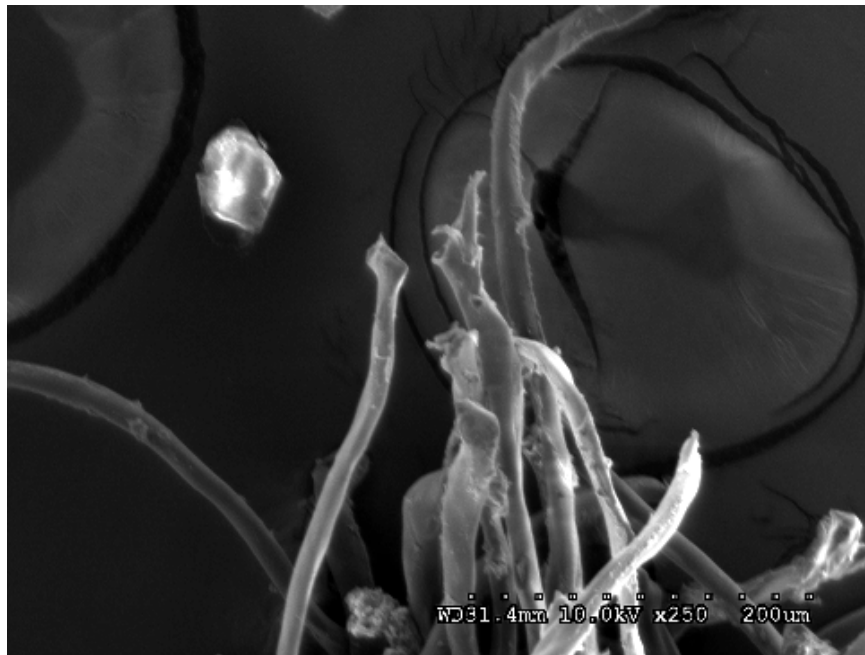
4.4.3.3 Hollander Reduced Material

The Hollander beater appears to have had a more intense action on the coating, Figure 4.34, where although the coated material after reduction still remains in the yarn form, the coating does not appear to bond individual fibres together. Most of the fibres have been separated and areas where fibres were previously adhered can be seen on the fibre surface as thicker, textured imprinted areas of coating. In comparison, the reduced uncoated material, Figure 4.35, shows that some fibres are relatively unaffected, maintaining a very smooth surface. However, other fibres have been considerably affected, evidenced by the lack of a circular cross-section. Fractures and abrasions are also apparent along the fibre axis caused by the beating action.

Fewer deposits can be seen on the fibres, in both Figure 4.34 and 4.35. This is due to the reduction being carried out in a liquid medium. Dust particles would be filtered out with the water as the samples were taken from the Hollander beater due to fibres being removed by hand. The samples taken from the beater would therefore contain less dust than the samples from the Laroche Cadette. Alternatively, less surface abrasion may be occurring on the yarns in the Hollander beater which utilises a metal bars giving a high impact chopping action rather than the pulling action employed by the pin clothing of the Laroche Cadette, abrade the fibre surface.

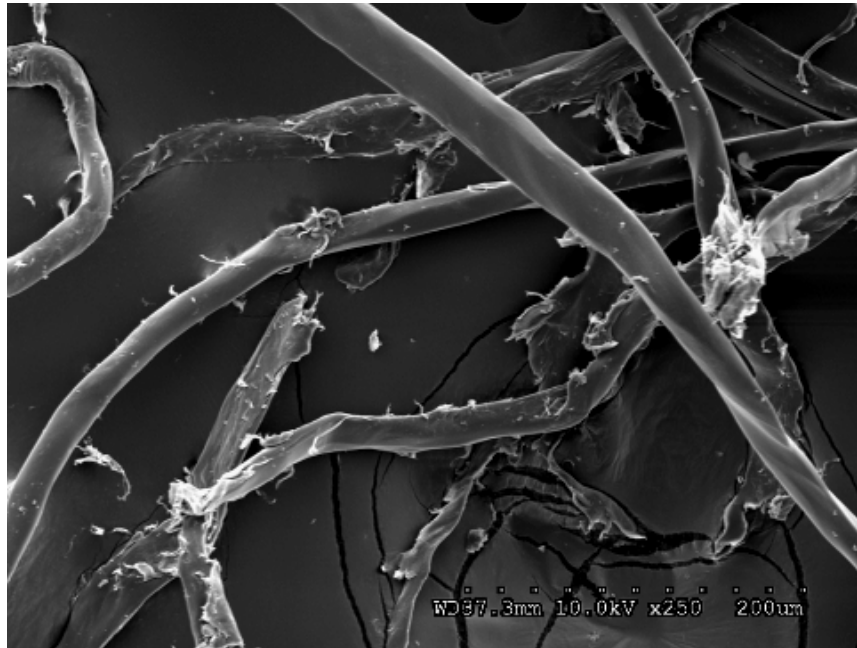


(a)



(b)

Figure 4.34: SEM Micrograph of Coated Material Reduced by Means of the Hollander Beater, at a Magnification of x250.



(a)



(b)

Figure 4.35: SEM Micrograph of Uncoated Material Reduced by Means of the Hollander Beater, at a Magnification of x250.

Breakage points seen in Figures 4.34 and 4.35 display a range of types of breakage occurring during fabric reduction within the Hollander beater. There are some break points with a pointed tip, whereas others are very blunt with a bulbous appearance. Pointed break points such as the one in the centre right position of Figure 4.34(b) are likely to have occurred due to localised abrasion at the break point. Figure 4.36 shows

two images of nylon fibre breaks that occurred through holding the fibre under tension against a rotating pin. The breaks demonstrate the angled wearing of the fibre surface until the material was reduced to a level where it can no longer support the tension. The resultant characteristic appearance of the fibre is of a thinned fibre cross-section, sometimes with axial splitting. Often, the two ends of the break are different, one having a smooth rupture and the other having a greater amount of splitting (Hearle, 1998). This thinned out appearance and axial splitting can be seen in many fibres (as shown in Figures 4.33 and 4.44).

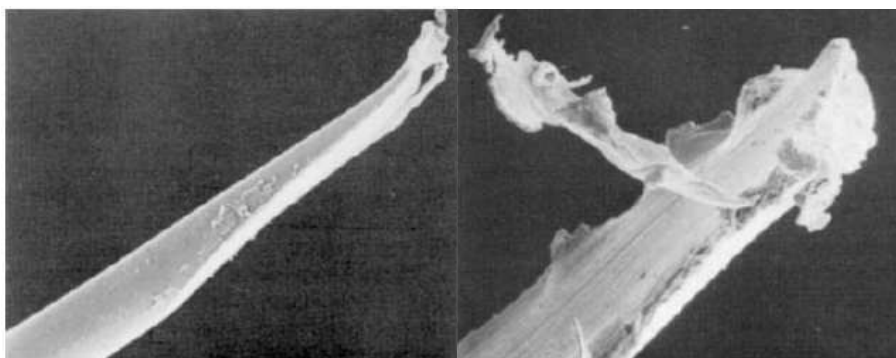


Figure 4.36: SEM Micrograph of Fibre Breaks Occurring from Nylon Fibre held under Tension against a Rotating Pin (Hearle, 1998)

The fibres with blunt, bulbous break points are likely to have been cut due to the metal bars of the beater roll and bed plate intersecting. Cut fibres can sometimes appear similar to tensile breaks where the object used is blunt however with sharper instruments more distinct break points are seen. Figure 4.37 illustrates the appearance of a nylon fibre cut with a knife, where a spreading appearance of the break is seen in the direction of the cut.

Scissor cuts are more distinct where two blades press together as shown in Figure 4.38. It is this appearance that is evident in the fibres reduced by the Hollander beater, for example the centre left fibre in Figure 4.34(b). Bulbous ends are also commonly found in fibres that have been cut, as the fibre heats up as the knife is drawn across it. A similar heating action will occur with the metal bars within the Hollander beater causing the bulbous fibre ends observed in Figure 4.34.

The uncoated fibre in Figure 4.35(b) may also have fractured due to impact. This process action causes fibres to initially flatten, followed by axial splitting and rupture. These characteristics can be seen in Figure 4.39.

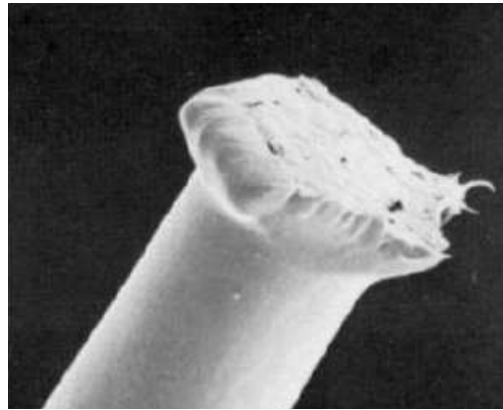


Figure 4.37: SEM Micrograph of Nylon Fibre Cut with a Knife (Hearle, 1998)



Figure 4.38: SEM Micrograph of Polyester Cut with Scissors (Hearle, 1998)



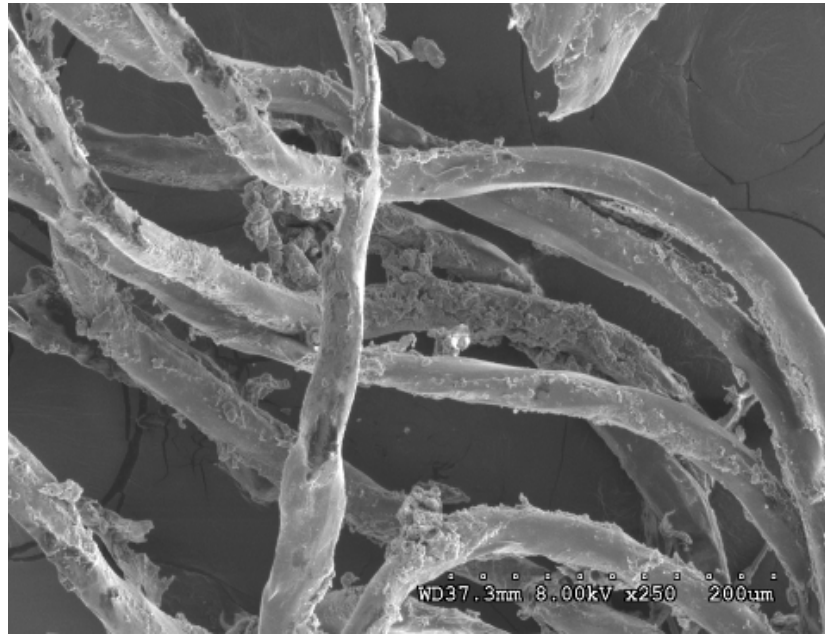
Figure 4.39: SEM Micrograph of Nylon Fibres Broken due to Impact (Hearle, 1998).

It is interesting to note that there are no visible fibres that have the cut appearance in Figure 4.35, where the fibres are uncoated. However this seems to be quite common in the fibres seen in Figure 4.34. It is likely that the increased stiffness that the coating

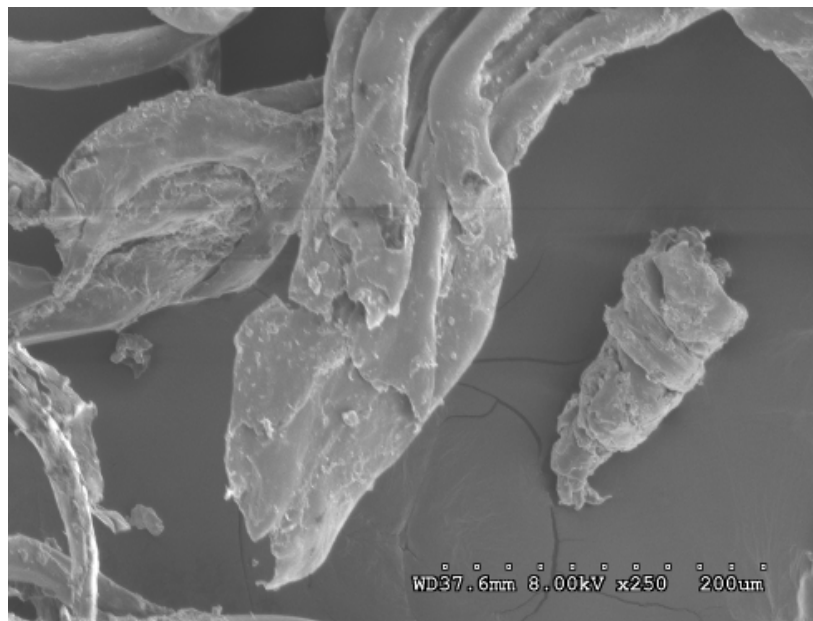
provides to the fibres causes the fibres to stand on end, allowing the metal bars of the Hollander beater to sever the fibre across cross-section performing a cutting action. In comparison the uncoated fibres are more likely to drape over the width of the bar causing an abrasive action or impact break. The energy required to break the coated fabric was also found to be less than that of the finished uncoated fabric in section 3.5.1. A clean break is therefore more likely to occur where less energy is required in the coated fabric, but an impact break will occur where a higher energy is required in the uncoated fabric.

4.4.3.4 Intimus Disintegrator Reduced Material

The textured coating illustrated in Figure 4.34(a) caused by physical rupture of the coating previously adhering fibres together can be seen again in Figure 4.40(a) which depicts fibres reduced by the Intimus disintegrator. This method of reduction was the most successful at separating yarns into a fibre form, when low batch sizes and pre-reduced waste was inputted as per trial B. It is therefore understandable that more areas of this textured coating would be seen on the fibres where separation has occurred. In comparison, the uncoated material seen in Figure 4.41 maintains its smooth appearance, showing little abrasive damage to the fibre surface. It is probable that melting at fibres has occurred during the reduction process, Figure 4.40(b) shows ends from a number of fibres that seem to be welded together. Similarly, in the uncoated fibre material in Figure 4.41(b), many fibre ends have a bulbous appearance indicative of melted ends. Figure 4.41(a) shows further good examples of a cut fibre at the top centre of the image, which has the characteristics seen in Figure 4.38. There is also evidence of impact breakages, seen in the flattening of fibres, Figure 4.40(b). There are particularly interesting fibre profiles depicted in Figure 4.41(b), the fibres have developed a bulbous ends which are not smooth. It is likely that these have occurred due to melting of the fibre, the bulbous end produced was more susceptible to abrasion than other areas of the fibre length.



(a)

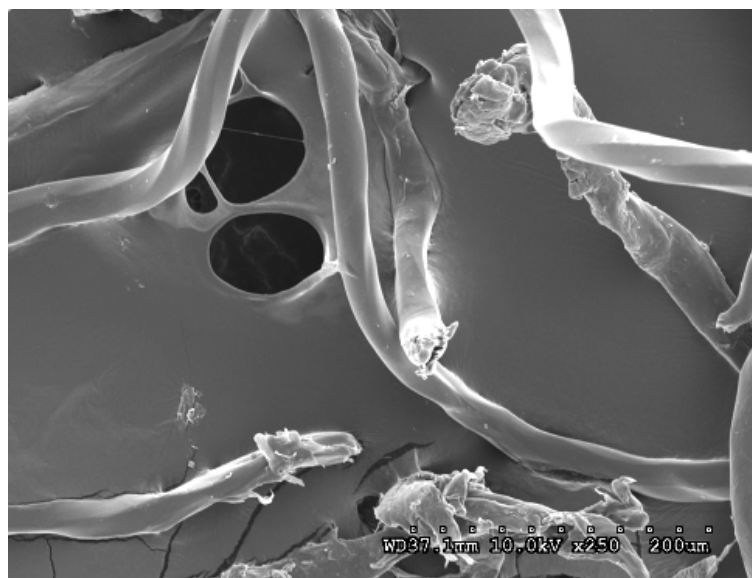


(b)

Figure 4.40: SEM Micrograph of Coated Material Reduced by Means of the Intimus Disintegrator, at a Magnification of x250.



(a)

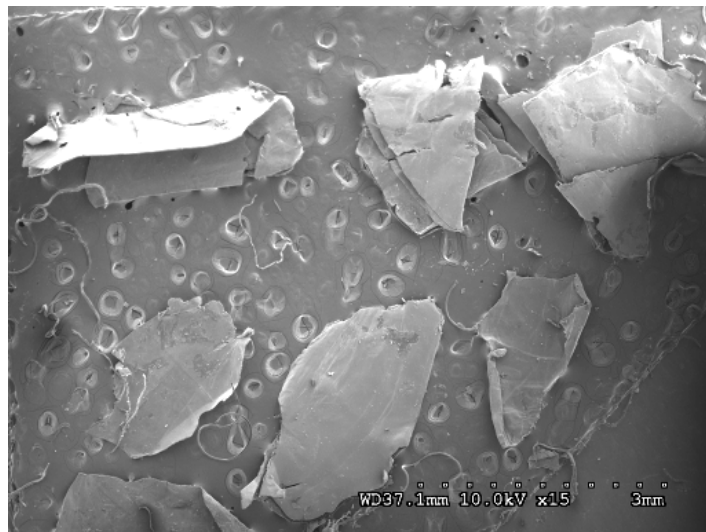


(b)

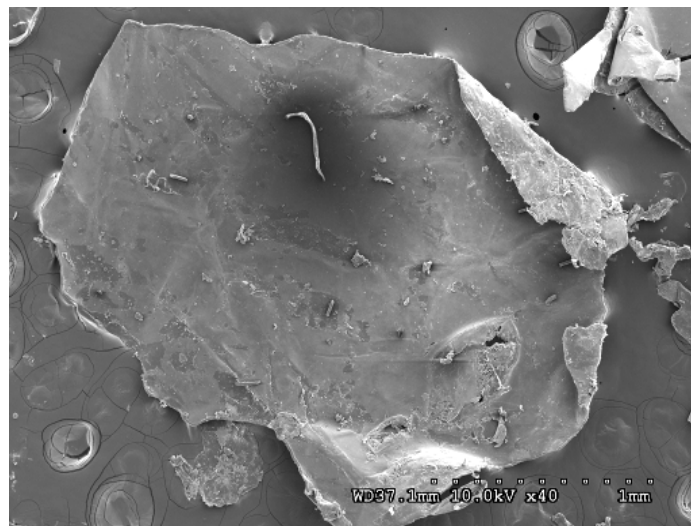
Figure 4.41: SEM Micrograph of Uncoated Material Reduced by Means of the Intimus Disintegrator, at a Magnification of x250.

The flake-like particles (illustrated in Figure 4.42 and 4.43), produced from the initial Intimus disintegration process have a smooth surface and flattened appearance. No bulbous areas or edge shrinking was observed which would have been expected to be seen from heating. It is therefore likely that the particles have gone through an impact or smearing action while in the melt stage before cooling, enabling complete transformation from fibres to particles.

Some debris can be observed on the particle surface, the majority of which look to be small pieces of remaining fibre. The fibre end seen in Figure 4.43(a) has a cut end, having its two ends compressed together. The reverse side of the particle seen in Figure 4.43(b), where a folded structure is evident, is less smooth than the first side. A layering type effect can be observed, possibly where fractured fibres and smaller particle pieces and debris have joined the particle infrastructure through further impact or smearing. There is little evidence of the coating material on the surface of the particle; it is likely that this has been combined with the nylon during the melting and impacting occurring in the reduction process.

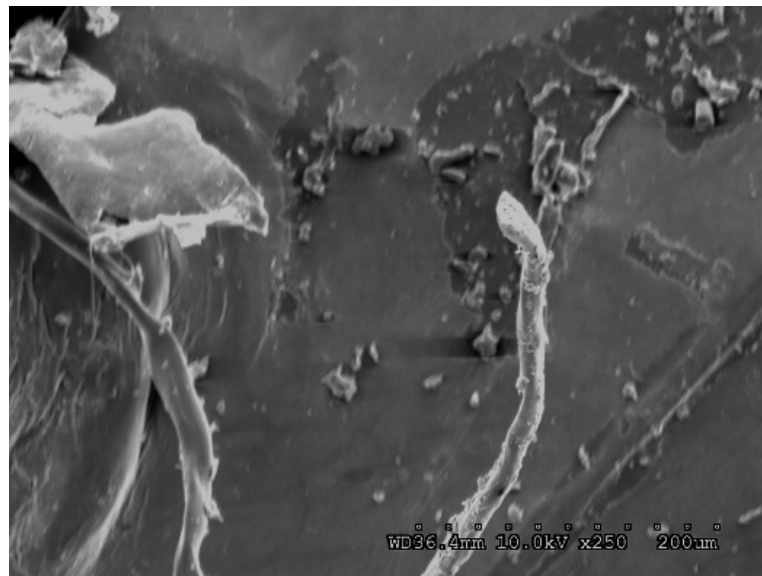


(a)

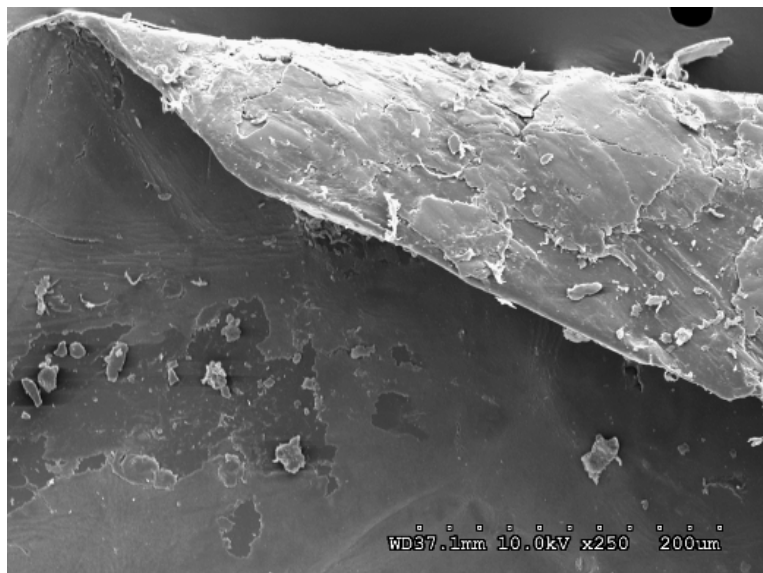


(b)

Figure 4.42: SEM Micrograph of Coated Material Reduced by Means of the Intimus Disintegrator, Forming Flake-like Particles, at a Magnification of $\times 5$ (image a) and $\times 40$ (image b).



(a)



(b)

Figure 4.43: SEM Micrograph of Coated Material Reduced by Means of the Intimus Disintegrator, Forming Flake-like Particles, at a Magnification of x250

4.5 Thermal Analysis

In addition to the problem of dealing with impurities, such as coatings, additives and dirt particles picked up during processing, there is also a problem in maintaining the polymer quality when polymers are recycled. Degradation of polymers will occur during their lifetime and in the recycling processes resulting in inferior quality

products with lower performance. Heat produced during the reduction processes will contribute to thermal degradation. Thermal analysis includes a number of techniques in which fibre properties are recorded while the material is heated. In this work, differential scanning calorimetry (DSC) was used to assess how the reduction processes affect the physical and chemical changes occurring in the samples during heating. Thermal gravimetry (TG) with infrared spectroscopy (IR) was also used to assess the temperatures at which the samples degrade and identify the volatile degradation products formed. The data from these analyses can be used to assess the quality of the polymers after the reduction processes. The melt flow index was also tested to assess how the molecular weight has been affected by the reduction processes.

The degradation of the coated material was also compared against the uncoated material using these techniques.

4.5.1 Materials

Mixed reduced coated and uncoated materials as previously discussed within this chapter were used for thermal analysis. These were compared to material prior to reduction, coated A, coated B and uncoated A, uncoated B which were two fabrics from the coated material and two from the uncoated material which made up a large proportion of the mixed waste reduced. All material tested, but reduced and pre-reduced was from the same waste batch and therefore the thermal history of each sample will be as comparable as possible given that it is a waste product that is being dealt with. However, the thermal history of the waste products is unknown.

Where the effect of the coating was assessed, two fabrics from pre- and post-coating stages of the same fabric specification T-00537, supplied by Heathcoat Fabrics and previously discussed in Chapter 3 were used. This fabric consists of a 2x2 twill weave using a single twist, 78 filament, 13 tex, multifilament textured yarn in both the warp and weft direction. This fabric is described as finished T-00537 (uncoated) and dipped T-00537 (coated) within this chapter.

4.5.2 Methods

4.5.2.1 Differential Scanning Calorimetry (DSC)

This technique measures and controls the temperature of sample and reference holders following a pre-determined time/temperature programme. The power difference needed to maintain both holders at equal temperature is measured allowing the thermal transitions of the sample to be monitored (Billmeyer, 1984). Tests were performed on a DSC-Q100 in standard mode using a heat/cool/heat cycle from -50°C to 270°C. This was performed on finished and dipped fabric to assess molecular weight change from this process. Coated samples pre- and post- reduction processes were then assessed. A sample size of 25mg in each case was used.

4.5.2.2 Thermogravimetric Infrared Analysis (TGIR)

This technique integrates standard Thermogravimetric analysis (TGA) with Fourier Transform Infrared Spectroscopy (FTIR) and is the most common form of an Evolved Gas Analysis (EGA) system. When the sample is heated, the volatiles released or combustion components are transferred to the IR cell where they can be identified (Perkin Elmer, 2009). Samples were prepared by drying in a vacuum oven at 100°C for 12 hours prior to testing to remove any moisture. Tests were carried out on a TG8000 EGA system made up of a Perkin Elmer Spectrum 100 spectrometer and Perkin Elmer STA 6000 Thermal analyser. Samples were subjected to heating from 30°C to 400°C whilst purged with nitrogen, and data analysed using Spectrum Timebase and Pyris software. Sample size of 25mg was used.

4.5.2.3 Melt Flow Index (MFI)

The melt flow index gives a comparison of the molecular weight of samples. A high MFI indicates a lower molecular weight and hence, increased degradation of the polymer. The effect of the reduction process and coating on the molecular weight was investigated. Melt flow tests were carried out at 275°C using a 2.16kg weight. The sample was packed into the cylinder and the weight added to extrude the molten polymer. Due to the viscosity of the polymer the time interval was measured for the entirety of the sample to be extruded and the mass of extrude then measured. From this information, the melt flow index was calculated, and normalised to a time period

of 10 minutes. This alternate method was used since the flow rate of the material tested was high and the material extruded from the cylinder in a shorter timeframe than the 10 minutes that the test is usually completed over.

4.5.3 Results and Discussion

4.5.3.1 Effect of the RFL coating on thermal properties

Figure 4.44 shows DSC curves of the finished and dipped fabric. In both cases, the curves show an endothermic response occurring. This depicts the melting phase change of the polyamide polymer. The dipped fabric has a slightly lower melting point than the finished fabric, illustrating that the polymer is of a lower grade, or that molecular weight degradation has occurred due to chain shortening. It is possible that the dipping process and predominantly the curing process which follows, caused heat degradation in the nylon polymer introducing a degree of depolymerisation (Kelen, 1983), however at the processing temperatures that would be required this is unlikely (Kohan, 1973). Bonding of RFL to the polymer chain will cause irregularities within the polyamide chain, and increase the distance between chains, this will limit the extent of crystallisation able to occur (Billmeyer, 1971). Hydrogen bonds are also formed between the RFL and the polyamide chain, restricting the amount of hydrogen bonding occurring between adjacent chains and form crystals (Billmeyer, 1971). The reduced crystallinity of the RFL coated polyamide would therefore cause a decrease in melting point.

During the second heating (Figure 4.44) two endothermic peaks are present. This is characteristic of partial melting and reorganisation (Jaffe, 1981) which will have occurred during the initial heating and cooling stage. The first peak represents the melting of crystallites formed in the previously amorphous regions during annealing, and the second relating to the melting of the orientated crystal structure.

The molecular reorganisation has affected the coated polymer more as increased energy is needed in order for the disorientated spherulites to melt in comparison to the organised crystal structure. By comparison, the uncoated polymer has rearranged, requiring more energy to melt the organised crystal structure.

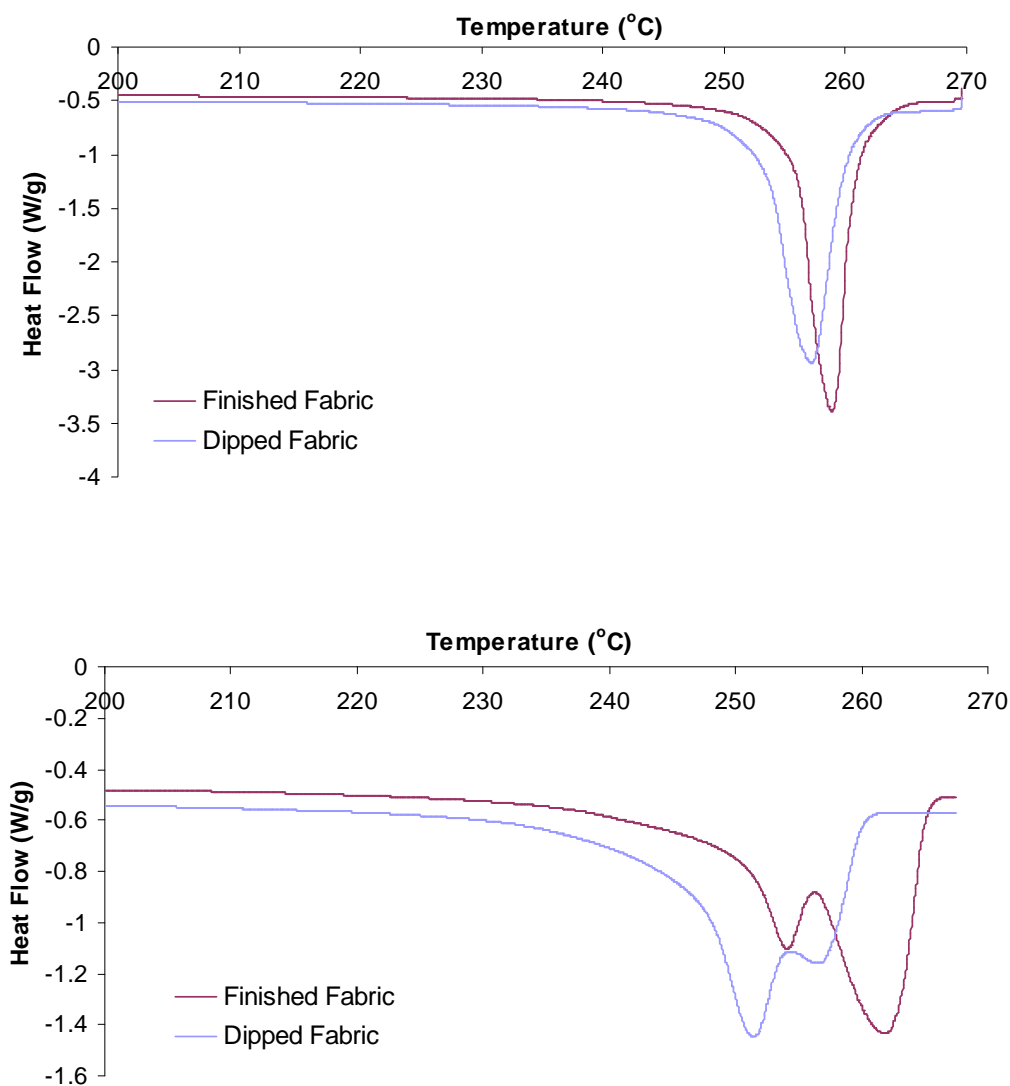


Figure 4.44: DSC Thermograms Showing the Initial (top) and Second (bottom) Heat Cycle of Finished (Uncoated) and Dipped (Coated) Fabric.

The melt flow index data in Table 4.3 shows particularly high flow rate for all samples, and hence low molecular weight, this could be due to the high temperature of 275°C that was used. However, comparing the samples against one another suggests that degradation has occurred from the fibre to the finished fabric. This is likely to occur during heat processes within the production such as yarn texturing and heat setting of the fabric, prior to fabric reduction. A decrease is seen in the melt flow of the dipped fabric. This suggests a molecular weight increase; however, this could also be due to the addition of bulky side chains which would be provided by the RFL groups attached to the main polyamide chain depicted in Figure 4.48.

Table 4.3: Effect of Coating on MFI

Sample	MFI (g/10min)
Nylon 66 Fibre	29.6
Finished Fabric	93
Dipped Fabric	43.6

The TGA analysis in Figure 4.47 shows that more significant weight loss occurs on the dipped fabric than the finished fabric. This is likely to be due to thermal degradation of the coated nylon producing volatiles that are lost during the heating process. This occurs gradually from approximately 100°C and becomes clearly evident at 300°C.

Thermal degradation of nylon is uncommon in processing, except in instances where temperatures reach over 310°C or where temperature is maintained over a number of days (Kohan, 1973). There are two kinds of reactions in polymers that may be induced through heat, depolymerisation and substituent reactions. Depolymerisation reactions result in the polymer backbone forming intermediate products similar to the monomer units used to create the polymer. Ultimately products may be monomers or volatile chain fragments. Alternatively, substituents attached to the backbone of the polymer molecules, change the repeat unit. This is known as a substituent reaction, the chain structure can remain intact but the volatile products produced can be different to the original monomer units (Grassie and Scott, 1985).

Studies on nylon detailed by Kohan (1973) suggest that decomposition of nylon either involves the fission of each bond in and adjacent to the amide group (Figure 4.45a) or that primary cleavage is at the C – N bond at an alpha position to the amide carbonyl (Figure 4.45b).



a. Bond cleavage in and adjacent to amide group.

b. Bond cleavage at C – N bond at an alpha position to the amide carbonyl.

Figure 4.45: Preferential Polymer Break Points in Thermal Degradation of Nylon.

A review carried out by Steppan *et al.*, (1991) summarises a number of chemical reactions that may occur. Figure 4.46 describes the simplest of these reactions, comparable to how adipic acid decomposes to cyclopentanone, water and carbon dioxide, Figure 4.46a. The nylon 66 chain can decompose from its end groups or internally as shown in Figure 4.46b and Figure 4.46c. The cyclopentyl chain end produced can degrade further forming an amide end group, cyclopentanone and carbon dioxide, Figure 4.46d (Steppan, 1991). Other reactions are possible with carbon dioxide, water and ammonia being common volatiles produced, where nylon decomposes to a crosslinked solid (Deopura and Mukherjee, 1997).

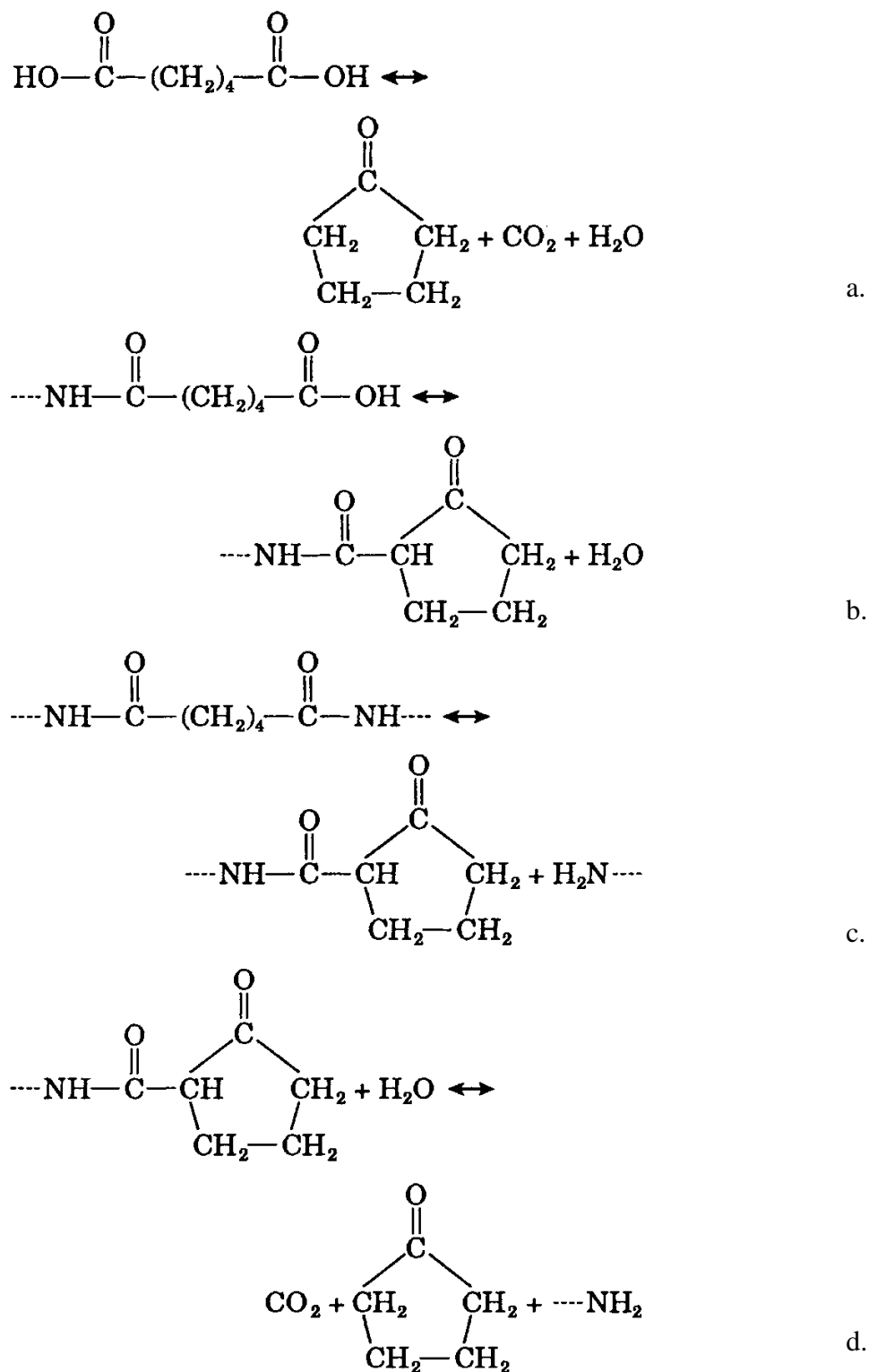


Figure 4.46: Degradation Reactions of Nylon 66 (Steppan et al., 1991).

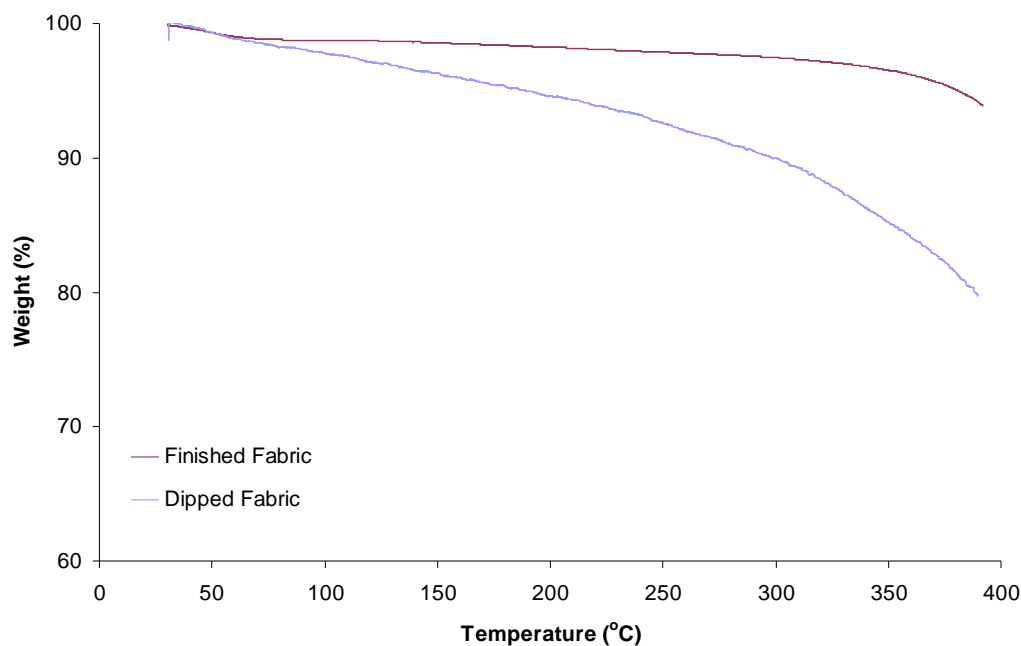


Figure 4.47: TGA Analysis of Finished and Dipped Fabric

Thermal degradation of nylon in nitrogen begins to occur at 300°C (Deopura and Mukherjee, 1997) and this behaviour can be seen to start to occurring in the finished fabric, Figure 4.47. The degradation of the dipped fabric occurs at a much lower temperature of around 70°C and is most likely to be due to bulky RFL coating side groups bonded to the nylon. The stability of nylons is associated with chain rigidity, for example in aromatic polyamides polymers formed with para-para orientation of the diamine and diacid results in a more stable polymer than para-meta orientation. This is due to the relative mobility of the para-para orientated chain. In less stable polymers the temperature at which catastrophic weight loss occurs is lowered. Meta-ortho orientated chains begin degrading at 200°C, ortho-meta at 300°C and para-para at 600°C (Kohan, 1973). Similarly the RF functionality, Figure 4.48, will cause the nylon polymer chain to become less mobile and the stability of the polymer will be affected, causing the decrease in temperature of onset of weight loss.

Weight loss could also be occurring due to the degradation of the coating only. This is likely to produce phenols as a product of the reaction. However, work on a similar formaldehyde Novolac resin structure by Sullivan (1991) found this to be stable to 220°C.

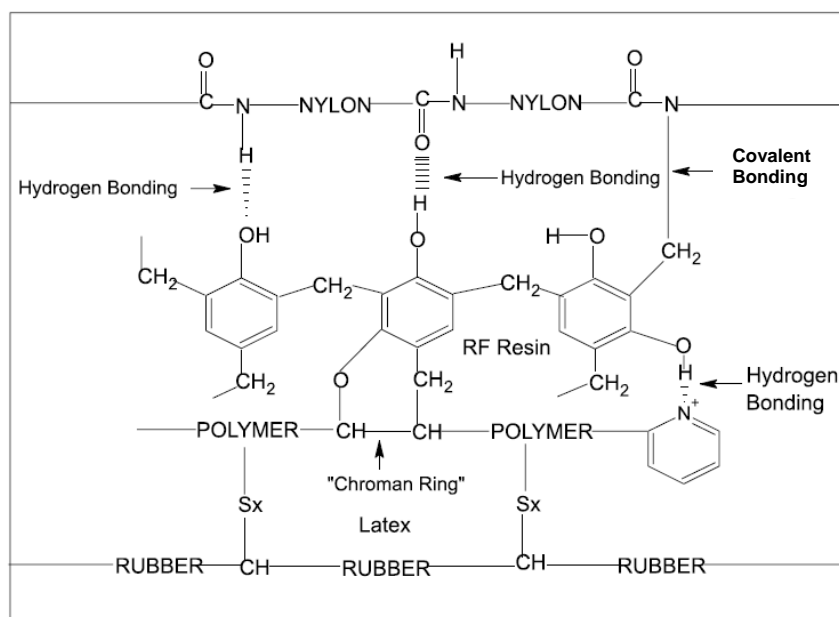


Figure 4.48: Structure of RFL Coated Nylon and Bonding Mechanism Involved
(Durairaj, 2005).

The infrared analysis shows both the finished and dipped fabric have the same degradation products, as identified by the peaks produced (Figure 4.49 and 4.50). The spectral bands present indicate thermal degradation of nylon, with production of water vapour, indicated through peaks at 3657 cm^{-1} , 3756 cm^{-1} and 1594 cm^{-1} representing symmetric stretch, asymmetric stretch and bending vibrations of covalent H – O bonds. Also, carbon dioxide is present having FTIR bands present at 2350 cm^{-1} representing an asymmetric stretch, and at 667 cm^{-1} representing a bending vibration of the CO_2 molecule. However, there does not seem to be any ammonia present, which would be represented through peaks at $3490\text{--}3180\text{ cm}^{-1}$, 1650 cm^{-1} and 1580 cm^{-1} or cyclopentanone which has peaks at $3000\text{--}2840\text{ cm}^{-1}$, 1747 cm^{-1} and 1153 cm^{-1} . Evidence of other nitric molecules and carbonyl groups are also present, the peak at $1570\text{--}1500\text{ cm}^{-1}$ could include C– NO_2 group ($1570\text{--}1540\text{ cm}^{-1}$), C–N=O ($1600\text{--}1500\text{ cm}^{-1}$) and the peak at $1800\text{--}1640$ could also include aldehydes ($1765\text{--}1645\text{ cm}^{-1}$) and ketones ($1725\text{--}1660\text{ cm}^{-1}$). This suggests that oxidative degradation is also taking place where aldehydes and ketones are common products (Kelen, 1983).

The volatiles, particularly water, are present at a constant rate, prior to the weight loss occurring during the heating of the finished fabric sample which was not the case for the dipped fabric, signifying that the presence of these volatiles may not have

occurred from degradation and are present from another source. However an increase is seen in the carbon dioxide (2350 cm^{-1} peak) at the point where weight loss starts to occur. The rate of loss of volatiles increases with temperature in the dipped fabric, reflecting the weight loss behaviour to concur with the degradation theory.

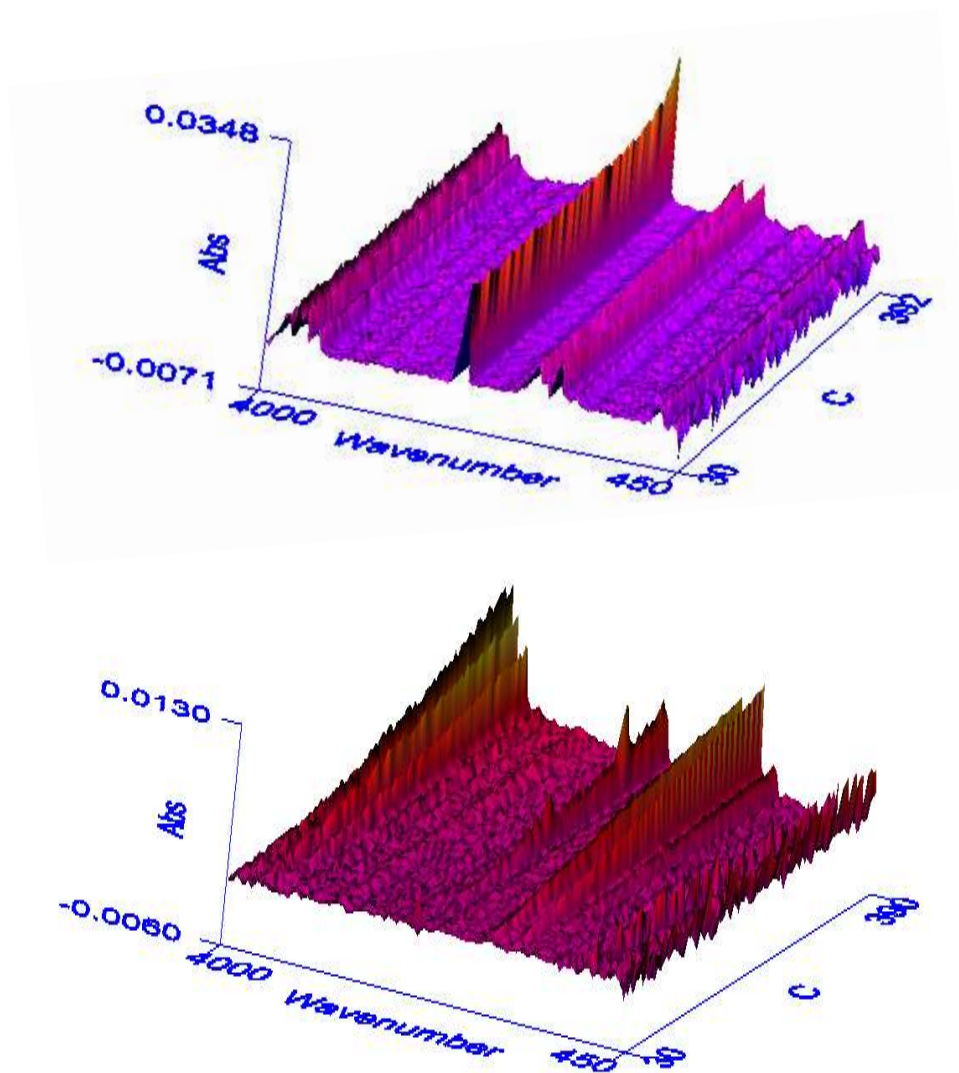


Figure 4.49: FTIR Spectral Analysis of Finished Fabric (top) and Dipped Fabric (bottom) in Relation to Temperature.

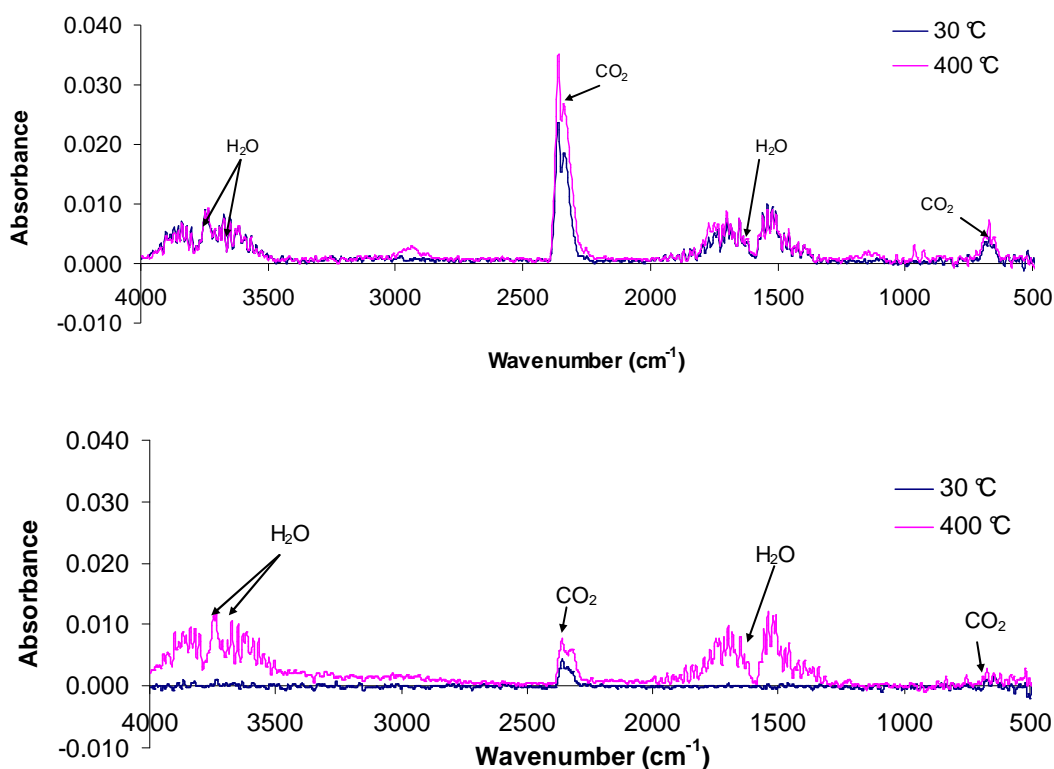


Figure 4.50: Identification of Volatiles Produced using FTIR Analysis from Finished (top) and Dipped (bottom) Fabric.

4.5.3.2 Effect of the reduction methods

DSC analysis of the coated fabric before reduction (Figure 4.51) shows similar results to the dipped fabric in Figure 4.44. Coated B fabric shows a slightly wider and lower intensity peak than coated A fabric, commonly this suggests that the thermal contact on the analysis equipment was poor (Gabbott, 2007), causing the sample to require more time to melt and hence only partially melting the sample in the given time. Alternatively lower broader endotherms may also indicate a comparatively less pure polymer (Wunderlich, 1981). It is likely that Coated B fabric has an increased amount of coating and therefore causing a broader peak to be produced due to increased contaminants to the polymer. The increased coating would also limit the ability of the polyamide to melt due to the increase in crosslinked the structure, causing partial melting. Both fabrics have the same melting point, and hence have a similar degree of polymerisation.

This partial melting has seemed to cause an increase in the organised crystalline structure within the polymer. The DSC results from the secondary heating show a double peak inferring partial melting and reorganisation (Jaffe, 1981), with the second peak, representing the organised crystal structure requiring more energy than the initial peak representing the disorientated spherulites. Conversely, where more complete melting occurred on the initial heating in coated A fabric, during the secondary heating more energy was required in the melting of the disorientated spherulites (represented from the first peak), indicating a less orientated structure has occurred from the heat, cool cycle.

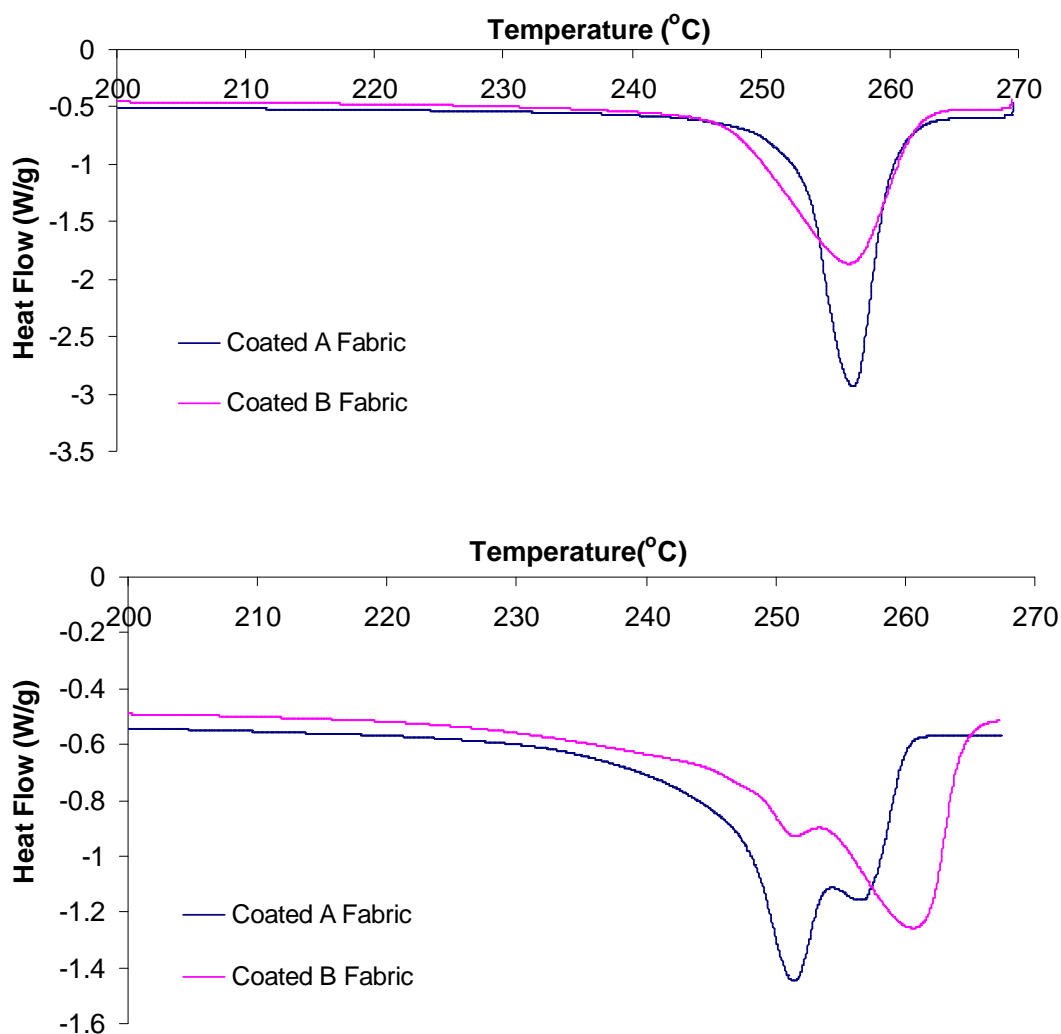


Figure 4.51: DSC Analysis Showing the Initial (top) and Second (bottom) Heat Cycle of Fabric Samples from Mixed Coated Waste Prior to Reduction.

The DSC analysis of the reduced samples, Figure 4.52, demonstrates the relative effect that each process has had on the polymer quality. There is little evidence that the Hollander beater has caused any molecular weight degradation to the sample, with the peak showing a similar melting point to that seen in the fabric samples depicted in Figure 4.51. The Laroche Cadette reduced coated waste showed a lower molecular weight to that reduced by the Hollander beater. However, there is little difference between the melting point of this and that of the initial waste fabric indicated in Figure 4.51, and therefore degradation is not evident. Conversely, the DSC thermogram of the Intimus disintegrator material shows a double peak occurring at a lower temperature indicating that significant heat was present in the reduction process resulting in reorganisation of the lamella within the crystal structure. A decrease in molecular weight was also seen, showing that this heat has caused the polymer to degrade. Furthermore, in the reduction process which produced the particulate, trial A, the DSC thermogram no longer shows any peak. This suggests that the polymer has fully degraded and formed a crosslinked solid, therefore melting does not occur within the temperature range measured. This result is consistent with the results seen in microscopic analysis in section 4.4.3. This confirms that the materials are thermally modified by the Intimus disintegration process as both sets of analysis show this to occur. The Laroche Cadette and Hollander beater do not thermally modify the material, also identified in both microscopy and thermal analysis, this is to be expected as these reduction methods are less harsh to the material, and the Hollander beater also uses water which acts to cool the material during the reduction.

Amorphous material can also occur when cooling is at a rapid enough rate to suppress crystals forming. This may have happened as the particles are ejected from the cutting zone, through the screen and into the air. As the particles are very small they have a high surface area to volume ratio and therefore will cool quickly. The secondary heating DSC curve shows similar reorganisation of the crystalline material once heated, as occurred in fabric samples.

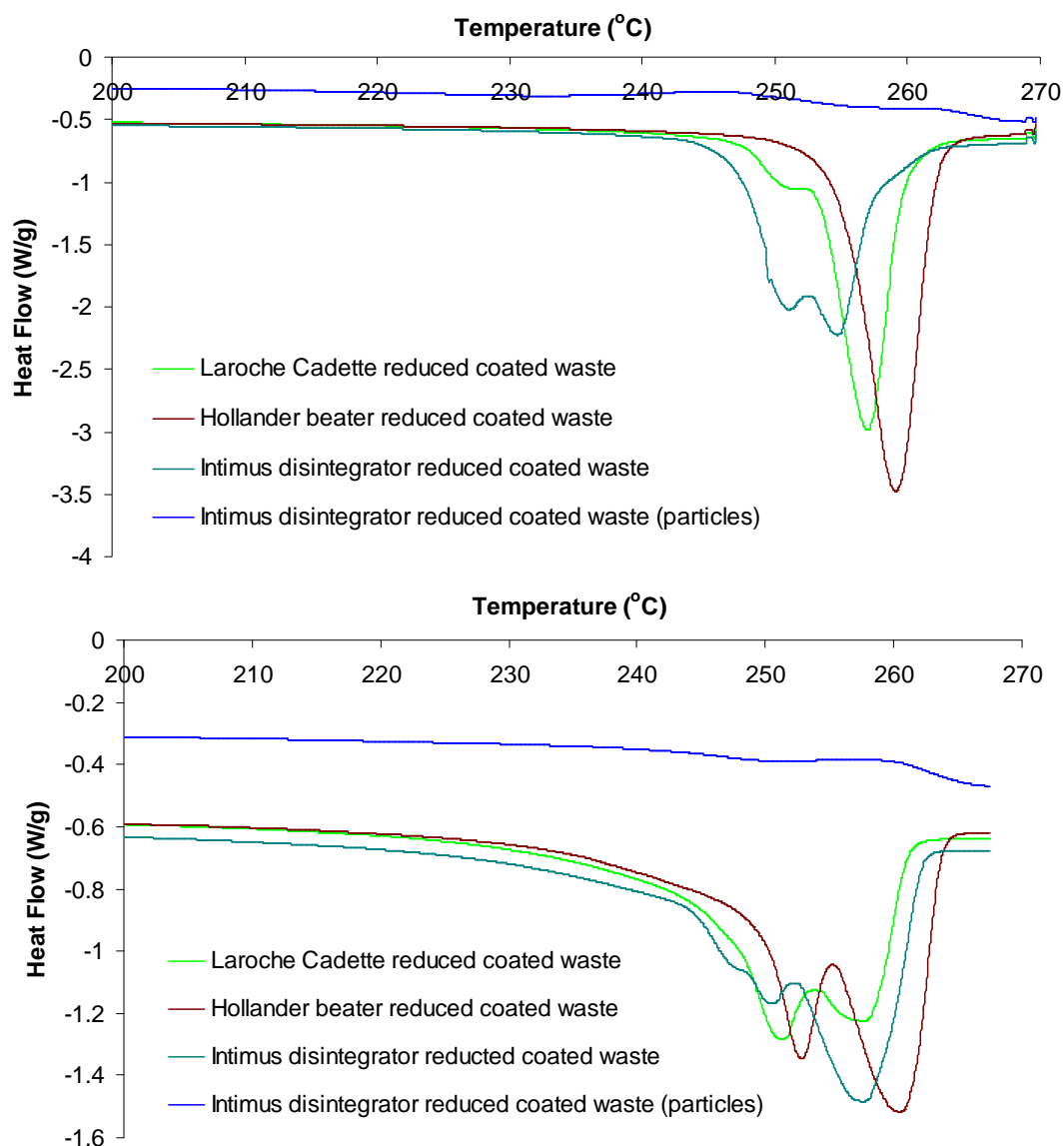


Figure 4.52: DSC Analysis Showing the Initial (top) and Second (bottom) Heat Cycle of Reduced Mixed Coated Waste.

The Melt Flow Index results in Table 4.4 agree with previous DSC data from the reduced material in Figure 4.51 and 4.52. The Hollander beater has the least effect on the molecular weight of the nylon, with the material behaving similarly to the fabric in the uncoated samples. The reduction processes where more heat due to friction have been involved caused increased degradation and reduction in molecular weight. The Laroche Cadette had the greatest effect on the molecular weight in the uncoated samples. Similarly in the coated samples, the Hollander beater reduced material experienced the least degradation during the process, having a MFI lower than the

initial fabric. This is likely to be due to the larger surface area of the reduced sample allowing melting to occur more quickly.

MFI results also show the Intimus disintegrated materials to be more degraded in the coated fibre sample than the uncoated fibre sample; this could be due to the reduced proportion of nylon 66 within the sample. Conversely, a decrease was observed in the MFI of the particles formed during reduction by the Intimus disintegrator, in comparison to both uncoated and coated fibres formed from this reduction method, suggesting an increase in molecular weight. However previous DSC results in Figure 4.51 suggest that the particles have formed into a cross-linked solid due to the degradation process. An increase in the number of polymer crosslinks will increase a polymer's viscosity, eventually producing a structure that is stable to heat as it cannot be made to flow or melt due to the crosslinks prohibiting molecular movement (Billmeyer, 1984). It is this increased stability to heat that has caused a reduced melt flow index rather than an increase in molecular weight.

Table 4.4: Effect of Reduction Method on MFI

Sample	MFI (g/10min)	Sample	MFI (g/10min)
Uncoated Fabric B	70	Coated Fabric B	31.1
Laroche Cadette reduced uncoated waste	160	Laroche Cadette reduced coated waste	108
Hollander Beater reduced uncoated waste	71	Hollander beater reduced coated waste	12.8
Intimus Disintegrator reduced uncoated waste	99.6	Intimus Disintegrator reduced coated waste (trial B – fibres)	207.6
		Intimus Disintegrator reduced coated waste (trial A - particles)	44.4

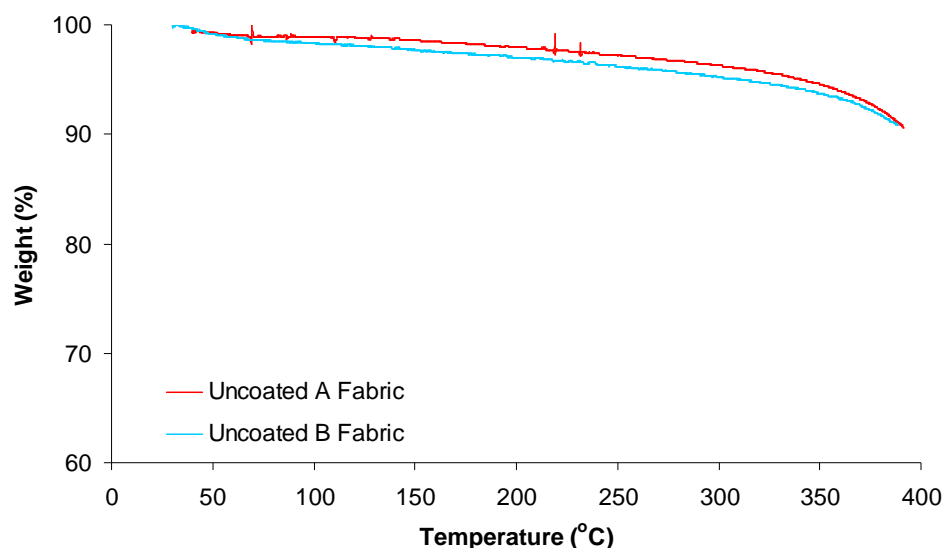


Figure 4.53: TGA Analysis of Fabric Samples from Mixed Uncoated Waste Prior to Reduction.

Analysis by TGA shows that very little degradation is evident in the uncoated fabric waste upon heating, Figure 4.53, little weight loss occurs in either fabric tested. Similarly the FTIR spectral analysis, Figure 4.54, does not show any evidence of volatiles produced during the heating process confirming little degradation has taken place.

The samples reduced by the Laroche Cadette and Intimus disintegrator also show little sign of degradation as evidenced by TGA analysis, Figure 4.55, proving that these forms of reduction do not lower the polymer quality of the uncoated fabric. The Hollander beater had the greatest effect on the polymer quality with subsequent heating causing a 20% weight loss, with degradation beginning to occur at a lower temperature (Figure 4.55). These results contradict those seen from MFI tests, shown in Table 4.4 which suggest that the Hollander degrades the polymer the least. This could be due to experimental error within the MFI test, since flow rate was high and a flow over a long timeframe could not be tested.

Volatiles produced in the heating of reduced samples, Figure 4.56, were negligible for the uncoated Intimus disintegrator reduced sample, agreeing with weight loss seen in Figure 4.55. However, volatiles increased with temperature in both the Laroche Cadette and Hollander beater reduced samples, as would be expected as degradation

occurs. FTIR absorptions seen previously were again evident, showing the production of water vapour and carbon dioxide (Figure 4.57). There was also evidence of cyclopentanone and ammonia in the Laroche Cadette FTIR spectra indicating that although less weight loss has occurred, a greater degree of degradation has occurred to the polyamide chain (Figure 4.57). This was not evident in the FTIR spectra from the Hollander beater sample.

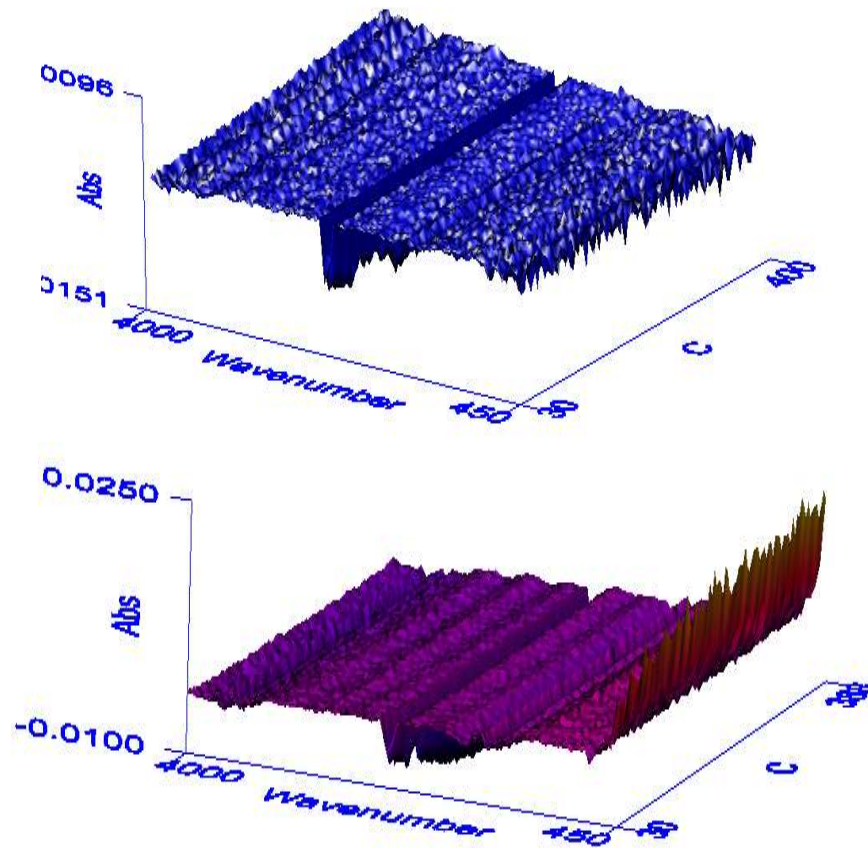


Figure 4.54: FTIR Spectral Analysis of Uncoated A Fabric (top) and Uncoated B Fabric (bottom) in Relation to Temperature.

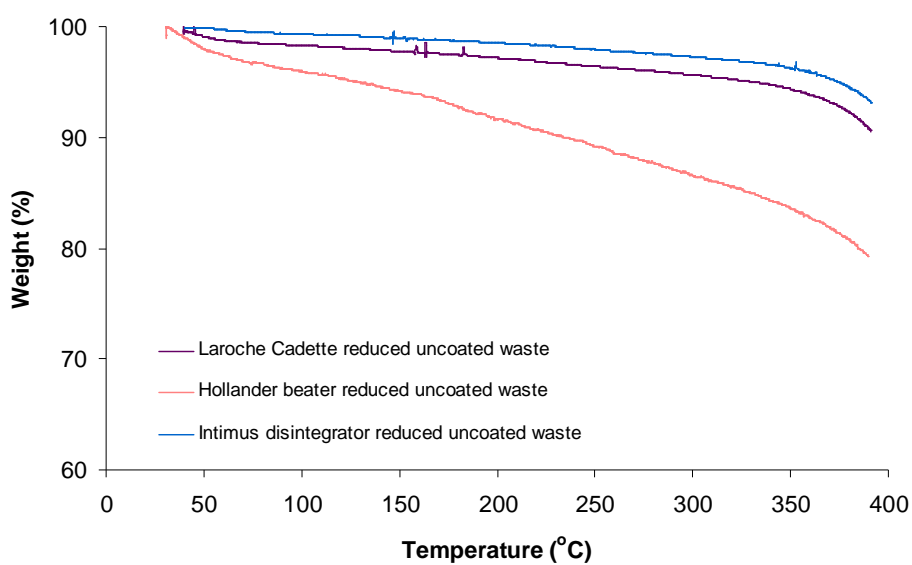


Figure 4.55: TGA Analysis of Reduced Mixed Uncoated Waste.

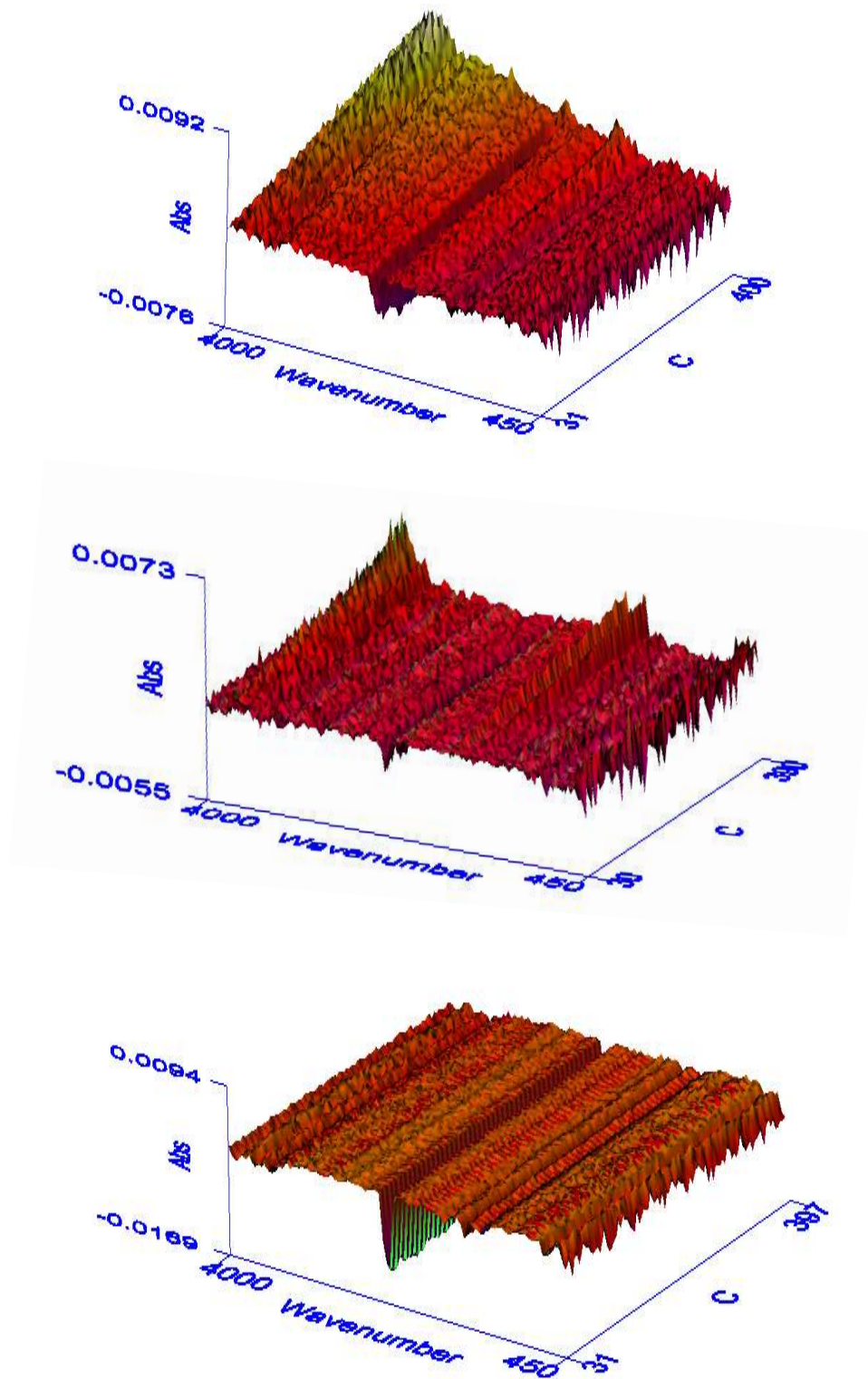


Figure 4.56: FTIR Spectral Analysis of Reduced Mixed Uncoated Waste in Relation to Temperature, Laroche Cadette (top), Hollander beater (centre) Intimus Disintegrator (bottom).

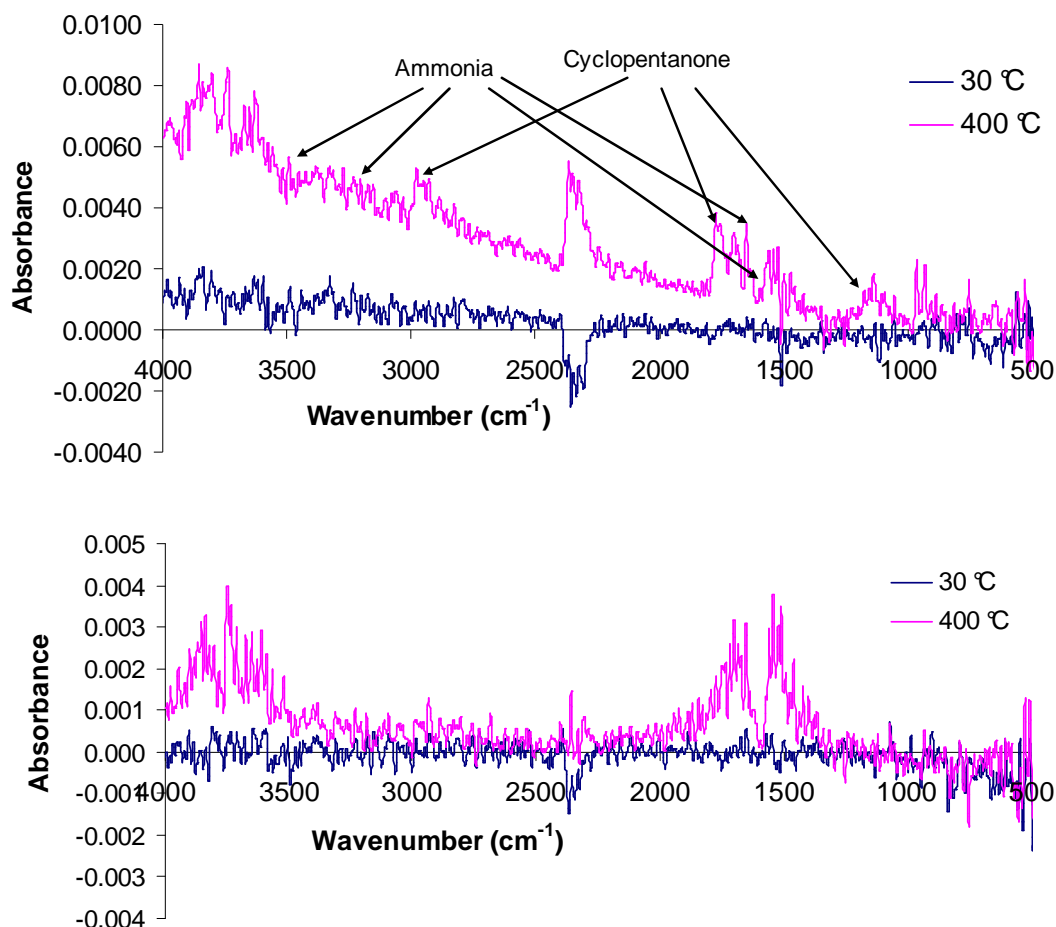


Figure 4.57: Identification of Volatiles Produced using IR Analysis from Laroche Cadette (top) and Hollander Beater (bottom) Reduced Uncoated Waste.

Dissimilar weight loss properties were observed in TGA analysis on the two coated samples prior to reduction, Figure 4.58. The coated B fabric had a higher rate of weight loss than the coated A fabric demonstrating that there is a difference in the polymer quality of coated waste prior to reduction.

It is likely that these changes occur due to differences in curing treatments. Volatiles produced from the coated A fabric during the heating are constant and can be identified as water vapour and carbon dioxide as previously seen (Figure 4.59). However, an increase in volatile production is seen in the coated B fabric coinciding with the weight loss (Figure 4.59). There is also a defined peak suggesting the presence of cyclopentanone at 2940cm^{-1} - 2886cm^{-1} (Figure 4.60). Coated B fabric therefore has more complete degradation in addition to increased weight loss.

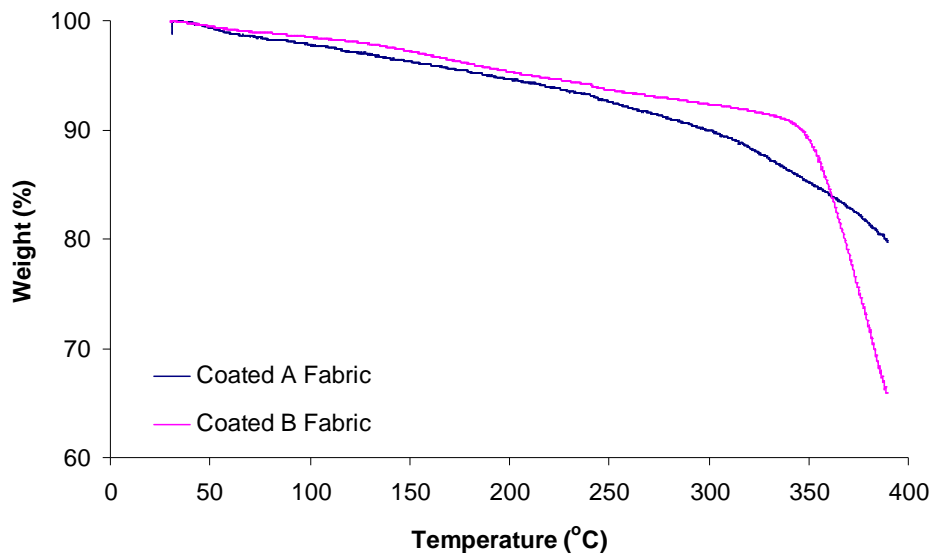


Figure 4.58: TGA Analysis of Fabric Samples from Mixed Coated Waste Prior to Reduction

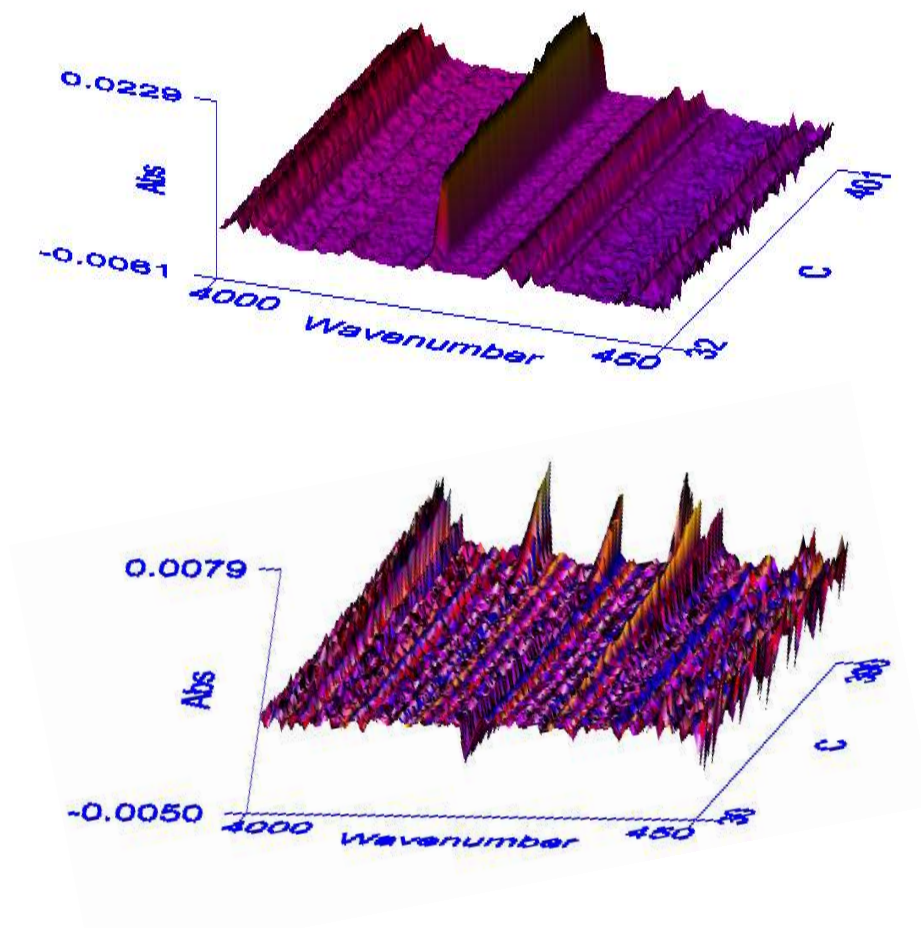


Figure 4.59: FTIR Analysis of Coated A Fabric (top) and Coated B Fabric (bottom) in Relation to Temperature.

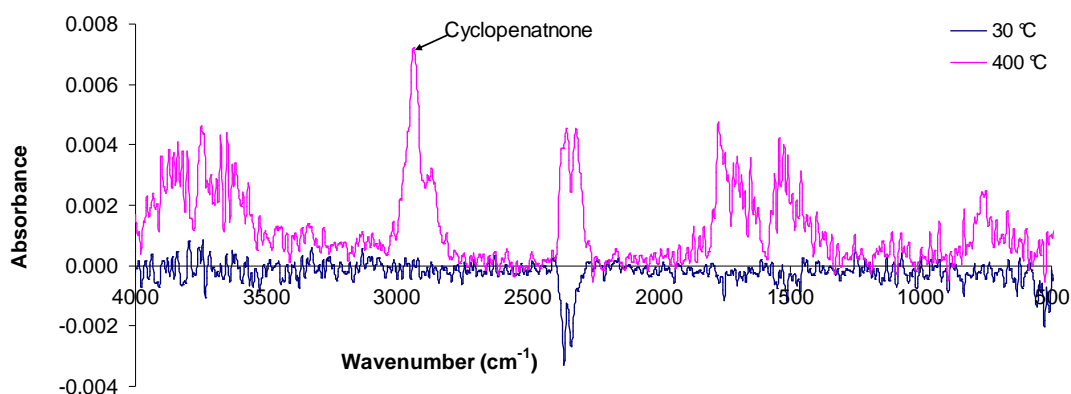


Figure 4.60: Identification of Volatiles Produced using IR Analysis from Coated B Fabric in Mixed Coated Waste Prior to Reduction.

As seen in the uncoated samples, coated waste reduced by the Intimus disintegrator producing fibres does not demonstrate significant weight loss from the heating procedure. The maximum weight loss is seen in the Laroche Cadette reduced sample (Figure 4.61). As previously shown, release of carbon dioxide and water vapour is evident in all samples (Figure 4.62 and 4.63). There was also evidence of cyclopentanone release, with a peak identified at 3000-2840 cm⁻¹ in the Intimus disintegrator reduced sample, demonstrating that although little weight loss occurs, more complete degradation was taking place.

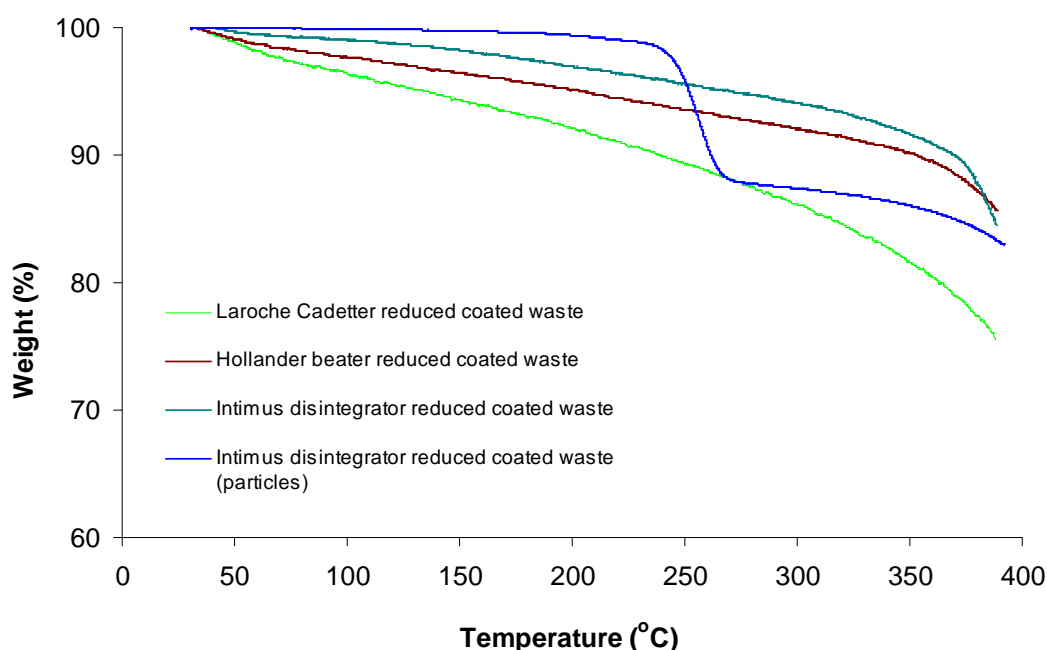


Figure 4.61: TGA Analysis of Reduced Mixed Coated Waste

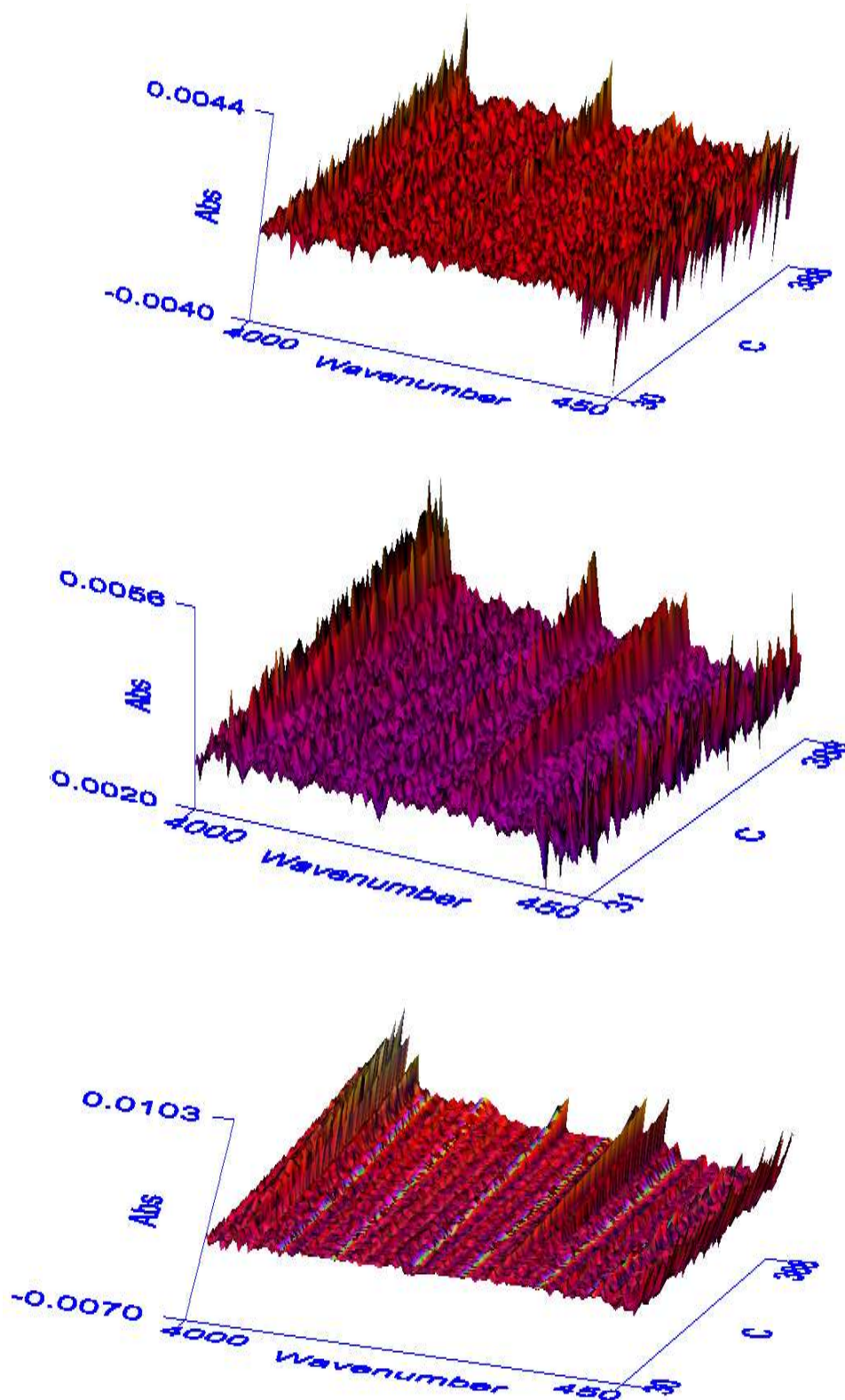


Figure 4.62: FTIR Spectral Analysis of Reduced Mixed Coated Waste in Relation to Temperature, Laroche Cadette (top), Hollander Beater (centre) Intimus disintegrator (bottom).

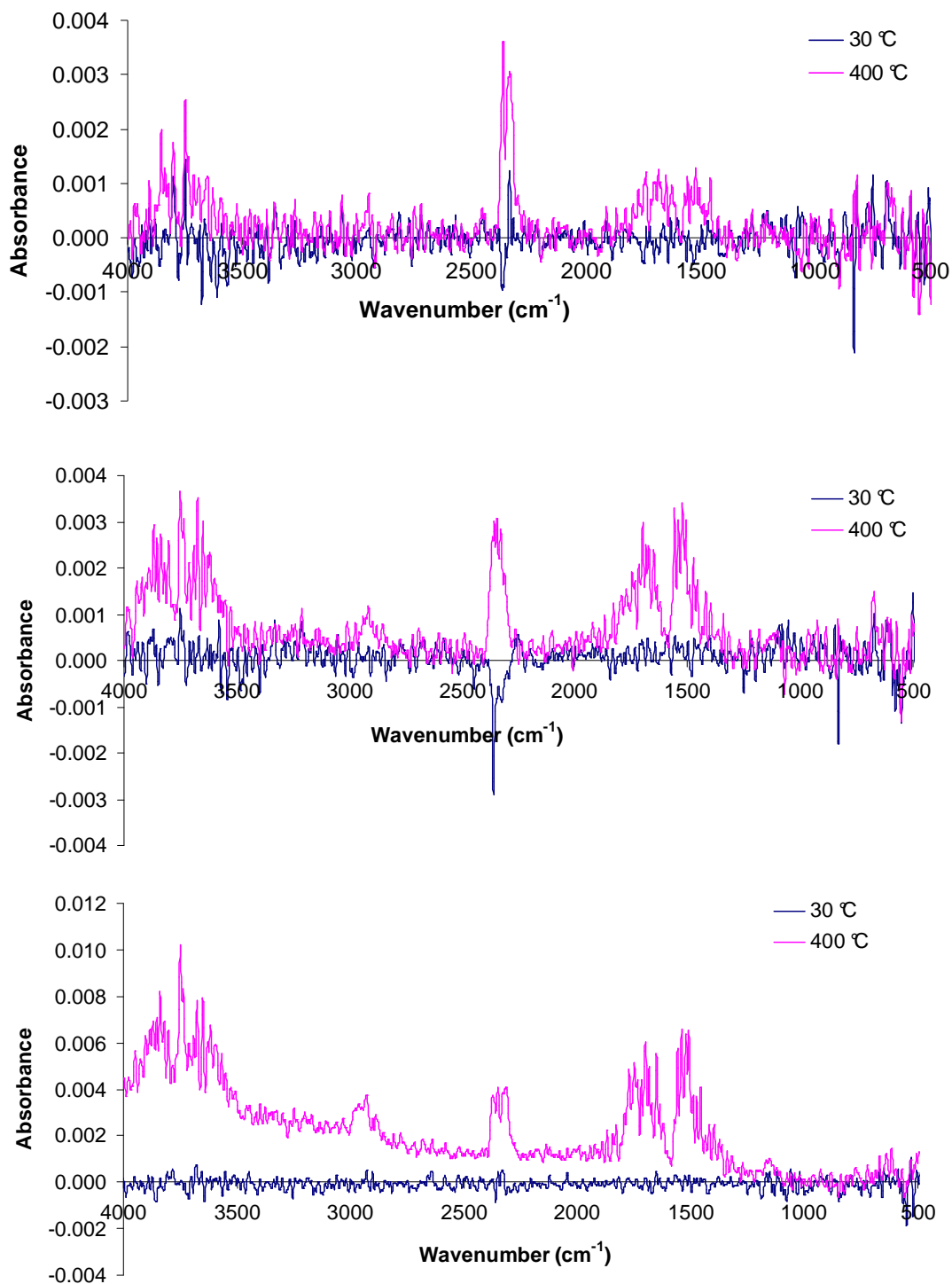


Figure 4.63: Identification of Volatiles Produced using IR Analysis from Laroche Cadette (top) and Hollander Beater (centre) and Intimus Disintegrator (bottom) Reduced Coated Waste.

The earliest onset of weight loss from degradation was seen in the Intimus disintegrator reduced (particle) sample where weight loss begins to occur at 250°C, and is rapid (Figure 4.61). This coincides with high levels of cyclopentanone and water vapour production, in addition to possible aldehyde, ketone and imide based species formation. An increase in carbon dioxide was seen at the later stages of the heating cycle near to 400°C (Figure 4.64 and 4.64). This sample has reduced quality and would not be suitable for processes requiring temperatures in excess of 250°C.

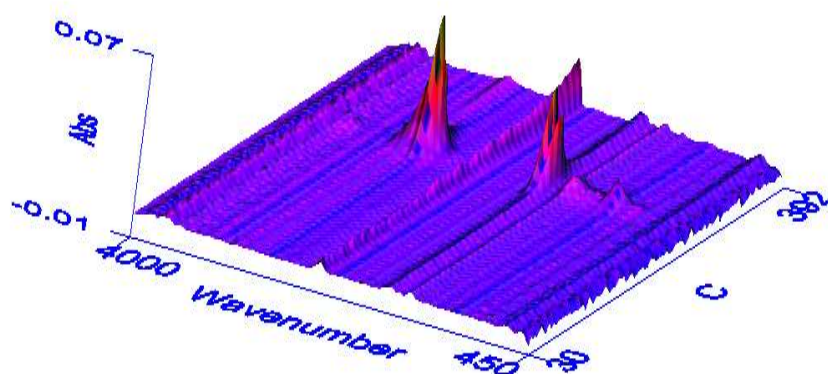


Figure 4.64: FTIR Spectral Analysis of Intimus Disintegrator Reduced Coated Waste (Particles) in Relation to Temperature.

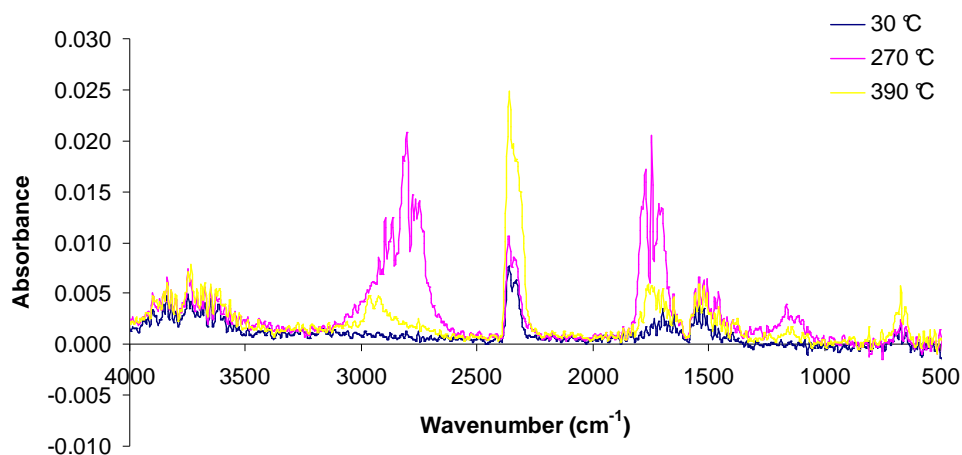


Figure 4.65: Identification of Volatiles Produced using IR Analysis from Intimus Disintegrator Reduced Coated Waste (Particles).

In summary, results from uncoated waste are inconclusive with MFI results suggesting that the Laroche Cadette causes the most degradation to the polymer, and little degradation occurs from the Hollander beater. Whereas, TGIR results show

degradation primarily from the Hollander beater, with little degradation occurring from either Laroche Cadette or Intimus disintegrator reduction methods. This could be due to experimental errors within the MFI tests, where short timeframes were used due to fast flow rates. Errors could also have occurred due to the nature of the material being tested, with different waste within the batch having different thermal histories which could not be controlled when directing the waste to alternate reduction processes.

The results for the coated waste were more conclusive with least degradation occurring in the Hollander beater in all tests. This is likely to be due to the water within the hollander beater providing a cooling mechanism throughout the reduction process to dissipate the heat produced due to friction between the beater rolls and fabric occurring during the reduction. The Laroche Cadette caused more degradation than the Hollander beater but less than the Intimus disintegrator in all tests. This is likely to be due to the high frictional heat that is built up during the process, which is unable to dissipate. This heat, however, is much lower than the heat produced from the Intimus disintegrator which is confined to a small space within the cutting chamber. All tests showed the coated material to degrade the most with the Intimus disintegrator reduction method.

4.6 Conclusions

Reduction methods affect fibres, coating and polymer quality in different ways. It is important when recycling that a suitable reduction method is chosen to optimise the quality of the material and product manufactured. The RFL coating on the fabric introduces secondary processing difficulties due to the material's behaviour owing to the bulky resin functionalities incorporated into the molecular structure. These difficulties are evident through increased viscosity, decreased melting point and the onset of thermal degradation at an earlier temperature.

The Laroche Cadette allows for long fibres to be produced, up to 160 mm, and is the most suitable for further textile processing. However the coating limits the fibre

length able to be produced to around 100 mm. The mechanical processing causes some surface abrasion to the fibre and coating, however, it does not affect the coating's adhesion to the polymer, and many fibres remain bonded together. The fibres break by tensile and twist forces causing short clean breaks. A decrease in molecular weight was observed for the uncoated polymer due to the reduction process, but little change to the degradation process seen post-reduction. The molecular weight was also lowered in the reduced coated waste, in addition to an earlier onset of degradation when heated again.

The Hollander beater in comparison produces much shorter fibres (12 - 32mm). Fibre length can be controlled to an extent by maintaining the space between the beater roll and bedplate, as shown in Hollander beater trial B, Figure 4.11; however, the fibre length range is high until full breakdown has commenced producing fibres of around 2 mm. It was observed that the Hollander beater was more likely to separate coated fibres; however, the coating still remains bonded to the fibre surface. Breakages occur due to the cutting and abrasion action causing a number of break appearances. The reduction causes the uncoated polymer to degrade at a lower temperature; however the Hollander beater reduction does not affect the coated polymer. Little change was observed to the molecular weight of the reduced material in either the uncoated or coated waste.

The Intimus disintegrator was able to produce the smallest fibre length and most suitable to be used as fillers or in polymer recycling at ≥ 3.2 mm. Fibres of longer lengths could possibly be created using a larger mesh screen. The process separates fibres and causes little abrasion, fibre breaks occurred primarily due to a cutting action. The coating also remained bonded to the fibres after this process. Heat produced in the process caused some melting of the fibres, which in turn affected the polymer, rearranging the crystalline structure thereby lowering the melting point of the nylon due to decreasing the molecular weight. However, little further degradation was observed when reheated until temperatures reached 350°C. The Intimus disintegrator was also able to produce particle flakes due to this melting of the polymer. This process caused significant degradation to the polymer resulting in a crosslinked structure rather than a crystalline polymer. The particles rapidly degraded further when heated to 250°C. The particles also had a reduced melt flow rate due to

the crosslinked structure inhibiting flow. Although the form of this material seems as though it would work well in plastic recycling, it is unlikely to be of use due to the extent of polymer degradation observed.

4.7 References

- BILLMEYER, F. W. (1984) *Textbook of Polymer Science*, New York, Chichester, Wiley.
- BOONSTRA, B. B. (1982) Reinforcement by Fillers. In Blow, C. M. & Hepburn, C. (Eds.) *Rubber Technology and Manufacture*. 2nd ed. London, Butterworth Scientific.
- DEOPURA, B. L. & MUKHERJEE, A. K. (1997) Nylon 6 and Nylon 66 fibres. In Gupta, V. B. & Kothari, V. K. (Eds.) *Manufactured Fibre Technology*. London, Chapman and Hall.
- DURAIRAJ, R. B. (2005) *Resorcinol [electronic resource]: Chemistry, Technology and Applications*, Berlin, Heidelberg, Springer-Verlag, Berlin, Heidelberg. Available at: <http://www.springerlink.com/content/m76682q537t4k566/>
- GABBOTT, P. (2007) A practical Introduction to Differential Scanning Calorimetry. [online] Available at:
http://media.johnwiley.com.au/product_data/excerpt/13/14051317/1405131713.pdf
[Accessed 1 September 2012]
- GRASSIE, N. & SCOTT, G. (1985) *Polymer Degradation & Stabilisation*, Cambridge, Cambridge University Press.
- HEARLE, J. (1998) *Atlas of Fibre Fracture and Damage to Textiles*. 2nd ed. Cambridge, Woodhead Publishing.
- JAFFE, M. (1981) Fibers. In Turi, E. A. (Ed.) *Thermal Characterization of Polymeric Materials*. New York, Academic Press.
- KELEN, T. (1983) *Polymer degradation*, New York
- KLEIN, W. (1986) *The Technology of Short - Staple Spinning*, Manchester, The Textile Institute.
- KOHAN, M. (1973) Preparation and Chemistry of Nylon Plastics. In Kohan, M. I. (Ed.) *Nylon Plastics*. New York, John Wiley & Sons.
- LAROCHE (2012) Our Activities - Cadette. OZ-média.

- MARTIN YALE INTERNATIONAL (2010) Intimus Power Disintegrator 200/410. Martin Yale International. [online] Available at: http://www.intimus.co.uk/data/media/38/3825_0x0_intimus_power_200_410_en.pdf [Accessed 23 April 2010].
- PERKIN ELMER (2009) *TG-IR Hyphenated Technology*, Perkin Elmer.
- SMOOK, G. A. (2002) *Handbook for Pulp & Paper Technologists*, Vancouver, Angus Wilde Publications Inc.
- STEPAN, D. D., DOHERTY, M. F. & MALONE, M. F. (1991) A simplified degradation model for nylon 6,6 polymerization. *Journal of Applied Polymer Science*, 42, 1009-1021.
- SULLIVAN, E. A. (1991) Thermal degradation of epoxy novolac-phenol formaldehyde novolac resin systems. *Journal of Applied Polymer Science*, 42, 1815-1827.
- SWANSON, J. W. (1964) Stock Preparation. In Britt, K. W. (Ed.) *Handbook of Pulp and Paper Technology*. London, Reinhold Publishing Corporation.
- UNIVERSITY OF MINNESOTA (1998) How Paper is Made. *Pulp & Fiber Products*.
- WUNDERLICH, B. (1981) The Basis of Thermal Analysis. In Turi, E. A. (Ed.) *Thermal Characterization of Polymeric Materials*. New York, Academic Press.

5.0 Recycling Fibres Using Paper Technology

5.1 Aim

This chapter explores the range of available paper technologies and their possible use in the recycling of waste textile fibres. The ability of RFL coated nylon to be made into paper will be assessed and evaluated as an alternative to textile or plastic recycling streams. In addition the potential use of centrifugal cleaners will be investigated with a view to the separation of recycled synthetic fibres.

5.2 An Overview of the Papermaking Process

In order to make paper cellulosic fibrous material is required. The material is initially pulped in order to separate the fibres, using either mechanical or chemical methods (Biermann, 1996). In addition depending on the type of paper required, bleaching of the pulp may also be necessary in order to impart a whiter colour to the paper. Beating or refining of the pulp is then undertaken and has the effect of hydrating the cellulose fibres causing them to swell and separate. Mechanical forces aid in the removal of the primary wall causing fibrillation and creating a fibrous form where hydrogen bonding can occur. The paper fibres can then be formed on a screen and water drained from the pulp mainly through gravity. The paper sheet is then pressed to remove excess water and left to dry (Biermann, 1996). Figure 5.1 outlines the steps required to manufacture paper in a modern paper mill.

It is worth noting that much of our used paper is recycled and goes back into the papermaking process for further use. This requires further processes such as deinking in order to make the cellulosic material suitable to be reused. This recycling process is relatively simple with the recycled pulp often being added to virgin pulp as an extender and subsequently being passed through the standard process to produce paper sheets.

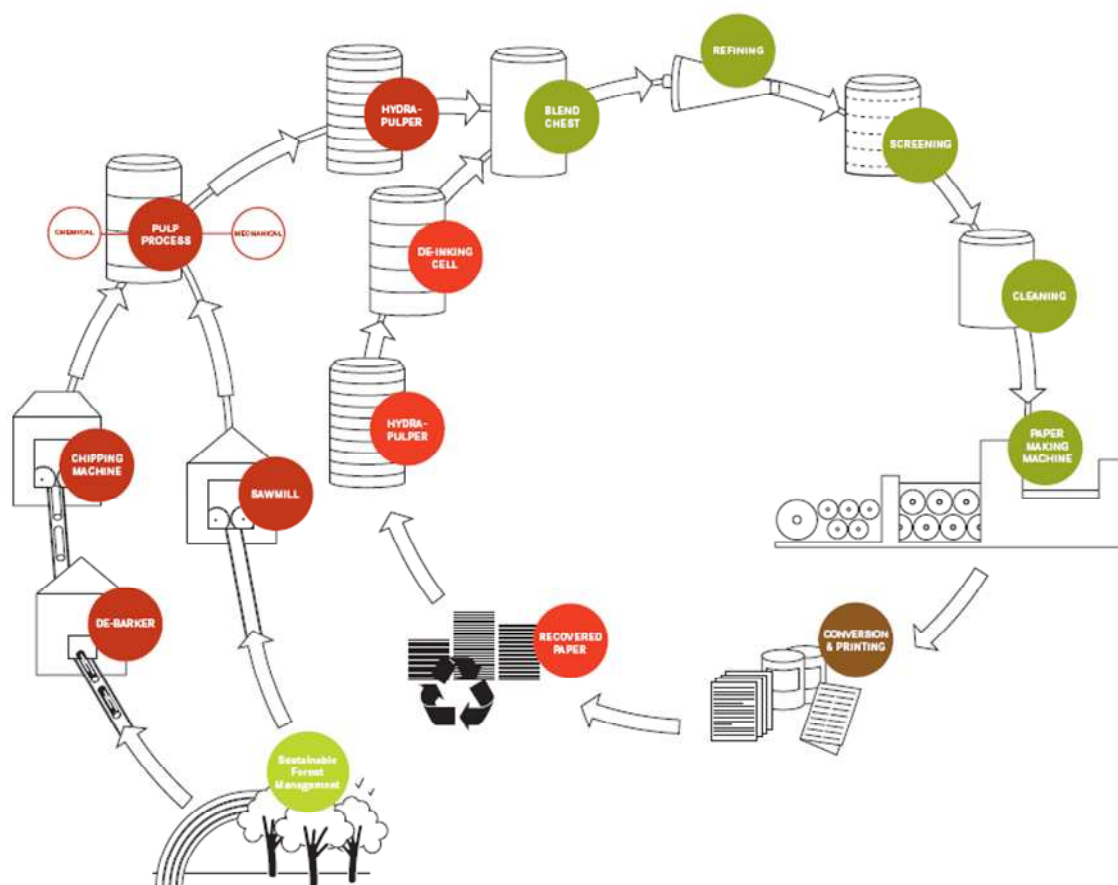


Figure 5.1: An Overview of Pulping and Papermaking Processes (Inform, 2009)

The following sections give a more detailed account of the different processes used within the paper industry.

5.2.1 Pulping

Pulping is any process in which fibrous material is reduced to a fibrous mass (Smook, 2002). Where wood is being pulped for use in the paper industry, the bonding within the wood structure must be broken. The disintegration/pulping can be achieved by chemical or mechanical methods, or a combination of both. Mechanical processes give a high yield of fibres in comparison to the original wood weight, typically at 85-95%, however short, impure fibres are produced that are often weak and unstable. Nevertheless good print quality paper can be achieved from this method of pulping. In contrast chemical pulping provides a low yield of fibres in comparison to the initial weight of wood, at around 40-55%, but the longer, purer fibres are both strong and stable. However the print quality for paper made from chemical pulps is lower than

that of mechanical pulps (Smook, 2002). By using a combination of these two pulping methods an intermediate yield can be produced at 55-85% with the required properties of the hybrid pulp able to be engineered to match the end use. Indeed often unique properties can be achieved (Smook, 2002).

Mechanical pulping can be achieved by grinding wood against a revolving stone that rotates at peripheral speeds up to 1000-1200m/min. The fibres produced are collected from the stone surface by use of water producing a fibre slurry which is passed through a screen to remove larger particles and thickened by removing water to form a pulp. The pulp produced from this method is known as stoneground pulp. Newer technology utilises wood chips which are shredded between two rotating disks and is capable of producing a more uniform and better quality pulp. The rotating disks are known as a refiner, and the pulp produced known as refiner mechanical pulp (RMP). RMP has a higher proportion of long fibres in comparison to stoneground pulp; however, further developments have now given rise to thermomechanical pulp (TMP). This method uses thermal energy in the form of a pressurised steam pre-treatment to soften the wood chips before being shredded in the refiner. The process decreases the energy needed to shred the wood chips and the resulting pulp is much stronger than RMP (Smook, 2002).

The process of chemical pulping involves the lignin within the wood chips being dissolved away to leave the constituent cellulose fibres. This is achieved by cooking the wood chips with chemicals in an aqueous acidic or alkaline solution at elevated temperature and pressure. The alkaline process is known as the kraft process and is one of the main pulps used in the modern paper industry due to the strength of the pulp produced and ease of chemical recovery (Smook, 2002).

5.2.2 Repulping, Beating and Refining

Often in paper making, the pulping does not occur at the same mill as the final paper production. Therefore dried pulp is often the starting material for many mills, and requires repulping and refining as the first stage of many papermaking processes. Repulping involves the dried baled pulp being dispersed in water to form a slurry and then refined and beaten further to prepare the stock for the papermaking process.

Optimal properties of the fibres can be created to give different paper qualities depending on the end product to be produced.

The aim of repulping is to loosen bonds between the fibres and evenly disperse the fibres within a suspension. The amount of repulping needed will depend on the final product to be produced. A common way of repulping is to use the hydropulper. It consists of a tub into which water and the pulp are added and agitated to disperse the fibres using one or more rotating devices at the base of the tub, Figure 5.2. Newer technology has seen a change in the rotor design so that they protrude further into the tank which allows the consistencies used in repulping to be increased to between 15% and 18%. An increased consistency provides more fibre to fibre friction, resulting in less energy needed to separate the fibres (Smook, 2002).

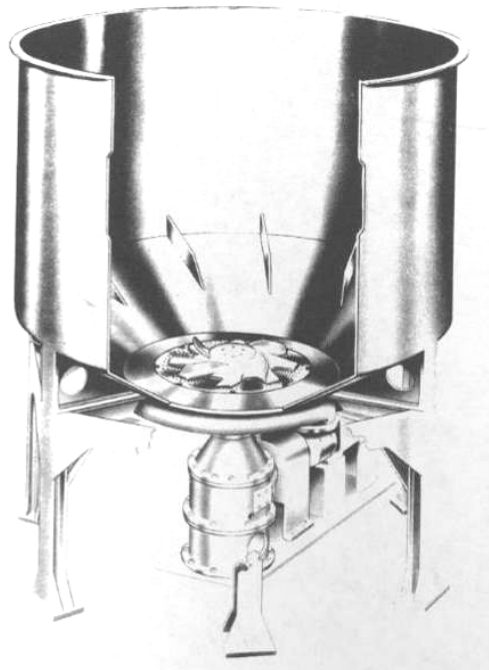


Figure 5.2: Illustration of a Hydropulper (Smook, 2002)

Beating or refining is necessary in papermaking in order to develop good fibre bonding within the finished sheet. After repulping the fibres are well saturated with water; however, without fibrillation of the fibres, sufficient bonds within the paper will not form. During the refining process, the primary cell wall of the fibre is partially removed. As the secondary cell wall is then exposed, the fibre swells further

causing the fibre to become more flexible. This process is known as internal fibrillation of the fibre. The fibre is made up of a microfibrillar structure which is loosened from the surface during the refining process. This causes an increase in surface area, known as external fibrillation. This increase in surface area enables more interfibre bonds to be formed, giving increased strength to the paper sheet formed (Roberts, 1996). Refining is achieved through a mechanical process where fibres are entrapped between rotating bars and stationary bedplates causing shear and normal stresses on the fibres. There are many types of refining and beating equipment that are used in the paper industry, all utilising this underlying mechanical action. Often the term beating indicates where a batch process is used, whereas refining refers to a continuous process. The Hollander beater, previously discussed in section 4.2.2 is one example of this type of technology. The use of Hollander beaters within paper mills was phased out in the 1970s, as they were seen to be too slow and expensive to operate. Modern mills now utilise either disk or conical refiners (Biermann, 1996). Due to this replacement in the operating commercial technology, there is now little current literature relating to the Hollander beater. It is now mainly utilised within hand papermaking studios (Lynch Adnams, 2004), or where stock is mixed for small paper machines (Degener, 2002). The replacement of this technology means that there are many unused Hollander beaters, which could be utilised within the recycling industry.

The Jordan, a type of conical refiner, and disk refiners are two continuous methods of refining pulp. The Jordan is made up of a tapered shell, with metal bars running down its length. A rotating cylinder also with metal bars, known as the plug, sits inside this shell. The cylinder axis and metal bars are oriented parallel to the direction of travel of the pulp slurry (Smook, 2002). Disk refiners are the most recent development within refining technology and can be classified into three types: a rotating disk with a stationary disc, two disks rotating in opposite directions, or one double sided rotating disk between two stationary discs (Smook, 2002). Higher consistencies are able to be achieved with disk refiners enabling better fibrillation of the fibres without cutting. They also have the advantage of being easier to maintain and have lower 'no load' energy consumption.

5.2.3 Screening and Cleaning

Before paper can be manufactured, it is important to remove any contaminants from the stock such as dirt, shives (small particles of under-fibred wood) and other foreign material. This is achieved through use of screens and cleaners to filter out unwanted particles. There are a number of different types of screen used and they are categorised by the method used to separate out the particles for example vibratory, gravity, centrifugal and pressure. The size of particle that is accepted depends on the size of the perforations on the screen. In order to stop the perforations from becoming blocked, the screens are equipped with cleaning devices which either continually or intermittently unblock the holes within the screen to ensure optimal efficiency. Cleaning devices are based on vibration, hydraulic sweeping action, back flushing and pulsation (Smook, 2002).

Within paper mills a number of screens are used, arranged in a cascade arrangement. This allows further concentration of unwanted particles, whilst allowing useable quality fibres to return to the system. The final reject stream is often refined further to capture “good” fibre which then passes through a further screen before returning to an earlier stage in the screening process. Centrifugal cleaners are also utilised within the cleaning process, separating material by density. Figure 5.3 illustrates a two stage primary screening system, with secondary screening and centrifugal cleaners for concentration of reject particles. This type of system would be used for the production of high quality TMP (thermomechanical pulp).

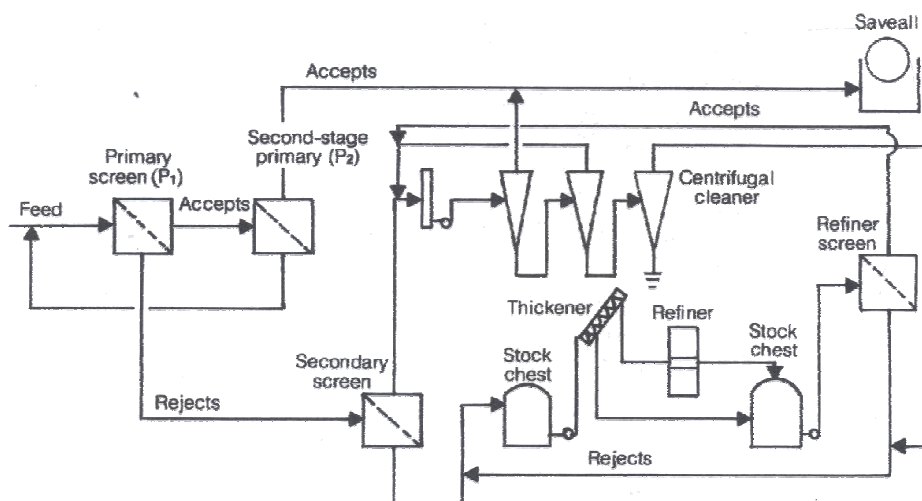


Figure 5.3: Diagram of Screening System (Smook, 2002)

Centrifugal cleaners were patented in 1891, becoming popular within mills by the 1950s. They are also known as a hydrocyclones, vortex cleaners and centricleaners. They are made up of a cylindrical body with a conical tip. Pulp is introduced into the cleaner at a tangent, at the top of the cleaner where the diameter is greatest. The overflow tip or vortex finder (“accepts”) and underflow tip (“reject”) nozzles are centred axially with the overflow at the top, and the underflow at the bottom, where the diameter is smallest, shown in Figure 5.4. Foreign particles are removed by both centrifugal force and fluid shear. This enables particles to be removed by both density and shape (Smook, 2002). The pulp is pumped through the inlet and a pressure drop is created within the hydrocyclone. The flow of the pulp is guided by the shape of the hydrocyclone, and causes a vortex flow pattern to be created. The flow rotates around the axis of the cleaner moving towards the underflow tip. As the diameter of the cleaner reduces, the rotation flow velocity increases. High centrifugal forces are, therefore, created near the centre, which force denser particles away from the “accepts” stream. The “accepts” stream is formed from the change in direction of the water flow at the tip of the centrifugal cleaner, as the outlet is too small for discharge of all the feed stock. The central “accepts” stream moves up the cleaner as an inner vortex due to the small conical tip preventing discharge. The flow, therefore, moves away from the tip until it is discharged from the overflow (Bliss, 1996). This flow movement is shown in Figure 5.5. The dirt particles continue in a downward current due to the centrifugal forces pushing outwards. At the tip of the cone, the dirt particles are pushed inwards, concentrating the particles, and are released as “rejects”. However an air core up the centre of the cleaner is also produced due to the hydraulic movements and this can cause problems if the underflow nozzle discharges to the atmosphere, and additional air can be drawn up from the underflow nozzle and be discharged with the “accepts”. Additional flow patterns within the centrifugal cleaner can also decrease the cleaning efficiency as the hydraulic energy is wasted. This effect has contributed to the development of many design modifications to limit unwanted flow patterns.

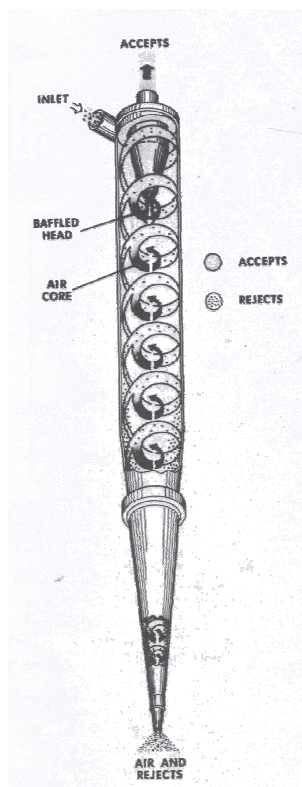


Figure 5.4: Centrifugal Cleaner (Smook, 2002)

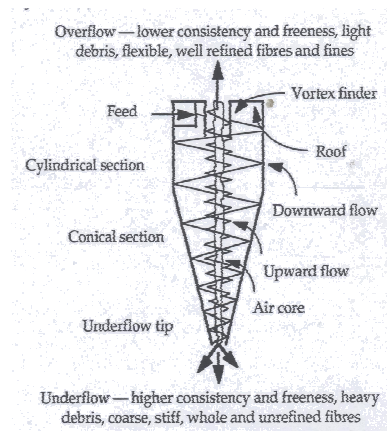


Figure 5.5: Flow Patterns within Hydrocyclones (Bliss, 1996)

The performance of the centrifugal cleaner is dependent on many variables such as the pressure drop, stock flow rate and feed consistency. Stock of low consistencies under 1%, are normally used for cleaning and above this consistency the efficiency is greatly reduced. Pressure drops of approximately 2 bar are typically used. Although in order to increase the centrifugal action, this pressure drop would be increased (Smook, 2002).

The design of the centrifugal cleaner has been modified in order to achieve removal of light debris rather than heavy debris. This is useful for foreign particles such as wax and plastics. Bliss (1996) outlined the machinery modifications and the resulting operating conditions in order to achieve machinery efficiency. The traditional centrifugal cleaner, as described above, is known as a forward flow cleaner. These can remove high density material of specific gravity in the range of 1 - 3.5g/cm² with the

reject material discharged at a consistency two to five times higher than that of the feed. The forward flow cleaner operating conditions are summarised in Figure 5.6

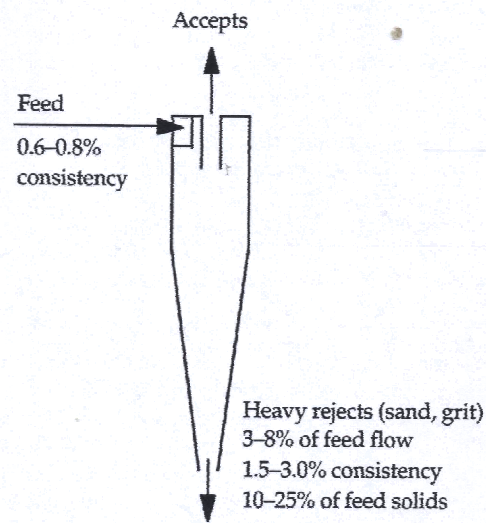


Figure 5.6: Forward Flow Cleaner Operating Conditions (Bliss, 1996)

The first modification to the forward flow cleaner was the core bleed cleaner which separates out lowest density material from the core of the cleaner as shown in Figure 5.7. This was the first time that low density particles were able to be separated from the pulp, and therefore, core bleed cleaners became very popular. However, problems arose in keeping the core bleed outlets clear and the efficiency in light weight contaminant removal was very low. The flow rate of the light weight and heavy weight “rejects” was also unable to be altered separately. Altering the accept pressure also changed the flow rate of the reject streams and led to a cleaner being developed to remove lightweight debris only.

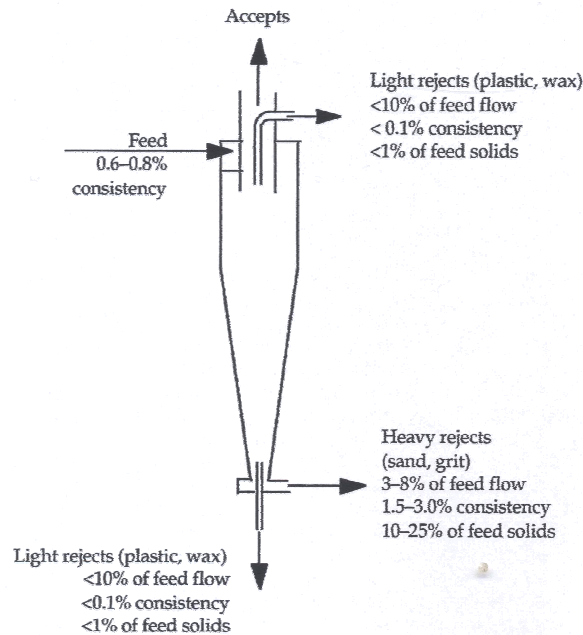


Figure 5.7: Core Bleed Cleaner (Bliss, 1996)

The main difference in the reverse cleaner from the forward flow cleaner is that the accepted pulp is collected from the underflow at the tip of the conical section of the cleaner; whilst the lightweight rejected pulp is outlet from the overflow. Reverse flow cleaners have oversized underflow outlets, which allows more pulp to be let out, rather than causing the upward flow. The cleaner also has smaller sized vortex finders letting only the particles with the lowest specific gravity through to the centre by the centrifugal action. They are also operated under much higher flow rates from underflow tip (“accepts”) at approximately 40 to 60% by volume of the feed flow. In comparison, the forward cleaner flow rate at the underflow tip (“rejects”) is 3 to 8% by volume of the feed flow. The “accepts” stream has a consistency only slightly higher than the feed consistency, making the cleaner operate more efficiently, while the reject stream has a very low consistency and very high volume. This high volume leads to further hydrocyclone processes needed to concentrate the unwanted material and allow useful fibrous material back into the process. Dilution between these stages, however, is not needed. Figure 5.8 summarises these operational differences.

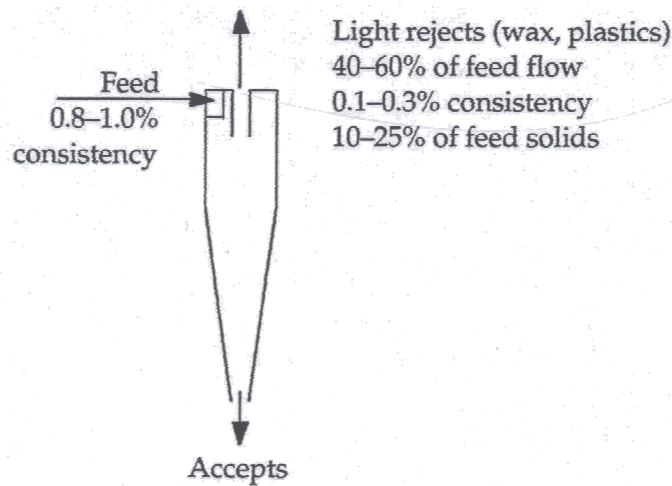


Figure 5.8: Reverse Cleaner (Bliss, 1996)

Through flow cleaners discharge both “accepts” and “rejects” from the conical tip of the cleaner. This operational system has proven to be the most effective cleaner for light debris removal and as there is no outlet at the top of the cleaner, no major flow reversal occurs. Therefore, less turbulence occurs within the hydrocyclone cleaner, and as a result better efficiency of the inlet pressure is achieved. Although the through flow cleaner has a much lower reject rate than the reverse cleaner, with only 1–4% w/w of the feed solids being rejected rather than the 10–25% w/w rejected in the reverse cleaner this means that less processing is needed to return good fibre to the system, giving a more efficient process. Figure 5.9 shows the operating conditions of the through flow cleaner.

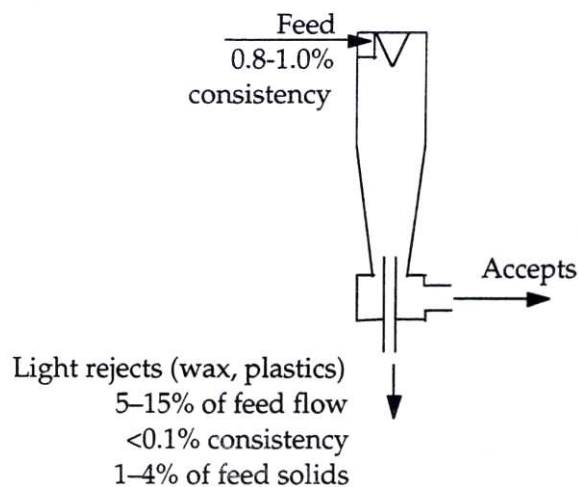


Figure 5.9: Through Flow Cleaner (Bliss, 1996).

There has been much research into the functioning of hydrocyclone cleaners and Bliss (1996) has provided an excellent review outlining the existing research, including: theoretical modelling of the fluid mechanics involved within hydrocyclones, efficiency trends and evaluation, and system considerations in mills. Perhaps one of the most interesting areas of research, particularly where use within the textile industry is concerned, is the fractionation properties that hydrocyclones can achieve (Gavelin and Backman, 1991, Kure et al., 1999, Lu and Liu, 2006, Scott and Abubakr, 1994, Wood, 1990).

Earlier research into the fractionation properties of hydrocyclones are related to the fractionation of coarse fibres. As printing technology developed in the 1980s there became a need for stronger paper with smoother surfaces. Gavelin and Backman (1991) suggested that hydrocyclone fractionation was an obvious way of achieving this through fractionation of the coarse fibres and upgrading reject material by further refining. It has been noted that the main cause for fractionation is the specific surface area of the fibres involved (Kure et al., 1999, Lu and Liu, 2006, Scott and Abubakr, 1994, Wood, 1990). However, the research has also identified other factors relating to the efficiency of the fractionation. Paavilainen (1992) fractionated fibres according to cell wall thickness and concluded that the efficiency was controlled by the accept to reject ratio, which could be altered by changing the tip size of the underflow outlet and the back pressure. It was also noted that the functional variables such as stock concentration, temperature, pressure drop and the mechanical treatment of the fibres involved could all affect the separation efficiency. Kure et al (1999) researched the separation of thick walled fibres within pulp and found fibres with thicker walls were outlet from the underflow, enabling further refining to take place. Fractionation was proven to be more effective where a larger proportion of thick walled fibres were present in the feed system.

Analysis of the fluid dynamics within hydrocyclones has found that hydraulic shear, hydraulic drag, density and centrifugal force all contribute to the separation (Scott and Abubakr, 1994). These forces created fractionation of longer stiffer, fibres with lower specific surface area, to the underflow of the hydrocyclone, whilst well refined, flexible fibres and short fines are fractionated to the overflow.

More recent research relates to the influence of the fibre properties on the fractionation effects and the production of mathematical models to represent fractionation. Park et al (2005) created a model estimating the drag coefficient on fibres which suggested that fibres with higher slip velocities were rejected from the underflow outlet. The slip velocity describes how the fibres move within the fluid and is increased by an increase in the velocity of the fluid, density of the fibres, and volume to area ratio. However, it would be decreased by an increased drag coefficient and the drag coefficient was, therefore, seen as a dominant variable. This was proven using hydrocyclone experimentation that showed where unbeaten fibres, were of a higher concentration within the reject stream. Lu and Liu (2006) calculated a separation index from their experimental work where the separation index is a ratio of the fibre fraction density function, of the overflow or underflow, to the feed. They found that there was a critical fibre length for any group of fibres to be fractionated. A higher proportion of fibres longer than this critical length would be found in the overflow stream, whilst a higher proportion of fibres lower than the critical length were found in the underflow stream. They also found the split ratio to be the most significant factor in fractionation of fibres. The split ratio is the ratio between the flow rates of the overflow and feed and the range of optimal split ratios to use was also calculated.

The geometry of the hydrocyclone has also been identified as an area that may affect the fractionation efficiency. Statie et al (2001) looked at each section of the hydrocyclone and found the main areas affecting fractionation were the angle of the conical chamber, the length of the vortex finder, the feed diameter, and the diameter of the vortex finder. It was found that a slight decrease in the conical chamber angle, and hence, a slight lengthening of the cone, increased the percentage of fibres that were discharged from the underflow. This trend was more pronounced on a denser fibre, showing a higher proportion of denser fibres would be rejected in comparison to the lower density fibres. An increase in the vortex fibre length increased the number of particles that were carried upwards to the overflow, with the trend more pronounced on less dense fibres. The feed diameter was proven to be the most important geometrical factor affecting separation. The difference in the percentage of the dense fibres and the less dense fibres that were outlet to the overflow increased from almost zero to 25% by varying the feed diameter. This was seen when the feed

diameter is half that of the annular chamber width. Similarly a decrease in the vortex finder diameter also slightly improved separation efficiency.

Fractionation of synthetic fibres was carried out by Ho et al (2000) in order to understand the fractionation process better. Nylon fibres were used with known lengths and coarseness. It was found that coarse, short fibres were rejected whilst fine, long fibres were accepted. The effect of flow rate and the feed consistency was investigated. At high flow rates of more than 60 kg/min, the “accepts” fraction consisted entirely of the fine fibres. However, the “reject” fraction contained a mixture of the coarse and fine fibres. Change in the feed flow also altered the consistencies of the “accept” and “reject” fractions. The “reject” consistency increased as the flow rate increased, whilst the “accepts” consistency decreased. However, the “reject” consistency was always higher than that of the “accepts”. Although the feed flow rate is linearly related to the pressure drop between the feed and the “accepts”, the feed consistency has no effect on the pressure drop. Fractionation of the fibres by length caused the consistency to have a great effect on the volumetric reject ratio (reject flow rate/feed flow rate %). However, this trend was not observed from fractionation by coarseness. It was suggested that this was due to the tendency of hydrocyclones to plug when using long, stiff fibres, and hence, flow rate of the “reject” fraction is lowered, where higher consistencies are used. The consistency and flow rate had little effect on the fractionation by length, with increased flow rate and consistency both resulting in a slight, no more than 0.1mm, increase in average length in both the “rejects” and the “accepts”.

Fractionation by length is now becoming a popular field of research. In addition to hydrocyclones, experimentation using rotating cones and flotation cells to fractionate pulp fibres into different lengths has also been investigated (Rewatkar and Masliyah, 1997. Eckert et al, 1997. Etkert et al, 2000) as cited in (Dabros et al., 2009). Air-sparged hydrocyclones were patented in 1981 (Miller, 1981) and this technology uses an injection of air bubbles in order to assist in the separation of fine particles and coarse particles in the mineral industry. Dabros et al (2009) used this technology to investigate pulp fibre fractionation by length. From this investigation he concluded that fractionation was most effective with high injection of air, low ratio of overflow

to underflow flow rates, and a dilute pulp feed. It was recommended that air-sparged hydrocyclones could prove very useful in fractionation within the pulp industry.

5.2.4 The Paper Machine

Once the pulp has been prepared, the paper making process can begin. There are many different types of papermaking machine that have been developed for particular types of paper. However, the Fourdrinier paper machine is probably the most widely known and offers a basic principle into the process of making paper. The pulp from the pipeline is distributed across the machine from front to back by the flow spreader, levelling out any consistency variations and cross current variations. A uniform jet is discharged from the headbox to the moving forming fabric and the water is then drained from the stock, forming the fibres into a continuous matted web. The Fourdrinier table is made up of suction pumps, which draw the water away from the paper sheet. Roll presses are then used to remove more water from the sheet. The pressure from these rolls consolidates the paper sheet, forcing the fibres together to allow bonding. The dryer section is made up of many steam heated rollers where the remaining water evaporates from the sheet surface and the fibre to fibre bonds are formed. The calender stack reduces the thickness of the paper and improves the sheet smoothness with the finished sheet wound onto a reel. Figure 5.10 shows a diagram of the Fourdrinier paper machine (Smook, 2002).

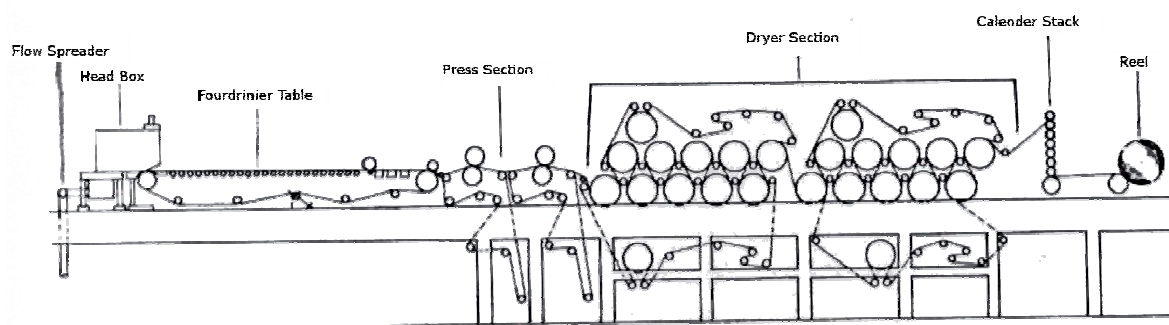


Figure 5.10: The Fourdrinier Paper Machine (Smook, 2002)

Alterations in this machine design include: twin wire formers, which use two wires to form the paper sheet, and the cylinder machine, which form the sheet on a cylinder rather than a table (Biermann, 1996).

5.3 Paper and Textiles

5.3.1 Textiles Fibres in Paper

Textile fibres have been used for many years within the paper industry. Cotton rags were in fact the main fibre source for paper in the late nineteenth and early twentieth centuries (Roberts, 1996). Many textile fibres such as cotton are cellulosic, and therefore, they form hydrogen bonds in the same way as wood pulp. However, virgin cotton fibres are much longer than wood pulp fibres and when used to make paper, virgin cotton fibres result in poor paper formation as the fibres do not distribute evenly within the web, due to their length. As cotton fibres are very popular within the textile industry its use in the paper industry would prove uneconomical due to the price of the cotton. Therefore, by using rag cotton from the textile industry, either pre-consumer or post-consumer which can be collected cheaply, these financial problems are alleviated. Rag cotton fibres are also shorter than virgin cotton at 10-45mm long. Cotton linters, the seed hair, can also be used within the paper industry, their length being much shorter than rag fibres at 1-2mm (Biermann, 1996). In addition the bonding properties of cotton are also different to those of wood pulp.

Cotton is made up of a pure cellulose structure, whereas, wood pulp also contains 15-25% of hemicellulose which is an unstructured polysaccharide of low molecular weight. It is thought that the hemicellulose contributes to the paper strength, either by interfibre hydrogen bonds or by disruption of the crystalline surface during the mechanical action imparted during pulp preparation (Roberts, 1996). The pure cellulose cotton fibres, therefore, have a lower bonding strength than wood fibres that include the hemicellulose component. The cotton is, therefore, often mixed with wood pulp to give stronger paper (Biermann, 1996).

Similarly other cellulosic fibres can be used within the paper industry such as bast fibres including hemp, jute and ramie. These are long fibres, generally 4mm to 60mm in length and are very strong. They are used for specific purposes such as cigarette papers, tea bags, sack paper and saturating paper (Biermann, 1996).

In addition to cellulosic fibres a number of synthetic fibres have been used in the paper industry. In the early twentieth century the development of synthetic fibres triggered a new interest within the paper industry to incorporate these new fibres into paper to give specific properties. In 1936 a German patent was granted to Eloed for his invention of a regenerated cellulose paper (White, 1993). Work followed on polyesters, polyamides and acrylics and in 1953 Arledter produced 100% synthetic fibre papers (White, 1993).

Synthetic fibres have been added to cellulosic fibres to achieve partially synthetic paper. Normally 5-10% synthetic fibre is used, but up to 20% has been used previously (White, 1993). The cellulose fibres provide the bonding performance characteristic, whilst the synthetic increase the product and process performance and reduce the negative effects of the cellulose fibres. These negative features include water retention which increases the processing costs to remove the water and can cause running problems. By blending different synthetic fibres with wood pulp a wide variety of product characteristics can be engineered (White, 1993).

An increased amount of synthetic fibre can be added to cellulose pulp if a binder is also used. As there is no bonding between the cellulose and synthetic fibres, binders enable the synthetic fibre to exhibit their properties in the final sheet. Synthetic fibres can make up between 20% and 50% of the fibre web using this technique. Binders are added by saturation of the fibre web in a polymer dispersion with the binder content used between 20% and 50% of the sheet weight. The sheet properties are also altered by the properties of the binder used. Where rubbery binders are used, paper with soft draping characteristics can be produced; whereas stiff binders give rigid sheets. This paper is treated much like conventional paper during its production with slight modifications to the stock handling. This form of synthetic paper has the advantage of being relatively cheap due to the wood pulp content present, whilst also having some properties of the synthetic fibres within the sheet. However, in order to fully utilise the properties of the synthetic fibres, entire synthetic sheets were developed (Hentschel, 1964).

Early work with synthetic paper proved difficult as the hydrogen bonding that imparted strength to cellulosic paper could not be achieved with synthetic fibres.

Research was therefore centred on bonding techniques in order to take advantage of the strong synthetic fibres within paper. Alternative bonding mechanisms were examined as a means to replace the hydrogen bonding. Hubbard et al (1955) described two new bonding methods: salt bonding and synthetic polymer bonding. Salt bonding utilises the way in which salt solutions act as swelling agents or solvents for fibre forming organic polymers. The salt solutions must be concentrated in order to act as a solvent. Dilute salt solutions are added to a synthetic fibre web, the excess water then evaporates, leaving a more concentrated form of the solution. The solution accumulates at the cross-over points of the fibres, increasing the concentration of the salt solution further. Once sufficient evaporation and accumulation of the salt solution has occurred, it becomes strong enough to act as a solvent to the organic polymer and gelatinisation of a portion of the fibre surface occurs. Gelatinisation of fibres at cross-over points in the fibre web cause adjacent fibres to coalesce. When complete evaporation of the water has occurred the polymer solidifies completing the bonding process. The paper is then washed and dried to remove the salt. The concentration of salt solution used for this process varies, depending on the fibre to be bonded and the temperature and pressure used in the forming of the sheet. Generally solutions of 2-10% are used with the salt used within the process selected depending on the polymer to be bonded. This is a very simple process; however, it has not become commercially acceptable due to a number of disadvantages. The salts used in the solutions are corrosive to metals, and therefore, damage the paper machinery. Salt bonded webs are also relatively weak in comparison to other methods of bonding. The unbonded weak webs also have to be handled on the machine before the bonding process is completed, methods for increasing the strength of the web whilst it is on the wire were therefore, still needed (Hentschel, 1964).

Polymer bonding involves using a binding polymer. The fibre sheet is saturated with the binder dispersion, in a similar way to salt bonding again with the carrier liquid evaporates concentrating the binding polymer at the fibre crossover points. Heat and pressure are then used to bond the web together. The binding polymer melts and fuses the fibres together at crossover points, bonding the web together (Hubbard et al., 1955). Again, this fibre web is very weak before bonding occurs, and therefore, needs to be handled very carefully before the binding polymer is added, causing problems in the manufacturing process (Hentschel, 1964). Alternatively the binding polymer can

be added by a precipitation method where the binder is added to the dispersed polymer, before the web is created. This also causes problems, due to the fact that the dispersed binding polymers do not have a natural affinity to the synthetic fibres. This method is, therefore, ineffective at binding the fibres. In order to alleviate these problems, small amounts of the binder dispersion can be sprayed onto the fibre web while it is still on the wire. This gives enough strength to the fibre web for its subsequent processing. The fibre web can then be saturated with binding polymer to give the paper better dry strength. Optimum properties are generally achieved where the binder content is 40% of the sheet weight (Hentschel, 1964). The polymers chosen are usually chemically similar to the fibres to be bonded and have elastic properties (Hubbard et al., 1955).

A similar bonding process using synthetic polymer binders with features similar to wood pulp has also been developed, in light of the problems mentioned with previous bonding methods. These polymers add sufficient strength to both the wet and dry fibre web, and therefore, the synthetic fibres can easily be processed on paper machinery (Hentschel, 1964). The fibrids, as these synthetic binders are known, are combined with synthetic fibres, to give properties similar to those of cellulosic pulps. When preparing these pulps, the synthetic fibres first have to be dispersed in water to create a slurry consistency of 0.05-0.1% w/w. The fibrids are dispersed in water using a hydropulper to a 1-3% w/w consistency and then opened up further, using a disk mill. The two dispersions are mixed together just prior to feeding the slurry to the headstock, which minimises flocculation of the fibres. Water is then also added to the head box to give a final stock consistency of 0.025%. The fibre web is then formed on the wire, and dried and processed in the conventional way. Due to the low consistencies used, an inclined wire is used to give good web formation. The speed is altered during drying to allow for the shrinkage difference in the synthetic fibres (Hentschel, 1961). The binders are melted to give the final bonding of the fibres and obtain the final dry sheet strength. This can be done with or without pressure to give different sheet properties. If no pressure is used, the final sheet will be soft and drapeable with a low density. Using pressure within a heated calender produces a dense sheet with more paper-like qualities, being stiff and having higher strength than sheets fused without pressure (Hentschel, 1964). Calendering is carried out at approximately 200°C, just above the fusing temperature of the fibrid. The sheet must

be raised uniformly to this temperature, and therefore, preheating of the sheet is often used to achieve higher calendar speeds. If pressure is not used the paper sheet (textryl) needs to be raised to a temperature of approximately 220°C for a sufficient length of time in order for the fibrils to fuse. The sheet will require support in this stage and textile pin stenters are often used although again some shrinkage may occur in this process (Hentschel, 1961). By using fibrils the paper sheet (or textryl) can be made to be chemically homogenous, as the fibril can be made from any synthetic polymer. Fibrils are, therefore, chosen to have the same chemical composition as the fibre. Using this method the fibril binder needs only to be 25% of the sheet weight in order to obtain maximum binding (Hentschel, 1964).

Since this development in binding of synthetic fibres to product webs, further work has been carried out regarding synthetic fibres with fibrillating qualities. White (1993) outlined numerous works carried out in the late 1970's and early 1980's where fibrillated manmade fibres have been used. These include biodegradable cellulose acetate with hydrophilic and thermoplastic characteristics, known as fibrets that can be used in wet-laid nonwoven processes. Also polyacrylonitrile fibres with fibrillating qualities, that when beaten, can form paper-like webs without the need of cellulose pulp. Film fibrillation can produce fibrillated fibres made from polyamides, polyesters and PVC so that they can be successfully used within papers. Also Kevlar pulp has been developed which can be used with or without other fibres to produce high performance webs. There is no clear line between synthetic paper made in this way and wet-laid nonwoven fabric, and as such nonwoven technology could be described as an area in which textile technology has completely overlapped with paper technology.

Recent articles on synthetic paper illustrate its popularity and increased demand (Larson, 2006, Licata, 1999, Thompson, 2004, Walsh, 2001), outlining where it is being utilised and information about its printing properties. Walsh (2001) also predicted that the synthetic paper market would increase at 8.4% per year in the years leading up to 2005, to give a total of 75 million kg. Modern synthetic paper is generally made from polyethylene, polypropylene, polystyrene or polyethylene terephthalate and it is combined with fillers such as titanium dioxide, calcium carbonate and silicas (Walsh, 2001). Synthetic paper has properties such as water

resistance, tear durability, smoothness, whiteness and can also be recycled easily. It, therefore, offers itself to products such as labels, brochures, manuals, speciality packaging, maps, menus and book covers (Larson, 2006, Licata, 1999, Thompson, 2004, Walsh, 2001). Much of the synthetic paper market concerns in-mould labels and rigid blow moulded containers where the synthetic paper labels become part of the container wall. Thus as the label is chemically composed of the same material as the rest of the packaging means that recycling of the entire product can be easily done without any separation stages.

Valeron DT has recently been introduced as a printable synthetic substrate for high strength tag and label applications and eliminates the need to laminate wood pulp papers for use in outdoor areas such as ski lift tags, fishing licences and plant tags in greenhouses and nurseries (Larson, 2006).

5.3.2 Paper in Textile Fabric

A method of making paper fabric was patented in 1886 (Wyman, 1886) and described the use of fine tissue paper, made of Manila hemp, which is cut into strips of 1cm. The strips are then wound onto bobbins before being immersed within a water bath to thoroughly wet them. The bath may also contain dye or size to impart colour or strength to the paper yarns. The strips are then twisted tightly using a twisting frame in order to obtain the paper yarn. Whilst still damp, the paper yarn is wound onto bobbins to be used as a weft in the fabric. This process removes kinks from the yarn and creates a more compact thread. The yarn can then be woven into fabric, still in a damp, pliable state using the paper yarn as the weft yarn. The inventor stated that the paper yarn can also be used as the warp, if it has been sized, but better fabric was created using a cotton warp with paper yarn weft. The resultant fabric is pliable, light, springy and cheap to produce. The Manila tissue paper used to make the paper yarns had a base weight of 4.3 kg per ream of with sheets being 60cm x 90cm. The patent does not specify the number of sheets to the ream, but using the standard of 500 sheets this converts to 15.5g/m².

Further technical adaptations, particularly throughout the 1930s to 1970s have been made to the methods of making paper yarn in order to get a stronger more flexible

yarn. In 1947 a paper yarn was patented that was flexible and strong enough to be used as weft in a needle or shuttle loom (Hamilton, 1946). This was created by having moisture entrapped within the yarn using a flexible film or coating. This coating also provided wet strength to the yarn enabling it to be woven without being broken. The twisting of the yarn is carried out using conventional methods. However, the coating is applied after the yarn has been partially formed but before the twisting operation is completed. Once woven into a fabric, the yarns could be modified to give the stiffness and body to the fabric. Another method for making paper yarns, patented in 1967 (Evans, 1967) describes a method of making a fine paper yarn from medium to heavy weight paper, of base weight between 3.5kg and 16kg per ream of 500 sheets, presuming sheet size of 60cm x 90cm this equates to 13 to 57 g/m². The paper has high elongation and does not require the yarns to be immersed in water before twisting and additionally the paper has a high fibre orientation, increasing the strength of the yarns produced. High fibre orientation in the machine direction is produced by forming the web with a high ratio of Fourdrinier wire velocity to stock in-feed velocity. Papers with 80% of fibres preferentially orientated in the machine direction were found to give the best results for this paper yarn. To give high elongation the paper is dried with the web in an unstretched condition in both the machine and cross directions. Papers were produced with a stretch of up to 13% in the machine direction; in comparison most papers have a stretch between 0.5 - 2% (Evans, 1967). Papers should have a stretch in excess of 4% to be efficient as paper yarns produced by this method, as the stretch increases the toughness of the paper. The paper is slit into ribbons of no more than 0.5cm, moistened and twisted using low speeds and high humidity, in excess of 70% relative humidity to produce the yarn (Evans, 1967).

Broughton and Wang (1955) investigated many of the factors involved in paper yarn manufacture, to give further understanding of their effect on the final yarn properties. They used a method in which paper strips 1.5cm were moistened before being twisted using a modified ring twister commonly used in the cotton industry. The effect of the mechanical factors: twist, size of traveller and feed roller design were investigated alongside the chemical factors: surface active agents and their concentration and temperature. The breaking strength of the paper yarns was found to have a linear correlation with the wet pick up, with optimum wet pick up being 40% irrespective of the number of twists imparted to the paper ribbon. The use of active wetting agents in

high twist yarns was, therefore, considered important, as due to the spinning speeds involved, the high twist yarns did not reach this moisture content. The concentration of the surfactant agents was not as important so long as the minimum surface tension was reached and anionic surfactants were found to be most effective processing additive. In addition the optimum twist of the yarn, much like in textile yarns, was found to be 1.8 turns/cm. It was also found that increased traveller weight gave increased breaking strength, as the yarn was more compact due to the increased tension imparted to the yarn during the spinning process. This relationship was also found to be linear.

Paper yarns have seen much use as backing for rugs and carpets, automobile seat covers and other upholstery applications (Broughton and Wang, 1955). Modern paper yarns are made in a similar way to those in the early 20th century, often using Manila hemp as the fibrous material from which the paper is made. The paper is slit to ribbon of 1-6mm width before being twisted into yarn and is able to withstand modern weaving and knitting production, and also go through dyeing and finishing processes. Fabric produced from these processes is light, strong and has little fuzz. It is smooth and also offers both good insulation and ventilation, making it ideal for dress fabric. (Oji Fiber Co, 2012).

5.3.3 Synthetic Paper Yarns

By combining the above two technologies of synthetic paper and paper yarns, Howell (1966) patented the synthetic paper yarn in order to achieve soft, drapeable paper yarns that would be suitable in apparel. Lightweight paper made from synthetic fibre bonded with fibrils was created. 15% to 60% by weight of fibrils are used within the paper with 85% to 40% staple synthetic fibre. The synthetic fibres used within the paper are 0.3cm - 2.5cm with a denier of 0.5 to 10 and bonding was achieved with no pressure applied to create a more drapeable paper. This paper was then cut into strips between 0.16cm to 3.17cm and twisted to form yarns. Twist in the yarn can be varied between 2-8 turns/cm and the denier of the yarn formed can be varied by altering either the weight of the paper used, or the width of the strip. The thickness of the paper used to make these yarns can be as low as 1.5mm or as much as 5mm and the yarns created have a high degree of bulk and covering power.

The yarns are suitable to be woven or knitted using conventional equipment and the fabrics produced from these yarns are said to have a cashmere-like hand. They are also able to withstand chemical and mechanical finishing treatments to further improve or create the desired properties. The yarns created from synthetic paper have a greater elongation and lower initial modulus than traditional paper yarns. In addition they are also tougher, more resilient and have a greater wet strength, making them capable of withstanding the durability and washability required for yarns used in apparel. The inventor (Howell, 1966) suggested uses in suits, dresses, skirts, blouses and shirts as well as upholstery fabrics such as curtains, automotive upholstery, seat covers, floor coverings and rug backing. The yarns could also be used in accessories such as bags and hats or in industrial uses such as electrical insulation and cable filler cords.

Despite the many uses suggested by the inventor, this invention does not seem to have been commercialised as no modern references to synthetic paper yarn have been found. However, it offers a potential use for recycled textile fibres that are too short to be twisted into yarns directly.

5.4 Experimental – RFL Coated Nylon 66 Paper Handsheets

The subsequent sections introduce the concept of utilising the RFL waste in paper form. Recycled RFL fibres were used alongside softwood fibres to produce paper handsheets and the properties produced are discussed.

5.4.1 Materials

Waste fabric from Heathcoat fabrics was used as the raw material within this study. The waste consisted of RFL coated fabric ends and selvages. The fabric was 100% nylon 66 of mixed specifications. The waste fabric was broken down in the Hollander beater as described in Section 4.2.2 using a 60 minute beating time adjusting the beater roll as described in Table 5.1. A consistency of 1% solids by weight was used in the beating process, using 5.6kg fabric with 560 litres of water. The reduction process by Hollander was chosen for this work since it produced a short fibre suitable

for introduction to paper which had not degraded in the reduction. Since the Hollander beater also utilised the fibre within a slurry in the reduction process, this slurry could also be used in the paper making process, whereas dry fibres would have required suspension in water prior to this work.

In addition to the RFL nylon pulp, Lapponia Pine softwood pulp obtained from Stora Enso mill was also used and was prepared using a disintegrator, to a count of 400 revolutions at a consistency of 1.5%. The softwood pulp was used as a binding medium within the paper sheet.

Table 5.1: Beating Procedure for Pulp Formation

Time (minutes)	Beater Roll Setting	Comments
	4TU	Fabric added to beater
0	4TU	All fabric incorporated. Time started.
15	1TU	Beater roll lowered
30	D	Beater roll lowered
50	1TD	Beater roll lowered
60	1TD	Beating stopped

5.4.2 Handsheet Formation

Paper sheets were formed using a mixture of softwood cellulose pulp and nylon pulp in order to impart sufficient paper strength through hydrogen bonding of the cellulose pulp. The cellulose pulp was used as a matrix in which the RFL coated fibres were held. Stock pulp slurries were formulated with varying percentages of nylon and softwood as summarised in Table 5.2. The volume of nylon pulp and softwood pulp required was calculated to give the correct percentage by weight of nylon and softwood fibre. The pulp was then diluted to give 12g of fibre in 4000ml of water giving a consistency of 0.3%. For each handsheet 400ml of pulp was used, giving handsheets of 1.2g (60 g/m²), as set out in the Tappi standard T205. For stocks of a higher nylon percentage, handsheets were also made at 2.4g (120 g/m²) and 3.6g (180 g/m²).

Table 5.2: Composition of Handsheets

Ratio of RFL coated nylon 66 fibres to cellulose fibres by weight	Weight of nylon fibres required for 12g slurry batch	Volume of 1.5% consistency nylon slurry (ml)	Weight of softwood fibres required for 12g slurry batch	Volume of 1.0% consistency softwood slurry (ml)	Total volume of pulp stock (ml)	Volume of water required to dilute to 4000ml
0:100	0	0	12	1200	1200	2800
50:50	6	400	6	600	1000	3000
60:40	7.2	480	4.8	480	960	3040
70:30	8.4	560	3.6	360	920	3080
80:20	9.6	640	2.4	240	880	3120
90:10	10.8	720	1.2	120	840	3160
100:0	12	800	0	0	800	3200

Paper handsheets were made following the paper TAPPI standard T205 sp-02. This method uses a sheet former which consists of a cylindrical tank above a metal wire mesh. The tank can be filled from below the wire from a tap, and pulp stock added from an opening at the top. The water was able to be drained through the wire, producing the paper sheet. To achieve this, the wire was first cleaned by turning on the water and rubbing the surface of the wire to remove any fibres. The sheet former was filled halfway with water before adding the amount of pulp stock required to make one sheet. More water was added until the water was at a depth of 350mm. The stock was agitated using the perforated stirrer and moved down and up 5 times within 6 seconds, keeping the perforated disk beneath the surface of the water. The perforated stirrer was then removed using one slow up and down movement. The drain was fully opened allowing the sheet to be formed on the wire. The paper sheet machine was then opened up, allowing the paper sheet to be accessed and couching to take place, removing all excess water from the sheet. Two sheets of blotting paper were placed on the drained paper sheet and the couch plate placed centrally on top of the blotting paper. The couch roll was placed in the middle of the couch plate and rolled back and forth 5 times, with no added pressure to the roll. The couch roll was then returned to the centre of the plate and lifted off. The couch plate was removed and the blotters lifted from the wire. The paper sheet adhered to the lower blotter and was removed from the wire. Ten handsheets were made in this way before being pressed together. The handsheets were pressed on the blotter and covered with a

polished plate. More blotters were used to separate each handsheet, and cover both the top and bottom of the pile. The press cover was then placed on top of the sheets and screwed into place. Pressure was raised to 345 kPa over 30 seconds, and maintained for a further 5 minutes. The stack of handsheets was removed from the press and the blotters removed from the handsheets, leaving them adhered to the polished plate. A second pressing was then undertaken at the same pressure for 2 minutes using dry blotters. The blotters were removed from the handsheets and the plates with attached test handsheets placed into drying rings. The drying rings ensure that the handsheets do not shrink during drying and each handsheet was in contact with the rubber seal of the drying ring above. A heavy weight, approximately 11kg, was placed on the stack of drying rings and the sheets were then left to dry overnight in a conditioned room at 23°C 50% RH. The paper handsheets were finally removed from the drying rings and gently peeled away from the polished plates.

5.4.3 Physical Testing of RFL Coated Nylon 66 Paper Handsheets

The physical strength of the paper was tested based on the TAPPI standard T220. The sheets were conditioned at 23°C and 50% RH, before testing the mass, thickness and tensile strength.

The weight of the sheets was measured individually, noting the handsheets with faults. As the sheets were of an area of 200 cm² the weight per unit area was calculated by multiplying the sheet weight by 50.

The thickness of the sheets was then tested using a Messmer deadweight micrometer. Each sheet was tested separately in three different places and the mean value calculated for each sheet, and the batch as a whole.

In order to test the tensile strength of the paper, the sheets were cut into strips 15mm wide and ten strips were made for each handsheet batch. Weak areas caused from thin areas within the sheet were avoided. The Instron 4411 tensile tester was used to test the strips with a gauge length of 100mm and crosshead speed of 10mm/minute. Tests were only carried out on samples up to 80% nylon as handsheets with higher ratios of nylon easily deformed under their own weight.

5.5 Results and Discussion – RFL Coated Nylon 66 Paper Handsheets

5.5.1 Forming of the Paper Sheet

Table 5.3 summarises the paper handsheets created and the types of faults observed. Figures 5.11, 5.12 and 5.13 show examples of the faults classes used to summarise the results.

Photographic evidence of the results of the sheet formation has also been taken as shown in Figure 5.14a-i. Images show a range of handsheets from each batch, selecting a variety of sheets with different levels of severity of faults.

Table 5.3: Summary of Handsheet Formation

Weight per unit area (g/m ²)	RFL coated nylon and softwood Fibre Content (%)	Number of Sheets Pressed ¹	Number of Sheets with no faults ²	Number of Sheets with small faults ³	Number of sheets with large faults ⁴
60	100 Softwood	8	8	0	0
60	50 Nylon – 50 softwood	11	11	0	0
60	60 Nylon – 40 Softwood	12	4	3	5
60	70 Nylon – 30 softwood	10	0	5	5
120	70 Nylon – 30 Softwood	6	1	0	5
60	80 Nylon – 20 Softwood	11	1	2	8
120	80 Nylon – 20 Softwood	7	0	1	6
120	90 Nylon – 10 Softwood	8	0	1	7
180	100 Nylon	5	0	0	5

¹ Further attempts to create sheets may have been made but discarded after couching due to disintegration of the sheet.

² To be considered as having no faults the sheet should have no holes and have a relatively even layer of fibres over the entire sheet. Some variance in sheet thickness may have occurred in these sheets. See Figure 5.11 for a pictorial example.

³ Small faults refer to small holes within the sheet, no larger than 2cm in diameter, or where the fibrous sheet is very thin showing an obvious weak point. See Figure 5.12 for pictorial example.

⁴ Large faults refer to any holes larger than 2cm in diameter or multiple holes smaller than this size on one sheet. It also refers to very large low fibre density areas within a sheet. See Figure 5.13 for pictorial example.



Figure 5.11: Example of a sheet with no faults



Figure 5.12: Photographic examples of sheets with minor faults such as the hole in the left sheet and small areas of thinness in the right sheet.

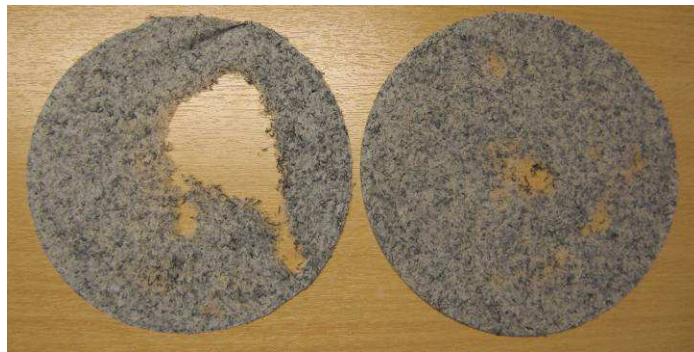


Figure 5.13: Photographic Examples of Sheets with Major Faults, such as the Large hole in the Left sheet and Many Smaller Holes and Large Areas of Thinness in the Second Sheet.

The 50% RFL coated nylon/50% cellulose sheets were relatively easy to form as the fibres were dispersed well in the pulp and formed an even layer on the wire. The fibres were able to be removed from the wire onto the blotting paper very easily, with

no disintegration of the wet sheet. The nylon and cellulose fibres held together well in the sheet and were resilient to handling.

When the percentage of RFL coated nylon 66 increased to 60% problems started to occur in the making of the sheets. The sheet was generally able to be removed from the wire without problems, although two out of the 10 sheets made did not adhere to the blotting paper sufficiently during removal. These sheets were therefore partly removed by hand. This was not hard to do as the majority of the sheet was already detached from the wire. Some fibres were left on the wire after the removal of the sheet. This caused unevenness in the thickness of the finished sheet. In addition, there were also problems with drainage not occurring evenly over the sheet. More than half of the sheets made had areas where no fibres were present. From the sheets with formation faults half were considered to be large enough gaps in the fibre mesh to be regarded as unusable. The drainage problem could be due to small nylon fibres becoming entrapped within the screen or could be due to poor suspension of the fibres.

Forming the 70% RFL coated nylon 66/30% cellulose and 80% RFL coated nylon 66/20% cellulose handsheets highlighted the same problems further. Fibres seemed to be dispersed well throughout the water; however holes did form within the sheets due to uneven layering of the fibres during draining. Where holes did not form there were obvious weak points within the sheet at thin areas. The main problem occurred when removing the wet sheet from the screen. The sheets needed to be couched twice in order for the sheet to be transferred to the blotting paper to continue with the pressing process. The sheets when dry were still very fragile and thin. It was thought that thicker sheets may be able to hold together when wet better than 60 g/m² sheets. Sheets of 120 g/m² (2.4g) were, therefore, also made for papers of higher nylon percentages.

The 70% RFL coated nylon 66 paper at 120 g/m² was able to be removed from the wire more easily as it adhered to the blotting paper better. There were still problems with the evenness of the paper and similar results were found with the 80% RFL coated nylon 66/20% cellulose 120 g/m² paper. Problems were observed in removing the sheets from the wire and the sheets were peeled off the wire by hand as they did

not adhere to the blotting paper. Due to the added thickness, there were fewer problems with tearing upon removal than the 60 g/m² sheet.

Although the success rate of paper formation was relatively low it was decided to continue to make some sheets at 90% RFL coated nylon 66/10% cellulose and 100% nylon but only at the 120 g/m² weight. However the 90% RFL coated nylon 66/10% cellulose was still difficult to remove from the wire and as the wet strength of the sheet was so low, the sheets were often ripped whilst peeling the sheet off the wire. Again the evenness of the sheet varied and the removal of the 120 g/m² 100% RFL coated nylon 66 sheet by hand was not possible as it disintegrated due to its low wet strength. 180 g/m² sheets were therefore made to ascertain the strength, in order to establish if the sheets were able to be removed from the wire. However even with added weight the wet sheets were still very delicate and were removed from the wire using a thin sheet of metal which was sliced between the nylon sheet and the wire. This was then able to support the weight of the nylon when transferring the formed paper to the blotting paper. However there were still problems in getting an even sheet and holes were observed in all five sheets that were formed. There was also an additional problem in removing the nylon sheets from the drying ring as the sheets were still very weak when dried, and therefore they ripped easily.



a. 100% softwood

b. 50% RFL coated nylon
66/50% softwoodc. 60% RFL coated nylon 66/40%
softwood

d. 70% RFL coated nylon 66/30% softwood

e. 70% RFL coated nylon/30%
softwood 120 g/m²

f. 80% RFL coated nylon 66/20% softwood

g. 80% RFL coated nylon 66/20%
softwood 120 g/m²h. 90% RFL coated nylon 66/10% softwood 120 g/m²i. 100% RFL coated nylon 66 180 g/m²

Figure 5.14: Photographs of Nylon Papers Formed from Various RFL coated Nylon 66/Cellulose Pulp Compositions

5.5.2 Physical Testing of Handsheets

The result from the grammage and thickness analysis are summarised in Table 5.4 and Figures 5.15 and 5.16, raw data is available in Appendix 2. Most handsheet weight per unit area was higher than the intended value, with increased variation in weight as the amount of nylon increased. This is likely to be due to the nylon fibres having a tendency to float in the fibre/water suspension, an increased number of nylon fibres would therefore be sampled in the first handsheets made from the fibre stock batch. As more handsheets were made the consistency of nylon was reduced more than that of the cellulose fibres, causing the fibre weight sampled for each sheet to be reduced. This was highlighted further in stocks containing a higher percentage of nylon fibres.

Table 5.4: Summary of RFL Coated Nylon 66/Cellulose Paper Weight per unit area and Thickness Results

Nylon content (%)	Intended weight per unit area (g/m ²)	Average weight per unit area (g/m ²)	Weight per unit area standard deviation (g/m ²)	Average Paper thickness (µm)	Thickness standard deviation (g/m ²)
0%	60	67.9	1.88	89	8
50%	60	75.1	5.08	240	19
60%	60	71.1	2.52	273	24
70%	60	65.5	4.30	259	48
80%	60	61	7.58	236	35
70%	120	128.9	9.87	488	55
80%	120	138.76	3.68	493	81
90%	120	128.99	10.35	490	68
100%	180	198.25	16.61	759	77

This variation in weight per unit area was observed when assessing the thickness of the handsheets, with higher nylon ratios having a higher variation of weight and thickness. However, the result for the 80% RFL coated nylon 66 handsheet, at 120g/m², is anomalous in having a smaller standard deviation than the 70% or 80% nylon at 60g/m² for weight per unit area, but a larger standard deviation for thickness. As faults occurred in the sheets, the weight per unit area was calculated for the full

web area inclusive of holes. This is therefore dependent on how the fibre stock was sampled. The standard deviation of the sheet thickness also highlights problems from faults, particularly where sheets were able to be produced with no holes, but included thin areas due to the drainage problems.

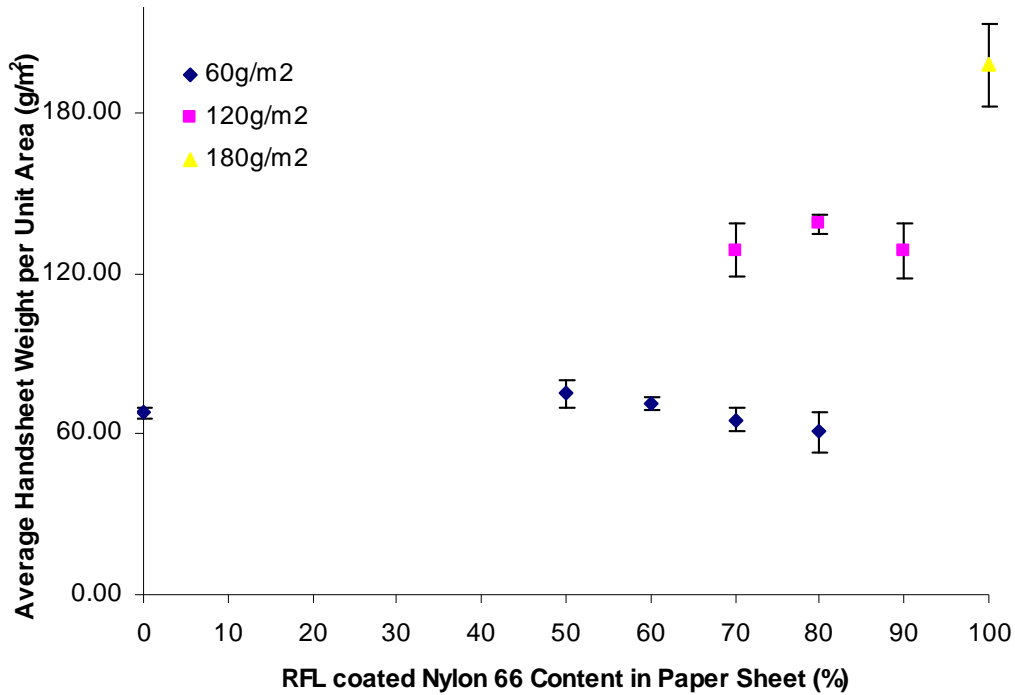


Figure 5.15: Weight per Unit area of Paper Handsheets Formed

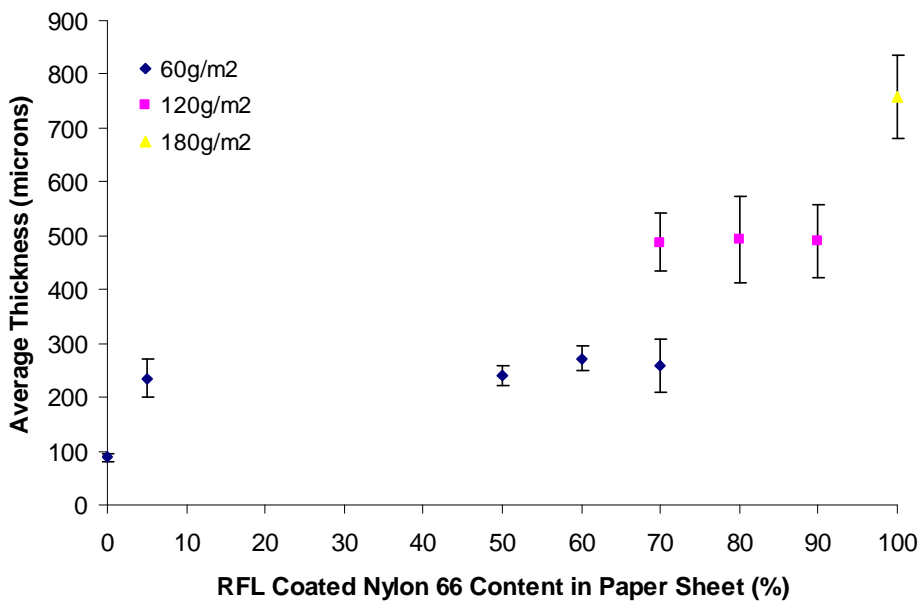


Figure 5.16: Thickness of Paper Handsheets Formed

It can be seen that the increase in the percentage of nylon used within the paper sheets dramatically affects the strength of the final sheet. Table 5.5 and Figure 5.17 summarise the tensile properties of the paper handsheets and the tensile index has been calculated using equation 5.1 so that results take into account the weight per unit area of the sheet, raw data can be found in Appendix 2.

$$\text{Tensile Index (N.m / g)} = 1000 \times \frac{\text{Tensile Strength (kN / m)}}{\text{Weight per unit area (g / m}^2\text{)}} \quad (\text{equation 5.1})$$

There is an exponential trend between the percentage of nylon within the paper handsheets and the tensile index (Figure 5.17). The curve has an R^2 value of 0.99902 showing a good fit has been produced. Reducing the amount of cellulose in turn reduced the amount of bonds that can hold the structure together. With an increase in the amount of nylon, the spaces between the cellulose fibres increased with the formation of interfibre bonding harder to achieve. As a result a small increase in the amount of RFL coated nylon 66 present can cause a more drastic effect on the loss of stress. This curve identifies the amount of RFL coated waste that could be utilised in this way where end use strength requirements are known.

Table 5.5: Summary of Tensile Properties

Nylon Percentage	Grammage g/m ²	Breaking Load (N)	Tensile Index (Nm/g)
0	67.91	68.83	67.56
50	75.11	9.42	8.36
60	71.40	3.94	3.68
70	65.50	2.55	2.60
80	60.99	1.26	1.38
70	128.85	4.23	2.19
80	138.76	1.64	0.79

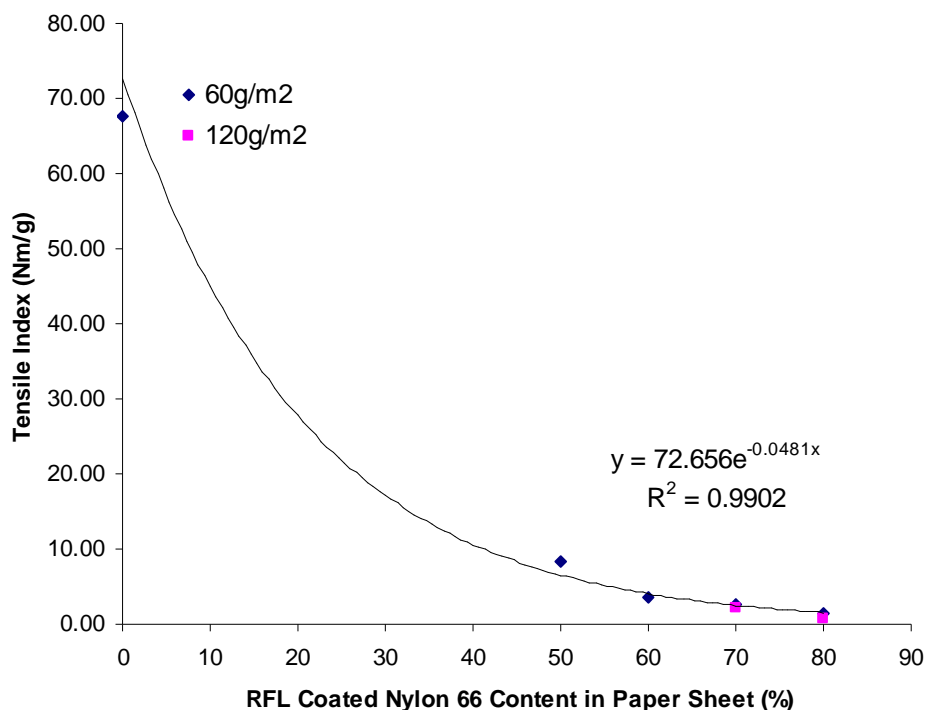


Figure 5.17: Tensile Index of Synthetic Nylon Fibre Paper Handsheets

5.6 Conclusion – RFL Coated Nylon 66 Paper Handsheets

The RFL coated nylon 66 paper created using cellulose to form a matrix of bonds entrapping the RFL coated nylon 66 within the structure has proved not to be effective with nylon quantities above 50%. This method of producing nylon paper does not seem to be feasible as a method of paper manufacture. Properties of the wet sheet seen in the production of the sheets would cause difficulties in manufacture and inefficient processing. An exponential relationship has been found between the quantity of RFL coated nylon 66 and the tensile index of the paper handsheets. This relationship could be used to assess the amount of RFL coated nylon fibre could be used where end use strength requirement are known. The properties of the final sheet are not sufficient for future production processes, such as creation of paper yarns, or to be used as paper products. It is thought that bonding using a synthetic polymer would be more appropriate and produce RFL coated nylon 66 paper with increased quality. This could be achieved using polyvinyl acetate (PVA) fibres and should be investigated further.

5.7 Experimental - Separation of Fibres

Paper technology can also be used to aid fractionation as described in section 5.2.3. Whilst examining how paper technology can be used to recycle RFL coated nylon 66 fibres it is important to see if benefits can be found from fractionation of fibres. Section 4.3.4 examined the variation of fibre lengths produced when RFL fabric was reduced to fibre form. In order to provide processing routes with useable fibre length distributions it an advantage to be able to separate fibres by length. The following sections introduce the concept of using centrifugal cleaners, traditionally used to remove unwanted particles in the paper industry, to separate long and short fibre lengths.

5.7.1 Materials

Nylon 6.6 fibres supplied by Goonvean Fibres, UK, were used for this section of work. Chopped flat fibre lengths of 3mm and 10mm were used as the base material and dyed red and blue, respectively, to identify/differentiate by colour.

Fast acid dyes were used to dye the fibres in order to minimise any transfer of colour to the other fibres during the subsequent processing. The fibres were placed in a polyester net bag and dyed in a drum machine and the following recipe used to dye the fibres at a 1% on mass of fibre shade and 40:1 liquor ratio:

- 1% Inratex B;
- 2g/l Ammonium Sulphate;
- Acetic acid to give pH 5-6.

The dissolved dye and was added to the water bath alongside the levelling agent ammonium sulphate. Dyeing was commenced at 40°C for 15 minutes before assessing the pH and adding the required amount of acetic acid. The temperature was then raised to 98°C over 30 minutes (2°C/min) and maintained for 30 minutes. The fibres were then rinsed and air dried.

5.7.2 Length Fractionation using Centrifugal Cleaners

1500g of the dyed long nylon fibre and 1500g of the dyed short nylon fibre were added to a hydropulper and 600 litres of water added to the fibre to give a stock consistency of 0.5%. The hydropulper was used to disperse the fibres within the water forming a stable fibre suspension. The suspension was then pumped to a tank, continuing to be mixed in order to keep the fibres in suspension. Both a forward flow cleaner and a through flow cleaner were used to allow separation into 4 outlets (each cleaner produces an overflow and an underflow). The fibre suspension was pumped to the centrifugal cleaners at an approximate rate of 50 litres per minute. The valves to the through flow cleaner were opened whilst leaving the forward flow cleaner valves closed, pumping the mixture to the through flow cleaner only. The valves were set so that the pressure going into the hydrocyclone was at 3 bar, and the outflow at 1 bar, giving a pressure drop within the hydrocyclone of 2 bar. The pump was then stopped and the valves changed to allow the mixture to go through the forward flow cleaner at the same rate. The inlet and outlet pressures were set as before giving a 2 bar pressure drop within the hydrocyclone. The fibre suspensions from the feed, the “accepts” (overflow) and “the rejects” (underflow) from the through flow cleaner, and the “accepts” and the “rejects” from the forward flow cleaner were collected. The fibres within the solutions were analysed both by colorimetric methods and numerical counting methods as described in the methods below.

5.7.3 Calculating the Consistency

In order for future sampling of the mixtures to be of equal amounts, the consistencies of the hydrocyclone mixtures had to be calculated.

The consistency of each fibre suspension was calculated by measuring the mass of 1 litre of the mixture. The water was then drained from the fibre using a paper handsheet machine to produce a fibre web. The fibre web was removed from the wire using blotting paper. The blotting paper and couching plate were placed on top of the fibre web. The couching roll was then rotated back and forth 3 times across the couching plate before lifting the fibre web, blotting paper and couching plate from the machine wire. Loose fibres that had not transferred to the blotting paper were then scraped off the wire and added to the fibre web. The fibre web was then dried in a

conditioned environment at 23°C and 55% relative humidity for 24 hours before weighing the fibre mass. The consistency of the mixtures was then calculated using the equation 5.2. The consistencies found are shown in the Table 5.6

$$\text{Consistency (\%)} = \frac{M_b}{M_a} \times 100 \quad (\text{equation 5.2})$$

Where M_a is the mass of the fibre suspension (fibre + water)

M_b is the mass of the fibre.

Table 5.6: Hydrocyclone Output Consistencies

Mixture	Consistency (%)
Feed	0.50
Through flow cleaner “accepts”	0.44
Through flow cleaner “rejects”	0.60
Forward flow cleaner “accepts”	0.63
Forward flow cleaner “rejects”	0.20

5.7.4 Colorimetric Analysis

In order to assess how much of each fibre had been eluted from the hydrocyclone as “accepts” and “rejects”, fibre webs were made from the five fibre suspensions and compared to standard fibre webs that had known amounts of long and short fibres. Comparisons were made, both by eye and using a colour measurement and a standard matching programme.

Four fibre webs from each of the 5 mixtures, and four of each standard were made. This enabled an opaque area to be created by layering the fibre webs so that the colour could be measured using a spectrometer.

5.7.4.1 Method to Produce Fibre Webs

The fibre webs were made using 2g of fibre for each sheet. As each mixture from the hydrocyclone has different consistencies, samples from each mixture were taken and diluted to give five litres of stock with a 0.2% consistency as shown in Table 5.7. The volume of mixture needed to give 10g of fibre was calculated, and to this 0.7g (7%)

PVA fibres were added in order to bond the nylon together. The PVAc fibres and sampled mixture were put in the disintegrator for a total of 5000 revolutions to ensure the PVA fibres dispersed evenly within the fibre mixture. The fibre mixture was then diluted to make five litres.

For the standard fibre webs, 10g of fibre, in the proportions noted in Table 5.8 below, and 0.7g (7%) of PVA fibres were measured. To this two litres of water were added and the mixture put in the disintegrator for 20,000 revolutions. An increased level of revolutions was used to ensure that the nylon fibres were fully dispersed within the water. To this another three litres of water were added giving a total of 10g of nylon fibre in five litres of water.

Table 5.7: Paper Handsheets Manufactured from Separated Fibres

Batch	Consistency of batch sample (%)	Volume of batch sample required to give 10g fibre (ml)	Volume of water required to dilute to 5 litres (ml)
Feed	0.50	2000	3000
Through flow “accepts”	0.44	2273	2727
Through flow “rejects”	0.60	1667	3333
Forward flow “accepts”	0.63	1587	3413
Forward flow “rejects”	0.20	5000	0

Table 5.8: Standard Paper Sheets Produced from Different Fibres

	Ratio of fibre short:long	Amount of short fibre (g)	Amount of long fibre (g)
1	100:0	10	0
2	90:10	9	1
3	80:20	8	2
4	70:30	7	3
5	60:40	6	4
6	50:50	5	5
7	40:60	4	6
8	30:70	3	7
9	20:80	2	8
10	10:90	1	9
11	0:100	0	10

A paper handsheet machine was used in order to produce the fibre webs from the fibre suspensions using a method based on the Tappi 205 sp-02 standard. The handsheet machine was half filled with water before adding 1000ml of fibre stock and topped up with water to the line 350mm above the wire. The perforated stirrer was then used, moving it up and down 6 times within the liquid to disperse the fibres evenly. Liquid was then drained from the fibre suspension forming the fibre sheet on the wire. The handsheet machine was opened and the fibre sheet couched using 2 sheets of blotting paper placed centrally on the fibre sheet. The couch plate and roll were placed centrally on top of the blotting paper. Couching occurs to remove the excess water from the fibre web, moving to couch roll back and forth 3 times with no added pressure being exerted before removing it from the middle of the couch plate. The number of rolls used in couching was decreased from 6 (outlined in Tappi standard 205 sp-02) to 3 in order to help in the fibre web adhere to the blotting paper. The blotting paper was then removed and lifted the fibre web from the wire to the blotting paper. The fibre web and blotting paper were then dried in an oven at 105°C for 30 minutes causing the PVA fibres to pass their glass transition point of 80°C bonding the nylon together. Once dry the fibre webs were able to be removed from the blotting paper.

5.7.4.2 Colour Difference Analysis

A Datacolor SF 600 DCI Spectraflash 600 spectrophotometer was used to measure the colour of the hydrocyclone fibre webs against the standard batches. The colour measuring programme, “colour tools” was used to carry out the colour analysis. The following set up was used for the colour measuring:

- Measurement Scale: Reflectance;
- Measurement Application: Colour Matching;
- Measurement Geometry: Diffuse illumination and 8° viewing;
- Illumination: Pulsed xenon filtered to approximate D₆₅;
- Specular: Exclude;
- Aperture: Small;
- UV filter: Off 0%.

The spectrophotometer was calibrated using reference materials with known reflectance. The black light trap was first used, followed by the white and green ceramic tiles, thus enabling accurate colour data collection. To measure the colour of the standards and the hydrocyclone batches, three fibre webs were used for each measurement to ensure an opaque area was achieved. The spectrophotometer measured the reflectance value for wavelengths between 400nm and 700nm at 10nm intervals. An average of 4 readings was taken for each standard and batch sample, with each reading being taken from a different area on the fibre web.

From these readings the colour tools programme calculated the three tristimulus values X, Y and Z and the chromaticity values x and y from the 1939 CIE colour space, the $L^*a^*b^*$ coordinates from the 1976 CIELAB colour space, the chroma and hue values (C^* and h) from the 1976 CIE LUV colour space.

The colour difference between the hydrocyclone batches and each standard was then calculated using both the CIE 76 (equation 5.3) and the CIE 94 (equation 5.4) colour difference equations.

$$\Delta E_{ab}^* = \sqrt{(L_2^* - L_1^*)^2 + (a_2^* - a_1^*)^2 + (b_2^* - b_1^*)^2} \quad (\text{equation 5.3})$$

Where ΔE_{ab}^* is the overall colour difference using the 1976 equation and L = lightness value, a = red/green value, b = yellow/blue value as shown in Figure 5.18(a).

$$\Delta E_{94}^* = \sqrt{\left(\frac{L_2^* - L_1^*}{K_L}\right)^2 + \left(\frac{C_2^* - C_1^*}{1 + K_1 C_1^*}\right)^2 + \left(\frac{h_2 - h_1}{1 + K_2 C_1^*}\right)^2} \quad (\text{equation 5.4})$$

Where, and ΔE_{94}^* is the overall difference using the 1994 equation and L = lightness value, C= chroma value and h=hue angle as shown in Figure 5.18(b). The value K in the 1994 equation is a weighting factor and depends on the colour application. For textiles $K_L = 2$, $K_1 = 0.048$ and $K_2 = 0.014$.

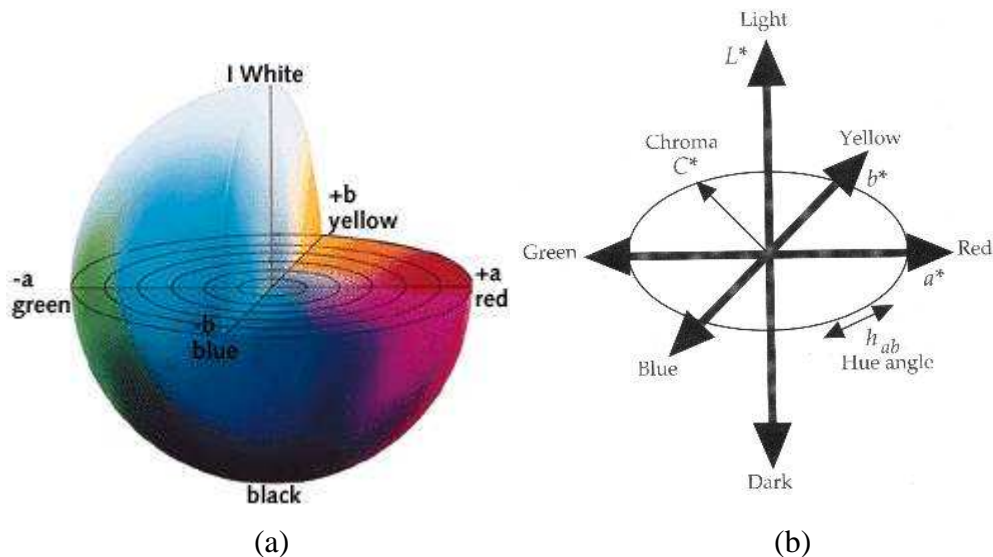


Figure 5.18 CIE $L^*a^*b^*$ colour model.

Each hydrocyclone batch was compared to each standard fibre web created with known long and short fibre quantities. The standard where the lowest colour difference value was seen, and therefore closest colour match between the hydrocyclone batch and the standards created was most representative of the long and short fibre content of the hydrocyclone batch. Therefore, for each hydrocyclone batch, the standard that has the closest match represents the proportion of long and short fibre within the outflow.

5.7.5 Numerical Analysis

Numerical analysis was also carried out on samples of the fibre suspension collected from the hydrocyclone separation. This was achieved by preparing slides, containing a sample of the solution and the number of coloured fibres on the slide could then be determined using a light microscope.

5.7.5.1 Slide Preparation – Fibre Analysis

Slides were prepared by adding 0.02g of fibres to one litre of water. The decreased fibre suspension was then stirred to ensure the fibres were fully dispersed. Slides were arranged on a hot plate and a pipette was used to transfer 2.5ml of the fibre suspension to each slide. The water evaporated from the slide leaving a number of fibres on the slide surface. This method was found to give a disproportionate number of short fibres in comparison to long fibres to what was expected. It is thought that this was due to the fibres being relatively inflexible and the long fibres larger than the pipette width resulting in a lower proportion of long fibres to be captured by the pipette in comparison to the short fibres having a length that could be captured by the pipette. The method was therefore changed to use a spoon rather than a pipette to transfer 2.5ml to the slides.

5.7.5.2 Counting Fibres

The number of each type of fibre on each slide was counted using a light microscope and recorded. Since the long fibres were often close together and the length of them longer than could be seen through the eyepiece difficulty in identifying full fibres was encountered. The ends of long fibres were, therefore, counted rather than identifying each fibre. This figure was then halved to give the number of long fibres present on the slide. A number of slides for each sample were created to give a total sample number of above 500 fibres for each batch.

5.8 Results and Discussion – Separation of Fibres

5.8.1 Colorimetric Analysis

Figure 5.19 provides a comparison of the 5 fibre suspensions collected: the feed, the through flow cleaner “accepts”, the through flow cleaner “rejects”, the forward flow cleaner “accepts” and the forward flow cleaner “rejects” in comparison to the standards made. This clearly shows that some fibre fractionation by length has occurred.

The eye is able to take into account certain aspects of this colour matching that spectrophotometer readings do not. For example, the long fibres had a tendency to flock together and, therefore, a lower density of long fibres could be seen around the outside of the fibre web resulting in a pinker appearance around the edges than in the middle of the fibre web. Figure 5.19 shows the visual colour of each standard and the visual colour of the hydrocyclone batches in comparison. The arrows show the decision on the closest standard to each hydrocyclone batch as expressed in Table 5.9.

Table 5.9: Visual Colour Matching of Hydrocyclone Separated Fibres

Batch	Closest Standard
Feed	70% long, 30% short
Forward flow “accepts”	80% long, 20% short
Forward flow “rejects”	20% long, 80% short
Through flow “accepts”	70% long, 30% short
Through flow “rejects”	100% long, 0% short

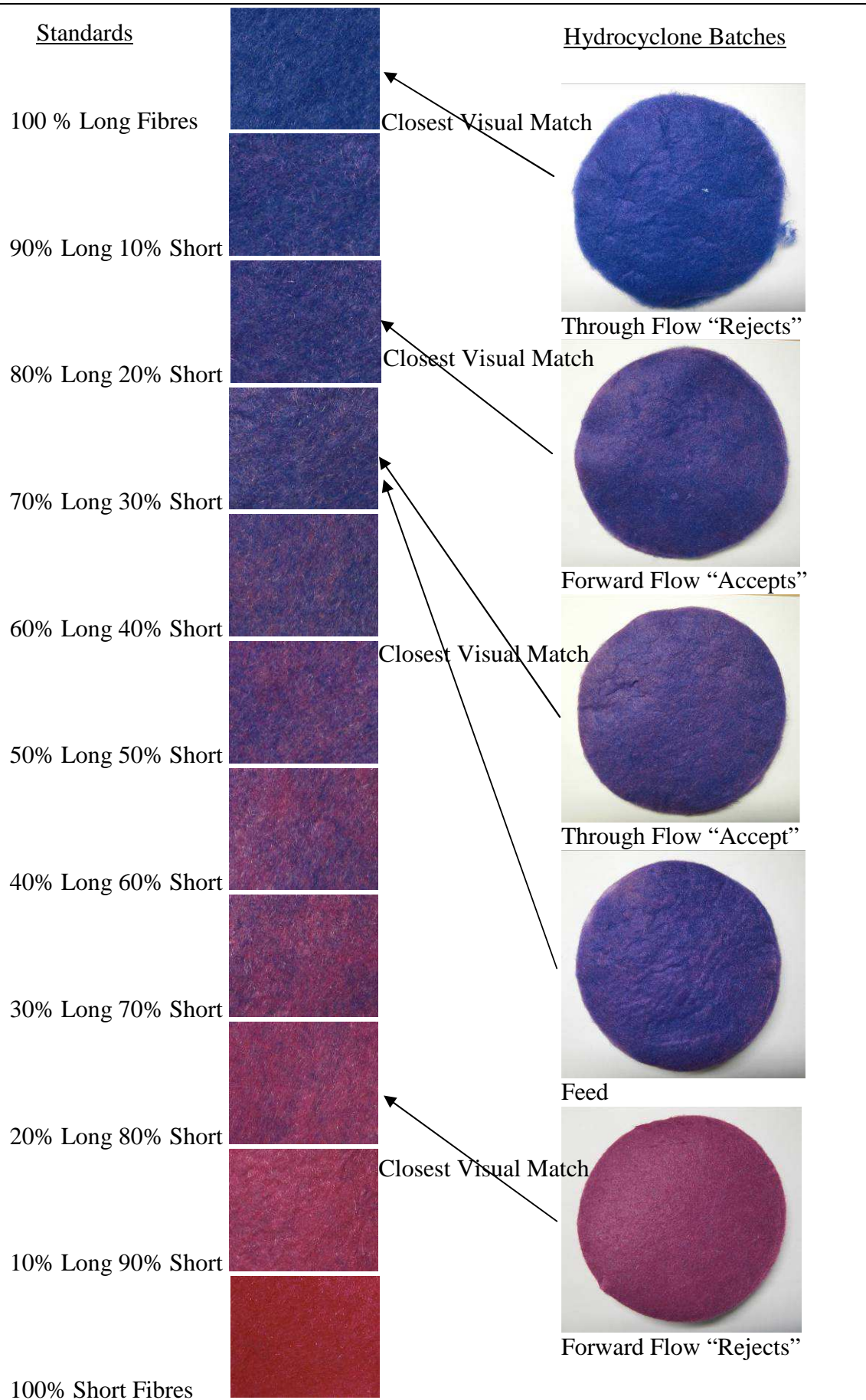


Figure 5.19: Visual Comparison Between Standard and Hydrocyclone Outlet Batches

Computational colour matching was also performed with the calculated ΔE_{ab} for each batch against each standard, Table 5.10, and Table 5.11 shows the ΔE_{94} values, the lowest colour difference is highlighted in bold for each batch.

Table 5.10: ΔE_{ab} Analyses of Batches against Standards with figures in bold showing closest standard for each hydrocyclone batch.

Standards ↓	Batches →	ΔE_{ab}				
		Feed	Forward flow “accepts”	Forward flow “rejects”	Through flow “accepts”	Through flow “rejects”
100% Long 0% Short		13.73	12.29	40.15	14.45	5.79
90% Long 10% Short		9.69	8.40	34.60	10.32	7.78
80% Long 20% Short		7.25	6.04	32.26	7.81	8.52
70% Long 30% Short		4.93	4.30	28.82	5.21	11.07
60% Long 40% Short		7.10	7.92	22.25	6.53	17.24
50% Long 50% Short		9.51	10.47	19.55	8.86	19.93
40% Long 60% Short		17.12	18.19	11.87	16.45	31.05
30% Long 70% Short		20.34	21.47	8.41	19.63	31.05
20% Long 80% Short		29.63	30.71	3.95	28.99	40.05
10% Long 90% Short		37.81	38.96	9.67	37.16	48.39
0% Long 100% Short		55.43	56.60	26.89	54.75	66.09

Table 5.11: ΔE_{94} Analyses of Batches against Standards

Standards ↓	Batches →	ΔE_{94}				
		Feed	Forward flow “accepts”	Forward flow “rejects”	Through flow “accepts”	Through flow “rejects”
100% Long 0% Short		4.97	4.52	14.24	5.28	2.00
90% Long 10% Short		3.59	3.25	12.08	3.92	2.43
80% Long 20% Short		2.56	2.26	11.04	2.88	2.47
70% Long 30% Short		1.60	1.54	9.58	1.88	3.32
60% Long 40% Short		2.28	2.67	6.98	2.22	5.36
50% Long 50% Short		3.09	3.50	5.97	2.98	6.22
40% Long 60% Short		5.66	6.06	3.18	5.54	8.57
30% Long 70% Short		6.42	6.83	2.22	6.28	9.43
20% Long 80% Short		30.89	32.42	2.01	30.11	42.19
10% Long 90% Short		34.42	35.87	6.46	33.69	45.03
0% Long 100% Short		38.88	40.18	14.09	38.25	48.26

The hydrocyclone has, therefore, fractionated the fibres into short fibres using the forward flow cleaner and long fibres using the through flow cleaner. Table 5.12 shows the summary of results from the colorimetric analysis and the visual analysis and computational analysis are very similar showing accuracy within these results.

However, there is some ambiguity within these results as the feed was known to have a proportion of 50% long fibres to 50% short fibres by weight.

Table 5.12: Summary of Results from Colorimetric Analysis

Hydrocyclone Batches	Visual Analysis Fibre Percentage	Computational Analysis Fibre Percentage
Feed	70% long, 30% short	70% long, 30% short
Forward flow “accepts”	80% long, 20% short	70% long, 30% short
Forward flow “rejects”	20% long, 80% short	20% long, 80% short
Through flow “accepts”	70% long, 30% short	70% long, 30% short
Through flow “rejects”	100% long, 0% short	100% long, 0% short

The reflectance spectra in Figures 5.20-5.23 show the position in the colour spectrum where the hydrocyclone batches differ from the standards. The main difference in colour between the feed and the 50% long, 50% short standard is the increased reflectance in the red areas of the spectrum between approximately 600nm to 680nm in the standard as shown in Figure 5.20. There are a number of reasons why this could have occurred, for example a disproportionate amount of long fibres could have been sampled due to the fact that the long fibres have a higher likelihood of flocking together and rising to water surface, whereas, the short fibres disperse evenly throughout the water. As the sample was taken from the top of the tank, a higher number of longer fibres than proportionate to the feed may have been sampled. However, the tank was continually stirred in order to avoid this problem.

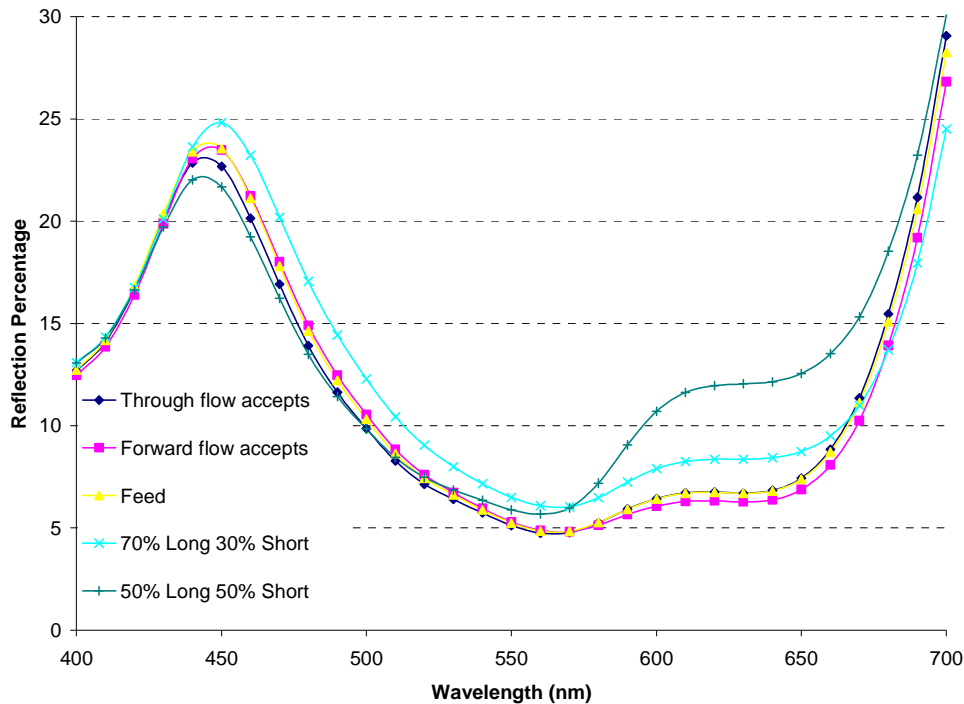


Figure 5.20: Reflectance Spectra of Feed, Forward Flow “Accepts” and Through Flow “Accepts” in Comparison to the 70% Long/30% Short and the 50% Long/50% Short Standards

The fact that the feed has almost identical reflectance patterns to the “accepts” outlet of both the forward flow cleaner and the through flow cleaner, as shown in Figure 5.23, leads to the potential ambiguity associated with the standards. It is likely that the “accepts” of both the forward cleaner and through flow cleaner have unchanged long and short fibre percentage from the feed fibre suspension. It is possible that the fibre suspensions made for the standards were less evenly dispersed than the batch fibre suspensions. As a result of this potential non-uniformity long fibres may be more likely to stick to the cylinder of the handsheet machine, or the stirrer than those long fibres within the batch fibre suspensions. The result would therefore be an overall increase in the redness of the fibre web.

Despite the ambiguity of the exact proportions of the fibres within the batches, these results show a very good separation of long and short fibres. The “rejects” from the through flow cleaner show a very close match to the standard with 100% long fibres. Assessment of the reflectance spectra, in Figure 5.21, it can be seen that the blueness of the batch is closer to the 90% long fibre standard. However this standard has an

increased reflectance in the red component of the colour spectrum in comparison to the 100% long fibres standard. This leads to the 90% long fibre standard having an overall colour difference higher to that of the 100% long fibre standard.

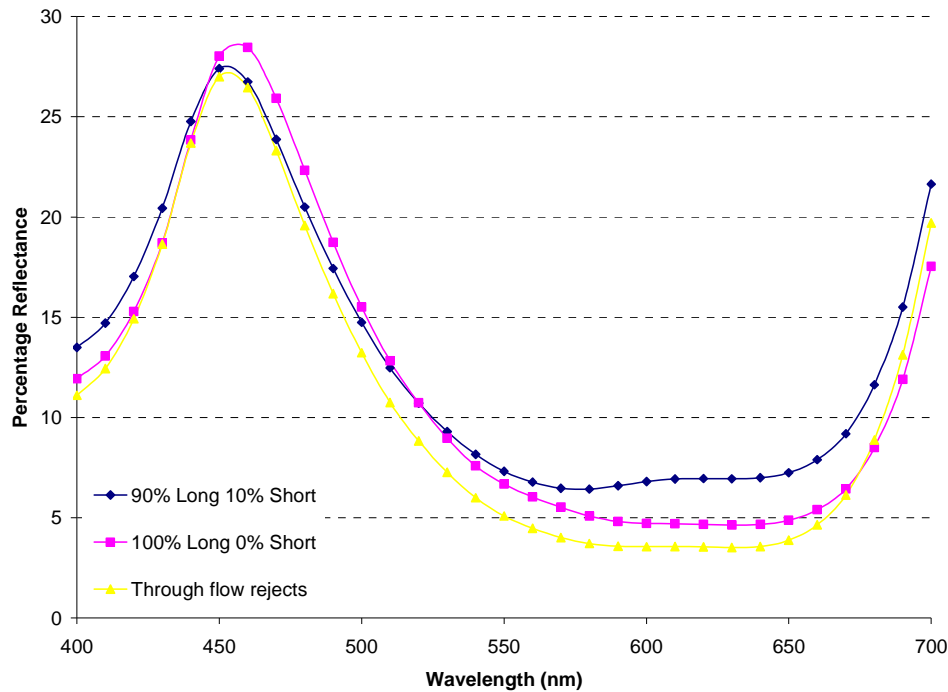


Figure 5.21: Reflectance of Through Flow “Rejects” in Comparison to the 100% Long Fibre and 90% Long Fibre/10% Short Fibre Standards

From the results it is apparent that the separation of the short fibres has not been as effective with the closest standard being 20% long fibres and 80% short fibres. The reflectance spectra in Figure 5.22, shows the blueness of the batch being closer to a different standard than the one shown as the lowest colour difference. In this case the blueness is closer to that of 30% long fibres and 70% short fibres. However in the upper end of the spectrum there is a closer match to the 20% long fibres, 80% short fibres.

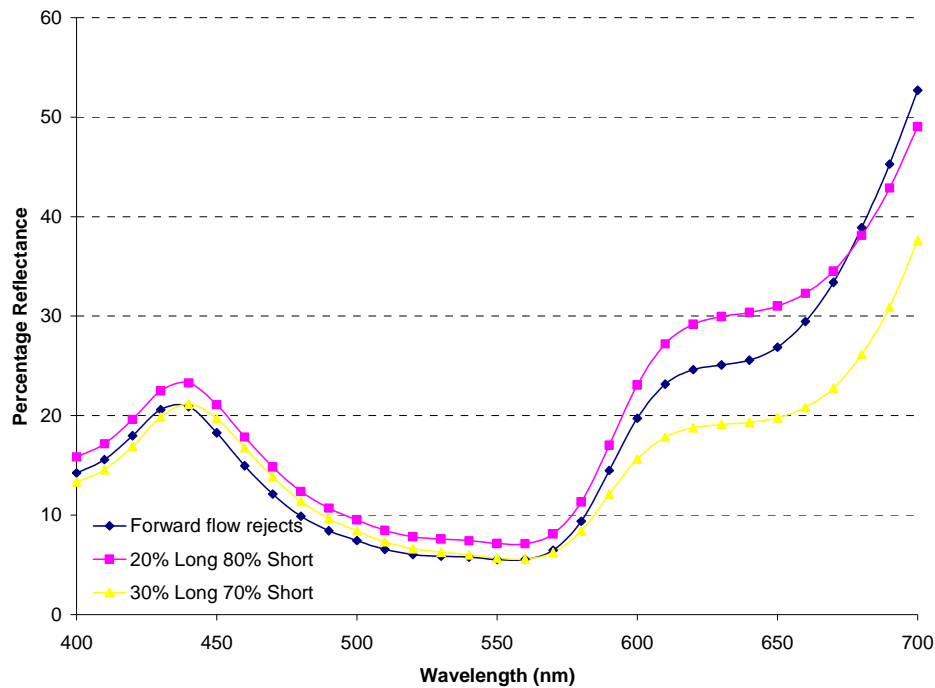


Figure 5.22: Reflectance of Forward Flow “Rejects” in Comparison to the 20% Long Fibre/80% Short Fibre and 30% Long Fibre/70% Short Fibre.

5.8.2 Numerical Analysis of Fibres

The results from the numerical counting analysis provided a similar outcome, showing very good separation of the short and long fibres within the reject outlets of the two cleaners. However, the proportions of fibres found in each batch from this method varied from that of the colour analysis. Table 5.13 and Figure 5.23 show the results from the numerical analysis of the five batch samples.

Table 5.13: Numerical Analysis of Batch Samples

Batch	Total number of fibres counted	Long fibres		Short fibres		Percentage increase from feed
		Number	Percentage	Number	Percentage	
Feed	671	113	16.8	558	83.2	N/A
Forward flow “accepts”	587	145	24.7	442	75.3	7.9% increase in long fibres
Forward flow “rejects”	755	19	2.5	736	97.5	14.3% increase in short fibres
Through flow “accepts”	845	163	19.3	682	80.7	2.5% increase in long fibres
Through flow “rejects”	550	338	63.8	192	36.2	47.0% increase in long fibres

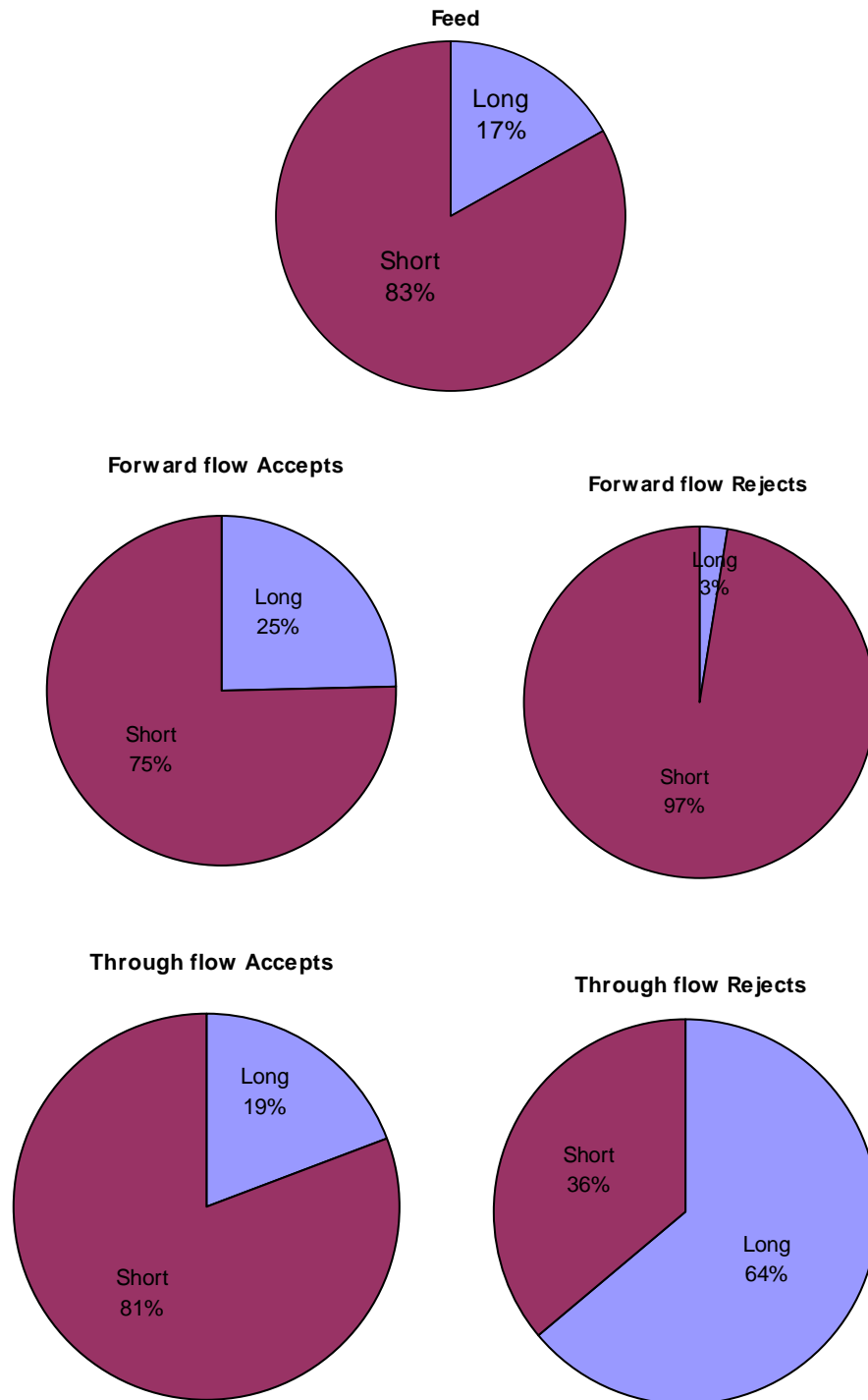


Figure 5.23: Pie Charts Showing the Proportion of Long and Short Fibres Counted within each Batch

As the feed input was 50% long fibres/50% short fibres by weight rather than number, the proportion of long to short fibres shown by this method is credible. The results indicate a good separation of the fibres for both long and short fibres. The forward flow cleaner has separated out short fibres almost completely from the long fibres,

whereas the through flow cleaners give a 47% increase in long fibres. This effective separation rate indicate that fibres would only need to be passed through the through flow cleaners a couple of times before practically full separation occurs.

5.9 Conclusions – Separation of Fibres

Rather than just looking at the proportion of fibres within each batch, it is vital to see the efficiency of the cleaners by calculating the percentage increase of the long and short fibres within the reject outlets of the hydrocyclone cleaners. The forward flow cleaner shows a 50% increase in short fibres from the feed, whilst the through flow cleaner shows a 30% increase in long fibres using the colorimetric analysis. Numerical analysis has indicated a 14% increase in short fibres in the forward flow cleaner “rejects” and 47% increase in long fibres in the through flow cleaners “rejects”. Both the forward and through flow cleaner provide sufficient efficiency to deliver almost full separation if the reject outlets were further separated using a bank of cleaners.

Table 5.14 summarises the efficiency of both cleaners from the two methods used to work out the fibre proportions. From this data it can be seen that by using a bank of cyclones, full separation would occur very quickly with a processing system similar to that shown in Figure 5.24 could be used in an industrial application. It is recommended that a system such as this could be used to separate the long RFL fibres from the short RFL fibres. The long fibres could then be utilised in textile processing streams whilst the short fibres are utilised in filler applications.

Table 5.14: Efficiency of Hydrocyclone Cleaners at Separating Fibres by Length

Cleaner	Efficiency by weight (colour analysis)	Efficiency by frequency (number analysis)
Forward Flow	+50% Short fibres in “rejects”.	+14% Short fibres in “rejects”
Through Flow	+30% Long fibres in “rejects”	+47% Long fibres in “rejects”

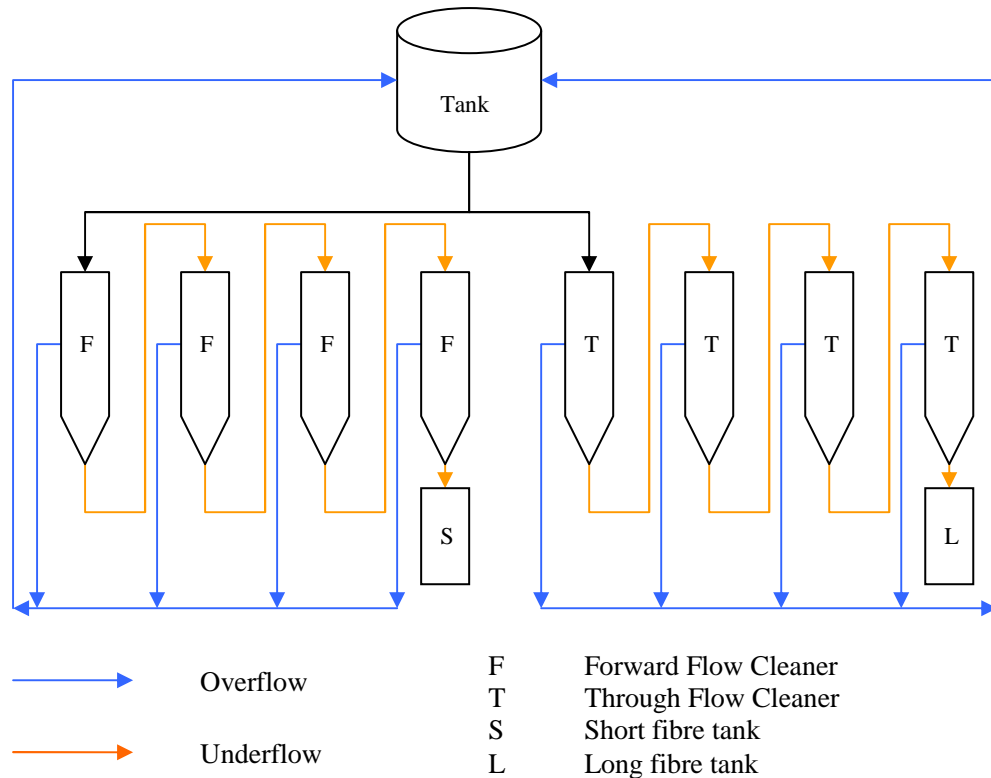


Figure 5.24: Recommended Processing Set up for an Industrial Application

The consistencies and the flow rate of the underflow outlets should also be considered with the forward flow hydrocyclone cleaner increasing the number of small fibres by 32% from the feed to the underflow outlet. The underflow outlet is only at a 0.2% consistency and a thickening stage would, therefore, also need to be used between each forward flow cleaner. The separation of the small fibres would take longer than that of the long fibres due to these thickening stages and the much decreased outlet flow of the forward flow cleaner. Although the rate of flow was not measured, there was an obvious decrease from the feed flow rate to the underflow rate. The feed flow rate was approximately 50 litres per minute and during the experiment only 8 litres of the forward flow underflow outlet solution was collected. It was estimated that the machine was running for 2 to 4 minutes and this gives an estimated flow rate of 2-4 litres per minute. It would therefore take much longer to collect the short fibres than that of the long fibres. In addition if the through flow cleaner underflow outlet was at a similar consistency and flow rate to that of the feed, there would not be a necessity for thickening stages between the through flow cleaners.

The results found from this investigation were found to agree with work by Ho et al (2000) where short fibres were rejected whilst longer fibres accepted. However, work by Ho et al shows a much higher percentage of long fibres than short fibres within the “accepts”, whereas in this work the “accepts” seems to have a similar proportion of long and short fibres as the feed. Their work was done using much shorter fibres of 1mm and 3mm, where the 1mm fibres were, therefore, rejected and the 3mm fibres accepted. The critical fibre length as suggested by Lu and Liu (2006) was expected to be somewhere between these two lengths in order to get this type of fractionation. The results found in this project have shown that fractionation has not occurred within the “accepts” outlet, showing that the critical fibre length is much lower than the average fibre length within the feed.

This experimentation shows that cyclone cleaners offer a very suitable method of separating fibres by length to be utilised in a number of production processes.

In order to use recycled fibres from industrial sources within optimum production processes it is an advantage to be able to separate out fibres by way of length and type. Once separated, fibres can be put through different processes to achieve a variety of products.

5.10 References

- BIERMANN, C. J. (1996) *Handbook of Pulping and Papermaking*, London, Academic Press Limited.
- BLISS, T. (1996) *Stock cleaning technology*, Surrey, Pira International.
- BROUGHTON, G. & WANG, J. P. (1955) An experimental study of the factors involved in the manufacture of paper yarn. *Tappi*, 38, 237-241.
- DABROS, M., AFACAN, A. & MASLIYAH, J., H. (2009) Fibre fractionation using air-sparged hydrocyclone. *The Canadian Journal of Chemical Engineering*, 87, 94-98.
- DEGENER, A. (2002) Interview with John Stahl. *Hand Papermaking*, 17, 23-29.
- EVANS, C. G. (1967) Method for Making Paper Yarn. *United Patent Office*. United States of America, Milliken Research Corporation.

- GAVELIN, G. & BACKMAN, J. (1991) Fraction With Hydrocyclones. *Pulping Conference*. Orlando, FL, USA.
- HAMILTON, K. (1946) Paper Yarn. *United States Patent Office*. United States.
- HENTSCHEL, R. A. A. (1961) Some new developments in synthetic fiber paper. *Tappi*, 44, 22-26.
- HENTSCHEL, R. A. A. (1964) Web Formation and Bonding. In Battista, O. A. (Ed.) *Synthetic Fibers in Papermaking*. New York, Interscience Publishers.
- HO, S.-L., REHMAT, T. & RICHARD, B. (2000) Fibre fractionation in hydrocyclones. *86th Annual meeting*. Montreal, Quebec, Canada, Pulp and Paper Technical Association of Canada.
- HOWELL, J. D. (1966) Synthetic Paper Yarn. *United States Patent Office*. United States of America, du Pont de Nemours and Company,.
- HUBBARD, J. K., KOONTZ, F. H., MCCARTNEY, J. R. & HENTSCHEL, R. A. A. (1955) Physical properties of papers from synthetic fibres. *Tappi*, 38, 257-261.
- INFORM (2009) Paper. [online] Available at: http://www.secret-life.org/paper/paper_environment.php [Accessed 7th August 2009].
- KURE, K. A., DAHLQUIST, G., ESTROM, J. & HELLE, T. (1999) Hydrocyclone separation, and reject refining, of thick-walled mechanical pulp fibres. *Nordic Pulp & Paper Research Journal*, 14, 100-104.
- LARSON, M. (2006) Synthetic paper makes inroads. *Converting Magazine*, October 2006, 32-35.
- LICATA, M. (1999) The truth about synthetic paper. *In-Plant Printer*, 39, 44-46 & 68.
- LU, X. & LIU, S. (2006) Evaluation of fractionation of softwood pulp in a cylindrical hydrocyclone. *Chinese Journal of Chemical Engineering*, 14, 537-541.
- LYNCH ADNAMS, S. (2004) Laura Anderson Barbata and the Yanomami of Venezuela. *Hand Papermaking*, 19, 33-38.
- MILLER, J. D. (1981) Air-sparged hydrocyclone and method. United States Patent. United States, University of Utah.
- OJI FIBER CO (2012) OJI FIBER Natural Filament Fiber OJO+. [online] Available at: http://www.ojifiber.co.jp/e_home/e_home.html [Accessed 26 August 2012].
- PAAVILAINEN, L. (1992) The possibility of fractionating softwood sulphate pulp according to cell wall thickness. *Appita*, 45, 319-326.

- PARK, S., VENDETTI, R. A., JAMEEL, H. & PAWLAK, J. J. (2005) The effect of fibre properties on fibre fractionation using a hydrocyclone. *Transactions of the Technical Section*, 31, 132-137.
- ROBERTS, J. C. (1996) *The Chemistry of Paper*, Cambridge, Royal Society of Chemistry.
- SCOTT, G. M. & ABUBAKR, S. (1994) Fractionation of secondary fiber - A review. *Progress in Paper Recycling*, May 1994, 50-59.
- SMOOK, G. A. (2002) *Handbook for Pulp & Paper Technologists*, Vancouver, Angus Wilde Publications Inc.
- STATIE, E. C., SALCUDEAN, M. E. & GARTSHORE, I. S. (2001) The influence of hydrocyclone geometry on separation and fibre classification. *Filtration & Separation*, 38, 36-41.
- THOMPSON, N. B. (2004) Synthetic Paper: The Real Deal. *Paper, Film & Foil Converter*, February 2004, 64.
- WALSH, K. (2001) Tearing Into Traditional Markets. *Chemical Week*, April 2001, 29.
- WHITE, C. (1993) *Synthetic fibres in papermaking systems (including wet laid nonwovens)*, Leatherhead, Surrey, Pira International.
- WOOD, J. R. (1990) Characterization of mechanical pulp fines with a small hydrocyclone. Part I: The principle and nature of the separation. *76th Annual Meeting of the Technical Section, Canadian Pulp and Paper Association*. Montreal, Quebec, Canada, Canadian Pulp and Paper Association.
- WYMAN, C. P. (1886) Method of Making Paper Fabric. *United States Patent Office*. United States.

6.0 Recycling of Fibres using Textile Technology

6.1 Aims

To investigate how the reduced RFL coated fibres behave under traditional textile recycling methods and to assess the viability of using friction spinning as a route to recycling the short fibres produced from fabric reduction.

6.2 Introduction to Carding and Friction Spinning

6.2.1 Carding

The aim of the card is to disentangle fibres from tufts into individual fibres. Carding also helps in the cleaning of fibres, reduction of neps, fibre alignment, blending and elimination of short fibres. The roller clearer card is made up of five types of rollers, the licker-in, main cylinder, doffer roller and worker and stripper rollers, the position of which are illustrated in Figure 6.1. In comparison flat cards use a number of flats that rotate about the cylinder, instead of the worker rollers. The surfaces of the rollers are covered in wire clothing which enables the fibres to be held in place by one surface, whilst being combed by the adjacent surface.

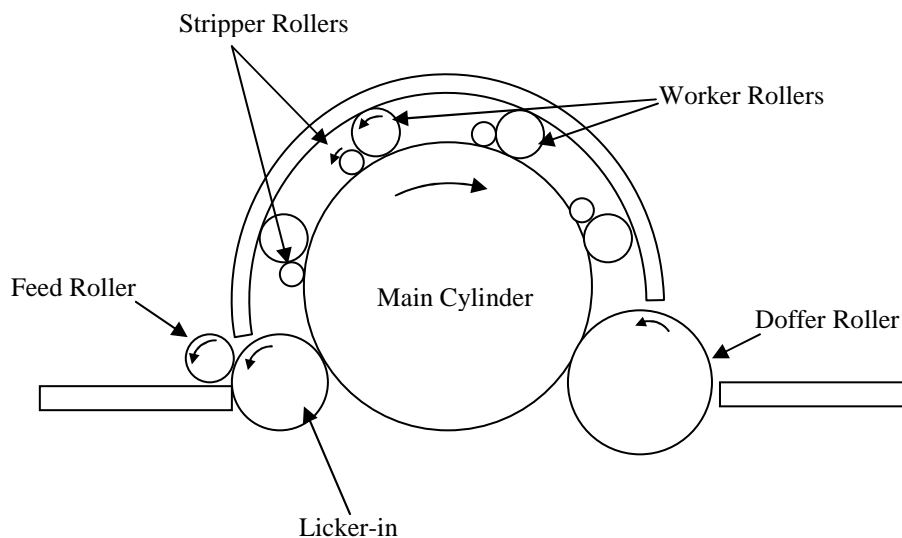


Figure 6.1: Position of Constituent Rollers on a Roller Clearer Card

The speeds of the rollers and the direction of the wires determine how the fibres are treated during the carding process. Where the wires are point-to-point and moving in the same direction but at different speeds there is a carding action, as shown in Figure 6.2. This occurs at the cylinder to worker roller contact points (where the linear speed of the cylinder is faster than that of the worker) and the cylinder to doffer contact point. The carding action will disentangle and align the fibres in the machine direction forming a web on the surface of the machine clothing on the main cylinder.

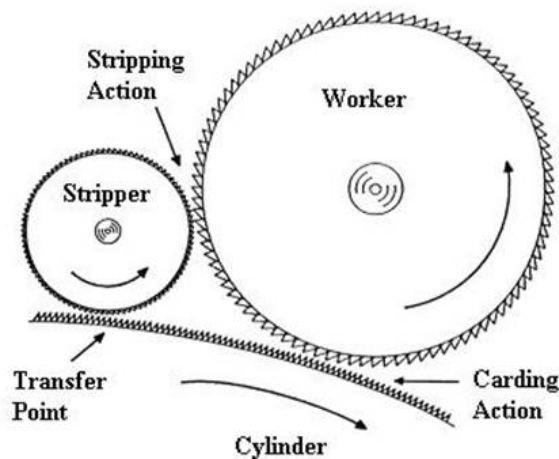


Figure 6.2: Carding and Stripping Actions (Dahiya et al., 2004)

Where the wires are facing the back edge of another set of wires the fibres will be removed, and stripping will occur, also illustrated in Figure 6.2. Stripping occurs at the licker-in to cylinder contact point, and the stripper roller to worker roller contact points (Klein, 1986).

6.2.2 Friction Spinning

In order to recycle fabrics using a primary approach, as outlined in section 2.3.1 by converting recycled fibres to new products, the reclaimed fibres need further processing. Common ways of re-utilising reclaimed fibres include nonwoven production and staple fibre spinning. Friction spinning is an ideal process for reclaimed fibres to be spun into yarns as it is able to employ shorter fibres than other spinning systems (Gulich, 2004). The spinning process consists of the following sequence of events: the opening and separation of fibres from a sliver or slivers, reassembling of individual fibres, twisting of the fibres and withdrawal of the yarn. This is done by feeding a mixture of fibres and air to a moving perforated surface. A

suction device ensures the fibres are assembled on the surface. The twisting occurs via a mechanical roller which forms a twisting zone where it meets the moving surface of fibres. The resulting yarn is withdrawn perpendicular to the moving surfaces, as illustrated in Figure 6.3 (Ishtiaque et al., 2003).

The friction spinning process avoids high centrifugal forces and high rotational speeds as twist is imparted by one rotation of the yarn, having a diameter of 0.15 - 0.30mm. By comparison rotor spinning requires one revolution of the rotor having a diameter of 38mm to insert one twist.

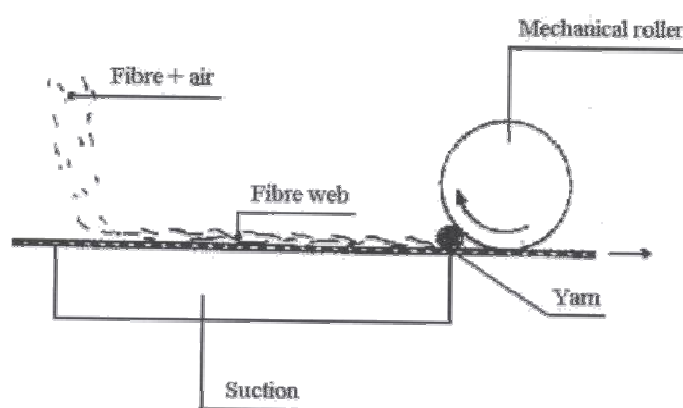


Figure 6.3: The Friction Spinning Process (Ishtiaque et al., 2003)

The DREF-1 friction spinner developed by Fehrer uses a single perforated cylindrical drum (Ishtiaque et al., 2003). The ratio of drum surface area to yarn surface area is kept large in order to keep the drum speed low. As there is no positive control of the assembly of the fibres, much slippage occurs between the roller and yarn, reducing the twist efficiency. The DREF-2 system, therefore, introduced the concept of enclosing fibre assembly between two perforated friction drums. By the two drums rotating in the same direction they act to collect the fibre whilst also spinning in the fibres to the open end of the yarn. The DREF-2 was available from 1977 and became the first friction spinning machine that became commercially popular. The DREF-2 consists of a specialised inlet system of rollers and a carding drum. The rollers provide the required draft to the sliver before the fibres are opened up with the card drum which is covered in saw-tooth wire clothing. The fibres are removed from the card by centrifugal force and supported within an airstream which transports the fibres to the nip of the two perforated friction drums. The rotation of the drums causes the

fibres to twist due to friction. Suction through the perforations of the drums also helps in this twisting process as well as assisting in the removal of dust, Figure 6.4. The DREF-2 system was restricted to spinning coarser yarns of 98-1181 tex (Ishtiaque et al., 2003).

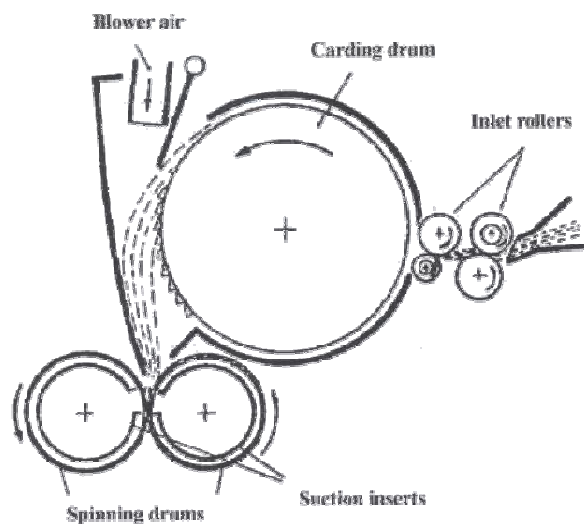


Figure 6.4: DREF-2 Spinning System (Ishtiaque et al., 2003)

The DREF-3 friction spinning machine was developed to improve the yarn quality, and broaden the yarn counts that could be achieved to include finer yarns of 33 tex. To achieve this it uses a core and sheath type spinning arrangement. It is also capable of producing multi-component yarns. The introduction of the DREF-5 friction spinning machine delivered a novel method of fibre feeding where rather than using five slivers, individual fibres from a single sliver were fed through a closed or partially open fibre duct to the spinning nip at an acute angle to the yarn axis. This caused the fibres to be as stretched as possible when being fed into the nip. The DREF-5 system offers yarns in the count range of 15 to 37 tex with production rates of up to 200m/min able to be achieved. The DREF-2000 friction spinner increased these production rates further to 250m/min and yarns of up to 41 tex could also be achieved. Either S or Z twist yarns can be produced on the DREF-2000 without changing the mechanical settings of the machine.

6.3 Recycling Fibres using Spinning Processes.

Recycled fibre is often turned into a commercial product by using friction spinning to create a yarn. Dref spinning machines solve problems previously encountered with ring and rotor spinning due to its versatility with fibre lengths and types. In ring spinning the draft rollers have to be set close enough to be able to control short floating fibres. This becomes difficult with particularly short fibres produced from opening of hard fabric waste (Cheng and Wong, 1997).

Much work has followed on the use of friction spinning with recycled fibre yarns (Hoenig, 1993), (Cheng and Wong, 1993), (Lenox-Kerr, 2000). Research has focused on producing yarns from opened waste spun at different carding drum and spinning drum speeds and determining the properties obtained; including strength and elongation as well as yarn hairiness and evenness (Cheng and Wong, 1997). Weaving of the recycled fibre yarns into fabrics to find the strength and abrasion resistance that can be expected from these yarns has also previously been undertaken by Cheng and Wong (1997). Much work has also been carried out regarding the properties of friction spun yarns in comparison to rotor and ring spun yarns (Huh, 2002), (Das and Mal, 2009).

Fibre lengths suitable for use in Dref machines has been stated to be 10-120mm for most fibres, with nylon and polypropylene more difficult to handle at longer lengths resulting in suitable lengths of 10-60mm (Lenox-Kerr, 2000). However experimental work on fibre length and the proportion of short fibres within the feed has not been extensively researched.

6.4 Experimental – Short Fibre Spinning.

Friction spinning has been highlighted as a possible option for spinning the recycled fibre, as it is able to spin fibres of lower lengths than other methods of spinning such as ring spinning. This work aims to show how the fibre length and the proportion of short yarns within the fibre feed affect the resultant yarn strength.

6.4.1 Materials

Virgin (ie previously unused) nylon 66 fibres provided by Goonvean fibres with lengths of 30mm, 25mm, 20mm, 15mm, 10mm and 4mm were used within this study.

6.4.2 Spinning Studies

Fibre webs were created with 50 g of fibre. The fibres were opened up by hand and laid over a 50 cm by 30 cm area on the conveyor. Where blends of fibre lengths were used the longer fibre was distributed over the area first and the shorter fibre scattered over the long fibre. This ensured an even proportion of long and short fibres throughout the web. The opened fibres were then fed into a Hatters roller and clearer card from the conveyor. The resultant web produced varied in its area density and therefore the web was folded over at both ends to produce an approximate consistent area density of 40 g/m².

The web was then folded in half lengthways to produce an 80 g/m² web narrow enough to be fed into the DREF 2 rollers. The carded web was fed into the feed rollers of the DREF 2 friction spinning machine with operating conditions as described in Table 1. A pre-spun yarn was wound onto a bobbin and the bobbin placed on the winding device. The yarn end was placed on the spinning zone in order to give an open end onto which the nylon friction spun yarn could form. A total of 20 yarns were produced with fibre length proportions shown in Table 2. In addition to these yarns 100% 10mm fibre webs were attempted to be spun but failed to spin successfully due to lack of cohesion of the web. Higher proportions of 4mm fibre could not successfully be fed into the roller and clearer card due to the gap between the conveyor and feed rollers.

Table 6.1: Operating Conditions of the DREF 2 Spinning Machine

Operation	Value
Inlet (rev/min)	154
Outlet (rev/min)	365
Friction Drum Speed (rev/min)	700 (increased to 850)
Delivery Speed (m/min)	100

Table 6.2: Specification of Yarns Produced

Yarn reference	Long fibre used	Long fibre percentage	Short fibre used	Short fibre percentage
1	30mm	100%	-	0%
2	25mm	100%	-	0%
3	-	0%	20mm	100%
4	-	0%	15mm	100%
5	30mm	75%	15mm	25%
6	30mm	50%	15mm	50%
7	30mm	25%	15mm	75%
8	25mm	75%	15mm	25%
9	25mm	50%	15mm	50%
10	25mm	25%	15mm	75%
11	30mm	75%	10mm	25%
12	30mm	50%	10mm	50%
13	30mm	25%	10mm	75%
14	25mm	75%	10mm	25%
15	25mm	50%	10mm	50%
16	25mm	25%	10mm	75%
17	30mm	75%	4mm	25%
18	30mm	50%	4mm	50%
19	25mm	75%	4mm	25%
20	25mm	50%	4mm	50%

6.4.3 Yarn Testing

Tensile tests were performed on each yarn to find their approximate strength using a Instron 4411 tensile machine. The British Standard, BS EN ISO 2062 *Textiles – Yarns from Packages – Determination of single-end breaking force and elongation at break using constant rate of extension tester*, was used as to carry out the tensile tests on the yarns. A gauge length of 250mm was used for the test with a rate of extension of 250mm/min. Six samples of each yarn were tested and the tenacity of the yarn was then assessed. As the linear density of the yarn varied throughout the bobbin due to

the differences in the fibre feed the linear density was measured for each yarn sample tested.

6.5 Results and Discussion – Short Fibre Spinning

Examination of the yarns produced from one length of fibre only indicated that the lower the fibre length used, the weaker the resultant yarn, Figure 6.5. Generally in friction spinning the longer fibres have a higher probability of damage during the spinning process as they may lap around the opening roller and have an increased tendency to buckle within the spinning zone. Using shorter fibres reduces the fibre damage caused and can improve the spinning efficiency (Ishtiaque et al., 2003). However, when using shorter fibres the strength of the resulting yarn is dependent on the friction properties between the fibres involved whereas yarns spun from longer fibres will rely on the breaking strength on the constituent fibres. These results agree correspond with the work by Louis et al (1985) who reported an increase in skein yarn strength of yarns produced with longer cotton fibres.

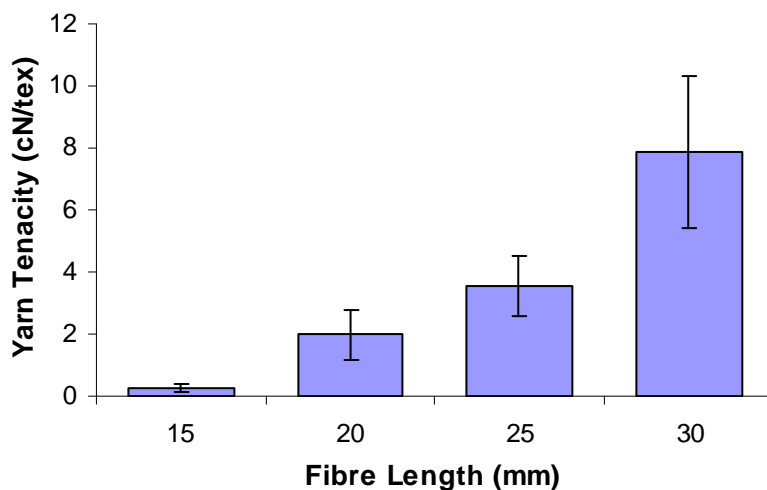


Figure 6.5: The Effect of Fibre Length on Yarn Tenacity

Increased percentage of short fibres within the produced yarns showed a number of effects. The 30mm/10mm blended yarn showed little alteration in its strength properties with an increase in the 10mm fibre composition. The 0% short fibre yarn and 50% short fibre yarn were proven to be statistically equivalent to a 95% confidence level using a t-test ($P=0.36$). This would suggest that friction forces were holding the short fibres within the yarn sufficiently and yarn breakage was due to

failure of the long 30mm fibres. The strength of yarn started to drop after increasing the percentage of short fibres over 50%, Figure 6.6. A t-test confirmed that these samples were statistically different to a 95% confidence level ($P=0.002$). The reduction of strength is most likely to be caused by the lack of long fibres which are contributing to the frictional forces holding the short yarns together and giving the yarn strength.

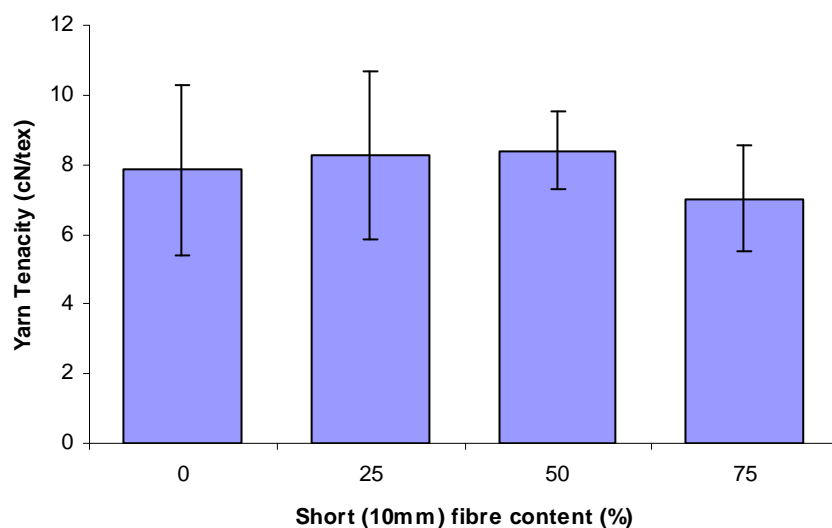


Figure 6.6: *The Effect of Fibre Percentage on Yarn Tenacity in a 30mm/10mm Blended Yarn*

This result was also reproduced in the 25mm/10mm blended yarn, Figure 6.7, where the 25mm fibres maintain the strength of the yarn samples between 25% and 50% 10mm fibre content (P value = 0.955 at 95% confidence level). At above 50% composition of the 10mm fibres the strength is reduced with the yarn containing 75% 10mm fibres significantly weaker using a 95% confidence test ($P=0.000$).

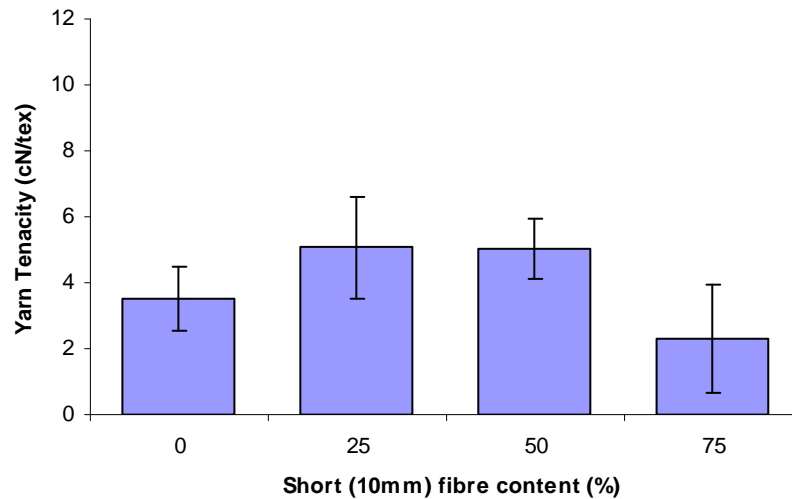


Figure 6.7: *The Effect of Fibre Percentage on Yarn Tenacity in a 25mm/10mm Blended Yarn*

A decrease in the overall strength of the 25mm/10mm blended yarns in comparison to the 30mm/10mm blended yarns can also be seen which agrees with previous data implying that shorter fibres will produce weaker yarns. As the strength of these yarns is dependent on the long fibres, the drop in length of the long fibre from 30mm to 25mm has affected the strength of all yarns produced.

The increase in short fibre percentage when using a short fibre of 15mm seems to have more effect on the strength of the yarn. The initial strength values at 100% of 30mm fibres and 100% of the 25mm fibres seems low as with the addition of 25% of the 15mm fibres the strength is increased, shown in Figure 6.8. It is possible that the 15mm fibres increase the uniformity and compactness of the yarn with increased friction between fibres. Increasing the percentage of short 15mm fibres further caused a steady decrease in yarn strength which shows that the strength of the yarn was dependent on both the long fibres (30mm and 25mm) and shorter 15mm fibres. As the percentage of the short fibre increases the lack of cohesion of the fibres causes the strength of the yarn to reduce. There is no difference in strength between yarns blended with 25mm and 30mm fibres when using the 15mm fibre as the short fibre, with t-tests proving equivalence between each pair of samples to a 95% confidence level ($P=0.205$, $P=0.243$, $P=0.440$ respectively for the 25% 15mm, 50% 15mm and 75% 15mm yarns).

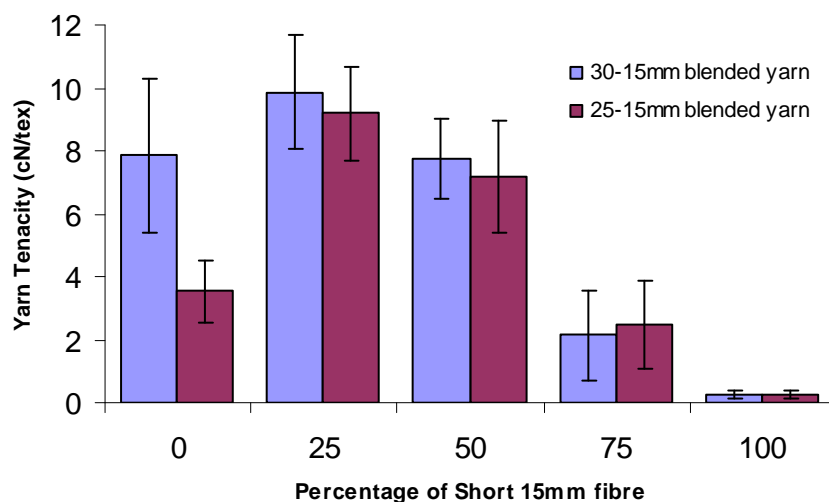


Figure 6.8: The Effect of Fibre Percentage on Yarn Tenacity in a 30mm/15mm and 25mm/15mm Blended Yarn

When even shorter fibres of 4mm are blended with longer fibres of 30mm or 25mm a more immediate change in the yarn strength was seen, Figure 6.9. It is unlikely that the 4mm fibres are offering significant strength to the yarn, instead they are held in place by the twisted 30mm fibres, which provide both the friction between the fibres and fibre length. The addition of the 4mm fibres to the blend has therefore caused the fibres to be less cohesive and results in a lower strength. The drop in strength is much less between the 0% and 25% of 4mm fibre percentages when using the 25mm fibre with t-tests proving an equivalence between these samples ($P=0.198$) to a 95% confidence level. In comparison, a significant drop in strength is seen from the 100% 30mm yarn to the 75% 30mm, 25% 4mm yarn ($P=0.000$), this could be due to the 100% 25mm yarn already having very low cohesion between the fibres. With a further increase of the 4mm fibre to a percentage of 50% both yarns showed an increase in yarn strength which was not expected. It is thought that this effect was due to production of a weaker web, resulting in the final yarn having a lower tex value due to breakages occurring to the web during feeding and short 4mm fibres being lost as fly material. The reduced material within the spinning zone would result in a higher twist taking place due to the lower circumference of the yarn, (Ishtiaque et al., 2003), and hence a higher tenacity. Raw data on the strength of these yarns can be found in Appendix 3.

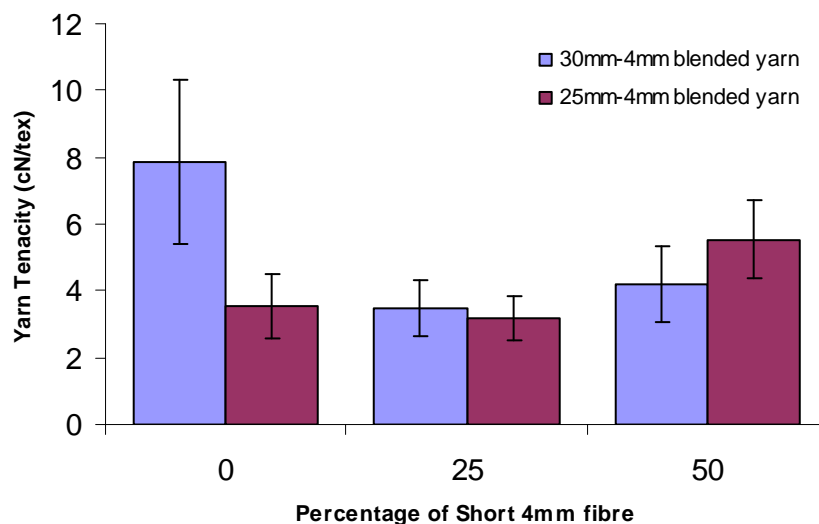


Figure 6.9: The Effect of Short Fibre Percentage on Yarn Tenacity in a 30mm/4mm Blended Yarn

6.6 Experimental – Web formation of RFL coated nylon 66 fibres

Web formation of RFL fibres was carried out in order to assess if textile processing could be advantageously used to recycle the Heathcoat waste.

6.6.1 Materials

RFL coated waste fabric from Heathcoat fabrics was used in this study. The waste fabrics were comprised of woven faulty fabric and selvages of mixed weaving specifications made from 100% nylon 6.6. The waste fabric was broken down using the Laroche Cadette shredder in order to produce longer fibre lengths suitable for textile production processes.

6.6.2 Carding

A Platt miniature trial roller card was used to produce the web, in order to assess how the fibres passed through the carding process. 100g of shredded fibre was placed on the conveyor of the card and the card was run at a speed of 1.62 metres per minute to produce the web. The miniature card did not have any numerical outputs of the operational variables.

6.7 Results and Discussion – Web formation of RFL coated nylon 66 fibre

Initial attempts to form a web using the miniature card resulted in problems in the feeding. Fibres were placed on the conveyor to transport them to the nip of the feed rollers, however due to slippage between the fibres and the conveyor belt when they reached this point the fibres were not fed successfully into the feed rollers but instead congregated at the conveyor end. There was also slippage between the feed roller and the fibres. The consequence of this is that very few fibres were fed to the card, and therefore a web could not be produced.

Cotton was used as a way of transporting the fibres to the card roller. Cotton was fed initially at 100% through the card. Cotton was then placed on the card conveyor with RFL coated fibres placed above at a ration of approximately 50:50. This was done in order to stop the RFL fibres slipping along the conveyor surface. Once the fibres were able to be transported to the card roller the web was able to be produced successfully, although easily broke at thin places that occurred due to lower feed levels. Figure 6.10 shows the resultant web that was able to be produced. Nevertheless it was evident an even web suitable for further processing, such as friction spinning, was unable to be produced using this method.



Figure 6.10: Photograph of RFL Fibre Web

It was thought the reason behind the troublesome processing of the fibre was due to its increased stiffness in its coated state. The stiffness of a fibre will affect how easily it is manipulated during processing. During carding the fibre is required to move as the machine clothing acts upon the fibres, be it in a carding or stripping operation, in order to align the fibres. Increased stiffness will cause the fibre to have difficulty in adjusting to the movements, (Klein, 1986). Instead they spring back to their original position after being manipulated by the card clothing which makes it difficult for the clothing on the main cylinder to hold the fibres in place, and rather than building up to form a web of the cylinder the fibres sit on the surface of the machine clothing and are easily removed, forming a very thin web.

The RFL coated fibres are also likely to have a lower coefficient of friction than fibres such as cotton. Due to the smooth surface of the fibres, they are less likely to entangle to form a cohesive web. Instead the individual fibres will pass over one another leading to the low strength of the web. The comparatively short fibres length of the RFL fibres to cotton fibres is another reason for less entanglement with one another. Shorter fibres will pass across fewer adjacent fibres within the web, and therefore have less opportunity to entangle. The longer RFL coated fibres are also thicker structures containing many filaments, and therefore, do tend to entangle with individual fibres due to their heavier weight.

Friction spinning was attempted on the small amount of fibre webs that were produced. This was not successful as the web was not strong enough for the inlet rollers to feed it to the carding drum. Because of this, the friction rollers did not have a constant supply of fibres to twist and open end of yarn was not able to be maintained. It was thought that if the web had been strong enough to produce a constant feed to the friction rollers, further problems may have occurred in the twisting process due to the fibre stiffness. During spinning fibres must be malleable enough to twist into shape, and bind one another together (Klein, 1986). If the fibres were unable to achieve they would likely be lost in processing. If a yarn was able to be produced it is likely to have been very hairy, with many fibre ends protruding from the surface.

6.8 Conclusions

Results in this chapter show that the fibre lengths achieved from the Laroche Cadette and Hollander beater reduction processes discussed in section 4.3.3 would be suitable for further processing using friction spinning providing that approximately 50% of long fibres, above 25mm are maintained in the reduced fibre.

However, the increased stiffness of the fibres due to the RFL coating causes problems during processing. Increased stiffness causes fibres to work against the forces imparted to them during carding and spinning, leading to spinning being an unviable commercial process for the RFL coated fibres. In order for textile processes to be suited to the RFL coated fibres it would be necessary to first remove the coating from the fibre, separating fibres and decreasing stiffness. Currently many of the fibres are in a thicker cut yarn form with the coating acting as an adhesive between the fibres. This causes them to have a much higher stiffness due to their increased diameter.

6.9 References

- CHENG, K. P. S. & WONG, K. F. (1993) From Rags to Yarn. *Textile Asia*, 24, 34.
- CHENG, K. P. S. & WONG, K. F. (1997) Processing and Properties of Yarns and Fabrics from Textile Production Waste. *1997 Recycling of Fibrous Textile and Carpet Wastes Conference*. Georgia, Georgia Institute of Technology.
- DAHIYA, A., KAMATH, M. G. & HEDGE, R. R. (2004) Dry Laid Nonwovens. [online] Available at: <http://www.engr.utk.edu/mse/Textiles/Dry%20Laid%20Nonwovens.htm> [Accessed 13 May 2012].
- DAS, A. & MAL, R. D. (2009) Studies on cotton-acrylic bulked yarns produced from different spinning technologies. Part 1: yarn characteristics. *Journal of the Textile Institute*, 100, 44-50.
- GULICH, B. (2004) What is machinery industry offering textile recycling? *Melliand International*, 10, 52-53.
- HOENIG, H. (1993) Textile Waste Recycling. *Textile Asia*, 24, 40.

HUH, Y. (2002) Analyzing structural and physical properties of ring, rotor, and friction spun yarns. *Textile Research Journal*, 72, 156.

ISHTIAQUE, S. M., SALHOTRA, K. R. & GOWDA, R. V. M. (2003) *Friction Spinning*, Manchester, The Textile Institute.

KLEIN, W. (1986) *The Technology of Short - Staple Spinning*, Manchester, The Textile Institute.

LENOX-KERR, P. (2000) Recycled Materials are Friction-Spun to Create High-Performance Yarns. *Technical Textiles International : TTI*, 9, 6.

LOUIS, G. L., SALAUN, H. L. & KIMMEL, L. B. (1985) Comparison of properties of cotton yarns produced by the DREF-3, ring, and open end spinning methods. *Textile Research Journal*, 55, 344.

7.0 Plastic Recycling

7.1 Aim

Plastic processing could be used as an alternative option for recycling of the RFL coated nylon 66 material. Preliminary investigations into two processing types: injection moulding and compression moulding are investigated in this chapter. Processing difficulties that arose from utilising the RFL coated material in these manufacturing techniques will be discussed and evaluated.

7.2 Introduction to Plastic Processing

There is a significant market for recycled plastics, the main reason for this being their reduced cost in comparison to virgin plastic with the added benefit of little alteration in their physical properties (Rosato, 1986). There are many ways of processing plastics and the choice often depends upon the product size and shape to be produced in addition to the plastic type, performance required and cost (Rosato, 1997).

7.2.1 Injection Moulding

In order to mould a plastic the material needs to be heated in order for it to be plasticised, maintained under pressure in order to take the shape of the mould, and cooled and released. An injection moulding machine consists of an injection unit and a clamping unit, as illustrated in Figure 7.1 (Rosato, 1997).

A typical injection moulding cycle, Figure 7.2, begins with the mould closing, the injection unit heats and transfers the material to the mould (Rosato, 1997). Work is done on the polymer using a screw device, causing heat to build up (this also aids pre-plastication of rubbers). The polymer is fed in a strip form between the barrel and the screw. Heat is controlled using a fluid, usually water or oil, which circulates around the barrel. At the point where the ram screw is fully forward the mould is fully filled and pressure is exerted consolidating the material, this is known as mould packing. At this stage the material also starts to cool and solidify, which continues in the dwell

time, also known as the mould cooling stage. This stage makes up half of the entire moulding cycle (Crowther et al., 1982). Once the plastic has solidified the mould is able to be opened and the mould ejected. “Change over time” is required for cleaning of the mould and the screw retraction must also be completed before the next cycle begins (Brydson, 1990).

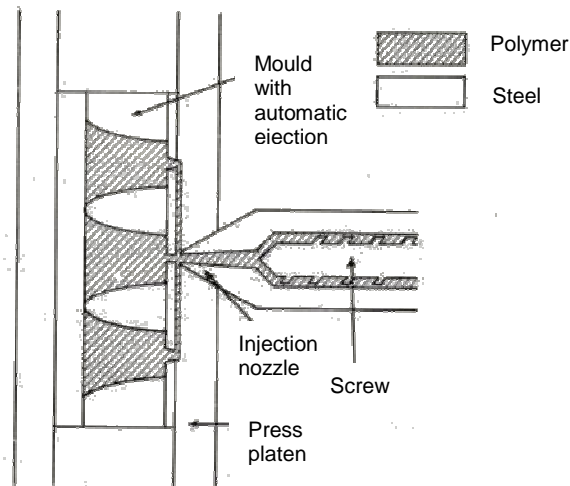


Figure 7.1: Injection Moulding (Crowther et al., 1982)

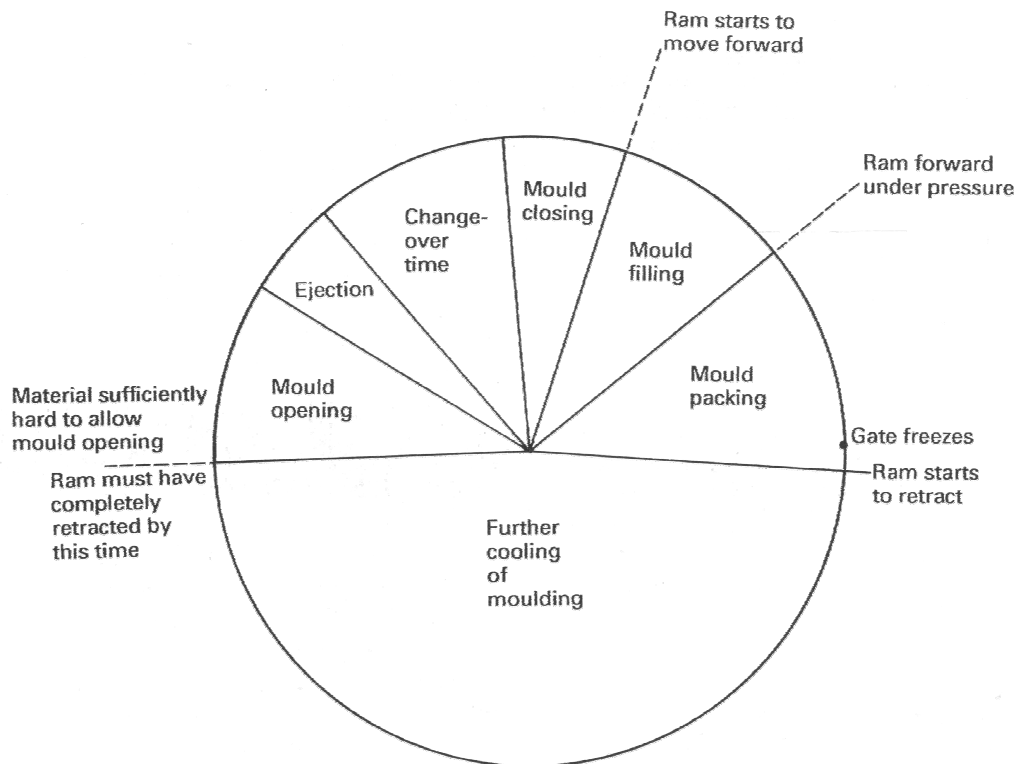


Figure 7.2: The Injection Moulding Cycle (Brydson, 1990).

7.2.2 Compression Moulding

Compression moulding in comparison is a more lengthy process as heating and cooling of the mould is required for each cycle, Figure 7.3. More material than required is charged into the mould cavity which is then closed under pressure. The material is heated within the mould to plasticize it and under pressure it flows to the shape of the mould, with excess material escaping as flash. (Thermosetting polymers will undergo polymerisation and crosslinking during this time (Brydson, 1990)).

Compression presses can consist of parallel platen or hinged platen. Hinged platen presses utilise fixed moulds and have reduced heat loss in comparison to parallel platen where loose moulds are used. This subsequently results in reduced cure time needed in hinged platen machines. Parallel platen machines on the other hand allow the operator to quickly access and clean the mould halves. Presses usually have semi-automatic controls in order to standardise mould close and cycle times. This in turn allows the product to be consistent with less rejects (Crowther et al., 1982). The platens utilise hydraulic pressure to bring them together, this can be by water or oil and give a loading from 7-14 MPa. Compression moulding is able to produce a wide range of components so long as the mould design basic. For intricate mould designs the cost for the mould is increased making this method less viable. Some designs may also be impossible to create a mould for.

Since plastics have different curing properties, the processing temperatures and cure times will vary to ensure that flow and crosslinking processes are controlled (Rosato, 1997). Typical compression moulding cycles, Figure 7.4 have an increased dwell time relative to injection moulding.

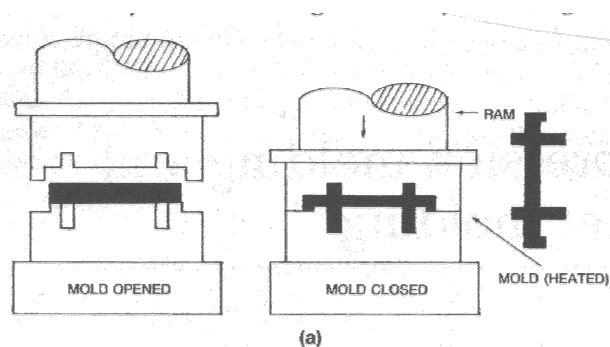


Figure 7.3: Compression Moulding (Rosato, 1997)

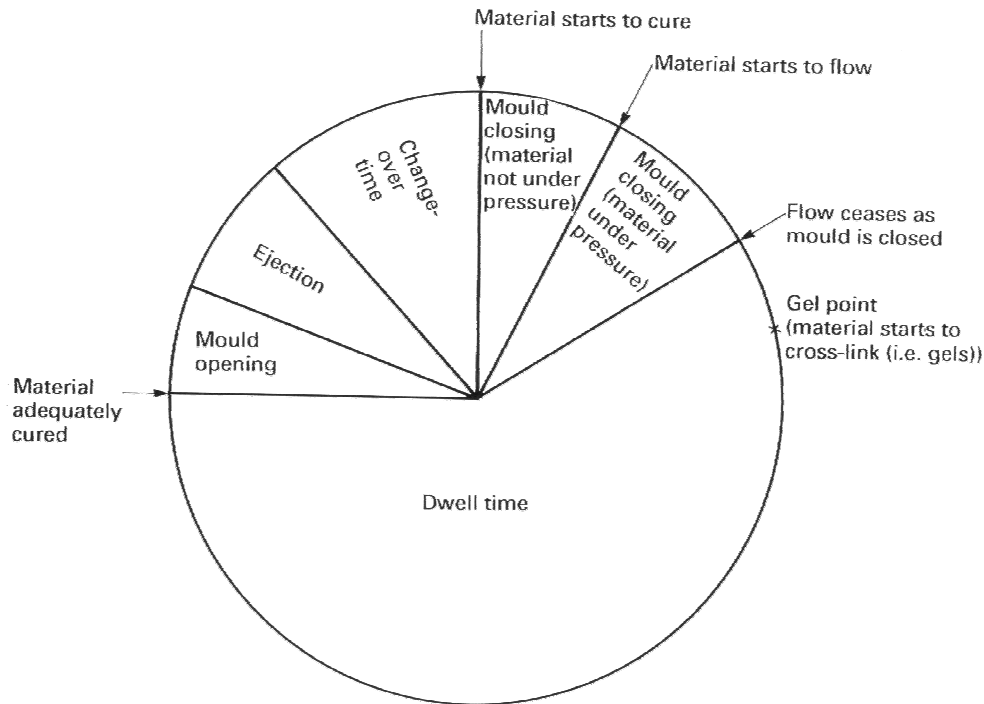


Figure 7.4: *The Compression Moulding Cycle (Brydson, 1990)*

Moulds used in compression moulding can be open flash, positive or semi-positive. Open flash moulds, Figure 7.5, require an excess of moulding powder to be loaded into the cavity which increases the pressure within the mould, enabling a good mould to be produced. Excess material is forced out as pressure is exerted onto the mould. This is the simplest kind of mould and can produce good quality products. Positive moulds allow a plunger to enter the mould cavity, trapping the plastic material within, and allowing the full pressure to be transferred to the charge material, Figure 7.6. An exact amount of charge polymer is required to be loaded, if too much is used the mould will not close sufficiently and if not enough is loaded the resulting moulded piece will be thinner than required. If air is trapped within the mould this can cause blisters to occur on the plastic's surface. Semi-positive moulds allow for flash to escape whilst still maintaining pressure on the polymer through a positive plunger and cavity shape (Rosato, 1997).

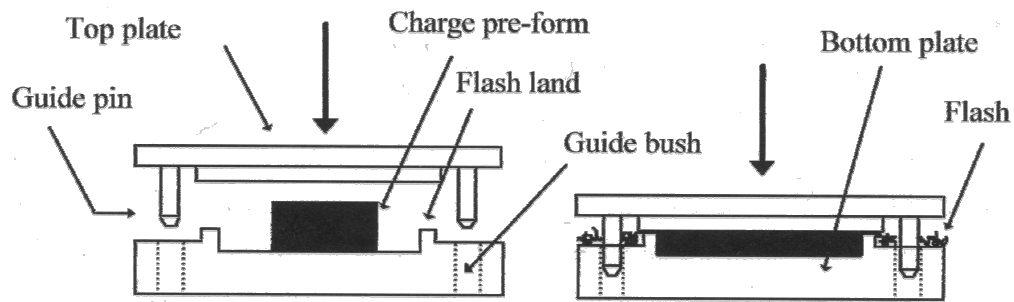


Figure 7.5: Open Flash Mould

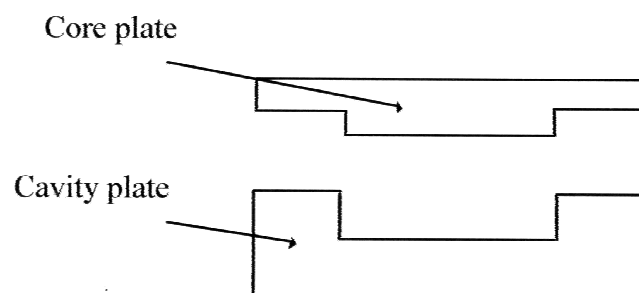


Figure 7.6: Positive Mould

In order to increase processing time, it is preferable to heat the mix prior to moulding. This can be done using water bath, ovens or microwaves and combined with compression moulding, however, transfer moulding and injection moulding incorporate this preheating into the moulding procedure. Transfer moulds are made up of the mould cavity which is mounted to another cavity. The prepared rubber mix is placed in the upper chamber and a ram is used to transfer the polymer to the mould cavity under pressure, this is known as transfer moulding.

7.3 Experimental

7.3.1 Injection Moulding

7.3.1.1 Materials

Coated waste fabric from Heathcoat fabrics was used as the raw material within this trial. The waste consisted of RFL coated nylon 66 in the form of fabric ends and selvages. The waste was broken down as discussed in section 4.3.2.3 using the Intimus disintegrator producing a particulate material. Prior to processing the material was dried in a vacuum oven at 100°C for 24 hours. The particulate material offered the best form for input to the injection moulding machine as this sample was the most dense out of the reduced samples. It also offered the best form for packing since more air is trapped between fibres, than particulate matter. In addition waste that had not been reduced was also used. The unreduced waste was chosen for this work due to its dense form and the ability to layer and compress the fabric.

7.3.1.2 Injection moulding settings

Injection moulding was performed using a Negri Bossi twin screw extruder with parameters as described in Table 7.1

Table 7.1: Injection Moulding Settings used in Study

Setting	Value
Barrel rear temperature	230°C
Barrel mid temperature	230°C
Barrel front temperature	230°C
Nozzle	55% (approx 220°C)
Injection pressure	40 bar
Screw Speed	50% (approx 130rpm)
Cooling time.	35 secs

7.3.2 Compression Moulding

7.3.2.1 Materials

Both RFL coated and uncoated nylon 66 waste from Heathcoat fabrics was used as raw material in the compression moulding trial. The waste was initially used in a reduced state using the particles produced from the Intimus disintegrator, the process of which is described in section 4.3.2.3. Following the initial trial, work was also carried out using the waste in fabric form. Material was dried in a vacuum oven at 100°C for 24 hours prior to processing.

7.3.2.2 Compression Moulding Parameters

Compression moulding of the Intimus disintegrator reduced particles was undertaken using a 127x76x1mm open flash mould, Figure 7.5. An open flash mould was created using a picture frame shaped metal piece, Figure 7.7, sandwiched between two metal plates. From an estimated density of 1.2 g/cm² for the waste material, it was calculated that approximately 11.5 g would be needed to fill the mould. As an extra 10% of material is required for sufficient pressure to build up within the mould, which is then expelled as flash, an additional gram of material was therefore incorporated to ensure that the mould would be fully filled and flash formed. The total amount of chip used was therefore 12.5 g. A hydraulic heated clamping unit, Tangyes Ltd Two speed Hydra-pak hand pump, was then raised to a temperature of 240°C and a pressure of 10 tonnes on a 10cm diameter (equivalent to 123 bar) was applied to the mould, Figure 7.8. Compression moulding parameters were later modified in order to optimise the moulding process.

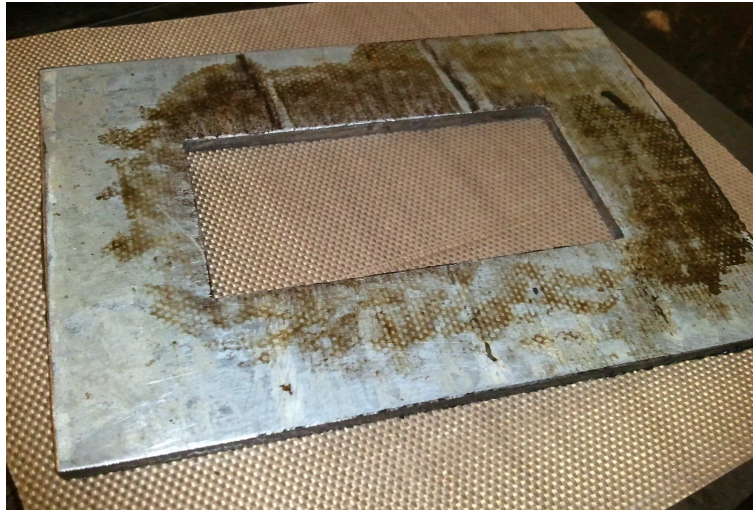


Figure 7.7: *Picture Frame Mould*

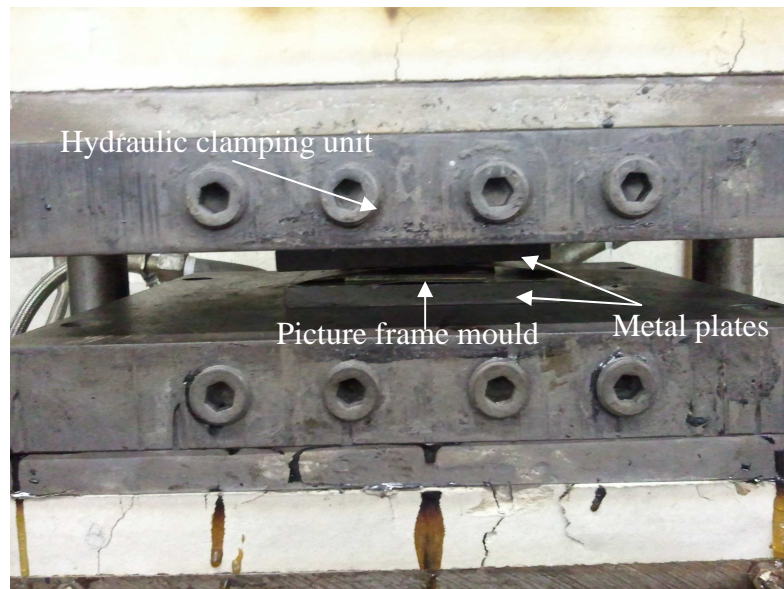


Figure 7.8: *Compression Moulding Construction*

Compression moulding of the fabric directly was attempted as much of the reduced material was of a lower quality due to degradation in the reduction stages. This was initially attempted with an open flash type mould (Figure 7.5) of dimensions 60x30x3mm, using a picture frame mould between two metal plates. The moulding parameters were changed in order to achieve better mouldings as described in the results, Table 7.2. These included:

- the total fabric weight used;
- the temperature of the platen and mould when the fabric was added;
- the temperature of the platen and mould when the cooling was initiated;
- the time the material was held at temperature before applying the pressure;
- the pressure applied.

The trial was repeated using a positive mould (Figure 7.6) of dimensions 112 x 51 x 2mm and the processing parameters were varied in order to optimise the moulding. Since there were some problems in removing the piece from the mould, the method was adapted to also include heat proof non-stick fabric within the positive mould.

The fabric pieces were cut to the size of the mould and layered in order to get the required polymer weight, Figure 7.9. The fabric layers were compressed using the metal plates, and further compression achieved using the hydraulic clamping unit.



Figure 7.9: Fabric Layers Prior to Moulding

7.4 Results and Discussion

7.4.1 Injection Moulding

The material was able to be extruded, however significant vapour emission occurred during the process, which created pressure on the screw and caused the screw to be pushed back. The material also began to spit occasionally, causing the material to be ejected as little balls. A moulding was therefore only attempted once due to safety issues, further the part produced also consisted of many voids. It is unknown as to whether the settings used would be suitable to produce satisfactory parts. Since the temperature used (230°C) was only slightly higher than the melting point of nylon 66

(220°C), reduction in temperature was likely to cause the polymer to solidify and would be unlikely to reduce the vapour emissions created.

This gaseous emission behaviour is comparable to that of processing damp nylon, or if the nylon has begun to degrade. From conclusions in Chapter 4, the quality of the particle form of Intimus disintegrated coated waste was found to be low and this is likely to have caused the problems experienced in the injection moulding trial.

7.4.2 Compression Moulding

Three plastic sheet samples were made up using compression moulding of the Intimus disintegrator reduced coated waste (particles); however, the resultant sheets were still weak with many voids. It was assumed that this was either due to the nylon flakes not melting sufficiently, or the pressure being too low. Voids occur due to air entrapment during the lay-up construction. Hand lay-up or low pressure processing methods are common causes of voids (Rosato, 1997). The material weight loaded into the mould was gradually increased in order to provide the flash build up and pressure required on the polymer in and to remove excess air from the system. The machine temperature was also increased to assist melting; however, an improvement was not seen in the strength of the resultant sheet. Parameters used are shown in Table 7.2.

Table 7.2: Compression Moulding Intimus Reduced Coated Waste (Particles)

Mould	1	2	3
Material weight (g)	12.5	13.5	15.0
Machine temperature (°C)	240	240	260
Pressure	10 tonnes/10cm diameter	17 tonnes/10cm diameter	30 tonnes/13cm diameter

Tables 7.3 to 7.6 summarise the characteristics of the samples created by compression moulding of the uncoated fabric and RFL coated fabric using both the open flash mould and the positive mould. Melt processing of the fabric was able to form plastic pieces with increased strength that were able to be removed from the mould. Where the RFL coating was also able to be integrated into the plastic pieces few problems other than additional vapour arising occurred. However, most pieces produced still

contained many voids and there was also a problem with discoloration of the uncoated polymer due to degradation. Figures 7.10 and 7.11 show examples of mould pieces produced. The discolouration of the uncoated nylon due to degradation during the compression moulding is particularly evident in Figure 7.10. The inherent colouring of the RFL coating makes it difficult to assess by eye if similar degradation has occurred to the nylon within the RFL coated moulded samples.

Figure 7.12 shows an example of the internal structure of the moulded plastic piece. The light micrograph of the cross-section of the moulded material indicates the presence of voids that will weaken the physical structure (Rosato, 1997). These may have occurred due to the weave structure and layered fabric pieces which would most likely cause air to be entrapped within the structure. Procedures such as applying a vacuum during the process or utilising rollers to squeeze air out during lay-up can be used to eliminate voids (Rosato, 1997).

Table 7.3: Compression Moulding of Uncoated Fabric using Open Flash Mould

Sample	1	2	3
Weight of fabric	4.5g	5.33g	6.15g
Weight of sample	4.33g	5.14g	5.21g
Temperature of polymer addition	180°C	200°C	230°C
Temperature of polymer heating	270°C	270°C	270°C
Time temperature held at 270°C before adding pressure	1 minute	1 minute	1 minute
Pressure	10 tonnes/13cm diameter	20 tonnes/13cm diameter	10 tonnes/13cm diameter
Comments	No flash formed. Some degradation.	Flash formed. Some degradation.	Increased flash. Less degradation.

Table 7.4: Compression Moulding of RFL Coated Fabric using Open Flash Mould

Sample	1	2	3
Weight of fabric	6.15g	6.15g	6.15g
Weight of sample	5.24g	5.21g	5.21g
Temperature of polymer addition	260°C	260°C	260°C
Temperature of polymer heating	270°C	270°C	270°C
Time temperature held at 270°C before adding pressure	1 minute	5 minutes	6 minutes
Pressure	0.8 bar	0.8 bar	1.6 bar
Comments	Nylon did not flow to fully fill the mould.	Flash formed. Polymer filled mould.	Flash formed. Polymer filled mould.



Figure 7.10: Example of a Moulded Piece Produced from Uncoated and RFL Coated Fabric using an Open Flash Mould

Table 7.5: Compression Moulding of Uncoated Fabric using a Positive Mould

Sample	1	2	3
Weight of fabric	20.0g	10.0 g (+ non stick sheets)	10.0g (+ non stick sheets)
Weight of sample	N/A	9.08g	8.71g
Temperature of polymer addition	260°C	270°C	270°C
Temperature of polymer heating	270°C	270°C	280°C
Time temperature held at 270°C before adding pressure	1 minutes	15 minutes	15 minutes
Pressure	0.8 bar	0.8 bar	0.8 bar
Comments	Polymer not fully melted, still in fabric form. Polymer stuck to mould.	Successful mould	Overfilled mould, problems extracting sample.

Table 7.6: Compression Moulding of RFL Coated Fabric using a Positive Mould

Sample	1	2	3
Weight of fabric	5.0g (+ non stick)	8.0g (+non stick)	10.0g
Weight of sample	5.00g	8.00g	8.76g
Temperature of polymer addition	180°C	180°C	180°C
Temperature of polymer heating	280°C	280°C	280°C
Time temperature held at 270°C before adding pressure	15 minutes	15 minutes	15 minutes
Pressure	0.8 bar	0.8 bar	0.8 bar
Comments	Fabric shrank within mould, too much space. Fabric not melted properly.	Still shrank slightly so more fabric needed.	Overfilled mould, problems extracting sample.



Figure 7.11: Example of a Moulded Piece Produced from Uncoated and RFL Coated Fabric using a Positive Mould

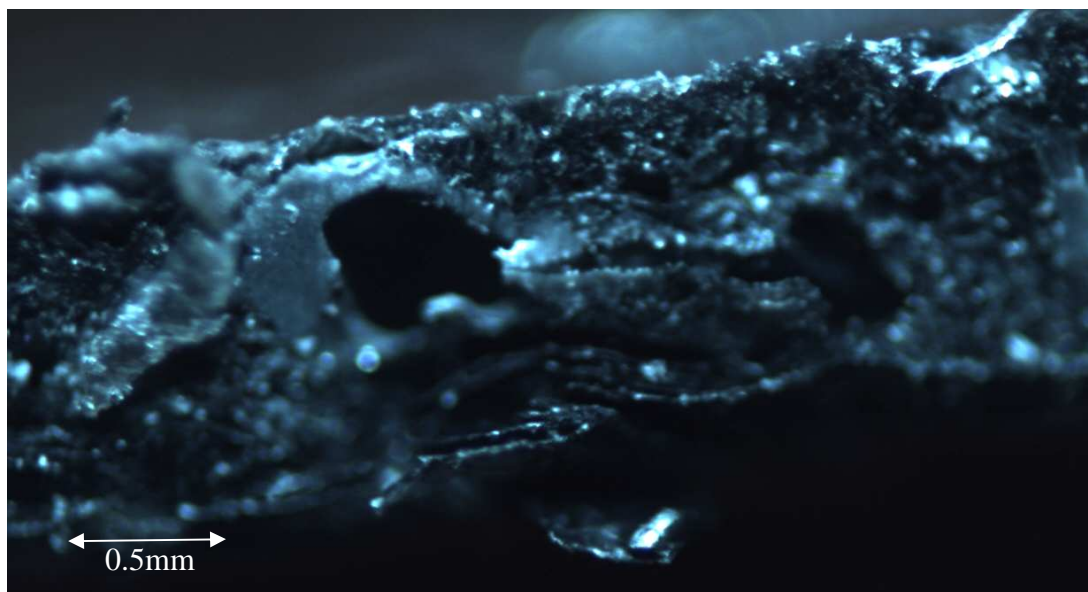


Figure 7.12: Light Micrograph Cross-section of Moulded Piece Produced from RFL Coated Fabric using an Open Flash Mould, with a Magnification of 5x.

There are many variables that would affect the void production within the plastic samples. Since this work is preliminary a full analysis of the void formation and the reasons behind this was unable to take place. It is likely that the particle size will have an effect on void formations, with smaller particles allowing the material to be more closely packed and therefore less voids produced. Densification processes are used in plastic recycling processes that allow the material to be more compact and hence have better handling within the melt processing (Scheirs, 1998). Smaller, denser particles would therefore produce better moulded pieces.

The coating is likely to cause the material to be more viscous due to the number of bulky side chains provided by the RFL as shown in Table 4.3. This makes voids more likely to be produced as the polymer does not flow into the air gaps as an uncoated polymer would. The bulky side chains of the RFL coating also cause the nylon to start to degrade at a lower temperature as discussed in section 4.5.3.1. The nylon degradation causes the production of gaseous products cyclopentanone and carbon dioxide. If this gas is unable to escape this will add the amount of voids formed. Since onset of degradation is earlier in the coated waste as shown in Figure 4.7 the gas production will occur over a longer period of time, causing more voids to occur in the plastic pieces made from the RFL coated waste than in the uncoated waste.

7.5 Conclusions

Preliminary work, discussed in this chapter, regarding recycling by melt processing, highlights the difficulties that would have to be resolved for this type of process to be utilised in recycling of the RFL coated waste, namely polymer degradation and formation of voids. Voids have been prevalent in samples due to the hand lay up and packing of the moulds. Reduction of voids by vacuum or roller methods to reduce air within the moulds could be used in an industrial environment.

Processing of the fabric directly enables fewer stages for the polymer to degrade, however shapes able to be moulded would be limited. It is interesting and encouraging to note that the nylon 66 was able to be processed with without prior removal of the RFL coating. Although problems may still arise in industrial processing due to the increased vapour evolution that the RFL coated materials produce when heated.

7.6 References

- BRYDSON, J. A. (1990) *Handbook for plastics processors*, Oxford, Heinemann Newnes in association with the Plastics and Rubber Institute.
- CROWTHER, B. G., EDMONDSON, H. M. & ELLIS, M. J. (1982) Processing Technology. In Blow, C. M. & Hepburn, C. (Eds.) *Rubber Technology and Manufacture*. 2nd ed. London, Butterworth Scientific.
- ROSATO, D. V. (1986) Summary - Mold with Profit. In Rosato, D. V. (Ed) *Injection Molding Handbook*. New York, Van Nostrand Reinhold Company.
- ROSATO, D. V. (1997) *Plastics processing data handbook*, London, Chapman & Hall.
- SCHEIRS, J. (1998) *Polymer recycling: science, technology, and applications*, Chichester, Wiley.

8.0 Using RFL Fibres as a Filler to Reinforce Rubber.

8.1 Aim

The aim of this chapter was to investigate whether RFL coated recycled fabric can be used as filler to reinforce rubber mouldings. The effect that the RFL coating has of the rubber produced and the way that recycled material quantity used has on the rubber properties was also investigated.

8.2 Rubber Technology

8.2.1 Introduction

Rubber, like textile fibres, is a polymeric material. As such, it is a compound of high molecular weight made up from of long chains of repeating molecules (Blow, 1982). Polymers can behave like viscous liquids if the links on the chain are free rotating and this allows flow and distortion of the material under stress. The polymer chain length and the presence of side groups restrict the movement of the chain causing viscoelastic properties (Blow, 1982). Crystallisation takes place when portions of the molecules rearrange to form crystallites. Other areas of the polymer chain, however, will remain amorphous. Crystallites occur in a time dependent process when the rubber is below its melting temperature, but by stretching the rubber rapidly crystallisation can also occur due to the polymer chains rearranging and aligning to become oriented (Blow, 1982). These properties give natural rubber high strength when un-compounded. Many synthetic rubbers are unable to form crystallites in this way due to the irregularity in the polymer molecular structure and therefore will have low strength in the gum state (Blow, 1982).

Early rubber technology depended upon natural rubber obtained from the wild, before being grown in rubber plantations. Natural rubber has substantial strength and

elasticity at room temperature, however, it is sensitive to both hot and cold temperatures and turns sticky when oxidised.

Natural rubber is a polymer of isoprene (C_5H_8) forming the structure shown in Figure 8.1. Once this became known, research focussed on alternative synthetic manufacturing routes, leading to a number of synthetic rubbers becoming available (Stern, 1982).

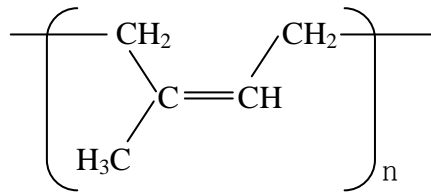


Figure 8.1: Polyisoprene Structure

Most synthetic rubbers are produced by first producing the monomer, and then by a polymerisation stage to form the polymers. Early synthetic rubbers were difficult to process due to their branched and irregular polymer chains. However, advances in polymerisation processing allowed straight chain derivatives to become commercially viable. Synthetic rubbers that are now available include: Styrene-Butadiene Rubbers (SBR), Polychloroprene Rubbers (CR), Ethylene-Propylene Rubbers (EPM and EPDM), Isobutene-Isoprene Rubbers (Butyl Rubber or IIR), Acrylonitrile-Butadiene Rubbers (NBR), Acrylic Rubbers (ACM), Fluororubbers and Silicone Rubbers (Stern, 1982).

SBR rubber, with which the work in this chapter has been undertaken, is a copolymer of styrene and butadiene forming the structure shown in Figure 8.2. This rubber is also used as part of the latex component of the RFL coating as discussed in section 1.2.3.2. Generally, commercially produced SBR use a styrene content of 23.5% (Brydson, 1988). SBR

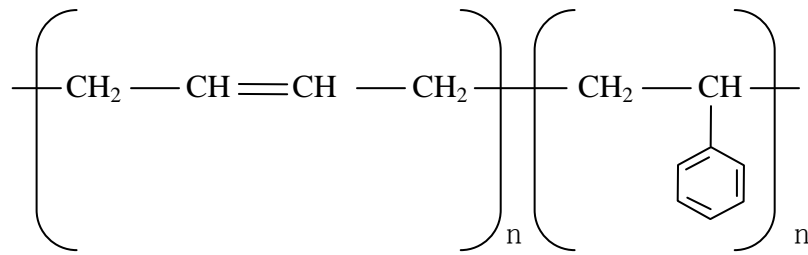


Figure 8.2: *Styrene Butadiene Rubber (SBR) Polymer Structure*

8.2.2 Vulcanisation

Vulcanisation is the chemical process in which cross-links are formed connecting the polymer chains. This restricts the movement of the molecules within the polymer chain, reducing its ability to crystallise. As such, this process enables the rubber to have improved elasticity and is stable at a wide temperature range, having constant modulus and hardness characteristics (Blow, 1982).

Vulcanisation was initially discovered by heating rubber in sulphur. Sulphur vulcanisation is still the most widely used form of curing rubbers commercially. The sulphur is able to bond with the polymer system, forming monosulphide, disulphide or polysulphide bonds, which connect the polymer chains, as shown in Figure 8.3. Additionally the sulphur can also form into pendant sulphides or cyclic monosulphides and disulphides, also illustrated in Figure 8.3 (Morrell, 1982). These latter types of bonds do not contribute to the polymer cross-linking mechanism and therefore cause the vulcanising process to be less efficient. In order to make the system more efficient in creating the cross-links, the use of accelerators and accelerator activators began to be used alongside the sulphur. Modern sulphur accelerated vulcanisation systems involve sulphur, an accelerator, an activator and a fatty acid (further detail in section 8.2.3.1) and require 15-20 minutes cure time at 140°C (Brydson, 1988).

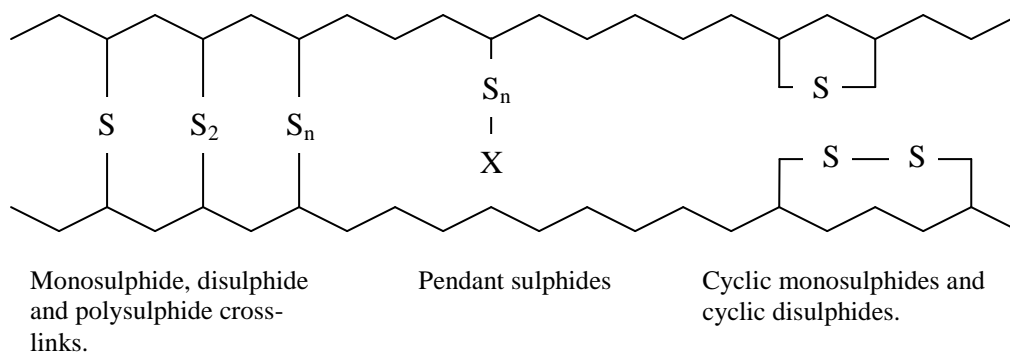


Figure 8.3: *Sulphur Bonding Structures in a Vulcanisate Network*

The vulcanisation process is often combined with the shaping of rubber pieces. This can be by compression moulding, using a cavity mould and heated plates, or by injection moulding where the rubber is forced into a cavity from an extruder (Blow, 1982).

8.2.3 Additives in Rubber

A number of additives are used in rubber to modify properties for the desired end use, both in natural rubber and in synthetic rubber. Early uses of additives in rubber included unsaturated oils as softeners, chalk to reduce cost, sand as an abrasive and zinc white and iron oxide as pigments. The need to modify the properties of rubber and reduce the costs involved led to a further number of liquids, resins and powders being evaluated in rubber compounds. Additives can be categorised into six functional types of material in rubber:

1. The polymer vulcanizing system;
2. Anti-ageing additives;
3. Fillers;
4. Softeners and plasticisers;
5. Resins and process aids;
6. Other specialty additives.

Despite their functions it is important that materials used as additives should also have the following features: be stable under processing conditions, not migrate from the rubber to an adjacent material, not interfere with the effects that other additives provide within the vulcanisate, be cheap and non-toxic (Brydson, 1988).

8.2.3.1 The Vulcanising System

Sulphur was initially discovered as a cross-linking agent and used alone, however this produces a slow reaction and much of the sulphur is inefficiently used as described in section 8.2.2. The use of accelerators alongside accelerator activators became commonplace, allowing vulcanising times to be controlled. Today the vulcanising system is made up of a vulcanising agent, an accelerator, an accelerator activator and a fatty acid. For the most common rubbers, natural rubber, SBR, IIR, Butyl Rubber, NBR and EPDM, sulphur is the cross-linking agent normally used. There are many choices of chemicals used as an activator but zinc oxide in the presence of the fatty acid stearic acid is a common preference. Different rubbers have different levels of reactivity, and therefore the chemicals used in the curing system must be chosen with this in mind. The formulations can also be changed to alter the cure time, scorch time and cure temperature of the mix or to change modulus, ageing properties, fatigue life and crystallisation tendencies of the cured rubber. Table 8.1 summarises how this can be achieved (Brydson, 1988).

Table 8.1: Controlling Vulcanizate Properties by Formulation Alteration

(Brydson, 1988)

Aim	Action	Functional Reason
Reduce the cure time.	Use a faster accelerator or increase the amount of accelerator level.	Accelerators help the reaction to be carried out more quickly and efficiently. Due to more efficient bonding this will also cause an increase in the vulcanisate modulus.
Reduce the cure time without affecting the modulus.	Increase the accelerator level but decrease the sulphur level.	By decreasing the sulphur level there are fewer sulphides to form linkages. By increasing the accelerator level the available sulphides tend to cross-link quickly and efficiently. The modulus avoids being altered as the reduction in sulphur means that the number of linkages does not increase.
Improve ageing resistance.	Use a high accelerator/sulphur ratio.	An efficient vulcanisation with substantial monosulphide linkages will be produced to give good ageing properties.
Improve low temperature properties.	Use a low accelerator/sulphur ratio to avoid efficient vulcanisation.	Regular monosulphide cross-linked rubbers have a higher tendency to crystallise, particularly in natural rubber. This causes them to become brittle at a higher temperature. A lower accelerator/sulphur ratio will cause less monosulphide linkages to be formed.
Increase cure temperature.	Increase the accelerator level without reducing the sulphur content.	By increasing the cure temperature, the time to optimum cure will decrease. In natural rubber the optimum crosslink density also decreases, causing a reduction in tensile strength, tear strength and other physical properties. Higher temperatures cause a higher number of monosulphide linkages to be formed but also a high proportion of cyclic and pendant sulphide groups. By increasing the accelerator level the crosslink density will be able to be increased.

In addition to sulphur, there are other cross-linking agents that can be used as additives for the vulcanising system. These include peroxides, phenolic resins and

nitroso and urethane-based systems (Brydson, 1988). As these systems are only used in specialised cases it is beyond the scope of this thesis to discuss these further.

8.2.3.2 Anti-degradant additives

In addition to changes in the vulcanisation formulation, the anti-ageing properties of rubber compounds can be improved by using extra additives. Depending on the rubber, the use of anti-ageing additives may be vital or only used to further improve properties for specific end use where requirements are strict. For some speciality rubbers they are unnecessary (Brydson, 1988).

Rubber can degrade in many ways; transforming to a tacky mass (perishing), formation of cracks (ozone attack) and through surface hardening. The most common degradation in natural and synthetic rubbers has been proven to be due to oxygen or ozone and as a result the main anti-degradants are antioxidants and anti-ozonates.

Hydrocarbon oxidation occurs in three stages, initiation, propagation and termination. Initiation occurs from the presence of free radicals which are created as a result of other reactions occurring during mechanical shear, UV radiation and thermal decomposition of weak bonds. The propagation stage results in more free radicals being formed enabling the reaction to continue. The reaction terminates by forming cross-links or by reaction with the oxygen forming non-radical products. In undergoing these processes chain scission may occur resulting in damage to the rubber composite (Brydson, 1988).

Additives can be used to stop the initiation reaction taking place, known as preventative antioxidants. These include:

1. Sequestering agents, which deactivate harmful metal ions such as copper and manganese;
2. UV absorbers;
3. Peroxide decomposition agents, which convert hydro-peroxide into an inert product;
4. Radical traps.

Preventative antioxidants are rarely used in rubbers instead additives that interrupt the propagation stage, known as chain breaking antioxidants are preferred. The requirements for the antioxidant will vary depending on the compound that is being produced. For example an antioxidant may be chosen for its good flex cracking resistance but produce poor heat resistance and metal inhibition. Both the polymer type and the vulcanisation system chosen will influence how the antioxidant performs in the compound.

Antioxidants that are used in rubbers can be classed into hindered amines and phenols. Amines generally offer better anti-degrading properties but result in staining of the compound. Phenols on the other hand do not stain but are less efficient (Brydson, 1988).

Ozone degradation is characterised by cracks perpendicular to the direction of stress. Deterioration occurs at the surface where the compound is open to attack from ozone in the atmosphere. There are two types of anti-ozonate used, p-phenylene diamines and waxes. Although p-phenylene diamines lead to improved anti-ozonate behaviour there are problems of toxicity, excessive volatility and interference with the cure. This leads to a limited choice on the market. Waxes are used at levels of 1-5% within the polymer compound. They act as an anti-ozonant by diffusing to the surface to form a protective layer. The wax melting point and the amount of side chain branching will affect how quickly this occurs, and therefore will also affect the choice of wax used for a particular rubber. If the diffusion occurs too quickly flakes will appear on the surface, however if diffusion occurs too slowly the wax will take too long to become effective as an anti-ozonant (Brydson, 1988).

8.2.3.3 Fillers

Fillers are often used in rubber composites simply to reduce cost. However they can also be used to change the mechanical properties of the rubber. They can therefore, be classified into inert or reinforcing fillers. Fillers are also classified by their size. Fillers in a powder form are known as particulate fillers. Alternatively fibres, yarn and other textiles can be used.

Types of inert fillers include untreated chalk and clays, although at fine particle grades these can have some reinforcing properties. The most popular reinforcing filler is carbon black. Silicas and silicates are also used as reinforcing fillers in specialised uses. Coupling agents can be used on inert fillers to enable them to chemically bond to the rubber molecule giving them a reinforcing property (Brydson, 1988).

How particulate fillers interact with an elastomer is dependent on a number of factors classified into the extensity, intensity and geometrical factors. The extensity factor relates to the amount of surface area or filler per cubed centimetre of compound. The intensity factor determines the specific activity of the filler surface per squared centimetre of interface. This is determined by the physical and chemical nature of the filler surface, and that of the elastomer being used. Geometrical factors that influence the fillers interaction are the structure of the filler (determined by its void volume), and the porosity of the filler. Out of these it is the surface area that is of most importance. Particle size and surface area vary significantly between fillers. Coarse inorganic fillers have a surface area of $1\text{m}^2/\text{g}$, whereas fine silicas are up to $400\text{m}^2/\text{g}$ and carbon blacks as high as $1000\text{m}^2/\text{g}$. The surface area of filler in contact with the elastomer not only depends upon the surface area per gram of filler but also on the amount of filler in the compound. In order to get sufficient reinforcement a particle should have a surface area of at least $6\text{m}^2/\text{g}$ within a rubber compound (Boonstra, 1982).

The physical adsorption properties of fillers tend to be more important than their chemical nature when looking at the effects the filler has on rubber composite properties. Carbon blacks with active adsorption sites rather than homogenous surfaces have been proven to give better reinforcing properties. It is unclear as to whether chemical bonds forming between the filler and the polymer increase the reinforcing properties of the filler, although increased bond formation does cause higher modulus of the compound (Boonstra, 1982). Coupling agents are often used with silicas in order to improve their reinforcing properties by forming bonds between the siloxyl group on the silica and with the rubber during vulcanisation. The specific surface activity of a filler can be difficult to measure, although it is clear that the chemical reactivity coupled with the surface area of the filler are the main factors responsible for the observed reinforcement.

The geometric structure of fillers determines the amount of voids that are likely to occur in the compound (Boonstra, 1982). This in turn relates to how much of the surface area of the filler is able to be in contact with the elastomer. Non-spherical particles have a packing within the compound that is less dense than spherical particles, and will leave a greater number of voids between particles. Inorganic and mineral fillers can have large differences in their geometry, depending upon how they form crystals. Particles are isometric when they are of equal size in all dimensions, such as spheres. Particles are more anisometric where one dimension is much smaller in relation to the other two dimensions, for example platelets. The most anisometric particles are where two dimensions are much smaller than the third, for example rods. In carbon blacks, increased anisometry results in decreased tensile strength, but a significant increase in abrasion resistance (Boonstra, 1982). Table 8.2 summarises work done by Horn (1969) cited by both Brydson (1988) and Horn (1982) which outlines the effect of on processing and vulcanisate properties, both in terms of size, relating to the above discussion on surface area of a filler, and in terms of increasing structure which is likely to also increase the anisometry of a filler.

Table 8.2: The Effect of Filler Particle Size and Structure on Rubber Properties (Horn, 1982)

Processing Property	Decreasing Particle Size	Increasing Structure
Loading capacity	Decreases	Decreases
Incorporation Time	Increases	Increases
Dispersability	Decreases	Increases
Viscosity	Increases	Increases
Scorch Time	Decreases	Decreases
Extrusion Shrinkage	Decreases	Decreases
Extrusion smoothness	Increases	Increases
Extrusion Rate	Decreases	Little
Vulcanisate Properties		
Rate of Cure	Decreases	Little
Tensile Strength	Increases	Decreases
Modulus	Increases to a maximum then decreases.	Increases
Hardness	Increases	Increases
Elongation	Decreases to a minimum then increases.	Decreases
Abrasion Resistance	Increases	Increases
Tear Resistance	Increases	Little
Flex resistance	Increases	Decreases
Heat Build up	Increases	Increases slightly

8.2.3.4 Softeners and Plasticisers

Plasticisers are used for the opposite effect of fillers, that is to soften the rubber. They may also reduce the cost and enhance the processing of the rubber. Plasticiser molecules work by pushing apart the rubber molecules causing a reduction in the glass transition temperature and melt viscosity of the uncured compound. The properties of the vulcanisate are also altered by adding plasticisers, causing a reduction in hardness. In order to work well as a plasticiser the following parameters should be met (Brydson, 1988):

1. The solubility parameter should be close to that of the polymer so that they are compatible;
2. The molecular weight of the plasticiser should be more than 300 to limit the volatility;
3. There should be interaction between the polymer and the plasticiser in order to avoid crystallisation of either one.

Plasticisers are often petroleum oil-based with molecules containing various ratios of unsaturated aromatic chains, saturated rings (naphthenic) and paraffinic side chains, Figure 8.4. Non-hydrocarbon materials are also often present in commercial oils where nitrogen, sulphur and oxygen can be present within the molecules.

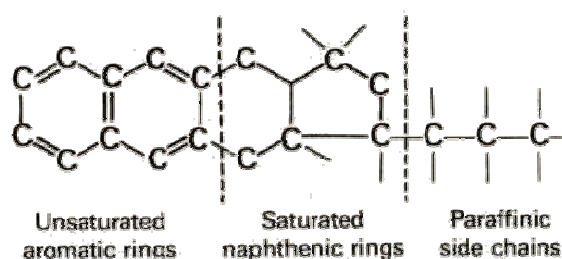


Figure 8.4: Molecular Structures in Plasticisers (Brydson, 1988)

The following factors should be taken into consideration when a hydrocarbon oil is selected as a plasticiser (Brydson, 1988):

1. The viscosity-gravity constant, which is a measure of the aromaticity of the molecule;
2. The oil viscosity, which depends on the structure and molecular weight;
3. The presence of nitrogen, oxygen or sulphur within the cyclic structure;
4. The oil loading required;
5. The price of the plasticiser.

Other than the price, these factors will affect both the processing of the compound and the properties of the resultant vulcanisate. Polar rubbers such as chloroprene rubber (CR) and nitrile butadiene rubber (NBR) are compatible with aromatic oils and rubbers that are more paraffinic such as ethylene propylene diene monomer (EPDM) and Isobutylene Isoprene Rubber (IIR) are compatible with paraffinic oils. An increase in the amount of plasticiser used will result in a reduced viscosity of the

rubber mix and therefore power consumption during mixing can be reduced. Addition of plasticisers also enables dispersion of other fillers as the shearing stress required can be reduced (Brydson, 1988).

In addition to oils esters and ethers can also be used as plasticisers (Brydson, 1988). These are used with NBR in particular, to lower the cold flex temperature. Ester and ether plasticisers can be further categorised into phosphates, phthalates, aliphatic esters, polyesters and polymerizable esters. Phosphates interact with the NBR and therefore do not have a great effect on lowering the cold flex temperature, alternatively phthalates and aliphatic esters are used which have a greater effect (Brydson, 1988). Phosphates tend to be used for their fire retardant properties.

8.2.3.5 Resins and process aids

Resins are used in rubber to aid in processing and function by having a lower viscosity than the rubber at processing temperatures. However at ambient temperatures they are harder than the rubber and act as a stiffening agent (Brydson, 1988) They can be classed into the following groups:

1. Phenolic resins;
2. Coumarone-indene resins;
3. High-styrene resins;
4. Cyclised rubber;
5. Coal tar pitch;
6. Petroleum pitches and petroleum resins;
7. Rosin related materials.

8.2.3.6 Speciality Additives

Other additives can be used in special occasions either to aid processing or to modify the vulcanisate properties (Brydson, 1988). They can be grouped according to their function as follows:

1. Abrasives;
2. Antistatic agents;
3. Blowing agents;
4. Colourants and white pigments;

5. Cork;
6. Electro-active materials such as magnetic powders and radiation absorbers;
7. Fire retardants;
8. Friction lubricants;
9. Glue;
10. Peptising agents (used to soften the rubber);
11. Re-odorants;
12. Tackifiers.

8.2.4 The Use of Textiles In rubber Technology

Textiles are commonly used to reinforce rubbers, providing additional strength to the rubber along the fibre direction, however limiting the extensibility. Products utilising textile reinforcement include tyres, hoses, and industrial belts (Redmond and Wood, 1982). Textiles can be used in fibre, yarn or fabric form, and properties of the final composite can be varied by choice of fibre, yarn twist and fabric construction. Common fibres used in rubber include rayon, nylon, polyester, steel, fibreglass and aramids (Redmond and Wood, 1982). Due to the one dimensional properties of fibres, (ie they have one dimension – length, that is substantially longer than the other 2 – height and width) and the 2-dimensional properties of fabrics (ie they have two dimensions – length and width, substantially longer than the third - height), appropriate textiles can be chosen to aid in the dimensional property requirements of the finished rubber product. In order for textiles to be successful in reinforcement of rubber products the following properties should be considered (Redmond and Wood, 1982):

1. Strength;
2. Dimensional Stability;
3. Flexibility;
4. Heat resistance;
5. Fatigue resistance;
6. Durability;
7. Temperature resistance.

8.2.5 Rubber Processing

In order to mix additives into the rubber it is necessary to soften the rubber. This is usually done by mechanical methods and through heat, however, peptisers can also be used (Crowther et al., 1982). Initially mills were used to process rubber and these have remained popular for laboratory use. Two roll mills consist of two rollers between which the rubber is passed through. The roll axes are horizontal and parallel to each other. It is possible to alter the distance between the rollers in order to change the work done on the rubber. The rollers can be powered using a double or single gearing system. Double gear mills have both rollers driven from a common backshaft, and were popular when steam engines were used to power them. Since the electric motors have become commonplace, single geared mills are now more widespread. Single geared mills have the back roll driven from the gearbox or backshaft and the front roll is powered from the back roll through roll end gears. Mills usually also contain a metal tray in order to collect droppings from the mill so that they can be reincorporated into the mix. They also contain guides to prevent the rubber being contaminated with grease from the gearing (Crowther et al., 1982).

In order to process rubber on a mill it is added to the top of the nip. A band of rubber comes through the nip and forms around the front roller. The ease of forming a band in this way varies according to the polymer used, varying the temperature and the nip size can aid in the band formation. Often the rubber band contains many holes initially, but with working of the rubber the band becomes smooth. The additives can then be put into the nip and any that fall out from the nip are returned to the nip until they are completely absorbed by the rubber (Crowther et al., 1982).

Internal mixers became more popular for mixing larger amounts of rubber and are more suitable for some types of synthetic rubber. Internal mixers are made up of two horizontal rotors containing protrusions, encased by a jacket, enabling work to be done on the rubber. There are different types of internal mixers; some incorporate a friction ratio into the rotor speeds, whilst others run at an even speed. The work on the rubber can either occur between the two rotors or between the rotors and the jacket. They also have a pneumatic ram to ensure that the rubber and powders maintain contact (Crowther et al., 1982). As the rubber compound is enclosed when mixed in

an internal mixer the time, power input and batch temperature are used to determine the end point of the mixing.

Once the rubber compound has been mixed there are a number of ways it can be shaped and processed further. It can be extruded using screw or ram technology to give a profiled strip of material. Alternatively it may be required to be calendered to produce a sheet. In order to otherwise shape the product moulding is used.

Moulding enables the rubber to be shaped and vulcanised at the same time by use of pressure and heat. Moulding can be done by compression, transfer or injection methods. These methods are discussed in section 7.2.

8.2.6 Applications of Rubber

The most widely produced rubber product is the tyre (Brydson, 1988). The design of the tyre is particularly important for steering control, stability and road holding and also affects fuel consumption (Blow, 1982). Transmission belting and conveyor belting are also applications of rubber of high importance. Rubber is also used in hosing in order to carry fluids and solids under a range of temperatures and pressures (Blow, 1982). In engineering applications rubber is often chosen for its flexibility, elasticity, and its impermeability to gases and liquids. It can therefore be used to isolate equipment from shock and vibration, as a seal, as a diaphragm to separate fluids yet transmit pressure differences and for rollers on machinery (Blow, 1982). Rubber is used in applications such as footwear, in which the waterproof and wear properties are utilised. On the other hand, sound absorbing and insensitivity to temperature properties allow it to be a good material for flooring (Blow, 1982). Uses of rubber are vast and wide and although plastics have replaced rubber in many products, as they are more easily processed and do not require a vulcanisation step, rubber still maintains its place as a key material in the design and engineering of many products (Brydson, 1988).

8.3 Recycling of fibrous waste in rubber

As landfill costs increase, waste products in manufacturing processes have become more costly to dispose of. Research has therefore been directed towards giving value to the generated wastes (Ferreira et al., 2011) (Rajaram et al., 2009) (Ali et al., 2011). Rubber technology repeatedly seems to provide an opportunity for such value added recycling to take place. This section focuses on how RFL fabric can be recycled and used as filler in rubber-based materials and the reinforcing properties it may offer. Similar work has been carried out on other fibrous material to assess how it behaves within rubber; the following section introduces some of this work.

8.3.1 Leather

Leather waste from shoe manufacturing processes has been demonstrated to be able to be recycled with rubber shoe soles, meeting the physical properties required for this application (Ferreira et al., 2010) (Ferreira et al., 2011). Within this research rubber compounds created from SBR and NBR with leather additions from 12.5 parts per hundred rubber (phr) to 300phr were tested for their rheometric and physical characteristics. Ferreira et al., (2010) found that increased amounts of leather fibres in SBR caused a decrease in the change of torque and an increase in the vulcanisation time during rheological experiments using a viscometer as the polymer is heated throughout the vulcanisation process. This suggested that the addition of leather fibres caused a decrease in the level of cross-linking and prohibited interaction between the vulcanisation additives and accelerator. In contrast when the leather fibres were added to NBR there was an increase in the change of torque and a decrease in the vulcanisation time, indicating that the leather fibres did not interact with the compound ingredients but promote the degree of cross-linking. Assessment of the physical properties of the rubber showed that the leather fibres caused an increase in the tear resistance properties up to an addition of 25phr. This was suggested to be due to the fibrous nature of the leather that prevents the growth of the specimen crack. Further addition of leather fibres caused a decrease in the tear resistance properties; although a sufficient level of tear strength was maintained for the rubber to be used for shoe components up to an addition of 100phr of leather waste. Addition of leather

fibres caused the tensile strength and elongation at break to decrease. However with adjustments to the vulcanisation system additives it was possible for the leather-rubber composites to have sufficient properties for use in shoe sole applications up to an addition of 20phr of leather fibres. The tensile strength was the limiting factor, rather than the elongation which was satisfactory until 50phr of leather fibres.

Further work by Ferreira et al (2011) repeated this work using an increased amount of finished tanned leathers to be more representative of the materials used in the footwear industry. In addition the effect of actual waste from both shoe upper roughing/carding leather waste and roughing sole waste and mixes of these was also analysed. These results agreed with previous work (Ferreira et al., 2010). Tear resistance saw an increase up to 25phr addition of leather fibres, whereas, tensile strength and elongation were shown to decrease. Incorporation of waste leather fibres, granules and dust was shown to increase the tear resistance to a maximum increase of 122% at 50phr in comparison to the control rubber sample that did not contain any recycled matter. Incorporation of more waste into the composite still showed a positive effect on the tear resistance in comparison to the control sample but to a lesser degree. Incorporating the sole waste alone also increased the tear resistance but to a lesser effect in comparison to the upper waste. Tensile strength and elongation at break increased with upper waste and sole waste to 20phr but further addition of waste caused a decrease in these properties. Incorporation of waste at this amount was proven meet standards for sole applications.

Similar work by Rajaram et al, (2009) characterise leather particulate-polymer composites from solid wastes produced in the leather manufacturing process such as chrome shavings and buffing dusts. Composites were made at 70:30, 60:40, 50:50 and 40:60 rubber to waste ratios and characterised for their strength, elongation, abrasion resistance, cyclic flexural endurance, hardness and density. Results showed that incorporation of the waste generally increased the composites physical properties. Abrasion resistance, hardness, and tensile strength were all found to increase with higher proportions of waste particulate. Flexural resistance was reduced but maintained at a satisfactory level even at the highest waste ratio. Elongation increased to a maximum at 60:40 polymer:leather ratio before reducing with further increase in waste in the composite. The study concludes that composites made from leather

wastes with NBR, SBR and neoprene provide good machinability and mechanical properties, and suggests that pre-treatment of leather waste could further enhance bonding between the polymer and the leather particles to increase flexural endurance and elongation properties.

8.3.2 Paper Fibres

Similar work has been completed with recycled newsprint paper waste. Nashar et al., (2004) studied the effects of newsprint fibre waste, both before and after treatment with sodium silicate and magnesium chloride, when used as fillers on the electrical and mechanical properties of natural rubber. Also the effect of newsprint paper waste used as filler in a butadiene acrylate copolymer (NBR), as an alternative to silica as a reinforcing material, was examined. Rubber compounds were made up using a vulcanisations system of sulphur, zinc oxide and stearic acid as activators, N-cyclohexyl-2-benzothiazole sulfenamide (CBS) as an accelerator. They found that increasing amounts of silica treated newsprint slightly decreased minimum torque values (M_L) in the vulcanisation process, whereas little change in minimum torque (M_L) was seen with increasing amounts of untreated newsprint waste. The equilibrium torque values (M_{HF}) increased with increasing filler content showing increased cross-linking density. The highest values were in untreated waste newsprint samples at 20phr. The optimum cure time, ie the time to reach a torque value of 90% of the equilibrium torque, defined by $T_c(90)$, generally decreased with increase of filler. The mechanical properties of the rubber compounds, including stress and yield, stress at rupture, strain at yield and strain at rupture, increased with the addition of filler content up to 20phr but decreased with further addition of filler. It was concluded that the optimum filler content was therefore 20phr. They also found that the adhesion system of silica treated waste was generally unnecessary for the newsprint fibres, only slightly improving the rheological properties. However, it did increase the maximum loading concentration to 40phr in the treated waste where the optimum mechanical properties were seen.

Further work has been carried out on newsprint fibres looking at fibres treated with polystyrene emulsion and used as a filler in styrene butadiene rubber (SBR) (Ali et al., 2011). The compounds were also irradiated and the mechanical and physical

properties of the rubber composites compared. Ali et al, (2011) found that mechanical properties such as tensile strength, elongation at break, stiffness and toughness were enhanced with both increased fibre content and increased radiation. Tensile strength was initially decreased with fibre loading with a minimum value at 7.5phr, further fibre loading increased the tensile strength to a maximum at 20phr. The stiffness and toughness of all the composites was increased with the maximum also occurring at 20phr.

8.4 Experimental

In order to assess the feasibility of using RFL coated waste fabric in rubber a range of rubber formulations were created using styrene butadiene rubber (SBR) and increasing the percentage of recycled material incorporated into the mix. Mixes were produced using both RFL coated nylon waste fabric and uncoated nylon waste fabric to assess how the RFL coating affects the reinforcing properties of the waste fabric when used as a filler. A control sample with no filler was also produced. The rheology of the rubber mix was investigated using an oscillating disk rheometer to assess the effect the recycled fibre content on the curing of the rubber compound. Vulcanised rubber sheets were then manufactured from the rubber mixes using a fixed cure time and the tensile and tear properties of the rubber vulcanite were established.

8.4.1 Materials

A mixture of waste fabric was provided by Heathcoat Textiles. The waste fabrics were primarily false selvedge offcuts from the weaving stage and faulty fabric offcuts from inspection and consisted of 100% nylon 6.6 fabrics of varied specifications. Waste fabrics were separated into RFL coated and uncoated forms for further processing. As described in section 4.3.1, all waste used throughout this study was from one batch of waste sent from Heathcoat Fabrics. Although specifications of all fabrics included in this waste is not possible, the raw material used within this study has remained as constant as possible given that it is a waste product that is being dealt with.

The fabrics were reduced using the beating process, utilising the Hollander beater reduction process, as described in section 4.3.2.2. A beating procedure based on the previous trial using 3.5 kg of fibre with 350 l of water with an extended total time of 90 minutes was used, adjusting the beater roll as described in Table 8.3. This reduction method was chosen as it was able to produce fine fibres by beating at the datum (D) or biting point of the Hollander beater, whilst maintaining polymer quality due to the cooling effect of the water during beating, as described in section 4.5.3.2. Smaller fibres enable better reinforcement due to the high surface area to weight ratio as described in section 8.2.3.3.

Table 8.3: Beating Cycle to Produce Recycled Filler

Time (minutes)	Beater Roll Setting	Comments
0	4TU	Fabric added to beater
	4TU	All fabric incorporated. Time started.
15	1TU	Beater roll lowered
30	D	Beater roll lowered
50	1TD	Beater roll lowered
90	1TD	Beating stopped

The produced slurry was filtered using a sieve lined with a muslin cloth to separate the fibres from the water. The fibres were left to air dry. This procedure was completed with both the coated and the uncoated waste fabric to produce a dust-like particulate to be used in the rubber mixes as seen in Figure 8.5.



Figure 8.5: Uncoated (left) and Coated (right) Beaten Waste Fabric used in Rubber Processing

Rubber formulations were prepared using styrene butadiene rubber (SBR), trade name Cariflex S 1502. The numerical suffix represents the grade of rubber with 1502 containing a non-coloured antioxidant as oppose to 1500 which contained a coloured antioxidant. A conventional sulphur vulcanisation system was used with zinc oxide, and stearic acid as activators and N-cyclohexyl-2-benzothiazole sulphonamide (CBS) as an accelerator.

8.4.2 Preparation of Rubber Formulations

Six rubber mixes were produced, increasing the fibre percentage from 12.5% to 37.5% using pure nylon waste and RFL coated waste. In addition a rubber mix using no filler was also made. Table 8.4 summarises the rubber mix batches that were produced and Tables 8.5-8.8 outline the formulations required to produce them. The rubber mixes were produced using a laboratory size, open, two roll mill, serial number M-0315, using the British Standard BS ISO 2393:2008, *Rubber test mixes – Preparation, mixing and vulcanisation – Equipment and procedures*, as a guide. The SBR rubber was first heated in an oven to 50°C to soften the rubber as the roll mill was unable to be heated. The SBR was then passed through the roll mill until a rubber band was formed on the front roll. The waste fabric filler was then added to the mix

and cuts were made across $\frac{3}{4}$ of the width of the rubber band from both directions, and the resultant flap folded over as a mixing technique, to incorporate the fibres into the rubber. Cuts were made approximately every alternate revolution of the mill roll. The zinc oxide, stearic acid and CBS were then added to the mix, for detailed compositions see Table 8.5-8.8. Cuts $\frac{3}{4}$ across the width of the rubber band were continued to mix the additives into the batch. Finally the sulphur was incorporated into the mix in the same way.

Where mixing of the formulations proved difficult, as discussed in section 8.5.1 lengths of the mix were removed from the roll and the additives were added to the top of the batch and the rubber mix folded over to sandwich the additives within. The batch was then passed through the roll mill and folded again. This procedure repeated until it was visually confirmed that the additives had been uniformly incorporated into the batch. Additives were added in the same order as previously mentioned also using this alternative method.

Due to the differences in behaviour of the mixes, the time to prepare the mixed varied between batch formulations. Also the nip pressure and roller speed were varied to achieve optimum behaviour of the rubber mix on the roll. The compounds were considered mixed into the rubber when no powder was observed on the rubber surface.

Table 8.4: Rubber Mixes Produced

Filler %	Filler (pph)	RFL Coated/Uncoated	Table Formulation
0	0	N/A	3.3
12.5	15.6	Uncoated	3.4
12.5	15.6	RFL Coated	3.4
25	36.3	Uncoated	3.5
25	36.3	RFL Coated	3.5
37.5	65.5	Uncoated	3.6
37.5	65.5	RFL Coated	3.6

Table 8.5: 0% Filler Formulation

Compound	Parts per 100 rubber (PHR)	Weight (g)
SBR	100	137.61
Recyclate	0	0
Zinc Oxide	5	6.88
Stearic Acid	1	1.38
CBS	1	1.38
Sulphur	2	2.75
Total		150

Table 8.6: 12.5% Filler Formulation

Compound	Parts per 100 Rubber (PHR)	Weight (g)
SBR	100	120.40
Recyclate	15.6	18.77
Zinc Oxide	5	6.02
Stearic Acid	1	1.20
CBS	1	1.20
Sulphur	2	2.41
Total		150

Table 8.7: 25% Filler Formulation

Compound	Parts per 100 Rubber (PHR)	Weight (g)
SBR	100	103.22
Recyclate	36.3	37.50
Zinc Oxide	5	5.16
Stearic Acid	1	1.03
CBS	1	1.03
Sulphur	2	2.06
Total		150

Table 8.8: 37.5% Filler Formulation

Compound	Parts per 100 Rubber (PHR)	Weight (g)
SBR	100	86.01
Recyclate	65.5	56.25
Zinc Oxide	5	4.30
Stearic Acid	1	0.86
CBS	1	0.86
Sulphur	2	1.72
Total		150

8.4.3 Cure Characterisation

Tests were carried out on the rubber mixes to assess the effect of increased fibre content, and the RFL, on the cure characteristics of the rubber. British standard ISO 6502:1999(E), *Physical testing of rubber – Part A60.1 Cure metering – Guide to the use of curemeters*, was followed to complete these tests. A Monsanto rheometer 100 was used alongside a data plotter to record the results. The Monsanto rheometer 100 is an oscillating disk rheometer and is set up as shown in Figure 8.6 in order to measure the torque of the rubber as it vulcanises with time at a set temperature. The polymer was placed within the vulcanisation chamber which was set to a temperature of 160°C and a pressure of 4136kPa. The disk was then oscillated through an arc of 3° by a motor operating at 100 rpm. The torque required to produce this oscillation was measured and recorded. The torque is proportional to the stiffness of the polymer specimen being tested, which increases as cross-links within the rubber are formed, and hence information on the vulcanisation characteristics of the specimen can be established.

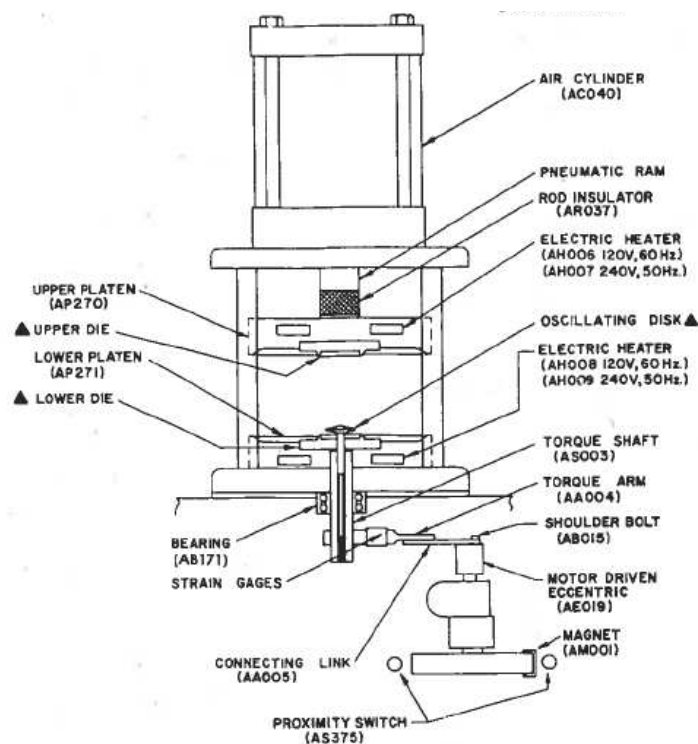


Figure 8.6: The Monsanto Rheometer 100 (Monsanto)

8.4.4 Vulcanisation Procedure

The rubber mixes were vulcanised to produce test sheets for physical testing of tensile and tear properties. BS ISO 2393:2008 was again used as a guide for this procedure. A mould of 155 x 155 x 3 mm was used, which was heated to 160°C using a press. Once the moulds had reached the required temperature, 60 g of the rubber mix was inserted into the mould and mould returned to the press. A pressure of 10 tonnes/10cm diameter (equivalent to 123 bar) was then applied to the mould using a Tangyes Ltd Two speed Hydra-pak hand pump. A vulcanisation time of 30 minutes was used for each rubber mix. The rubber composites were then removed from the mould at left to cool at room temperature.

8.4.5 Physical Test Methods - Tensile Properties.

British Standard BS ISO 37:2005, *Rubber, vulcanized or thermoplastic – Determination of tensile stress-strain properties*, was used to test the vulcanized specimens to find the effect the filler content and RFL has on the tensile properties of the rubber. Dumb-bell test pieces, 115 mm in length and 25 mm wide were cut using a

die and cutter to produce samples with a test length of 33 mm and width of 6 mm. A Hounsfield tensile tester and Hounsfield 100R extensometer were used alongside a PL4 recorder from JJ instruments to test the samples, using a 500 N load cell and a gauge separation of 20 mm. The samples were extended at a constant rate of 200 mm/min and the load recorded. Three test pieces were tested for each sample.

8.4.6 Physical test methods - Resistance to Tearing.

British Standard BS ISO 34-1:2010, *Rubber, vulcanized or thermoplastic – Determination of tear strength, method B, procedure (b): Using an angle test piece with a nick*, was used to test the vulcanized sheets for tear strength. Angle test pieces were cut using a die and cutter, and tested using a Zwick Z050 tensile tester using a constant extension rate of 500 mm/min and a gauge separation of 60 mm. As nicks were used in the specimen this test only provides information on tear propagation rather than initiation. Four test pieces for each sample were tested.

8.5 Results and Discussion

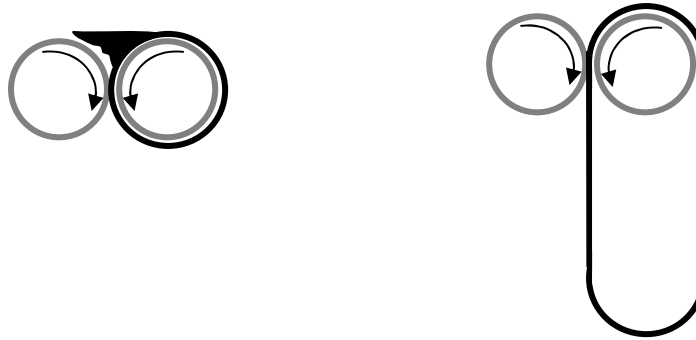
8.5.1 Preparation of Specimen

For good rubber processing the rubber should form a tight band on the front roll of the mill, excess rubber should be accumulate at the nip of the rollers where it is constantly worked and manipulated. This arrangement is illustrated in Figure 8.7a. This formation of the rubber band allows the additives to be mixed into the rubber using the $\frac{3}{4}$ cut and fold method stated in British Standard BS ISO 2393:2008.

The SBR rubber proved difficult to work with initially. This was due to its inability to break down upon kneading and working of the rubber. This is one of the main differences between SBR rubber and natural rubber and as a result it is necessary to increase the rubber's viscosity to provide good dispersion of particles and ease of flow during processing (Brydson, 1988). As the mill used did not have the capabilities to heat the rubber, the rubber took longer to plasticise, even with prior heating using an oven. As a result it tended to break up into lumps rather than form a band on the

roll. When a band formed it often contained many holes initially but as the rubber was worked further this smoothed out. This processing problem would have been eased by utilising a roll mill that has capabilities to heat the rolls to 50°C and a thermostat to regulate and control the temperature.

Once the band had been formed on the front roll, processing became easier, and the rubber was able to be manipulated more easily. For the sample containing no filler, the additives were able to be added and mixed into the rubber at this stage and were dispersed throughout the rubber. For samples containing the recycled fillers, further difficulties arose as the filler amount increased. The recycled filler was added to the rubber after a band had been formed on the front roll but before the vulcanisation system additives were added. For samples containing 12.5% of filler materials, the recycle was able to be added to the rubber fairly easily. The rubber band was maintained on the front roll facilitating the $\frac{3}{4}$ cutting of the rubber and in turn the dispersion of the filler and vulcanising additives. However, increased filler caused the rubber to become less tacky and instead of maintaining a band on the roll, the band length increased and formed a loop as shown in Figure 8.7b. This in turn caused problems in cutting and mixing of the rubber as the rubber tended to move and buckle on the roll due to the cutting force used. As the cut folded edge passed through the nip point of the rollers, rather than reforming into the band and the rubber dispersing across the working width of the mill, the band width became uneven and the band was more likely to break. Static electricity also became a problem as the rubber band slipped on the rollers.



a. Ideal mixing rubber behaviour – tight rubber band formed on front roll and excess rubber material at nip.

b. Problematic rubber behaviour - rubber band loosens on front roll, no excess rubber material and nip. Material is able to slip causing cutting problems and static charge.

Figure 8.7: Rubber Behaviour During Milling

Brydson (1988) explains how this behaviour is due to the molecular weight distribution of the rubber material. Low molecular weight molecules prevent tearing by allowing a viscous flow, whereas high molecular weight molecules provide elastic strength. By having a broad molecular weight distribution, both these attributes can be maintained, improving the milling behaviour. It would seem that the addition of the recycled filler causes the viscous flow to be reduced and hence excess rubber is not maintained at the nip and instead it is passed through the nip of the rollers and causes the rubber band to increase in length. The processing of rubber with this recycled filler could therefore be improved by using an SBR rubber with a higher proportion of low molecular weight molecules. Brydson (1988) also suggests that better processing during milling can be obtained in the following ways:

1. by incorporating vinyl groups to the chain ($-\text{CH}=\text{CH}_2$);
2. by broadening the molecular weight distribution;
3. by using long chain branching;
4. by increasing the styrene content (C_8H_8);
5. by blending the high molecular weight polymer with oil.

Due to these processing problems the method for mixing the filler and additives into the SBR rubber was altered as discussed in section 8.4.2. By using this method for the 25% uncoated filler and 37.5% filler samples all the rubber mixes were able to be

formulated successfully. Figure 8.8 and 8.9 show the final rubber mix samples prior to vulcanisation.

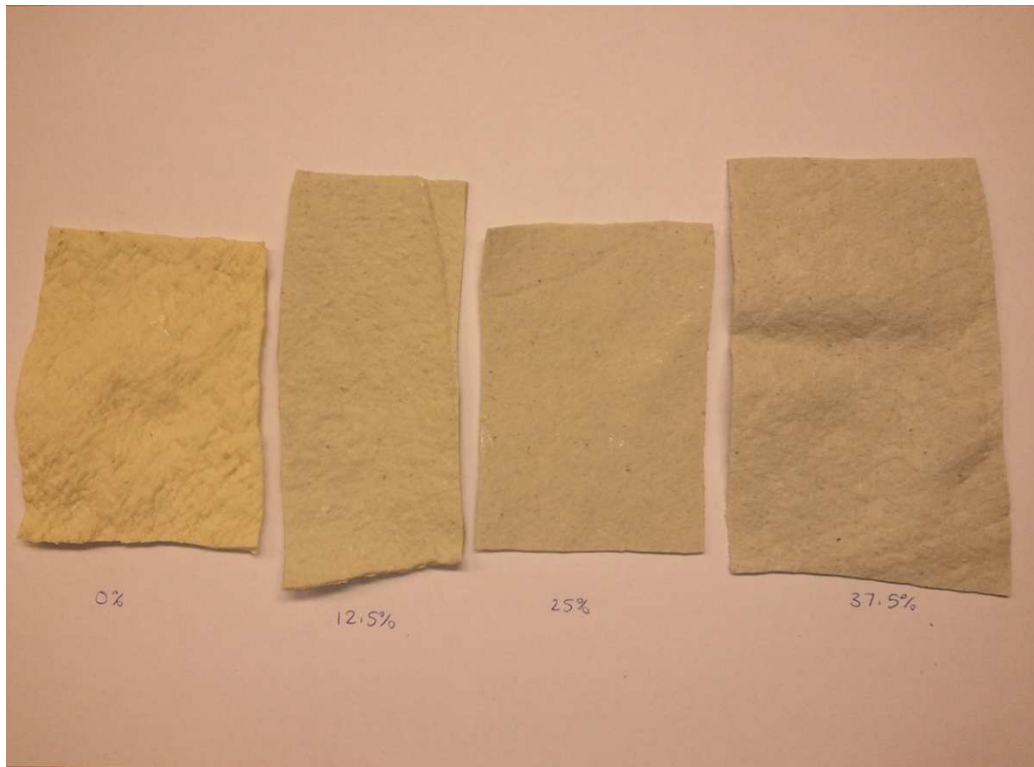


Figure 8.8: Rubber Mixes Incorporating the Uncoated Waste Reduced using the Hollander Beater.

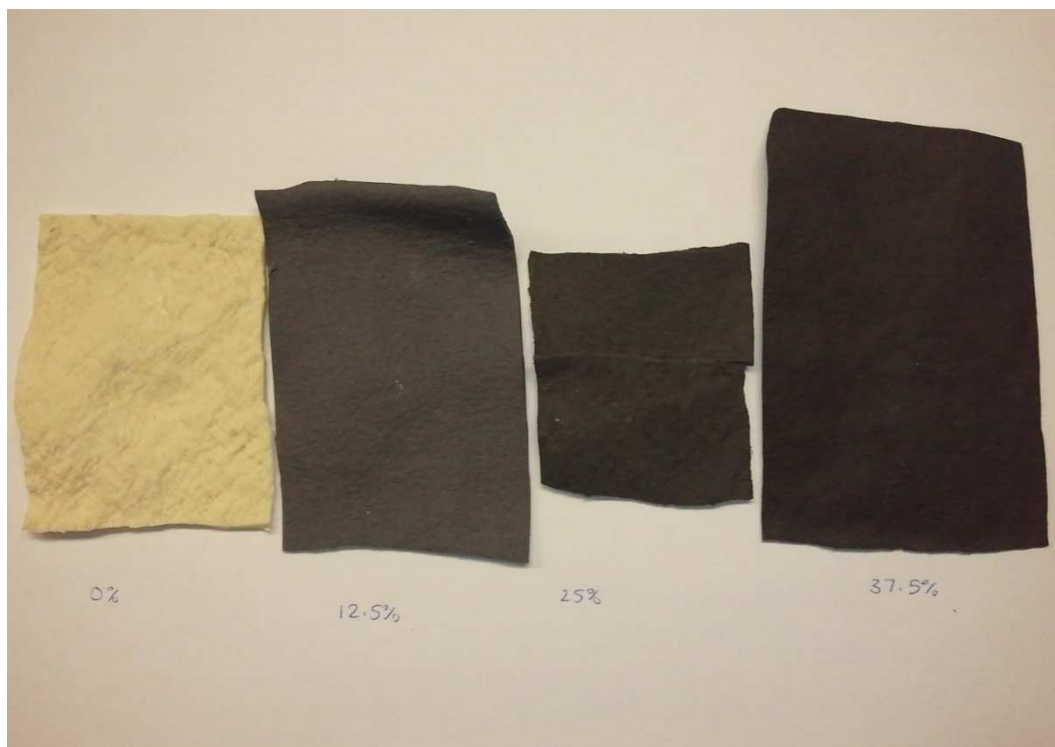


Figure 8.9: Rubber Mixes Incorporating the RFL Coated Waste Reduced using the Hollander Beater.

8.5.2 Cure Profile

A cure trace of a polymer depicts its stiffness against time during the vulcanisation process and can be broken down into the following features (Monsanto):

1. Initially the stiffness reduces as the polymer softens due to the increased temperature;
2. A time of delay, before the stiffness rises due to increased cross-links being formed;
3. Levelling of the stiffness as the optimum cure time is reached. In some instances the torque does not level but continues to rise, this is known as a marching modulus. (Brydson, 1988).

The following measurements are used to compare rubber cure traces:

1. The minimum torque, M_L ;
2. The time to cure onset or scorch time, $t_s(x)$ (where x is a defined amount of increase above M_L . $x = 5\%$ in below calculations);
3. The cure time to (x) percent of full cure development - $t_c(x)$ (usually $x = 90\%$);
4. The equilibrium torque - M_{HF} ;
5. The cure rate index, calculated using equation 8.1. This gives an approximate rate of cure, proportional to the average slope of the cure rate curve in the steep region. (Monsanto)

$$\text{Cure Rate Index} = \frac{100}{t_c(x) - t_s(x)} \quad (\text{equation 8.1})$$

Where $t_c(x)$ = cure time to $x\%$ of full cure development ($x=90$ is conventionally used)
and $t_s(x)$ = onset of cure/scorch time at $x\%$ above M_L ($x=5$ is conventionally used)

Figure 8.10 shows a typical equilibrium curve with these measurements indicated.

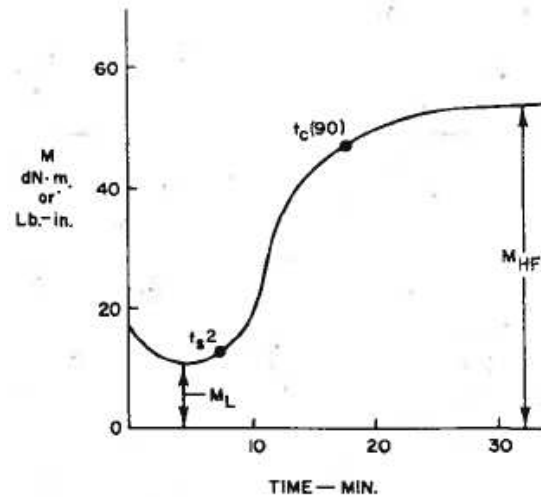


Figure 8.10: Typical Cure Trace (Monsanto)

Both the amount of filler added to the rubber, and whether the filler consisted of the RFL coated matter or the uncoated matter, had an effect on the vulcanisation properties of the rubber. Figure 8.12 shows the full cure traces for each of the mixes produced, and Tables 8.9 and 8.10 summarise these results using the terms mentioned above. Generally the increase in filler used causes the mix to cure at a faster rate ($t_c(90)$ decreases) and reach an increased level of stiffness (M_{HF} increases). The RFL within the filler also causes further increase in stiffness (M_{HF}) and although the rate of cure is similar the curve shifts to a lower temperature. These trends can be seen in Figures 8.13 to 8.15.

The rheometric curves produced all plateau on reaching the maximum torque. This is an indication of the stability of the material and the cross-links that have been formed during the vulcanisation. The vulcanisation of the test sheets was carried out for 30 minutes. From Figure 8.11 it can be seen that this vulcanisation time of 30 minutes used to produce the rubber sheets for testing the compounds physical properties will be fully vulcanised, yet it will not have caused any degradation to the rubber sheet by due to the heating over a lengthened time, as no reversion is identified on the curve.

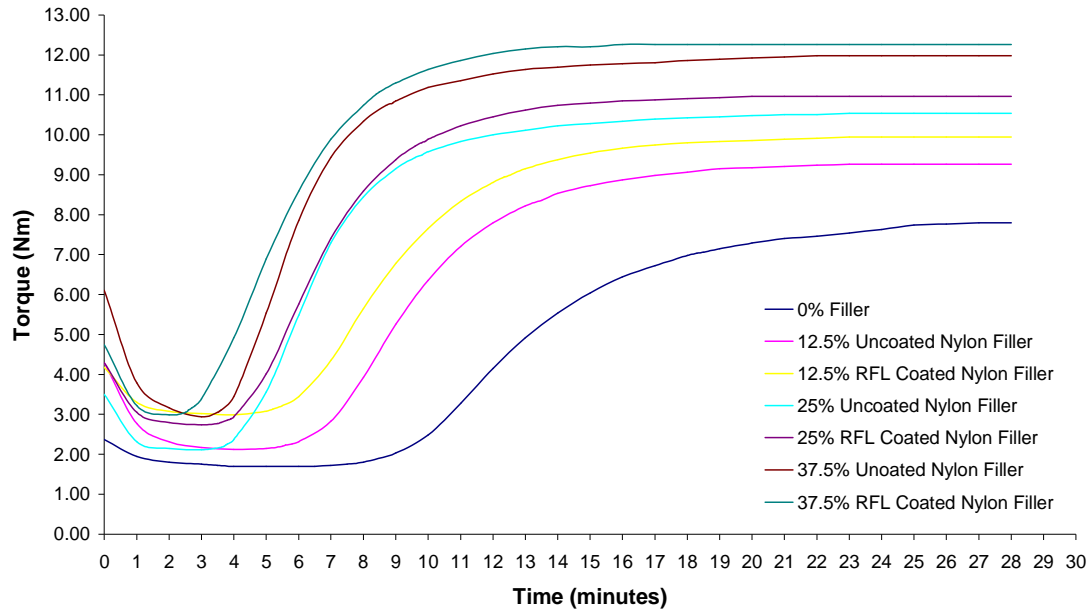


Figure 8.11: The Effect of Filler Percentage and RFL Content on Rubber Cure Time

Table 8.9: Summary of Cure in Uncoated Nylon Filler

Sample	M_L (Nm)	$t_s(5)$ (min)	$t_c(90)$ (min)	M_{HF} (Nm)	Cure Rate Index
0% Filler	1.70	7.5	18.3	7.8	9.26
12.5% Uncoated	2.12	5.6	13.5	9.27	12.66
25% Uncoated	2.12	3.75	9.8	10.54	16.53
37.5% Uncoated	2.94	3.6	8.9	11.98	18.87

Table 8.10: Summary of Cure in RFL Coated Nylon Filler

Sample	M_L (Nm)	$t_s(5)$ (min)	$t_c(90)$ (min)	M_{HF} (Nm)	Cure Rate Index
0% Filler	1.70	7.5	18.3	7.8	9.26
12.5% RFL coated	2.99	5.2	12.4	9.94	13.89
25% RFL coated	2.74	3.9	10.0	10.96	16.53
37.5% RFL coated	2.99	2.7	8.4	12.26	17.54

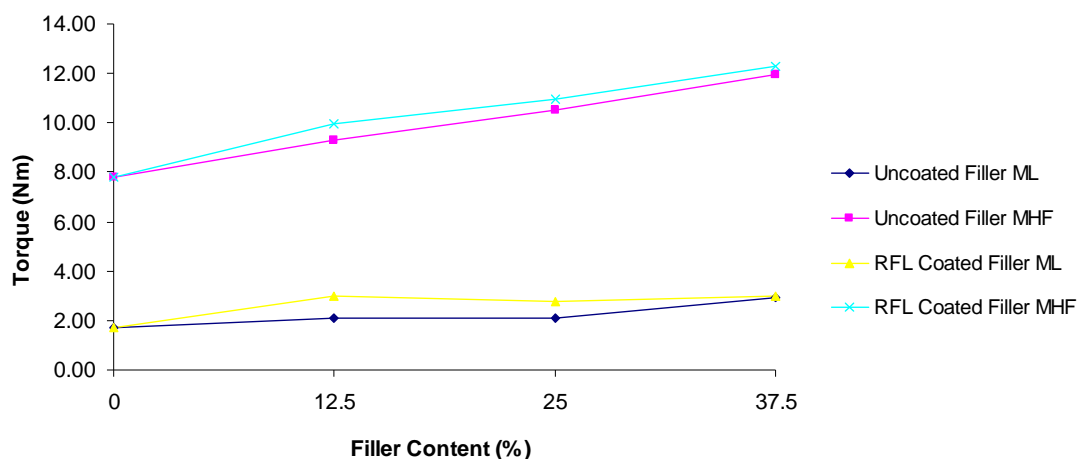


Figure 8.12: The Effect of Filler on Minimum (M_L) and Maximum (M_{HF}) Torque

The minimum torque (M_L) relates to the viscosity of the mix, and how malleable the rubber will be. The added filler has not had a dramatic effect on this property (Figure 8.12), suggesting that it should be able to be processed in a similar way to the SBR rubber with no filler. The scorch time, which decreases with increased filler quantity (Figure 8.14), also relates to the processability. This implies that the rubber with the recycle as filler would reach its flow state quicker than rubber with no filler and therefore be able to be processed and moulded in a shorter period of time.

The maximum torque (M_{HF}) is an indication of the number of cross-links that are formed in the compound. The M_{HF} increased in both the RFL and uncoated recycle compounds with increased filler loading, with the RFL filler showing slightly higher stiffness than the uncoated filler (Figure 8.12). This suggests that the RFL coating on the nylon aids in the cross-link formation, presumably due to the surface chemistry of the polymer and the RFL coating, which is designed for adhesion to rubber and therefore a higher number of crosslinks are formed. However, the increase of the filler loading used has a more dramatic effect on the cross-link formation. The vulcanisation time ($T_c(90)$) is also decreased (Figure 8.13), this shows that the filler does not prohibit the interaction between the sulphur and the accelerator within the vulcanisation system but instead, that the presence of the recycle as a filler aids in the interaction of reagents utilised in the vulcanisation reaction.

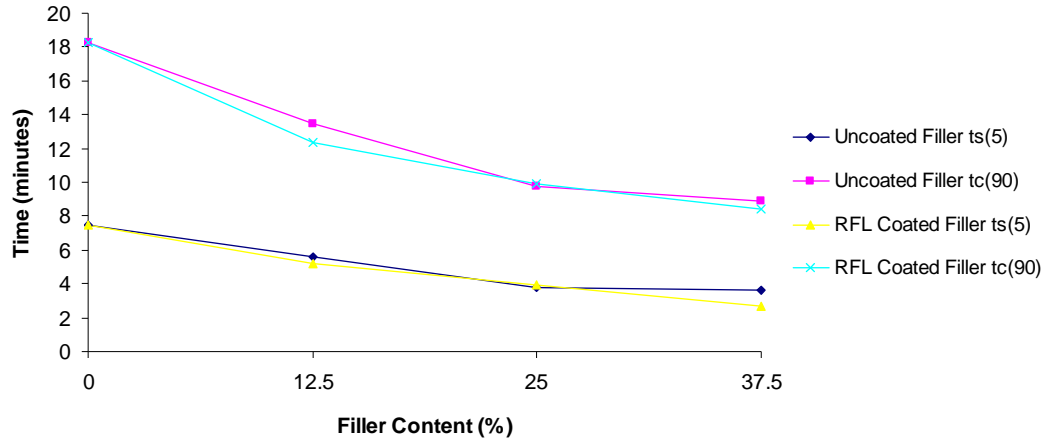


Figure 8.13: The Effect of Filler on Scorch Time ($t_s(5)$) and Cure Time ($t_c(90)$)

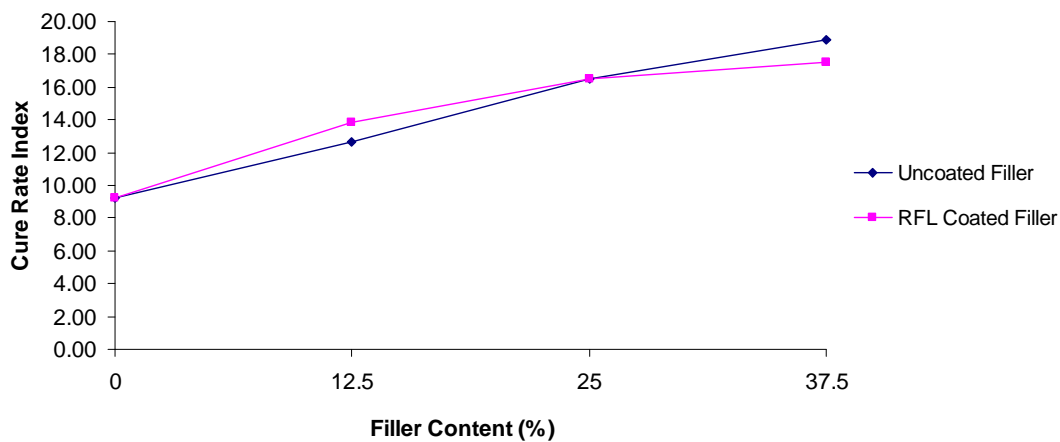


Figure 8.14: The Effect of Filler on Cure Rate Index

Literature suggests that the cure time can be related to the pH of the filler, with more acidic fillers causing the reaction time to be reduced (Boonstra, 1982). Results show that the RFL coated filler has a slightly lower cure time than the uncoated filler as seen in Figure 8.14. This could be due to the above reason; however the difference seen here is thought to be insignificant and more likely due to slight differences in filler amount and distribution occurring at the mixing stage. The surface chemistry of the filler plays an important role in the initial reaction prior to the cross-linking taking place. In order to evaluate a filler's potential to be used as a reinforcement filler the M_{HF} value is examined to assess the increase in maximum torque during vulcanisation as the filler loading is increased. The relative increase in M_{HF} (α) can be calculated using equation 8.2.

$$\alpha = \frac{M_{HF(X)} - M_{HF(0)}}{M_{HF(0)}} \quad (\text{equation 8.2})$$

Where: α = the relative increase in M_{HF} ,

$M_{HF(x)}$ = M_{HF} value of rubber with x% filler,

$M_{HF(0)}$ = M_{HF} value of rubber with no filler.

By plotting the α values for a number of filler content percentages, a straight line is formed, with the gradient (α_F) characterising the reinforcing property of the filler. Table 8.11 and Figure 8.15 depict this property. An increased gradient value or reinforcement factor (α_F) suggests a better reinforcing structure has been produced. This calculation confirms the reinforcing effect of the RFL coated filler, in comparison to the uncoated nylon filler. However, the additional reinforcement the coating provides is only slight, having a reinforcement factor of 0.016 over the uncoated nylon filler, which is 0.014.

Table 8.11: Reinforcement Factor

Sample	M_{HF} (Nm)	Relative increase in M_{HF} - α
0% Filler	7.8	0.00
12.5% Uncoated	9.27	0.19
25% Uncoated	10.54	0.35
37.5% Uncoated	11.98	0.54
12.5% RFL coated	9.94	0.27
25% RFL coated	10.96	0.41
37.5% RFL coated	12.26	0.57

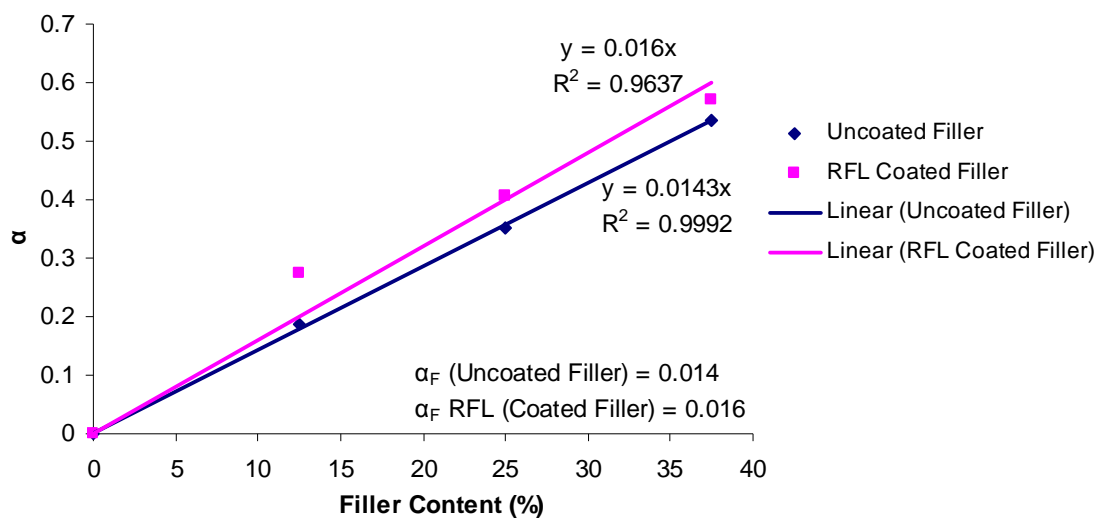


Figure 8.15: The Effect of RFL on Filler on Reinforcing Factor (α_F)

8.5.3 Curing of Rubber Sheets

The rubber sheets were all able to be vulcanised, using a cure time of 30 minutes. Figure 8.16 depicts the moulded sheets formed. On removing of some rubber sheets from the mould, it was evident that the filler in some samples had not been dispersed as well as had originally been anticipated from the mixing stage. There were defects in some of the sheets that manifested as fibrous dry patches near to the edge of the rubber sheet. These were present on both sides of the sheet suggesting the defect was throughout the entire thickness of the sheet. This problem was only evident in the uncoated samples and was most prominent on the 25% sample, not as may be expected on the 37.5% sample. This suggests the problem was due to the mixing process rather than the amount of filler incorporated into the rubber as an increased amount of filler was able to be incorporated into the rubber sheet with better results. This is likely to be due to the mixing, where a heated mill was unable to be used and subsequent problems occurred when the recycled material was added as filler as explained in section 8.5.1. Figure 8.17 shows the defects present on the 25% uncoated filler sample. Poor dispersion can have knock-on effects regarding the compound's properties such as tensile strength, and elongation.



a. 0% Filler



b. 12.5% Uncoated

c. 25% Uncoated

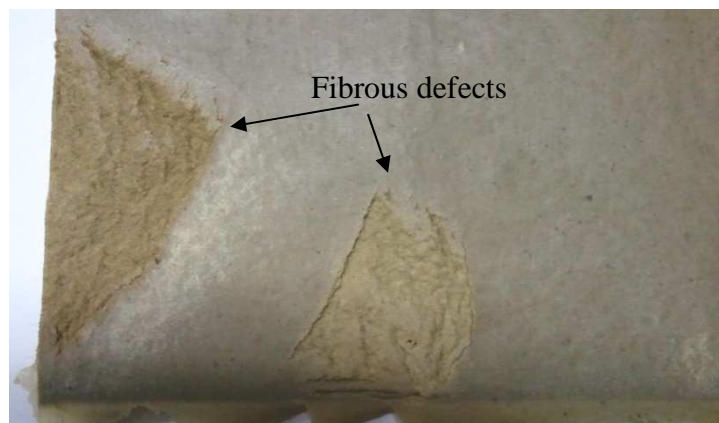
d. 37.5% Uncoated



e. 12.5% RFL

f. 25% RFL

g. 37.5% RFL

Figure 8.16: Vulcanised Moulded Rubber Sheets.**Figure 8.17: Defects in 25% Non-Coated Rubber Sheet.**

8.5.4 Tensile Properties.

Fillers are used in the rubber industry in order to increase the strength of synthetic rubbers. In order to get maximum strength and reinforcement within a synthetic rubber it is necessary that fine particulate is used and is dispersed well throughout the rubber. Carbon blacks and reinforcing silicas are generally used in the highest strength rubbers and can produce strengths in the region of 18-23 MPa (Jacques, 1982) at a 50 pph filler formulation.

From the results shown in Table 8.12 and Figure 8.18 it can be seen that the increasing the amount of RFL coated filler used in the compound has caused the tensile strength to increase to 3.97 MPa, for the 37.5% filler compound (equating to 65.5 pph). In comparison the uncoated nylon filler enabled the strength of the compound to increase, reaching its optimum strength of 3.01 MPa in the 25% filler (36.6 pph) compound. Further addition of the uncoated fibre caused the strength of the compound to drop. This shows that the RFL filler is more effective at reinforcing the rubber at higher loading levels. These results are not comprehensive enough to show whether the strength of the RFL coated filler compound has been fully optimised using this loading of filler or if increasing the filler further would increase the strength. However, as the increase in strength is at a plateau, it suggests that much higher tensile strength would be difficult to achieve.

Table 8.12: Tensile Strength of Rubber Sheets

Sample	Average Thickness (mm)	Width (mm)	n	Extension at Break (%)	Force at break (N)	Tensile Strength at Break (Mpa)
0% Filler	2.40	6.00	1	94	22.34	1.55
			2	80	20.78	1.44
			3	112	25.45	1.77
			Average	95.33	22.86	1.59
			SD	16.04	2.38	0.17
			Variance	16.83	10.41	10.41
12.5% Uncoated	2.79	6.00	1	165	36.62	2.19
			2	141	36.88	2.20
			3	128	37.14	2.22
			Average	144.67	36.88	2.20
			SD	18.77	0.26	0.02
			Variance	12.98	0.70	0.70
25% Uncoated	2.53	6.00	1	49.5	44.39	2.92
			2	40.5	48.47	3.19
			3	42	44.39	2.92
			Average	44.00	45.75	3.01
			SD	4.82	2.36	0.16
			Variance	10.96	5.15	5.15
37.5% Uncoated	3.08	6.00	1	15.5	34.29	1.85
			2	18.5	28.57	1.54
			3	32.5	34.29	1.85
			Average	22.17	32.38	1.75
			SD	9.07	3.30	0.18
			Variance	40.93	10.19	10.19
12.5% RFL	2.69	6.00	1	148	43.90	2.72
			2	90	45.45	2.82
			3	135	41.82	2.59
			Average	124.33	43.72	2.71
			SD	30.44	1.82	0.11
			Variance	24.48	4.17	4.17
25% RFL	2.66	6.00	1	55	58.16	3.65
			2	40.5	72.96	4.58
			3	71	56.12	3.52
			Average	55.50	62.41	3.92
			SD	15.26	9.19	0.58
			Variance	27.49	14.72	14.72
37.5% RFL	3.00	6.00	1	13	66.33	3.68
			2	13.6	79.59	4.42
			3	30.8	68.37	3.80
			Average	19.13	71.43	3.97
			SD	10.11	7.14	0.40
			Variance	52.83	10.00	10.00

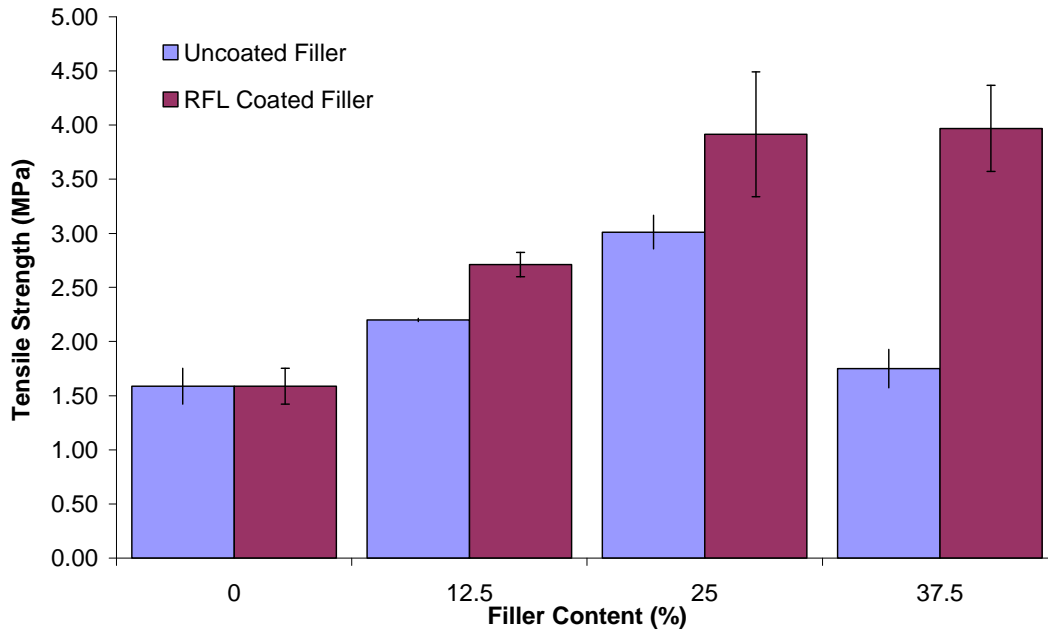


Figure 8.18: The Effect of Recycled Filler Content on Tensile Strength of Rubber Compounds.

The RFL coated fibres were able to enhance rubber strength at high loading capacities in comparison to the uncoated fibres. This is therefore an opportunity to add value to the waste produce and enable higher volumes of the waste to be dealt with. The reason for the RFL coated filler producing increased strength at higher loading in comparison to the uncoated fibres which cause a drop in tensile strength at high loadings could be due to a number of factors particularly due to failure to disperse the uncoated filler throughout the mix as discussed in section 8.3.3. However, there is no explanation for why the RFL coated fibres would disperse better the uncoated fibres in general, and a decrease is also seen in tensile strength at a 37.5% filler content which looked to have better dispersed filler.

The rheological results discussed in section 8.3.2 would suggest that the uncoated filler compounds should continue to increase in tensile strength at higher loadings as the vulcanisate became stiffer as shown by the increase in M_{HF} signifying an increased amount of cross-links had been formed. These cross-links should translate to increased strength.

The main factors responsible for reinforcement are the surface area of the filler and the chemical reactivity (Boonstra, 1982). The RFL coated filler and the uncoated filler

are likely to have a similar particle size as shown in the results in section 4.3.4.2 Figure 4.9. A difference in particle size would explain the reduced tensile strength seen in the 37.5% loaded rubber sheet. Decreased particle size will result in an increased surface area per gram of filler. This enables the rubber to form more cross-links with the particles and increase in strength. In order for a particle to provide reinforcement it is required to have a surface area of $6\text{m}^2/\text{g}$ (Boonstra, 1982). Since the Hollander beater produced similar sized fibre length in the reduction of the RFL coated fabric and the surface area of the filler used was not determined.

The increased surface activity of the RFL coated fibres in comparison to the uncoated fibres is a likely reasoning for increased strength at higher filler loading capacity. The RFL coating is designed to increase the reactivity of the nylon to rubber. The latex within the coating contains high numbers of unsaturated carbon-carbon bonds which increase the surface reactivity of the filler (Durairaj, 2005). In comparison the nylon is only able to bond through hydrogen bonding or through the amide group, hence there are fewer reactive sites. As the beating process does little to remove the coating it is likely that the particles have been able to bond with the rubber to form stronger cross-links than the uncoated nylon is able to achieve.

In addition to the specific surface activity the geometric structure of the fillers will also determine the reactivity seen (Boonstra, 1982). The geometric structure determines the amount of voids that are likely to occur in the compound. Larger particles are harder to disperse into the matrix and hence are more likely to cause voids in the compound, decreasing the strength. This may have occurred in the 37.5% uncoated filler compound. The rod-like shape of the fibres will increase the likelihood of voids forming due to the anisometry of the filler, which causes packing to be less dense. The amount of the surface area of the filler that is in contact with the elastomer is therefore reduced, decreasing the amount of bonds that can be formed. The RFL coated and uncoated fibres were reduced to a similar length, however, since the coating was unable to be removed, and the RFL fibres often remained bonded together due to the coating it is likely that the RFL reduced by the Hollander beater could have been more spherical in shape than the uncoated Hollander beater reduced waste, enhancing the bonding capabilities further.

Although both the coated and uncoated fillers serve initially to increase the tensile strength of the SBR rubber, the strength that is achieved is much lower than what could be achieved from carbon black or silica, which is as much as 18-23 MPa (Jacques, 1982). Accordingly it is also still too weak for many other applications. For example, in shoe soles, a popular application of SBR rubber, the minimum tensile strength is specified to be 8 MPa (Ferreira et al., 2010). The maximum tensile strength of 3.97 MPa, achieved by using the RFL coated filler, is only half the specified strength needed for shoe soles.

There was also a dramatic drop in the extension of the rubber at higher loadings as shown in Figure 8.19. The highest extension was seen at 12.5% filler (15.6 pph) in both the RFL coated and the uncoated filler samples, with results from the two samples being statistically similar to each other ($P=0.397$). The extension recorded is fairly low for SBR rubber which has been quoted at 500% for reinforced vulcanisates by Brydson (1988). The low extension suggests that the polymer chain motions have been restricted; this could be due to high number of cross links forming with the sulphur, or due to reactions occurring with the sulphur producing cyclic or pendant sulphides. The presence of the filler could also be inhibiting the polymer chain movement.

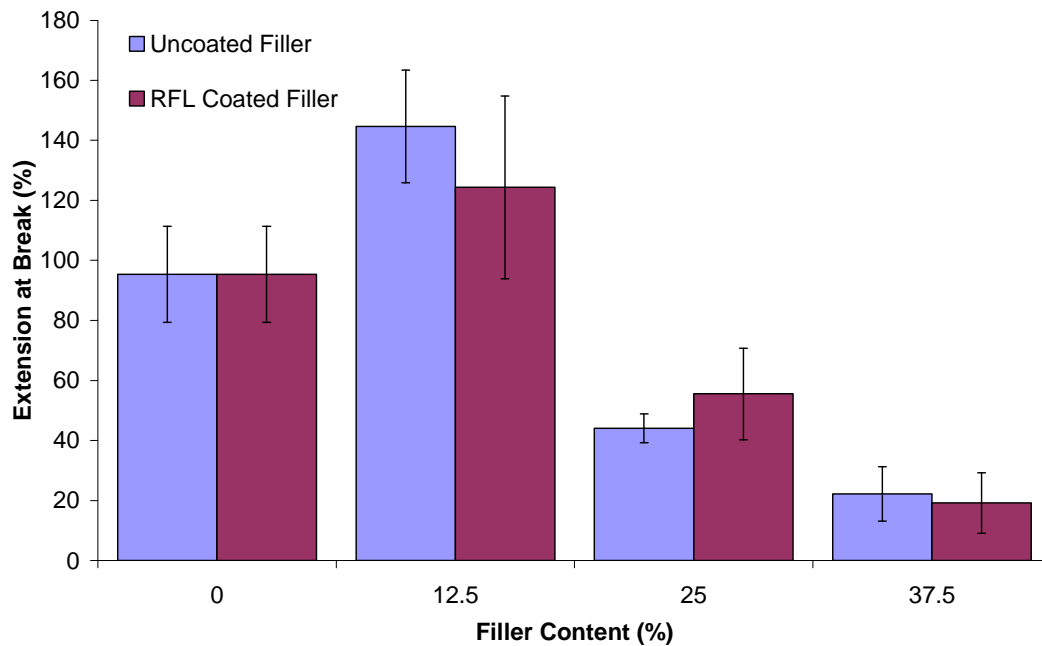


Figure 8.19: The Effect of Recycled Filler Content on the Tensile Extension of rubber compounds.

8.5.5 Resistance to Tearing

Tear strength is an important property of rubber, as products are often subjected to cyclic stresses from repeated or periodic flexing or compression. The initiation and development of cracks from this is a common cause of failure in products. Abrasion can also form cracks which would be weak points likely to propagate due to tearing and cause failure (Brown, 2006).

Table 8.13 and Figure 8.20 show the results from the angle tear tests completed. The recycle fillers have had a marked effect on the tear strength of the rubber with 25% RFL coated filler loading increasing the tear strength by 2.5 times that of the compound with no filler. The uncoated filler increased the tear strength at 25% filler loading even further. 25% of filler (equivalent to 36.3 pph) produced the optimum tear strength for both the uncoated and RFL coated filler. However the uncoated filler was able to give increased tear strength comparable to the 37.5% compound with RFL coated filler but was able to achieve in this level with only 25% fibre content, and consistently performed better than the RFL coated filler at each loading.

Table 8.13: Tear Strength of Filled Rubber Sheets

Sample	Thickness (mm)	n	Maximum Force (N)	Tear Strength (kN/m)
0% Filler	2.49	1	21.55	8.64
		2	15.35	6.15
		3	15.32	6.15
		4	13.42	5.38
		Average	16.41	6.58
		SD	3.54	1.42
		Variance	21.59	21.59
12.5% Uncoated	2.74	1	31.89	11.62
		2	36.24	13.21
		3	29.46	10.74
		4	29.23	10.66
		Average	31.71	11.56
		SD	3.25	1.19
		Variance	10.26	10.26

25% Uncoated	2.63	1	53.78	20.48
		2	52.42	19.96
		3	50.85	19.36
		4	41.36	15.74
		Average	49.60	18.88
		SD	5.63	2.14
		Variance	11.35	11.35
37.5% Uncoated	3.07	1	58.80	19.16
		2	44.74	14.58
		3	60.83	19.82
		4	53.019	17.28
		Average	54.35	17.71
		SD	7.21	2.35
		Variance	13.26	13.26
12.5% RFL	2.74	1	24.29	8.88
		2	24.90	9.10
		3	26.62	9.73
		4	26.58	9.71
		Average	25.60	9.35
		SD	1.19	0.43
		Variance	4.64	4.64
25% RFL	2.67	1	47.94	17.97
		2	46.27	17.34
		3	36.76	13.77
		4	48.65	18.23
		Average	44.90	16.83
		SD	5.52	2.07
		Variance	12.30	12.30
37.5% RFL	3.05	1	51.54	16.91
		2	44.62	14.64
		3	52.42	17.20
		4	46.44	15.23
		Average	48.75	15.99
		SD	3.81	1.25
		Variance	7.82	7.82

As the RFL coated samples performed better in the tensile tests, it was expected that they would also perform better in the tear tests due to an increased number of cross-links having been formed. The RFL coated fibres and uncoated fibres behave similarly to each other with increased filler content with t tests between RFL coated and uncoated samples finding $P=0.226$ in 25% filler content samples and $P=0.266$ in 37.5% filler content samples. The uncoated fibre sample, however, had significantly higher ($P=0.040$) tear strength than the uncoated sample at a filler loading of 12.5%. The reasoning for the uncoated filler to perform better at a 12.5% fibre content could

be due to fibre size, geometric factors or dispersion. Although some literature suggests that decreased filler particle size will result in increased tear strength of the compound (Brydson, 1988), (Horn, 1982), others argue that the effects of particle size are only slight, particularly in SBR (Jacques, 1982). This could enable other physical phenomena to make a resultant difference to the tear strength. The fibrous nature of the filler will prevent the growth of crack propagation (Ferreira et al., 2010).

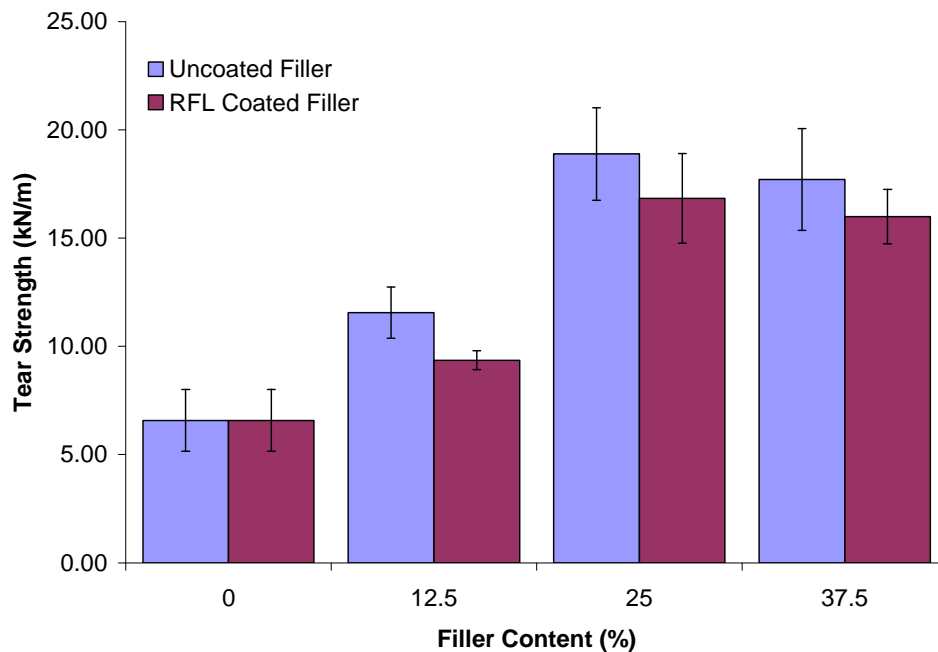


Figure 8.20: *The Effect of Recycled Filler on Tear Strength of Rubber Compounds.*

It is also possible that the strength seen by the 12.5% uncoated sample could be due to differences in the way that the uncoated and RFL coated filler compounds transfer the load to the tear site. A common problem in the test method used is that energy applied to the test piece is dissipated in stretching the arms of the sample, rather than tearing it (Jacques, 1982). This could have occurred in this study, where the uncoated filler samples have taken a higher load, due to its more malleable nature, whereas, the less pliable RFL coated filler samples transfer the load directly to the tear site.

In both cases the recycle filler is able to provide a reinforcing capacity to the compound. The tear forces measured are also in the range specified for certain applications. Rubber used in footwear is required to have a tear strength of 7 kN/m for normal wear and 10 kN/m for demanding wear (Ferreira et al., 2011). The recycle fillers enable these strengths to be met.

8.6 Conclusions

Recycling RFL coated fabric through reduction by Hollander beater and incorporation into rubber as filler is a possible alternative to current waste disposal used. The particulate is able to be incorporated into the rubber at high loadings. There is also an opportunity to ease the processing stages by using plasticisers to improve the viscous flow of the polymer and hence allow the filler to be better integrated into the compound.

A reinforcing effect in rubber was identified from use of both the uncoated nylon and the RFL coated nylon, providing an alternative to other reinforcing fillers on the market, and a way of utilising the waste products. Further work could be done to attempt to enhance the strength of the composites by altering the ratios of the vulcanisation system reagents used, as the final tensile strengths were lower than expected and would need to be increased for most product specifications. If the dispersion properties of the higher loaded compounds were also improved this could result in higher tensile strengths being produced.

Increased loading of both fillers resulted in increased physical properties up to 25% loading (36.3 pph) of filler. Further loading, although increasing the tensile strength in the RFL coated filler compound, had little effect on tear strength and caused a reduction in strength of the uncoated filler compound.

There was little overall difference seen between the RFL coated nylon and the uncoated nylon waste. The most significant difference being the drop in tensile strength of the uncoated filler compound from 25% loading to 37.5% where the RFL coated filler compound continued to increase in strength, enabling the RFL fibre reinforced composite to have 127% increase in strength to the uncoated fibre reinforced composite. This suggests that RFL coated waste would be best utilised at higher loadings. This enables higher volumes of material to be recycled in this way and is a key finding in this research. Value is able to be added to the material this way since due to the reinforcing factor that the RFL fibre provides to the rubber composite. Tear strength of 10 kN/m specified for products such as demanding footwear was able to be met due to the incorporation of the recycle fillers into the rubber.

8.7 References

- ALI, M. A., EL-NEMR, K. F. & HASSAN, M. M. (2011) Waste newsprint fibers for reinforcement of radiation-cured styrene butadiene rubber-based composites - Part I: Mechanical and physical properties. *Journal of reinforced plastics and composites*, 30, 721-737.
- BLOW, C. M. (1982) An Outline of Rubber Technology. In Blow, C. M. & Hepburn, C. (Eds.) *Rubber Technology and Manufacture*. 2nd Ed. London, Butterworth Scientific.
- BOONSTRA, B. B. (1982) Reinforcement by Fillers. In Blow, C. M. & Hepburn, C. (Eds.) *Rubber Technology and Manufacture*. 2nd ed. London, Butterworth Scientific.
- BROWN, R. (2006) *Physical Testing of Rubber*, New York, Springer
- BRYDSON, J. A. (1988) *Rubbery materials and their compounds*, London, Elsevier Applied Science.
- CROWTHER, B. G., EDMONDSON, H. M. & ELLIS, M. J. (1982) Processing Technology. In Blow, C. M. & Hepburn, C. (Eds.) *Rubber Technology and Manufacture*. 2nd ed. London, Butterworth Scientific.
- DURAIRAJ, R. B. (2005) *Resorcinol [electronic resource]: Chemistry, Technology and Applications*, Berlin, Heidelberg, Springer-Verlag Berlin Heidelberg.
- FERREIRA, M. J., ALMEIDA, M. F. & FREITAS, F. (2011) Formulation and characterization of leather and rubber wastes composites. *Polymer Engineering & Science*, 51, 1418-1427.
- FERREIRA, M. J., FREITAS, F. & ALMEIDA, M. F. (2010) The Effect of Leather Fibers on the Properties of Rubber-Leather Composites. *Journal of Composite Materials*, 44, 2801-2817.
- HORN, J. B. (1982) Materials for Compounding and Reinforcement. In Blow, C. M. & Hepburn, C. (Eds.) *Rubber Technology and Manufacture*. 2nd ed. London, Butterworth Scientific.
- JACQUES, J. E. (1982) Principles of Compounding. In Blow, C. M. & Hepburn, C. (Eds.) *Rubber Technology and Manufacture*. 2nd ed. London, Butterworth Scientific.
- MONSANTO Monsanto Rheometer 100 User Guide.
- MORRELL, S. H. (1982) The Chemistry and Technology of Vulcanisation. In Blow, C. M. & Hepburn, C. (Eds.) *Rubber Technology and Manufacture*. 2nd ed. London, Butterworth Scientific.

NASHAR, D. E. E., ABD-EL-MESSIEH, S. L. & BASTA, A. H. (2004) Newsprint paper waste as a fiber reinforcement in rubber composites. *Journal of Applied Polymer Science*, 91, 469.

RAJARAM, R., RAJNIKANTH, B. & GNANAMANI, A. (2009) Preparation, Characterization and Application of Leather Particulate-Polymer Composites (LPPCs). *Journal of polymers and the environment*, 17, 181.

REDMOND, G. B. & WOOD, J. O. (1982) Materials for Compounding and Reinforcement - Textiles In Blow, C. M. & Hepburn, C. (Eds.) *Rubber Technology and Manufacture*. 2nd ed. London, Butterworth Scientific.

STERN, H. J. (1982) History. In Blow, C. M. & Hepburn, C. (Eds.) *Rubber Technology and Manufacture*. 2nd ed. London, Butterworth Scientific.

9.0 Conclusions and Further Work

9.1 Conclusions

The European Waste Framework Directive 2008/98/EC and The Waste (England and Wales) Regulations encourage businesses, organisations and waste handlers to prevent, re-use and recycle waste in order to limit the disposal of waste. In addition landfill tax is continuing to rise until 2014/2015 at which point “active” waste will cost £80/tonne to dispose of by landfill. In keeping with this, Heathcoat Fabrics is exploring ways to recycle their Resorcinol Formaldehyde Latex (RFL) coated nylon 66 waste.

In this study the effect of the RFL coating on the fabric properties was analysed with respect to the stiffness, tensile strength and tearing properties. It was found that the RFL coating caused the fabric to have increased stiffness in the warp direction and decreased tear strength, in comparison to uncoated fabric. This was primarily due to the yarns having less ability to move within the fabric structure. The coating therefore, enables fabric reduction by tear propagation for example in pin penetration shredding techniques used in the Laroche Cadette shredder, however will inhibit yarn breakdown to fibre as the coating penetrates into the yarn, bonding the fibres together. An increase in tensile strength was observed but reduced energy is required to reach break point, meaning that the coating should also aid impact forms of reduction such as the hollander beater.

Three reduction methods were assessed, the Laroche Cadette shredder, the Hollander beater and the Intimus disintegrator:

- 1) The Laroche Cadette produced the longest fibres, up to 160mm in uncoated fabric and 100mm in coated fabric. The coating was relatively unaffected from the reduction procedure. A slight lowering of molecular weight was observed with earlier onset of degradation occurring in reduced material in comparison to fabric samples;

- 2) The Hollander beater produced an intermediate fibre length of 12 mm – 32 mm, with opportunity to control the fibre length through the beater roll setting, where at Datum fibres of 2mm were produced. Coating was still evident on the fibres post reduction by this technique. Minor degradation was seen in uncoated fabric, with onset temperature of degradation reduced; however the coated fabric was unaffected. Reduction in molecular weight of either the coated or uncoated fabric was not observed. Water used within this process reduces heat build up which causes degradation in alternate processes;
- 3) The Intimus disintegrator produced small fibre lengths of less than 3.2mm. Heat build up was an obvious problem in this reduction method with melting and smearing occurring causing reduction to a particulate form. Significant degradation was observed producing a cross-linked structure with degradation onset at 250°C. If heat was controlled, melting was avoided; producing fibres, with slightly lower molecular weight from degradation. Coating remained bonded to the fibres and more fibre separation occurred.

A number of fibre processing methods were assessed for their viability to be used to recycling the material with varying success:

- 1) Synthetic paper production required a minimum of 50% cellulose pulp to ensure sufficient bonding within the fibre web. Paper was produced, using the RFL fibres reduced by the Hollander beater method, having a tensile index of 8.36Nm/g and weight per unit area of 75.1g/m². The tensile index (y) of paper was found to be exponentially related to the RFL coated nylon 66 fibre content (x) with the relationship $y=72.656e^{-0.0481x}$, enabling recycled fibre content to be maximised where a strength requirement is known. Commercial uses for this product are unknown;
- 2) Carded webs were unable to be produced for textile processing of the RFL fibres reduced using the Laroche Cadette shredder due to the increased stiffness of the fibres, and decreased surface friction of the fibres. However, work was carried out confirming that the short fibre lengths of 10mm produced from the Hollander beater would be sufficient to form yarns, although increased fibre length of 25 and 30mm enhanced yarn strength. Fibre blends of long (30mm) and short (10mm) fibres were able to be friction spun to 75% short fibre with only a small drop of 10% in

strength. Using blends of long (25mm) and short (10mm) affected yarn strength more drastically with a drop of 67% occurring when decreasing the long fibre length from 30mm to 25mm in the 75% short fibre (10mm) yarns. So long as 50% long fibres (25mm or more) was maintained in the blend sufficient yarn strength of at least 5cN/tex for further processing could be achieved. Fibres with lengths as low as 4mm could be spun as the short fibre at this blend;

- 3) Separation of fibre lengths for specific lengths was achieved through use of the through flow hydrocyclone “rejects” for separation of long fibres (10mm) and the forward flow hydrocyclone “rejects” for separation of short fibres (3mm). It is recommended that this separation of fibres is used in order to deliver waste fibres of improved length uniformity for subsequent product processing.

Polymer processing routes of melt processing and use within the rubber industry were also assessed:

- 1) Injection moulding of the Intimus Disintegrator reduced particulate was not found to be viable due to excess gas production and high number of voids within the moulded piece;
- 2) Moulded pieces were able to be produced from uncoated and RFL coated waste by compression moulding on a small scale. More work is needed to analyse the voids within the pieces and the method developed to reduce the quantity of voids. The effect this process has on degradation of the polymer is also unknown;
- 3) The Hollander beater reduced waste was also successfully used as filler within rubber at a level of up to 37.5% fibres by weight. The RFL coated nylon 66 fibre waste filler enabled a 127% increase in strength from the uncoated nylon 66 waste filler in the 37.5% filler content rubber composites. This enables a value to be added to the RFL coated fibre, and an increased quantity able to be recycled as filler. Rubber composite tear strengths above that specified for demanding footwear of 10kN/m were able to be achieved by using the RFL nylon 66 waste as filler.

Contrary to what might be expected it can be beneficial to use the RFL coated nylon 6 waste, without the need to first remove the coating and remove contaminants. By retaining the waste in a rubber processing route the RFL coating can be advantageous due to improved interfacial adhesion between particles and the rubber matrix, translating to increased tensile strength of the rubber composites.

From this study it has been established that the promising route to recycle RFL coated nylon 66 waste is as shown in Figure 9.1, where the rubber created with the RFL coated nylon 66 fibres meet the specification to be used for products such as demanding footwear.

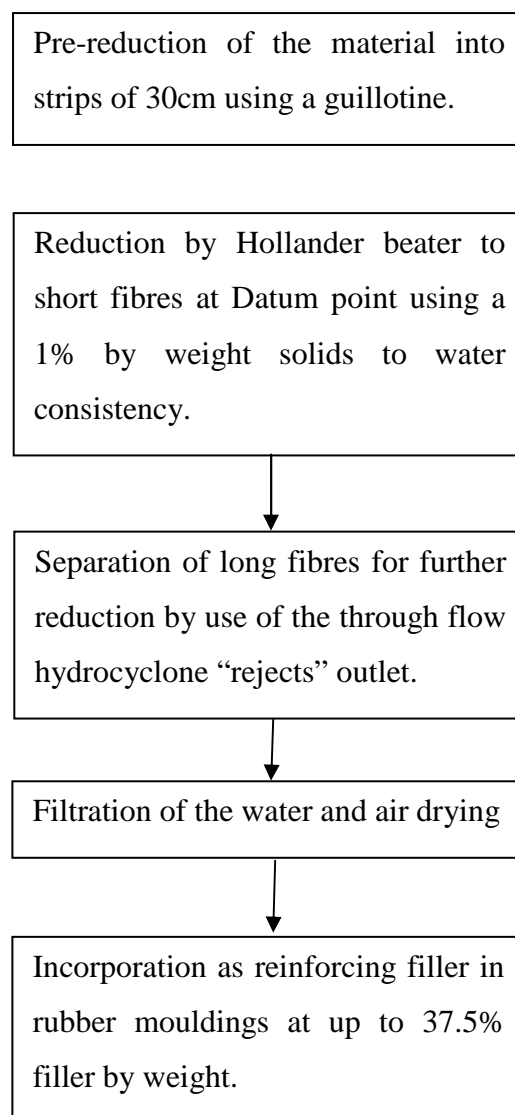


Figure 9.1: Recommended recycling processing route for RFL coated nylon 66 fibres

9.2 Further Work

It is apparent that leaving the RFL coating in place would be advantageous and identifying processing routes that are capable of handling the coated fibres and products that utilise their properties would be the preferred choice. Since the Hollander beater provided the optimum way of reduction, causing little degradation and enabling yarns to be broken up to individual fibres whilst maintaining the coating on the fibre surface, further work could be done to increase the throughput of this batch process to assess whether it could cope with the high quantity of RFL waste produced by Heathcoat Fabrics. This could be done by using higher consistency of solids within the fibre slurry formed. Assessment would be required to see if this affected the fibre size produced.

Further work is required in looking at fibre separation techniques, such as the hydrocyclone to assess processing capabilities with RFL coated fibres. This could enable optimum sized particles for the recommended recycling processing route to be removed from the reduction process, whilst larger fibre lengths are filtered back into the Hollander beater. This method was proved using uncoated fibres but the increased density of the RFL coated nylon 66 fibres could make a difference to the fibre sizes that are outputted from the hydrocyclone. The capability of the hydrocyclone to process this material has also not been challenged, and has the possibility to cause blockages at the underflow outlet which would need to be investigated and overcome.

Using the RFL fibres as a filler in rubber has proven to be the most viable method of recycling the coated waste, due to the reinforcing factor they offer to the rubber composite. Work to address the optimum particle size or fibre length of the RFL coated material for use as filler could be researched further in order to produce rubber pieces with most favourable properties for specific products, and enable further reinforcement to be created between the RFL nylon 66 fibre waste and the rubber matrix. Section 8.2.3.3 discusses how the surface area of filler per cubic centimetre of compound affects the reinforcement provided in addition to the chemical nature of the particle. Since the RFL coated nylon 66 particles already have beneficial surface activity, further work could be concentrated on finding optimum particle size, geometry and packing to enable maximum surface area of filler per cubic centimetre

of compound and hence optimum reinforcement to be produced. Fibre configurations and incorporating yarn strands into rubber could also be evaluated.

Further work outside of the recommended processing route could also be studied further in order to find alternative recycling routes for the fibres, and increased products in which they could be used. Work utilising short RFL fibres in synthetic paper using synthetic polymer binders as described in section 5.3.1 could achieve higher percentage of recyclate within paper prototypes. Further work would also be required to assess product opportunities for this technology, this could be by way of insulating materials or filters for example.

Yarn production methods failed due to stiffness of the fibre. Chemical methods to remove the RFL coating could be examined in order to introduce greater flexibility into the fibres in order to allow carding to occur. Physical methods of removing the RFL coating or increasing the flexibility of the coated fibres, such as etching could also be researched, however methods such as this are likely to have a substantial effect on the processing cost.

Work to assess the voids in plastic melt processing is required to develop this technique. Current prototypes consist of many voids, which will affect the strength. Voids are formed due to insufficient pressure on the mould during forming, or due to gases being formed in the process. Processing methods to limit void formation should be trialled and characterisation of voids occurring and their effect on the materials properties such as strength should be assessed.

Appendix 1: Fabric Properties

Sample		Breaking Load (N)	Tensile Strength (kN/m)	Strain (%)	Displacement at Max load (mm)	Modulus (MPa)
Loomstate Warp	1	490.7	9.814	61.486	122.971	16.600
	2	515.4	10.308	64.778	129.556	16.554
	3	563.0	11.260	71.327	142.654	16.219
	4	505.0	10.100	69.160	138.320	15.424
	5	558.7	11.174	70.112	140.224	17.176
	Mean	526.6	10.531	67.373	134.745	16.395
	S.D	32.54	0.651	4.115	8.230	0.642
	C.V	6.18	6.180	6.107	6.108	3.919
Minimum	490.7	9.814	61.486	122.971	15.424	
Maximum	563.0	11.260	71.327	142.654	17.176	
Loomstate Weft	1	422.3	8.446	40.334	80.668	33.852
	2	453.8	9.076	46.403	92.805	28.510
	3	447.5	8.950	41.362	82.724	38.863
	4	462.4	9.248	45.050	90.100	34.982
	5	418.5	8.370	42.804	85.608	36.133
	Mean	440.9	8.818	43.191	86.381	34.468
	S.D	19.49	0.390	2.521	5.043	3.815
	C.V	4.42	4.421	5.838	5.838	11.069
Minimum	418.5	8.370	40.334	80.668	28.510	
Maximum	462.4	9.248	46.403	92.805	38.863	
Finished Warp	1	671.4	13.428	59.712	119.424	23.055
	2	691.5	13.830	64.691	129.382	22.435
	3	720.8	14.416	63.702	127.405	23.481
	4	690.2	13.804	64.458	128.916	21.826
	5	701.2	14.024	66.401	132.802	21.622
	Mean	695.0	13.900	63.793	127.586	22.484
	S.D	18.00	0.360	2.486	4.971	0.790
	C.V	2.59	2.590	3.896	3.896	3.515
Minimum	671.4	13.428	59.712	119.424	21.622	
Maximum	720.8	14.416	66.401	132.802	23.481	
Finished Weft	1	493.7	9.874	73.037	146.074	14.197
	2	484.0	9.680	72.395	144.790	14.100
	3	503.6	10.072	73.765	147.530	14.670
	4	504.7	10.094	71.268	142.535	15.827
	5	495.3	9.906	71.126	142.251	14.734
	Mean	496.3	9.925	72.318	144.636	14.706
	S.D	8.41	0.168	1.134	2.268	0.686
	C.V	1.69	1.695	1.567	1.568	4.668
Minimum	484.0	9.680	71.126	142.251	14.100	
Maximum	504.7	10.094	73.765	147.530	15.827	
Coated Warp	1	757.9	15.158	50.169	100.338	34.674
	2	778.0	15.560	50.491	100.983	35.049
	3	785.2	15.704	51.214	102.427	35.507
	4	765.1	15.302	49.460	98.920	35.059
	5	777.4	15.548	49.395	98.790	38.048
	Mean	772.7	15.454	50.146	100.292	35.667
	S.D	10.99	0.220	0.757	1.515	1.363
	C.V	1.42	1.422	1.510	1.510	3.822
Minimum	757.9	15.158	49.395	98.790	34.674	
Maximum	785.2	15.704	51.214	102.427	38.048	
Coated Weft	1	431.3	8.626	56.259	112.517	15.930
	2	462.1	9.242	58.945	117.890	17.098
	3	391.3	7.826	58.694	117.387	13.654
	4	393.8	7.876	58.749	117.499	13.681
	5	375.8	7.516	56.482	112.963	13.601
	Mean	410.9	8.217	57.826	115.651	14.793
	S.D	35.16	0.703	1.334	2.669	1.625
	C.V	8.56	8.559	2.307	2.308	10.984
Minimum	375.8	7.516	56.259	112.517	13.601	
Maximum	462.1	9.242	58.945	117.890	17.098	

Sample	Bending Length (cm)					
	Warp			Weft		
	Loomstate	Finished	Coated	Loomstate	Finished	Coated
F1	1.4	1.75	4.00	2.40	1.35	2.30
F2	1.5	1.85	3.90	2.20	1.30	2.45
F3	1.3	1.85	3.95	2.15	1.30	2.35
B1	1.85	1.65	4.10	2.25	1.50	2.20
B2	1.85	1.75	4.35	2.25	1.45	2.10
B3	1.9	1.65	3.95	2.45	1.40	2.10
Mean	1.63	1.75	4.04	2.28	1.38	2.25
S.D	0.26	0.09	0.17	0.12	0.08	0.14
C.V	16.16	5.11	4.10	5.12	5.90	6.29
Minimum	1.30	1.65	3.90	2.15	1.30	2.10
Maximum	1.90	1.85	4.35	2.45	1.50	2.45

	Tearing Resistnace - Maximum Load (N)					
	Across Warp			Across Weft		
	Loomstate	Finished	Coated	Loomstate	Finished	Coated
1	56.10	52.08	31.81	53.95	52.75	21.61
2	52.21	54.09	32.88	53.28	54.49	20.67
3	54.09	50.06	32.75	53.95	53.82	22.41
4	50.46	51.94	31.67	54.09	51.40	22.01
5	-	53.69	32.34	-	52.08	20.67
Mean	53.22	52.37	32.29	53.82	52.91	21.47
S.D	2.43	1.61	0.54	0.36	1.26	0.79
C.V	4.56	3.06	1.68	0.68	2.38	3.66
Minimum	56.10	54.09	32.88	54.09	54.49	22.41
Maximum	50.46	50.06	31.67	53.28	51.40	20.67

Appendix 2: Paper Physical Testing

Handsheet Weight

GSM	Sheet	Nylon Percentage							
		0 Faults	50 Faults	60 Faults	70 Faults	80 Faults	90 Faults	100	
60	1	65.3 N	72.0 N	74.7 N	59.3 N	58.9 N			
	2	65.2 N	69.9 N	76.5 N	62.1 N	62.1 N			
	3	66.7 N	66.5 N	68.6 N	64.8 N	57.4 N			
	4	68.9 N	71.7 N	69.9 Y	63.1 N	46.7 Y			
	5	68.7 N	70.3 N	68.1 Y	67.7 Y	54.5 Y			
	6	67.7 N	79.4 N	71.9 N	71.1 Y	58.6 N			
	7	70.3 N	78.3 N	68.2 N	63.1 N	69.6 Y			
	8	70.0 N	78.8 N	71.5 N	73.4 Y	66.2 Y			
	9	68.6 N	79.9 N	71.5 N	63.6 Y	68.2 Y			
	10		78.9 N	72.4 Y	66.9 Y	67.8 N			
	11		80.7 N	71.6 Y		68.8 Y			
	12			72.2 N					
	Average	67.9	75.11	71.4	65.5	61.0			
	SD	1.88	5.08	2.52	4.30	7.58			
120	1				110.20 Y	142.50 Y	130.50 Y		
	2				127.90 Y	136.90 Y	137.35 Y		
	3				132.85 Y	144.15 Y	125.40 Y		
	4				138.80 Y	139.85 Y	133.65 Y		
	5				133.60 Y	138.50 Y	134.40 Y		
	6				129.75 Y	134.25 N	125.05 Y		
	7					135.15 Y	138.95 Y		
	8						106.65 Y		
	Average				128.85	138.76	128.99 Y		
	SD				9.87	3.68	10.35 Y		
180	1								181.90
	2								222.95
	3								189.35
	4								195.50
	5								201.55
	Average								198.25
	SD								15.61

Handsheet Thicknesses

60 g/m²

		60 gsm																			
Nylon %	Sheet	0				50				60				70				80			
		n1	n2	n3	Average	n1	n2	n3	Average	n1	n2	n3	Average	n1	n2	n3	Average	n1	n2	n3	Average
	1	82	88	86	85	242	240	248	243	271	290	248	270	194	300	360	285	228	228	207	221
	2	86	82	87	85	238	211	271	240	266	230	278	258	251	185	235	224	240	196	197	211
	3	85	82	83	83	222	242	217	227	260	321	323	301	303	262	233	266	182	173	200	185
	4	86	86	88	87	202	230	226	219	250	276	230	252	243	245	228	239	226	242	231	233
	5	99	122	91	104	251	253	219	241	292	277	267	279	322	380	351	351	221	209	202	211
	6	91	91	95	92	222	246	238	235	266	302	294	287	270	318	284	291	222	218	233	224
	7	89	88	93	90	253	260	237	250	250	282	283	272	213	240	247	233	261	291	276	276
	8	86	89	89	88	194	271	243	236	270	294	247	270	241	233	212	229	243	267	228	246
	9	91	85	90	89	258	262	258	259	304	291	300	298	233	218	256	236	298	337	240	292
	10					242	272	245	253	254	272	253	260	235	253	216	235	248	256	230	245
	11					247	230	244	240	216	290	283	263				233	284	228	248	248
	12									250	274	262	262								
Thickness (µm)	Mean				89				240				273				259				236
	SD				8				19				24				48				35

120 g/m²

		120 gsm												180 gsm			
Nylon %	Sheet	70				80				90				100			
		n1	n2	n3	Average	n1	n2	n3	Average	n1	n2	n3	Average	n1	n2	n3	Average
	1	485	511	595	530	471	290	524	428	456	440	415	437	771	816	664	750
	2	513	436	330	426	475	492	606	524	470	530	461	487	762	723	612	699
	3	487	510	532	510	363	521	616	500	382	512	445	446	687	780	680	716
	4	475	485	503	488	507	526	544	526	546	540	507	531	780	787	921	829
	5	478	551	507	512	481	582	582	548	457	545	535	512	845	785	772	801
	6	487	448	449	461	437	531	415	461	566	422	691	560				
	7					542	423	435	467	485	571	466	507				
	8									425	480	416	440				
Thickness (µm)	Mean				488				493				490				759
	SD				55				81				68				77

Tensile

Nylon - 0% 60 g/m²

	Maximum Load (N) (N)	Tensile Strength (kN/m) ()
1	75.360	5.024
2	66.390	4.426
3	66.740	4.449
4	60.990	4.066
5	66.360	4.424
6	69.690	4.646
7	70.170	4.678
8	76.590	5.106
9	73.020	4.868
10	62.950	4.197
Mean	68.826	4.588
S.D.	5.114	0.341
C.V.	7.431	7.431
Minimum	60.990	4.066
Maximum	76.590	5.106

Nylon - 50% 60 g/m²

	Maximum Load (N) (N)	Tensile Strength (kN/m) ()
1	9.168	0.611
2	11.660	0.777
3	9.866	0.658
4	8.497	0.566
5	9.181	0.612
6	9.463	0.631
7	9.987	0.666
8	9.101	0.607
9	8.215	0.548
10	9.034	0.602
Mean	9.417	0.628
S.D.	0.955	0.064
C.V.	10.145	10.145
Minimum	8.215	0.548
Maximum	11.660	0.777

Nylon - 60% 60 g/m²

	Maximum Load (N) (N)	Tensile Strength (kN/m) ()
1	3.369	0.225
2	3.168	0.211
3	4.537	0.302
4	5.060	0.337
5	4.215	0.281
6	3.007	0.200
7	2.738	0.183
8	2.510	0.167
9	5.570	0.371
10	5.221	0.348
Mean	3.940	0.263
S.D.	1.119	0.075
C.V.	28.401	28.401
Minimum	2.510	0.167
Maximum	5.570	0.371

Nylon - 70% 60 g/m²

	Maximum Load (N) (N)	Tensile Strength (kN/m) ()
1	2.725	0.182
2	3.758	0.251
3	2.362	0.157
4	2.430	0.162
5	2.470	0.165
6	2.752	0.183
7	1.315	0.088
8	2.872	0.191
9	2.523	0.168
10	2.295	0.153
Mean	2.550	0.170
S.D.	0.604	0.040
C.V.	23.678	23.678
Minimum	1.315	0.088
Maximum	3.758	0.251

Nylon - 80% 60 g/m²

	Maximum Load (N)	Tensile Strength (kN/m)
1	1.758	0.117
2	1.664	0.111
3	1.825	0.122
4	1.168	0.078
5	1.557	0.104
6	0.819	0.055
7	0.510	0.034
8	1.423	0.095
9	0.926	0.062
10	0.953	0.064
Mean	1.260	0.084
S.D.	0.449	0.030
C.V.	35.645	35.645
Minimum	0.510	0.034
Maximum	1.825	0.122

Nylon – 70% 120 g/m²

	Maximum Load (N)	Tensile Strength (kN/m)
1	3.302	0.220
2	2.604	0.174
3	4.577	0.305
4	4.282	0.285
5	3.463	0.231
6	4.631	0.309
7	4.671	0.311
8	5.785	0.386
9	6.550	0.437
10	2.470	0.165
Mean	4.234	0.282
S.D.	1.311	0.087
C.V.	30.968	30.968
Minimum	2.470	0.165
Maximum	6.550	0.437

Nylon – 80% 120 g/m²

	Maximum Load (N)	Tensile Strength (kN/m)
1	1.879	0.125
2	1.799	0.120
3	1.101	0.073
4	1.919	0.128
5	1.651	0.110
6	1.718	0.115
7	1.114	0.074
8	1.839	0.123
9	1.383	0.092
10	2.027	0.135
Mean	1.643	0.110
S.D.	0.331	0.022
C.V.	20.176	20.176
Minimum	1.101	0.073
Maximum	2.027	0.135

Appendix 3: Yarn Physical Testing

Sample Number	Fibre length Percentages		Tex	Tensile Strength (cN)	Tenacity (cN/tex)
	Long Fibre	Short Fibre			
1	100% 30mm		240.00	2133.00	8.888
2			473.00	2451.00	5.182
3			255.00	2110.00	8.275
4			480.00	2388.00	4.975
5			468.00	3690.00	7.885
6			213.00	2817.00	13.225
7			213.00	2432.00	11.418
8			228.00	2357.00	10.338
9			510.00	2966.00	5.816
10			248.00	2859.00	11.528
11			215.00	2144.00	9.972
12			425.00	1956.00	4.602
13			445.00	3603.00	8.097
14			515.00	3420.00	6.641
15			518.00	2894.00	5.587
16			435.00	3485.00	8.011
17			468.00	3105.00	6.635
18			510.00	4076.00	7.992
19			535.00	2805.00	5.243
20			470.00	3082.00	6.557
Mean			393.20	2838.65	7.843
S.D.			126.05	597.73	2.447
C.V.			32.06	21.06	31.204
Minimum			213.00	1956.00	4.602
Maximum			535.00	4076.00	13.225
1	75% 30mm	25% 10mm	270.00	2654.00	9.830
2			285.00	2689.00	9.435
3			483.00	2671.00	5.530
4			345.00	4289.00	12.432
5			263.00	2930.00	11.141
6			260.00	2299.00	8.842
7			270.00	2992.00	11.081
8			373.00	1383.00	3.708
9			363.00	3150.00	8.678
10			325.00	3612.00	11.114
11			273.00	2630.00	9.634
12			458.00	3427.00	7.483
13			420.00	2683.00	6.388
14			435.00	4156.00	9.554
15			420.00	4234.00	10.081
16			460.00	3042.00	6.613
17			360.00	1694.00	4.706
18			388.00	2652.00	6.835
19			483.00	2958.00	6.124
20			438.00	2687.00	6.135
Mean			368.60	2941.60	8.267
S.D.			78.98	748.09	2.426
C.V.			21.43	25.43	29.340
Minimum			260.00	1383.00	3.708
Maximum			483.00	4289.00	12.432
1	50% 30mm	50% 10mm	233.00	1844.00	7.914
2			283.00	2659.00	9.396
3			225.00	1781.00	7.916
4			270.00	1591.00	5.893
5			295.00	1993.00	6.756
6			235.00	2009.00	8.549
7			270.00	2534.00	9.385
8			220.00	1804.00	8.200
9			235.00	2110.00	8.979
10			243.00	1734.00	7.136
11			263.00	2270.00	8.631
12			223.00	1804.00	8.090
13			243.00	2332.00	9.597
14			225.00	2220.00	9.867
15			263.00	2046.00	7.779
16			238.00	2003.00	8.416
17			225.00	1897.00	8.431
18			240.00	2507.00	10.446
19			230.00	1667.00	7.248
20			220.00	2083.00	9.468
Mean			243.95	2044.40	8.405
S.D.			22.25	298.99	1.128
C.V.			9.12	14.62	13.425
Minimum			220.00	1591.00	5.893
Maximum			295.00	2659.00	10.446
1	25% 30mm	75% 10mm	248.00	1970.00	7.944
2			260.00	2046.00	7.869
3			240.00	2436.00	10.150
4			278.00	2187.00	7.867
5			263.00	1949.00	7.411
6			278.00	1542.00	5.547
7			288.00	1403.00	4.872
8			285.00	2341.00	8.214
9			250.00	2177.00	8.708
10			245.00	2154.00	8.792
11			250.00	1858.00	7.432
12			255.00	1671.00	6.553
13			235.00	1765.00	7.511
14			260.00	1474.00	5.669
15			248.00	1060.00	4.274
16			255.00	1592.00	6.243
17			263.00	1365.00	5.190
18			253.00	1634.00	6.458
19			263.00	2097.00	7.973
20			255.00	1439.00	5.643
Mean			258.60	1808.00	7.016
S.D.			14.34	370.11	1.513
C.V.			5.55	20.47	21.568
Minimum			235.00	1060.00	4.274
Maximum			288.00	2436.00	10.150

Sample Number	Fibre length Percentages		Linear Density (Tex)	Tensile Strength (N)	Tenacity (N/tex)
	Long Fibre	Short Fibre			
1	100% 25mm		177.00	613.40	3.466
2			134.00	285.90	2.134
3			130.00	605.40	4.657
4			175.00	590.40	3.374
5			131.00	406.00	3.099
6			267.00	728.90	2.730
7			267.00	1114.00	4.172
8			264.00	1219.00	4.617
9			275.00	1247.00	4.535
10			266.00	904.70	3.401
11			133.00	630.90	4.744
12			150.00	581.20	3.875
13			143.00	467.10	3.266
14			127.00	546.30	4.302
15			232.00	840.30	3.622
16			213.00	951.70	4.468
17			205.00	771.80	3.765
18			186.00	283.20	1.523
19			163.00	530.20	3.253
20			216.00	347.70	1.610
Mean			192.70	683.26	3.531
S.D.			54.18	287.92	0.965
C.V.			28.11	42.14	27.330
Minimum			127.00	283.20	1.523
Maximum			275.00	1247.00	4.744
1	75% 25mm	25% 10mm	133.00	502.00	3.774
2			143.00	543.60	3.801
3			203.00	1380.00	6.798
4			118.00	295.30	2.503
5			123.00	416.10	3.383
6			128.00	304.70	2.380
7			138.00	794.60	5.758
8			138.00	460.40	3.336
9			190.00	786.60	4.140
10			170.00	907.40	5.338
11			165.00	698.00	4.230
12			193.00	1164.00	6.031
13			158.00	833.60	5.276
14			178.00	1051.00	5.904
15			250.00	1668.00	6.672
16			290.00	1481.00	5.107
17			233.00	1507.00	6.468
18			145.00	1176.00	8.110
19			140.00	883.20	6.309
20			138.00	838.90	6.079
Mean			168.70	884.57	5.070
S.D.			46.09	410.15	1.557
C.V.			27.32	46.37	30.706
Minimum			118.00	295.30	2.380
Maximum			290.00	1668.00	8.110
1	50% 25mm	50% 10mm	290.00	2087.00	7.197
2			278.00	1463.00	5.263
3			283.00	1285.00	4.541
4			268.00	1440.00	5.373
5			290.00	1419.00	4.893
6			318.00	1718.00	5.403
7			253.00	1401.00	5.538
8			253.00	1262.00	4.988
9			273.00	1197.00	4.385
10			240.00	1191.00	4.963
11			233.00	1015.00	4.356
12			250.00	1234.00	4.936
13			235.00	1066.00	4.536
14			243.00	983.90	4.049
15			258.00	1635.00	6.337
16			295.00	885.90	3.003
17			260.00	1215.00	4.673
18			288.00	1332.00	4.625
19			298.00	1605.00	5.386
20			265.00	1722.00	6.498
Mean			268.55	1357.84	5.047
S.D.			23.52	292.47	0.918
C.V.			8.76	21.54	18.181
Minimum			233.00	885.90	3.003
Maximum			318.00	2087.00	7.197
1	25% 25mm	75% 10mm	260.00	1252.00	4.815
2			283.00	174.50	0.617
3			225.00	401.30	1.784
4			243.00	194.60	0.801
5			238.00	1019.00	4.282
6			235.00	255.00	1.085
7			235.00	847.00	3.604
8			220.00	895.30	4.070
9			223.00	531.50	2.383
10			238.00	120.80	0.508
11			258.00	1255.00	4.864
12			223.00	260.40	1.168
13			220.00	273.80	1.245
14			198.00	953.00	4.813
15			220.00	138.30	0.629
16			258.00	692.60	2.684
17			228.00	122.10	0.536
18			250.00	518.10	2.072
19			253.00	139.60	0.552
20			280.00	990.60	3.538
Mean			239.40	551.73	2.302
S.D.			21.44	399.82	1.640
C.V.			8.96	72.47	71.237
Minimum			198.00	120.80	0.508
Maximum			283.00	1255.00	4.864

Sample Number	Fibre length Percentages		Linear Density (Tex)	Tensile Strength (N)	Tenacity (N/tex)
	Long Fibre	Short Fibre			
1	75% 30mm	25% 15mm	395.00	3528.00	8.932
2			325.00	3129.00	9.628
3			335.00	3487.00	10.409
4			418.00	2984.00	7.139
5			325.00	2686.00	8.265
6			343.00	2094.00	6.105
7			423.00	3787.00	8.953
8			385.00	3117.00	8.096
9			355.00	4262.00	12.006
10			428.00	4145.00	9.685
11			400.00	3576.00	8.940
12			330.00	3777.00	11.445
13			350.00	3635.00	10.386
14			343.00	4021.00	11.723
15			360.00	3234.00	8.983
16			345.00	3110.00	9.014
17			330.00	3960.00	12.000
18			320.00	3334.00	10.419
19			320.00	4115.00	12.859
20			348.00	4216.00	12.115
Mean			358.90	3509.85	9.855
S.D.			35.93	561.63	1.798
C.V.			10.01	16.00	18.241
Minimum			320.00	2094.00	6.105
Maximum			428.00	4262.00	12.859
1	50% 30mm	50% 15mm	300.00	2887.00	9.623
2			363.00	2043.00	5.628
3			333.00	2889.00	8.676
4			275.00	2698.00	9.811
5			258.00	1944.00	7.535
6			255.00	1952.00	7.655
7			243.00	1385.00	5.700
8			233.00	1654.00	7.099
9			240.00	2447.00	10.196
10			235.00	1706.00	7.260
11			248.00	2227.00	8.980
12			238.00	1933.00	8.122
13			223.00	1478.00	6.628
14			288.00	2460.00	8.542
15			330.00	2097.00	6.355
16			355.00	2474.00	6.969
17			318.00	2544.00	8.000
18			328.00	2494.00	7.604
19			323.00	2411.00	7.464
20			345.00	2491.00	7.220
Mean			286.55	2210.70	7.753
S.D.			46.81	440.82	1.268
C.V.			16.33	19.94	16.358
Minimum			223.00	1385.00	5.628
Maximum			363.00	2889.00	10.196
1	25% 30mm	75% 15mm	273.00	158.40	0.580
2			298.00	443.00	1.487
3			298.00	590.60	1.982
4			303.00	1413.00	4.663
5			288.00	959.70	3.332
6			295.00	136.90	0.464
7			295.00	169.10	0.573
8			295.00	612.10	2.075
9			318.00	1162.00	3.654
10			328.00	1443.00	4.399
11			320.00	524.80	1.640
12			298.00	434.90	1.459
13			295.00	716.80	2.430
14			348.00	800.00	2.299
15			325.00	147.70	0.454
16			340.00	669.80	1.970
17			290.00	1274.00	4.393
18			303.00	111.40	0.368
19			330.00	280.50	0.850
20			313.00	1089.00	3.479
Mean			307.65	656.84	2.128
S.D.			19.25	441.44	1.427
C.V.			6.26	67.21	67.082
Minimum			273.00	111.40	0.368
Maximum			348.00	1443.00	4.663

Sample Number	Fibre length Percentages		Linear Density (Tex)	Tensile Strength (N)	Tenacity (N/tex)
	Long Fibre	Short Fibre			
1			270.00	59.06	0.219
2			250.00	48.32	0.193
3			249.00	24.16	0.097
4			299.00	103.40	0.346
5			181.00	29.53	0.163
6			255.00	37.58	0.147
7			196.00	122.10	0.623
8			236.00	97.99	0.415
9			216.00	55.03	0.255
10			279.00	60.40	0.216
11		100% 15mm	248.00	48.32	0.195
12			242.00	59.06	0.244
13			248.00	32.21	0.130
14			223.00	24.16	0.108
15			257.00	55.03	0.214
16			281.00	76.51	0.272
17			300.00	115.40	0.385
18			304.00	110.10	0.362
19			238.00	25.50	0.107
20			273.00	81.88	0.300
Mean			252.25	63.29	0.250
S.D.			32.84	32.11	0.129
C.V.			13.02	50.73	51.614
Minimum			181.00	24.16	0.097
Maximum			304.00	122.10	0.623
1			218.00	2266.00	10.394
2			225.00	2287.00	10.164
3			258.00	2250.00	8.721
4			270.00	2494.00	9.237
5			233.00	2314.00	9.931
6			240.00	2534.00	10.558
7			273.00	2205.00	8.077
8			268.00	2777.00	10.362
9			240.00	1423.00	5.929
10	75% 25mm	25% 15mm	253.00	2157.00	8.526
11			243.00	2039.00	8.391
12			258.00	2286.00	8.860
13			275.00	2624.00	9.542
14			240.00	2091.00	8.713
15			253.00	1897.00	7.498
16			243.00	3048.00	12.543
17			233.00	2290.00	9.828
18			273.00	2240.00	8.205
19			230.00	2526.00	10.983
20			225.00	1597.00	7.098
Mean			247.55	2267.25	9.178
S.D.			17.89	369.14	1.503
C.V.			7.23	16.28	16.372
Minimum			218.00	1423.00	5.929
Maximum			275.00	3048.00	12.543
1			400.00	2140.00	5.350
2			368.00	2510.00	6.821
3			378.00	3654.00	9.667
4			383.00	2843.00	7.423
5			355.00	2894.00	8.152
6			375.00	2391.00	6.376
7			370.00	2914.00	7.876
8			373.00	2599.00	6.968
9			380.00	1913.00	5.034
10	50% 25mm	50% 15mm	360.00	3702.00	10.283
11			370.00	2658.00	7.184
12			383.00	2162.00	5.645
13			398.00	3519.00	8.842
14			380.00	1173.00	3.087
15			370.00	2848.00	7.697
16			365.00	3250.00	8.904
17			385.00	3075.00	7.987
18			378.00	2075.00	5.489
19			353.00	3117.00	8.830
20			373.00	2200.00	5.898
Mean			374.85	2681.85	7.176
S.D.			12.12	634.92	1.763
C.V.			3.23	23.67	24.571
Minimum			353.00	1173.00	3.087
Maximum			400.00	3702.00	10.283

Sample Number	Fibre length Percentages		Linear Density (Tex)	Tensile Strength (N)	Tenacity (N/tex)
	Long Fibre	Short Fibre			
1	25% 25mm	75% 15mm	360.00	342.30	0.951
2			375.00	127.50	0.340
3			330.00	208.10	0.631
4			340.00	1197.00	3.521
5			363.00	1134.00	3.124
6			348.00	1094.00	3.144
7			343.00	1421.00	4.143
8			358.00	1017.00	2.841
9			340.00	1036.00	3.047
10			340.00	302.00	0.888
11			330.00	1428.00	4.327
12			315.00	430.90	1.368
13			373.00	1638.00	4.391
14			360.00	1294.00	3.594
15			380.00	1201.00	3.161
16			365.00	230.90	0.633
17			360.00	452.30	1.256
18			330.00	600.00	1.818
19			353.00	1470.00	4.164
20			360.00	771.80	2.144
Mean			351.15	869.79	2.474
S.D.			17.28	490.91	1.383
C.V.			4.92	56.44	55.888
Minimum			315.00	127.50	0.340
Maximum			380.00	1638.00	4.391
1	100% 20mm		215.00	519.50	2.416
2		219.00	159.70	0.729	
3		210.00	346.30	1.649	
4		198.00	405.40	2.047	
5		207.00	585.20	2.827	
6		285.00	426.80	1.498	
7		191.00	253.70	1.328	
8		218.00	365.10	1.675	
9		324.00	818.80	2.527	
10		231.00	256.40	1.110	
11		354.00	746.30	2.108	
12		328.00	677.90	2.067	
13		219.00	408.10	1.863	
14		321.00	887.20	2.764	
15		334.00	634.90	1.901	
16		245.00	455.00	1.857	
17		252.00	357.00	1.417	
18		184.00	193.30	1.051	
19		259.00	614.80	2.374	
20		328.00	1468.00	4.476	
Mean			256.10	528.97	1.984
S.D.			56.04	300.88	0.815
C.V.			21.88	56.88	41.092
Minimum			184.00	159.70	0.729
Maximum			354.00	1468.00	4.476
1	75% 30mm	25% 4mm	375.00	1166.00	3.109
2			403.00	1319.00	3.273
3			385.00	1333.00	3.462
4			348.00	1510.00	4.339
5			392.50	1485.00	3.783
6			377.50	1757.00	4.654
7			352.50	1774.00	5.033
8			390.00	1616.00	4.144
9			347.50	1111.00	3.197
10			370.00	1101.00	2.976
11			392.50	1452.00	3.699
12			435.00	567.80	1.305
13			390.00	1446.00	3.708
14			415.00	1251.00	3.014
15			392.50	1208.00	3.078
16			382.50	1515.00	3.961
17			357.50	1089.00	3.046
18			360.00	1030.00	2.861
19			370.00	1619.00	4.376
20			357.50	928.90	2.598
Mean			379.68	1313.94	3.481
S.D.			22.89	298.86	0.832
C.V.			6.03	22.75	23.914
Minimum			347.50	567.80	1.305
Maximum			435.00	1774.00	5.033

Sample Number	Fibre length Percentages		Tex	Tensile Strength (cN)	Tenacity (cN/tex)
	Long Fibre	Short Fibre			
1	50% 30mm	50% 4mm	460.00	2373.00	5.159
2			580.00	1553.00	2.678
3			485.00	1985.00	4.093
4			495.00	1192.00	2.408
5			532.50	1850.00	3.474
6			470.00	1950.00	4.149
7			472.50	2526.00	5.346
8			500.00	2170.00	4.340
9			430.00	1730.00	4.023
10			455.00	2513.00	5.523
11			450.00	1138.00	2.529
12			475.00	2658.00	5.596
13			427.50	2259.00	5.284
14			477.50	2322.00	4.863
15			542.50	1193.00	2.199
16			497.50	1584.00	3.184
17			547.50	1984.00	3.624
18			487.50	2646.00	5.428
19			435.00	2430.00	5.586
20			467.50	2192.00	4.689
Mean			484.38	2012.40	4.209
S.D.			40.65	484.82	1.158
C.V.			8.39	24.09	27.523
Minimum			427.50	1138.00	2.199
Maximum			580.00	2658.00	5.596
1	75% 25mm	25% 4mm	395.00	1632.00	4.132
2			400.00	1007.00	2.518
3			410.00	1001.00	2.441
4			402.50	1083.00	2.691
5			422.50	1106.00	2.618
6			412.50	1181.00	2.863
7			415.00	1450.00	3.494
8			407.50	1344.00	3.298
9			415.00	1730.00	4.169
10			425.00	1583.00	3.725
11			415.00	1389.00	3.347
12			425.00	1003.00	2.360
13			402.50	1188.00	2.952
14			387.50	1421.00	3.667
15			425.00	1070.00	2.518
16			407.50	1227.00	3.011
17			390.00	1705.00	4.372
18			390.00	1168.00	2.995
19			420.00	931.50	2.218
20			402.50	1719.00	4.271
Mean			408.50	1296.93	3.183
S.D.			12.10	266.35	0.687
C.V.			2.96	20.54	21.575
Minimum			387.50	931.50	2.218
Maximum			425.00	1730.00	4.372
1	50% 25mm	50% 4mm	142.50	468.50	3.288
2			170.00	900.70	5.298
3			170.00	1067.00	6.276
4			177.50	1247.00	7.025
5			157.50	898.00	5.702
6			162.50	793.30	4.882
7			242.50	1753.00	7.229
8			232.50	1177.00	5.062
9			255.00	1259.00	4.937
10			250.00	1732.00	6.928
11			220.00	1082.00	4.918
12			270.00	1929.00	7.144
13			260.00	1282.00	4.931
14			160.00	1035.00	6.469
15			190.00	1236.00	6.505
16			197.50	920.80	4.662
17			262.50	1340.00	5.105
18			215.00	1162.00	5.405
19			210.00	1227.00	5.843
20			252.50	774.50	3.067
Mean			209.88	1164.19	5.534
S.D.			41.58	350.17	1.170
C.V.			19.81	30.08	21.147
Minimum			142.50	468.50	3.067
Maximum			270.00	1929.00	7.229